UNIVERSITY OF CALIFORNIA

SANTA CRUZ

Beyond Glucose Recognition: Development of a Multiwell Assay for the Recognition of Sugars and Sugar Derivatives as GI Permeability Markers

A dissertation submitted in partial satisfaction
of the requirements for the degree of

DOCTOR OF PHILOSOPHY

In

CHEMISTRY

by

Angel Resendez

June 2017

The Dissertation of Angel Resendez
is approved:

Professor Bakthan Singaram, Research Advisor

Professor Pradip K Mascharak, Chair

Professor R. Scott. Lokey

Tyrus Miller
Vice Provost and Dean of Graduate Studies

TABLE OF CONTENTS

List of Schemes

CHAPTER 1:

CHAPTER 2:

CHAPTER 3:

CHAPTER 4:

List of Figures

CHAPTER 1:

CHAPTER 2:

CHAPTER 3:

CHAPTER 4:

List of Tables

CHAPTER 1:

CHAPTER 2:

CHAPTER 3:

CHAPTER 4:

Beyond Glucose Recognition: Development of a Multiwell Assay for the Recognition of Sugars and Sugar Derivatives as GI Permeability Markers

Angel Resendez

Abstract

Gastrointestinal barrier dysfunction is now recognized as an early event in the pathogenesis of several problematic diseases, such as inflammatory bowel disease (IBD), Parkinson's disease, Crohn's disease, celiac disease and type 1, 2 diabetes mellitus. Gastrointestinal permeability can be assessed noninvasively by analyzing saccharide markers in urine such as sucrose, lactulose, mannitol, and the synthetic sweetener sucralose. Current methods for analyzing these markers require expensive and time consuming instrumentation such as high performance liquid chromatography/mass spectrometry (LC/MS). An alternative approach has been taken by assembling a two-component fluorescent probe that comprises a boronic acid substituted bipyridinium salt (BBV) as the receptor and a fluorescent reporter dye (HPTS) in which the system operates at physiological pH. We have shown that using our two component probe small intestinal permeability can be determined by rapidly measuring the lactulose and riboflavin ratios. To improve the current system, we pursued an array based system containing a triad of the boronic acid sugar receptors. Through this array, it was possible to discriminate between low and increased small intestinal permeability by analyzing various lactulose and mannitol mixtures.

Additionally, an assay to measuring sucralose for colonic permeability was developed. Since sucralose can survive the metabolic pathways of the gut microbiome, it is deemed as an excellent marker to use for measuring permeability in the colon. We have shown a proof of concept that using our chemical assay, sucralose can be measured with sensitivity in the range it is expected to appear in actual samples.

Dedication

I dedicate this dissertation to my hard working parents, without their exemplary example and sacrifices I would not be where I am today. Para mi familia Resendez, este esfuerzo no lo hubiera logrado sin su apoyo. Los quiero mucho.

Acknowledgements

I have been fortunate to have the amazing support from various groups of people during my time at UCSC. From my early beginnings as an undergraduate student navigating the realm of higher education and now as a graduate student, I am grateful for finding fantastic programs meant for helping the lost souls. From the EOP to ACE, and to the STEM diversity programs, all have greatly contributed to my success.

Bakthan Singaram, thank you for being a great mentor and providing me the opportunity to work in your lab. You are a fantastic educator I strive to be one day and you have always inspired me to pursue practical scientific solutions when approaching problems. Thank you Pradip Mascharak for being a supportive chair and I am grateful to have had the opportunity to briefly work on a project with your group. Thank you, Scott, for being a replacement as a reader in my committee, wishing your group and your company all the best.

We are the last ones standing Rachel, Murphy, and Gaby. You all have made the journey more enjoyable and have kept each other upright during the ups and downs. In the end, we look back at it and laugh at those times. Thank you for being the support system that was needed to get through this chapter of my life. I was very fortunate to have worked with fantastic undergraduate students, such as Jasmeet, Adriana, Ruth, Priera, Isaac, and Kelsey. Watching you all grow and become your own version of a scientist has been a fruitful experience.

Finally, I would like to acknowledge my partner in crime, Jessica Macias, you have always been by my side from the beginning and have made graduate school that much more possible to achieve. Your support and love has been instrumental for my success. We both have grown together and separately, which makes us the chingones that we strive to be. I would not be the person I am today without you and I am eternally grateful to have found a person like you.

CHAPTER 1

Molecular Recognition of Saccharides: Design, Significance, and Applications

1.1. Introduction

Up until the last three decades, researchers have focused on areas of developing detection systems for nucleic acids, proteins, and lipids. Carbohydrates not being coded in the genome, are complex, and have only more recently received increased attention through expanding fields of glycobiology and carbohydrate chemistry.[1] A major theme in these areas of research has been the development of analytical tools or sensors for the analysis of carbohydrates in aqueous media, from monitoring blood glucose levels, to detecting glycan biomarkers for diagnostics.

Molecular recognition of carbohydrates and its derivatives has become an important area of research as carbohydrates play a significant role in metabolic pathways of cells that contributes widely to overall homeostasis of a living organism. More specifically, carbohydrates and its derivatives (as complex oligomers) can be involved in protein function regulation,[2] cell-cell recognition,[3] cellular signaling,[4] and in its simplest form acts as energetic molecules (i.e. glucose). One example of the level of complexity is demonstrated in Figure 1.1, where α-D-glucose is polymerized into an oligomer of trimers.

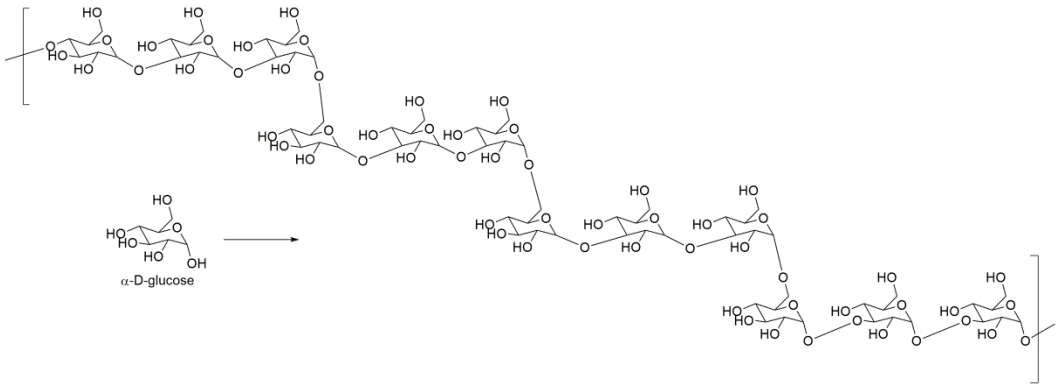

Figure 1.1. From the simplest form of glucose to a branching of trimers comprised of glucose.

The complexity of these carbohydrate targets can create particular challenges when working with synthetic receptors (chemosensors). In such systems, the issue of selectivity arises where having one particular receptor binding to glucose over other carbohydrates that may be present in the sample can be a difficult task to achieve. From this, researchers have made significant efforts in designing synthetic receptors that are highly selective for their targets or have some level of selectivity. Other key feature in the design of chemosensors that play an important role is the solubility and sensitivity of them. Variations of different chemosensor assemblies have been synthesized modulating the receptor unit to accommodate target (carbohydrate) interaction by either covalent or non covalent interactions. Herein, chemosensors that will be described and discussed are fluorescent based chemosensors where upon interaction with the receptor unit, there is a change in the photophysical characteristic (i.e. emission intensity, wavelength, and/or lifetime), and such a change can provide a variation in the absorbance and fluorescence, which indicates carbohydrate binding.

1.2. Current Demand for Developing Fluorescent Systems Based on Boronic Acids for Carbohydrates

The design and synthesis of chemosensors for biologically important molecules has developed into a major research area. Progress has been driven by advances in the analytical capabilities of biologists and chemists and from medical professionals whose practices lay increasing emphasis on accurately monitoring a patient's biochemical balance. In particular, medical providers are interested in the accurate and real-time measurement of blood glucose levels because of its central role in various metabolic processes. For example, control of blood glucose concentration is of critical importance for patients suffering from diabetes mellitus, a disorder affecting many millions of people worldwide.[5, 6] Diabetes mellitus is the major cause of blindness, heart diseases, kidney failure, and amputations among working-age adults around the world.[7] Regular testing of blood glucose levels and insulin administration at the proper time can dramatically reduce the long-term complications of insulin-dependent diabetes. Practically, all commercially available glucose sensors are electrochemical devices that function by measuring the product of glucose oxidation catalyzed by an enzyme, such as glucose oxidase (GOD) demonstrated in Scheme 1.1. In the presence of oxygen, glucose is converted to gluconolactone with the reduction of the cofactor FAD to $FADH_2$ which reduces oxygen to hydrogen peroxide. This conversion is measured electrochemically by the reduction-oxidation reaction of peroxide and the electron outputs are quantified by a silver electrode.[8]

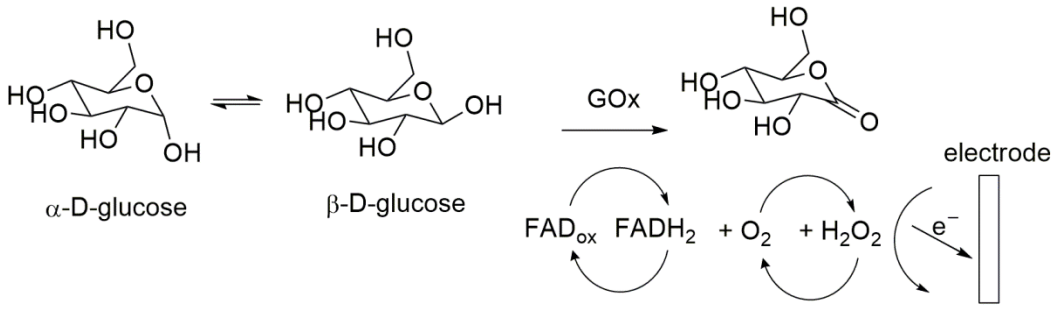

Scheme 1.1. Oxidation of D-glucose by glucose oxidase

Enzyme-based sensors currently available for self-monitoring of glucose concentration in whole blood can be too expensive for the millions of diabetics in third-world countries. From the increasing demand of having robust and cost effective sensors for glucose, has generated novel applications from the boronic acid functional group for developing synthetic receptors by developing fluorescent based systems. Thus, new approaches to glucose sensing in diabetes are being actively explored. Amongst these, fluorescence based systems are receiving the most attention, partly by the advantages fluorescence has to offer.[9]

1.3. Properties of Fluorescence

Compared to electrochemical analysis, fluorescence can offer extremely sensitive measurements. Early examples have demonstrated the ability to perform single-molecule detection using fluorescence. Fluorescence is the phenomenon of the emission of a light photon by a molecule or material after initial electronic excitation in a light-absorption process. Fluorophores (fluorescent molecules) can be characterized by their ability to absorb light of a particular wavelength, and emit a photon with a longer wavelength. This process can be described by the electronic state Jablonski diagram (Figure 1.2).

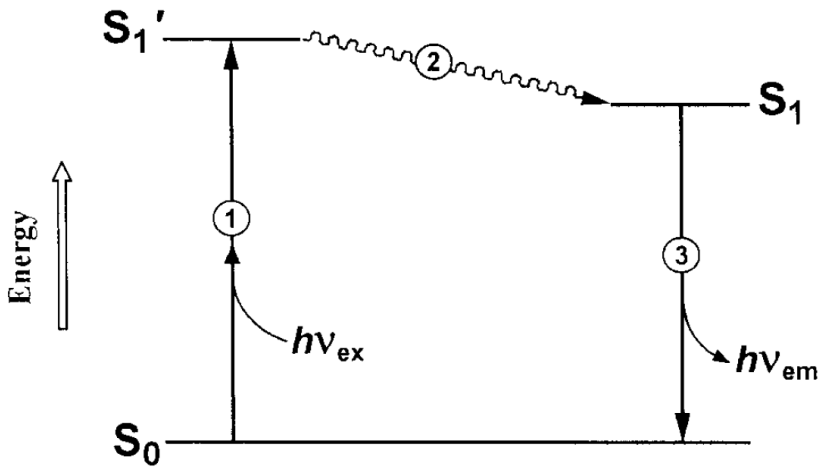

Figure 1.2. Jablonski diagram showing the three stages of the fluorescence process.

After absorptive excitation of the fluorophore by an external source (lamp or laser) supplying a photon with energy $h\nu_{ex}$, it is excited from the electronic ground state S_o, to an excited singlet state S_1'. The time it remains in this excited is referred to the

fluorescence lifetime (τ). The time range of fluorescence lifetime depends on both the fluorophore and its interaction with the local environment. Thus, for organic dyes it is in the picosecond (ps) to nanosecond (ns) time range (10^{-9}-10^{-12} s).

The second stage of fluorescence, non-radiative deactivation, is a process by which the excited fluorophore loses energy and relaxes to a lower excited singlet state (S_1' $\rightarrow$ S_1). This decay process occurs when the excited fluorophore transfers its vibrational and/or rotational energy to other molecules in its environment through collisional interactions shortening the fluorescence lifetime. Finally, the fluorophore returns to the ground state from the relaxed singlet state ($S_1 \rightarrow S_o$) and emits a photon with energy $h\nu_{em}$. The energy of the emitted photon $h\nu_{em}$ is lower (longer wavelength) than the excitation photon due to the non-radiative decay process.

1.3.1. Fluorescence Spectroscopy

The proper selection of excitation and emission wavelength is important for conducing fluorescence experiments. When a fluorescence spectrum is taken, a fluorescence excitation is nearly identical to an absorption spectrum and is depend on the same parameters of Beer's Law. It is also depended on the quantum yield of the fluorophore, the power of the source, and the fluorescence collection efficiency of the instrument. Fluorescence intensity (F) can be measured at the given wavelengths of excitation and emission. Its dependence on emission wavelength F^{max} (λ_{em}) gives the fluorescence emission spectrum. Usually, the fluorescence spectrum is shifted with

respect to the excitation spectrum to longer wavelength and this shift is referred to the *Stokes shift* (Figure 1.3).

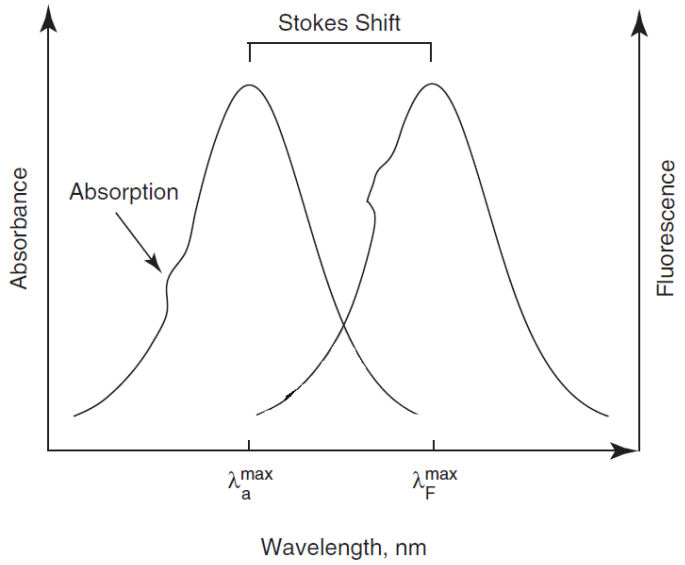

Figure 1.3 Typical absorption/excitation (left) and fluorescence emission (right) spectra.

The wavelength at which the excitation spectrum displays a maximum intensity is referred to as the $\lambda_a = \lambda_{ex}$. The energy differences between λ_{ex} and λ_{em} (Stokes Shift) are an important parameter to consider when choosing fluorophores for chemosensor design to help reduce light scattering. Therefore, excitation and emission wavelength should always be separated and fluorophores with a large *Stokes shift* are preferred.

1.3.2 Fluorescence Quenching

In addition to fluorescence emission spectra, the quenched state ("off") is as equally as important as other parameters of a fluorophore. Fluorescence quenching refers to any process that decreases the fluorescence intensity of a given fluorophore.[10] Of the possible quenching mechanism that exists, the two will be discussed here: dynamic (or collisional) and static quenching. Both of these types of quenching require a quencher molecule to come into physical contact with the fluorophore.

In dynamic quenching, the effect of quenching competes with the emission in time and is determined by the diffusion of a quencher molecule (Q) in the medium and its collisions with the excited dye. The fluorophore then returns to the ground state, but without emitting a photon. Neither molecule is chemically altered during the process. In this case, the relative intensity F_o/F is strictly proportional to the change of the fluorescence lifetime, τ_o/τ, where F_o and τ_o correspond to conditions without quencher, [Q] is the concentration of quencher, and K_v is the dynamic Stern-Volmer quenching constant. The dynamic quenching can be quantified by fitting the data to the following Stern-Volmer equation:[10]

$$\frac{F_o}{F} = \frac{\tau_o}{\tau} = (1 + K_v[\mathrm{Q}]) \qquad (1)$$

In static quenching, the fluorophore (in the excited and ground state) forms a non-fluorescent complex, with the quencher F-Q (Scheme 1.2)

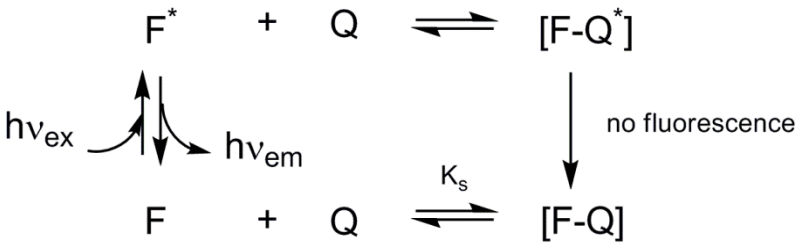

Scheme 1.2. Process of static quenching by complex formation of fluorophore (F) and quencher (Q) to form [F-Q].

Any fluorescence observed is from the uncomplexed fluorophore, which is unperturbed by Q, so $\tau = \tau_o$. The static Stern-Volmer quenching constant K_s is also the association constant, K_a for complex formation.

$$K_a = K_s = \frac{[F-Q]}{[F][\mathrm{Q}]} \tag{2}$$

The static quenching constant can be determined by using:

$$\frac{F_o}{F} = 1 + K_s[\mathrm{Q}] \tag{3}$$

Plotting F_o/F with respect to [Q] provides a Stern-Volmer plot. The quenching constant K_s or K_v can be obtained from the slope of the line displaying dependence of intensity. In this case, the nature of the quenching process is unknown. To determine whether the quenching is purely dynamic or static temperature studies must be conducted. Dynamic quenching is dependent on the frequency and force of intermolecular collisions, increases with increasing temperature. Conversely, static

quenching decreases with an increase in temperature, since higher temperatures will decrease the stability of the non-fluorescent ground state complex by disruption of the complex. Absorption measurements can also provide information to distinguish between the static or dynamic quenching. Since dynamic quenching occurs only in the excited state, the absorption spectrum will remain unperturbed. While static quenching the complex formation occurs in both the excited and ground states of the fluorophore, the absorption spectrum will have noticeable changes.

Cases where fluorescence quenching occurs through both static and dynamic mechanisms, a Stern-Volmer plot will display a trend with upward (exponential) character. To account for this, a quenching "sphere of action" model was developed.[11] This model considers the fluorophore molecule embedded in a sphere of a particular volume, and assumes that if a quencher molecule enters that sphere, it will instantly quench the fluorophore. By fitting the Stern-Volmer plot to equation 4, both static and dynamic quenching constants can be determined.[12]

$$\frac{F_o}{F} = (1 + K_s[\mathrm{Q}])\, \mathrm{e}^{V[Q]} \qquad (4)$$

Static quenching remains as K_s, but the dynamic quenching is represented by V. For the Singaram-Wessling two-component system that is reported throughout the chapters described here, apparent Stern-Volmer quenching constants were obtained from this equation.

1.4. Evolution of Boronic Acids As Carbohydrate Receptors

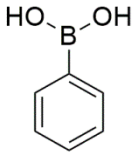

1

Due to the increasing demand for providing a sensing system for monitoring the debilitating disease of diabetes, boronic acids were turn to as a possible solution to traditional methods of finger pricking to provide capillary blood and measured by amperometric enzyme methods. A boronic acid compound was first used in 1954 by Kuivila and coworkers and noticed that boronic acids complexed with saccharides and polyols, postulating the formation of a cyclic ester.[13] Excess of phenylboronic acid **1** was taken and to it was added a solution of sugar alcohol, such as sorbitol and upon addition a white solid appeared. Elemental analysis demonstrated the ester product formed. Few years later, Lorand and Edwards reported the first quantitative evaluation of saccharide by boronic acid in 1959, reporting the first stability (affinity) constants for multiple polyol compounds.[14]

Since this pioneering work, various research groups have embarked on designing, developing, and discovering new systems based on boronic acids for quantifying saccharides in aqueous solution. Before going into selected examples, boronic acid chemistry will be discussed in detail. The applications of boronic acids in the design of chemoreceptors can be attributed from boron's electronic character such that the boron atom of a boronic acid in its neutral form has an open shell (empty *p*-orbital, six valence electrons) and therefore, is electron deficient. The presence of this open

shell gives boronic acids its Lewis acidity. Consequently, it has a high tendency to react with a Lewis base to reach the stable octet form (Scheme 1.3.).

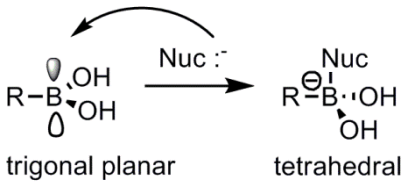

Scheme 1.3. Change in geometry undergone at the boron center when the vacant p orbital is filled by an attacking Lewis base (nucleophile).

Trisubstituted boron atoms have a sp^2 trigonal planar geometry. Nucleophiles or Lewis bases can donate electron density to the vacant p orbital, resulting in a change in geometry, and ultimately, to sp^3 hybridization. Based on this property, boronic acid have been exploited as receptors for diol containing molecules, such as carbohydrates forming a boronic acid-diol complex. Boronic acids reversibly form a 5- or 6-membered cyclic diol boronate complex upon association between arylboronic acid and *cis*-1,2-diols or *cis*-1,3-diols respectively as depicted in Scheme in 1.4. Because of its Lewis acidity character, boronic acids have their intrinsic pK_a, but the pK_a is not the same that is usually to describe Brønsted acids. It is a measure of the proton released from a water molecule.

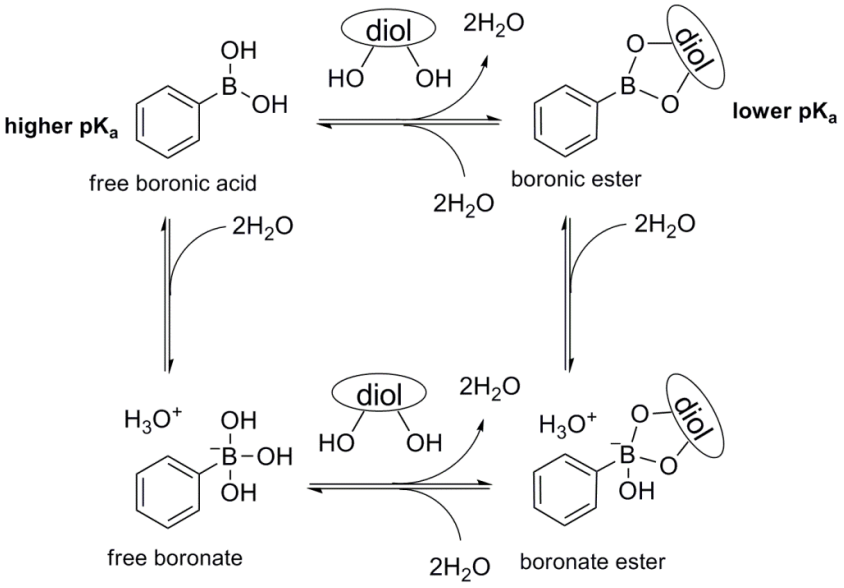

Scheme 1.4. Reversible binding equilibria between aryl boronic and a diol model compound.

It is generally understood that upon association of a diol to form the cyclic boronic ester (top right), there is a shift in the pK_a of the boronic acid due to the bond angle suppression, increasing the boron atom's Lewis acidity. This results in the boronic ester ionizing water to become attacked by the hydroxide anion forming the boronate ester (bottom right). Also, the free boronic acid can be converted to the free boronate (bottom left), and then bind to the diol to form the boronate ester complex. Thus, optimal binding of diol depends on the interplay of the pK_a value of the boronic and diol, the solution pH, and the nature and concentration of the buffer solution.[15] Although not always the case, but boronic acids with low pK_a values tend to have high binding affinities.[16, 17] Additionally, because of its strong Lewis acidity in an

aprotic solvent, boronic acids can react with a variety of Lewis bases, such as hydroxyl, sulfhydryl, and amino groups as well as fluoride and cyanide.

Russell first described the use of a fluorescent boronic acid for glucose recognition in a 1992 patent.[18] It utilized an azo dye substituted with a boronic acid (2) and was able to recognize different carbohydrates in aqueous solution (Figure 1.4).

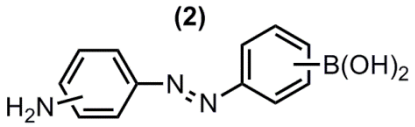

Figure 1.4. The boronic acid functionalized azo dye (**2**) that was first used to quantify the presence of carbohydrates in aqueous solution.

1.5. Fluorescent Chemosensors Based on Boronic acids

Since the early efforts by Lorand and Edwards and Russell's patent application, the main concepts utilized in the design of fluorescent chemosensors based on boronic acids can be categorized into four types of signal modulation systems; such as Photoinduced Electron Transfer (PET), Fluorescence Resonance Energy Transfer (FRET), Internal Charge Transfer (ICT), and External Charge Transfer (ECT).

1.5.1 Internal Charge Transfer Chemosensors

In an ICT-type system, the boronic acid is directly attached covalently to a fluorescent molecule with a significant orbital overall for electronic coupling. Altering the electron distribution of the fluorescent moiety often results in a change to both the fluorescent intensity and wavelength emission. Similar to Russell's system, Yoon and Czarnik took advantage of the affinity of boronic acids to diols by substituting a fluorophore anthracene with a boronic acid to give 2-anthrylboronic acid (**3**).[19] This chemosensor provided a fluorescence excitation and emission at 365 and 415 nm respectively (Figure 1.5). The binding studies for glucose were carried out in pH 7.4 phosphate buffer containing 1% DMSO demonstrating an "on-ff" fluorescent system.

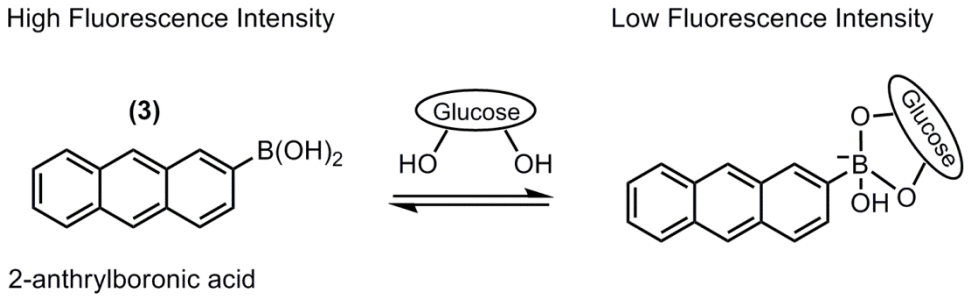

Figure 1.5. Binding of glucose to 2-anthrylboronic acid (**3**) resulted in the less fluorescent boronate ester.

This chemosensor system can be considered to be an ICT-type system due to the decrease in fluorescence intensity, which was about 30% decrease.[19]

Another early ICT-type system described by Nagai and coworkers where they reported the 5-indolylboronic acid (**4**) which exhibited fluorescence quenching upon binding of mono, di and oligosaccharides.[20] This system exhibited an excitation and emission of 290 and 361 nm respectively (Figure 1.6).

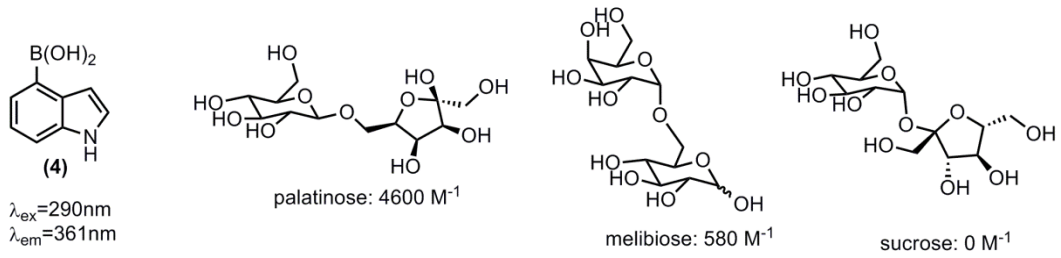

Figure 1.6. 5-indolyl boronic acid (**4**) and binding constants to the studied disaccharides. Studies performed in 20 mM phosphate buffer and 1 % DMSO.

The highest binding affinity for this system was achieved for palatinose, a reducing disaccharide with 4600 M^{-1} association constant, 580 M^{-1} for melibiose, and no binding affinity was observed for the non-reducing saccharide sucrose. A general pattern that the target carbohydrate must be a reducing disaccharide can be inferred.

Shinkai and coworkers later expanded on the ICT system and prepared a series of arylboronic acid analogues and studied the binding to fructose. A biphenyl (**5**) and napthalene (**6**) derivatives were most notable. Both of these demonstrated strong emission intensities and efficient reduction of fluorescence (Figure 1.7). Excitation and emission wavelengths for these arylboronic acid derivatives range between 230 nm and 338 nm excitation for (**5**) and 324 nm and 376 emissions for (**6**). The

emission was reduced by 70% and 82% respectively in water:DMSO (99:1) at pH 3. No emission was observed at pH 11.[21]

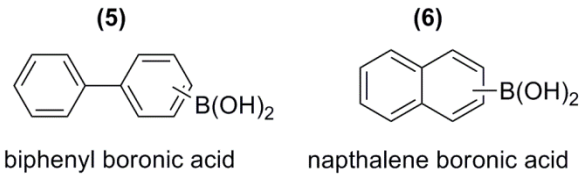

Figure 1.7. Biphenyl (**5**) and napthalene (**6**) boronic acid derivatives.

Unfortunately, the excitation and emission wavelengths used for these boronic acid derivatives are in the UV range which can interfere with the auto fluorescence from biomolecules present in a biological sample.

Lakowicz and DiCesare expanded on the work of Shinkai and coworkers by investigating a series of boronic acid functionalized stilbene derivatives. This stilbene derivatives contained electron withdrawing or donating groups in the 4'-position of the stilbene derivatives. Amongst the derivatives with donor or withdrawing groups, the withdrawing cyano group attributed to the stabilization of a donor-acceptor interaction between the functional group and the boronic acid (Figure 1.8).[22, 23]

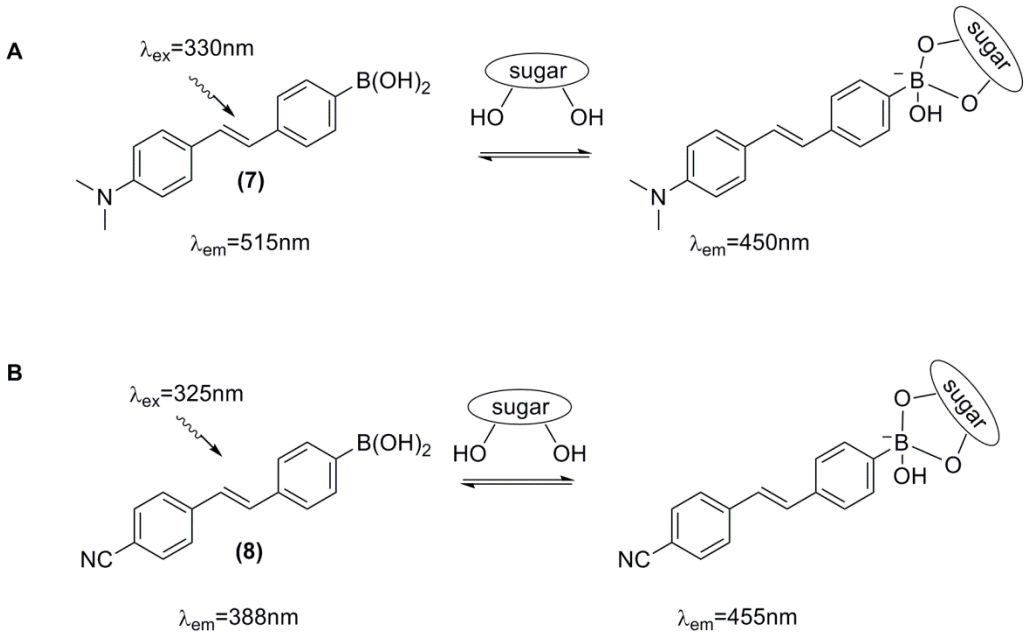

Figure 1.8. A. Stilbene functionalized boronic acid with an electron donating group. Receptor (**7**) exhibiting a blue shift in emission wavelength upon sugar binding. **B.** Stilbene functionalized boronic acid with an electron withdrawing group (**8**) exhibiting a red shift in emission wavelength upon sugar binding.

Stilbene derivative (**7**) demonstrated to have apparent binding constants if 23 M^{-1} and 400 M^{-1} to glucose and fructose respectively. The stilbene derivative (**8**) provided slightly higher binding affinity to glucose and fructose with apparent binding constants of 55 M^{-1} and 1500 M^{-1} respectively. Although effective in binding to glucose and fructose, these boronic acids derivatives lack solubility in water and all studies needed to be conducted in methanolic-aqueous buffer solutions.

Few years later, Wang and coworkers developed a novel ICT fluorescent boronic acid based on quinolines with improved photostability and solubility. Two chemosensors were prepared, 5-quinoline boronic acid (**9**) and 8-quinoline boronic

acid (**10**), which demonstrated λ_{ex} and λ_{em} values of 315 nm and 425 nm for (**9**) and 314 nm and 417 nm for (**10**) respectively (Figure 1.9).[24,25]

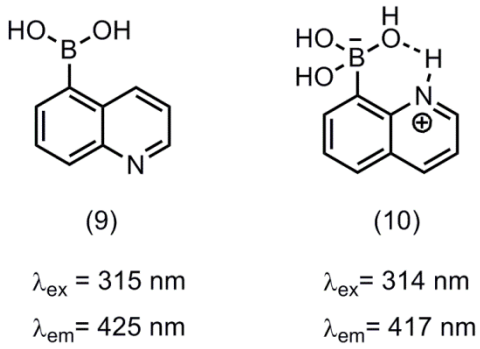

Figure 1.9. Quinoline boronic acid derivatives (**9**) and (**10**) in their neutral and zwitterionic form at pH 7.0 with their respective excitation and emission wavelengths.

The 5-quinoline boronic acid derivative exhibited an eight times larger binding constant between fructose compared to the 8-quionline boronic acid (**9**) and fructose. Additionally, ^{11}B NMR titrations showed that the derivative (**9**) existed as a neutral boronic acid and derivative (**10**) existed as the zwitterionic form at pH 7. The lack of binding affinity to fructose by (**10**) can be rationalized by the intramolecular hydrogen bonding stabilization between the boronate and quinoline hydrogen. This interaction could hinder the formation of the fructose boronate triester.

1.5.2 Photoinduced Electron Transfer Chemosensors

Despite successful efforts in having the boronic acid moiety directly attached to the fluorophore unit, there remains an unmet need in exploring other variations of the chemosensing element. An alteration of the chemosensing element that was taken advantage by James and coworkers, was attaching a linker moiety in between the boronic acid receptor and the fluorophore. In these systems, carbohydrate binding can cause a fluorescent modulating process, such as photoinduced electron transfer (PET), to be enhanced or interrupted. In a PET system, the fluorescent moiety is attached to the boronic acid receptor through a spacer. Early reports of this work stem from the classical example developed by Shinkai and James, who attached a boronic acid receptor to an anthracene fluorophore (**11**) by way of an amine linker (Figure 1.10).[26, 27] Having this proximal amine linker arm in between the fluorophore unit and the boronic acid receptor can offer unique advantages, such as lowering the pK_a of the neighboring boronic acid and the amine group could serve as an "off-on switch". The amine's ability to lower the pk_a of a boronic acid has been previously demonstrated the N-B interaction by Wulff and coworkers.[28, 29]

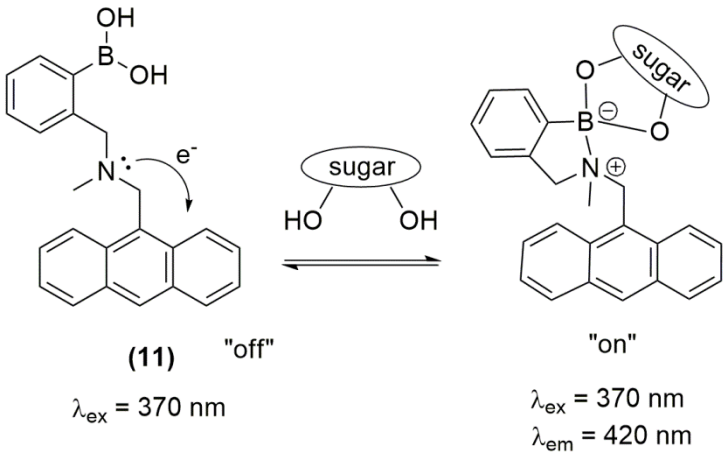

Figure 1.10. Anthracene functionalized boronic acid with an amine linker arm (**11**) and its respective excitation and emission wavelengths. Illustration of "off-on switch" after diol complexation.

This anthracene bridged to a phenylboronic acid moiety (**11**) by a tertiary methylene amine exhibited an excitation and emission of 370 nm and 420 nm after condensation of a saccharide. In the absence of saccharide, the lone pair of the amino group quenches the fluorescence. While in the presence of a saccharide, the N-B interaction is enhanced due to the increased Lewis acidity of boron and modulates the florescence of nearby anthracene. This chemosensor demonstrated to work effectively over a broad range pH range.[30] The structural dependence of (**11**) upon changing pH is illustrated in Scheme 1.5. The amino group is protonated at low pH, thus, unable to quench the fluorescence of the anthracene moiety. The chemosensor (**11**) is also non fluorescent at high pH, since the arylboronic is fully converted to the boronate form.

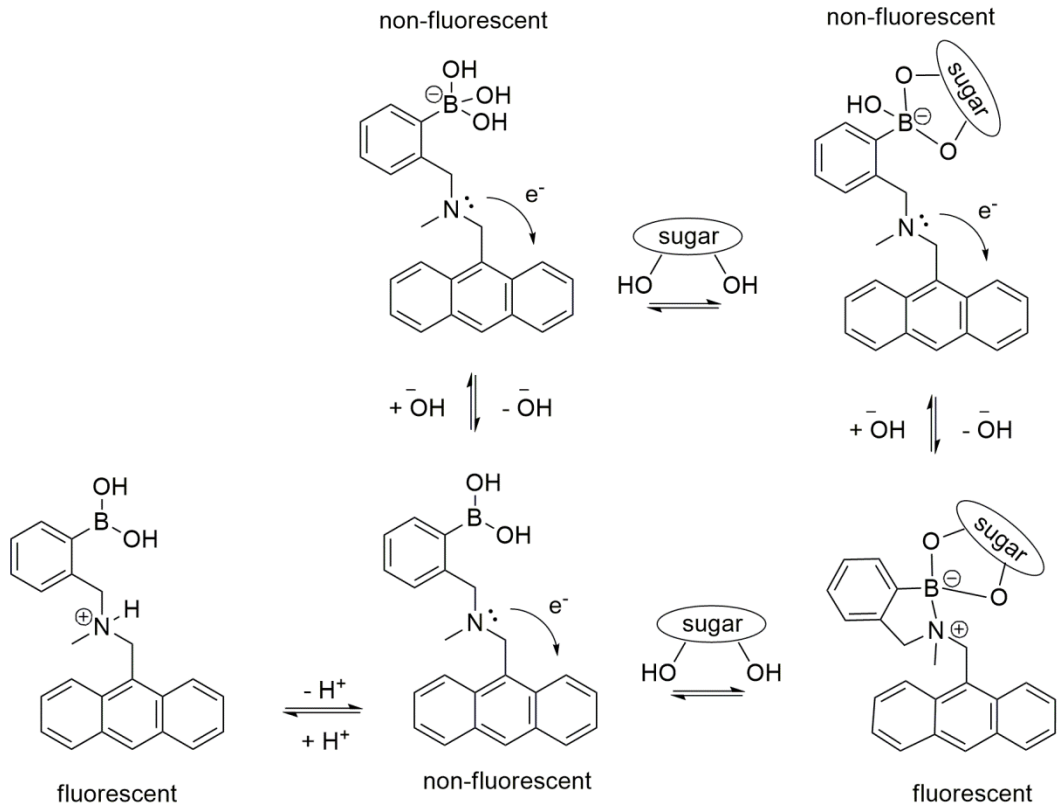

Scheme 1.5. Structural effects of (**11**) from pH modulation and after saccharide addition.

In addition, the fluorescence does not increase with high pH in the presence of saccharide since the boronic acid is already converted to the boronate form. This chemosensor can only operate in the pH range that will not produce a false positive signal from amine protonation and a false negative from high pH that results from the boronate formation upon saccharide addition.

From this basic unit, Shinkai and James and coworkers, further improved on chemosensor (**11**) to a diboronic acid system (**12**) by adding an additional amine linker arm linked to a phenylboronic acid. The goal of introducing a second boronic

acid motif was to promote bidentate binding for saccharides and potentially have selectivity for glucose over fructose (Figure 1.11).[27]

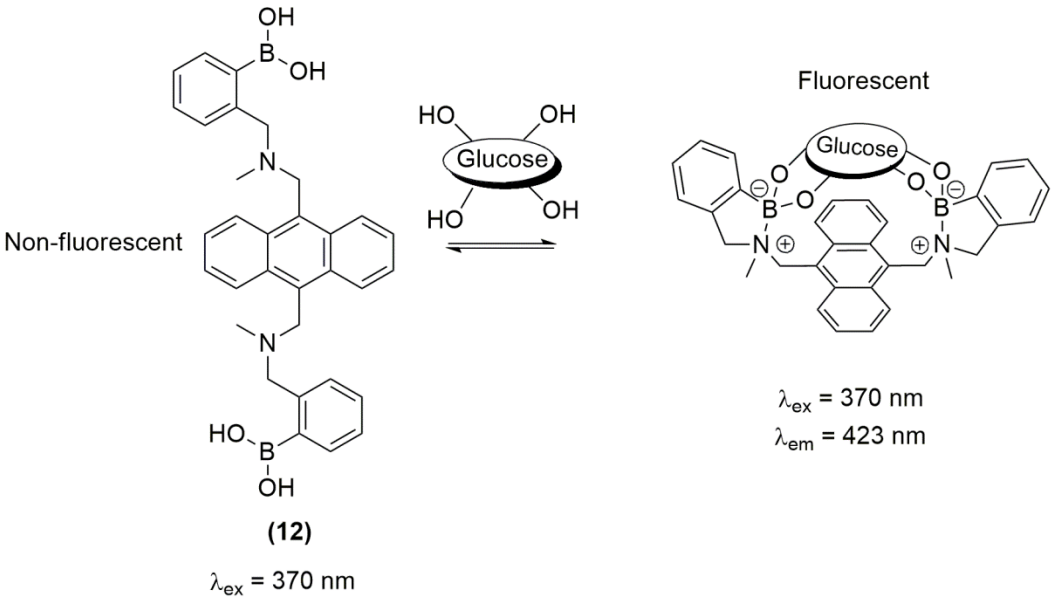

Figure 1.11. The bidentate PET-chemosensor by Shinkai and James with selective glucose binding.

The diboronic acid (**12**) had an appropriate distance between the boronic acid receptors to achieve a 1:1 stoichiometry bidentate binding for glucose. This receptor achieved higher selectivity for glucose over fructose and galactose with apparent binding constants of 4000 M^{-1} , 320M^{-1} , and 160 M^{-1} respectively. Based on ^{1}H NMR structural elucidation of the glucose and (**12**) complex , there was substantial evidence demonstrating that binding occurred at the 1,2 and 4,6 diol sites in the alpha-D-glucopyranose form of glucose. This was one of the first examples to

illustrate selective bidentate binding for glucose over fructose with a selectivity ratio of glucose/fructose of 12.5:1.

1.5.3 Photoinduced Electron Transfer Chiral Chemosensors

To further improve on the bidentate ability of the fluorophore-linker-boronic acid motif system, James and coworkers went on to develop the first chiral chemosensor based on boronic acids. Chiral binaphthol were coupled to diboronic acids by an amine linker, which demonstrated to have moderate glucose selectivity. The chiral binol chemosensor (**13**) of R and S configuration were examined for its enantioselectivity for glucose at pH 6 (Figure 1.12).[31]

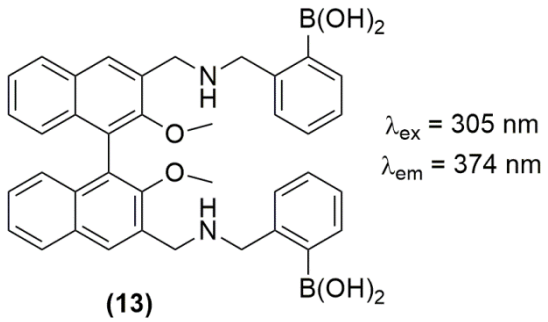

(13)

Figure 1.12. The chiral binol chemosensor (**13**) with its respective excitation and emission wavelengths.

This chiral binol derivative (**13**) showed apparent binding affinity for glucose with values of K_R = 201 M^{-1} and K_S = 146 M^{-1} with enantioselectivity of K_R/K_S ratio of 1.4:1. Enantioselectivity was not observed at pH 8, since glucose was bound to the binol derivatives with similar strengths with K_R = 242 M^{-1} and K_S = 232 M^{-1}.

Although not as selective for glucose, the binol chemosensor (**13**) demonstrated excellent binding affinity and chiral discrimination to sugar alcohols, such as sorbitol.[31] For sorbitol, a K_R value of 1130 M^{-1} and K_S = 5880 providing a K_R/K_S value of 1.1:5.88 at pH 6, little selectivity was obtained at pH 8. All of the measurements were carried out in 50 % methanol in water NaCl buffer, due to the poor solubility of the binol chemosensor.

Thus far, all of the aforementioned systems are considered as one-component systems and it was not until the research program from the Singaram research group that introduced a two-component system based on boronic acids for the recognition of saccharides. Through this work it became a goal of our research group to develop an implantable sensor that can be used to continuously monitor glucose concentration in people suffering from diabetes. An application for continuous glucose sensors would be beneficial in hospitals; they are necessary for implementing tight glycemic control in the operating room and in the Intensive Care Unit.[32,33]

1.6. Singaram-Wessling Two-Component System

Before we started our research, coupling of the modulation of fluorescence quenching with glucose binding to a boronic acid relied exclusively on the use of a single sensing moiety containing both receptor and fluorophore, as described previously. To increase glucose selectivity in these systems, the concept of bidentate binding via diboronic acids has been utilized.[26, 34-38] In this approach, the molecular probe contains two arylboronic acid moieties spatially disposed in a way that allows for cooperative binding to a single glucose molecule, the entire assembly being coupled to a fluorophore reporter. For a given diboronic acid-containing scaffold, the spacing between the boronic acids can be adjusted through synthetic modifications to create a glucose-specific binding pocket. The synthetic challenge, associated with all the one-component systems, can be avoided by employing a modular approach to the sensor design, where the receptor and the indicator moieties exist as covalently discrete entities. This technique has been used in well-known indicator displacement assays (IDA).[39, 40]

Our approach to monosaccharide sensing has also relied on a modular two-component design. In our system, fluorescence is quenched by a boronic acid-substituted viologen receptor not directly bonded to the fluorophore. Monosaccharide binding to the boronic acid diminishes the efficacy with which the fluorescence emission is quenched by the viologen. Thus, the intensity of fluorescence emission can be correlated with monosaccharide concentration. This two-component approach

avoids the synthetic difficulties associated with combining the fluorophore and receptor in a single sensor molecule and allows for considerable versatility in choosing each component. For example, the structure of the receptor can be modified to improve quenching ability or to provide selectivity for one monosaccharide over another without having to modify the structure of the dye. At the same time, fluorophore units can be interchanged without any synthetic modification of the receptor, making it possible to use numerous, commercially available fluorescent dyes. This is a considerable advantage of our two-component approach, since synthetic transformation can cause unwanted changes in the photophysical properties of the dye. Unlike a standard IDA, the indicator in our system is displaced by the analyte from an allosteric interaction, wherein the analyte does not compete at the same binding site with the indicator. In contrast, it binds at another site (allos stereos *Greek* "other object"), thereby inducing a decrease in the affinity of the indicator for the receptor. We call this new type of assay an "allosteric indicator displacement assay" (AIDA) (Figure 1.13).

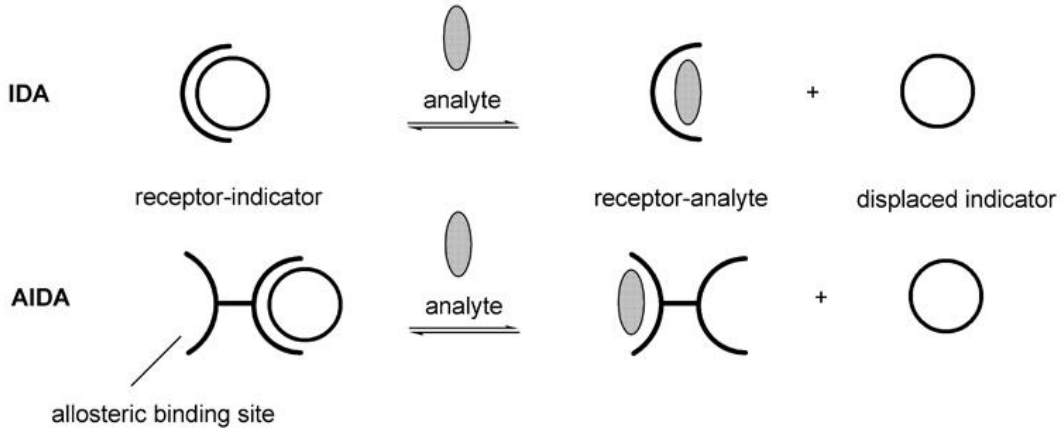

Figure 1.13. Comparison between an indicator displacement assay (IDA) and an allosteric indicator displacement assay (AIDA).

The first use of an AIDA as a probe for saccharide sensing was reported by the Singaram group in 2002.[41] Progress in this endeavor is well documented in a series of papers by the Singaram group detailing the chemistry of this system and the development of sensors based on immobilization of the sensing components in a hydrogel.[42-53] The original goal of this research was to produce a fluorescence-based sensor for glucose that could operate in vivo. The goal of this dissertation research was to utilize the chemistry to develop a high throughput assay for measuring specific sugar markers in human urine and exploring the two-component system for its ability to discriminate between sugar alcohols and sugar acids of interest. The Singaram-Wessling two-component system is compromised of the anionic fluorescent dye, 8-hydroxypyrene, 1,3,6-trisulfonic acid trisodium salt (HPTS), and a boronic acid–appended viologen (BBV) that acts dually as a quencher and receptor. In the absence of sugar, a ground state complex is formed due to the coulombic attraction between

the anionic dye and cationic quencher with a decrease of fluorescence intensity as compared with free HPTS. When a saccharide binds, the boronic acids are converted to tetrahedral anionic boronate ester, which neutralizes the cationic viologen, diminishing its quenching efficiency and liberates HPTS. The fluorescent signal generated upon dissociation of the ground state complex is directly proportional to sugar concentration (Scheme 1.6).

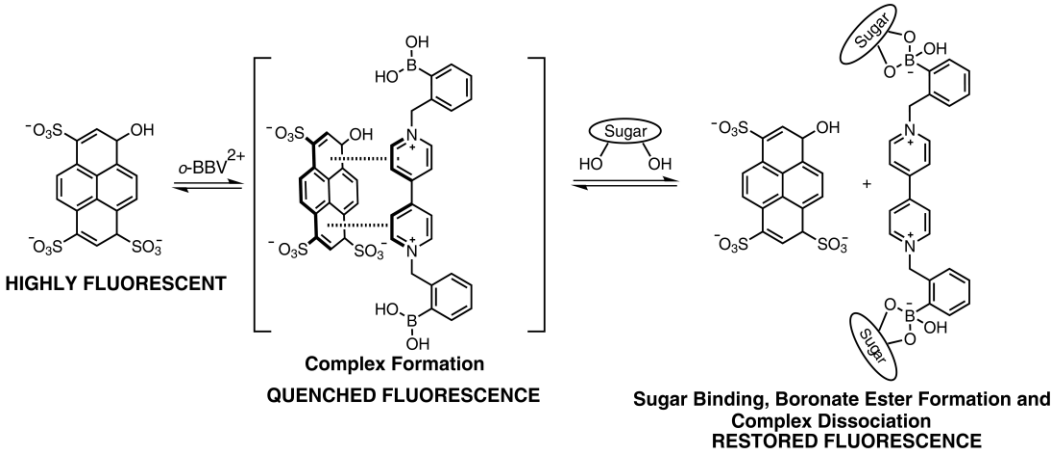

Scheme 1.6. Proposed mechanism for fluorescence signal generation upon recognition of sugar analyte with 4,4'-*o*-BBV receptor.

The dye and quencher as two discrete entities can provide better selectivity and sensitivity over saccharides of interest. This also allows the quencher to be readily modified without altering the photophysical properties of the reporter dye. Because of the ionic nature of these receptors, they are water soluble at physiological pH even in the absence of sugar. In addition, varying ratios of receptor to reporter dye can be used to modulate fluorescence response.

Among the various quenchers screened in the early stages of the glucose sensing project, viologens stood out because of their superior ability to quench the fluorescence of many dyes. Our hypothesis was that boronic acid substituted viologens could be combined with a fluorophore to sense glucose. Viologens are characterized as good electron acceptors.[54] Although methyl viologen (MV^{2+}) is the most widely studied and most often utilized of these compounds, numerous viologens with different redox potentials have been prepared. Several excellent reviews of viologen chemistry are available.[55-58]. Importantly, although viologens are, by one definition, the salts of 4,4'-bipyridinium several other bipyridinium and phenanthrolinium salts share many of the properties as the former. Thus, we have chosen to use the term "viologen" for all such compounds as they all show similar ability to quench fluorescent dyes and have the bipyridinium cores. These electron accepting viologens and related heterocyclic, aromatic, dinitrogen-containing compounds have been found to quench the luminescence of both simple dyes[59-61] and macromolecular fluorophores.[62-65]

The ability of these compounds to quench fluorescence of anionic fluorophores stems at least partly because they contain two positive charges. The positive charges of the viologen facilitate two possible processes: electron transfer and Coulombic attraction. The relatively modest fluorescence quenching of an anionic dye molecule by nonionic 4,4'-dipyridyl follows simple Stern-Volmer kinetics and appears to occur exclusively through dynamic, or collisional quenching. Quenching with a cationic

viologen, however, is dramatically enhanced as a result of electrostatic attraction. This results in static quenching through complex formation between dye and quencher.[66] The quenching ability of viologens encouraged us to proceed with the synthesis of boronic acid substituted viologens beginning with 4,4'-N,N'-bis(benzyl-2-boronic acid) bipyridinium dibromide (4,4'-*o*-BBV^{2+}) and study their ability to quench HPTS. Synthetically, the preparation of 4,4'-*o*-BBV^{2+} is very similar to that of benzyl viologen (BV^{2+}) (Scheme 1.7).[41]

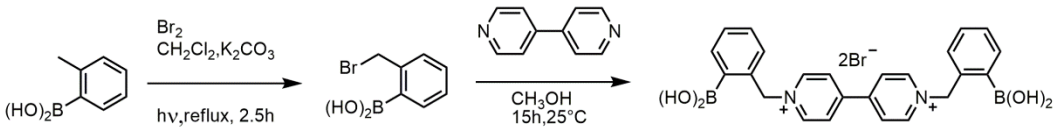

Scheme 1.7. Initial synthetic route for 4,4'-o-BBV^{2+}.

The signal transduction in this system is thought to be derived from two separate, reversible complex formation of 4,4'-*o*-BBV^{2+}/HPTS and 4,4'-*o*-BBV^{2+}/monosaccharide. In the absence of sugar 4,4'-*o*-BBV^{2+} and HPTS form a photo-inactive complex while in the presence of sugar, 4,4'-*o*-BBV^{2+} forms a boronate ester-complex. The boronate ester formation converts the dicationic viologen to a neutral zwitterionic species. Neutralization of charge results in a loss of electrostatic attraction and subsequent dissociation of the 4,4'-*o*-BBV^{2+} and HPTS complex. Evidence for this mechanism is observed in the UV-Vis spectra where addition of fructose or glucose results in regeneration of the free HPTS (Figure 1.14).

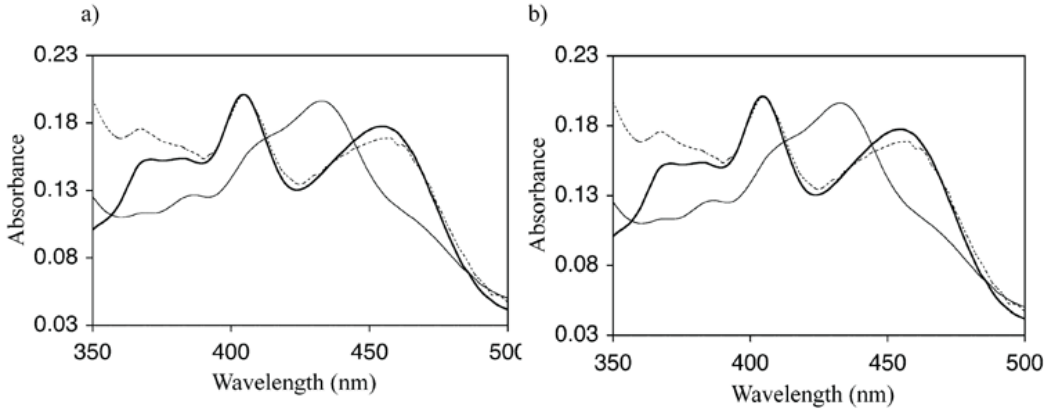

Figure 1.14. a) UV-Vis absorption spectra of HPTS (lx10^{-5} M, solid line) ; HPTS (3x10^{-4} M) with 4,4'-*o*-BBV^{2+} (3x10^{-4} M, light solid) **;** HPTS (1x 10^{-5} M) with *o*-BBV^{2+} (3x10^{-4} M, dashed line) and fructose (1800 mg/dL) b) UV-vis absorption spectra of HPTS (lx10^{-5} M, solid) ; HPTS (lx10^{-5} M) with 4,4'-*o*-BBV^{2+} (3x10^{-4} M); HPTS (lx10^{-5} M. light solid) with 4,4'-*o*-BBV^{2+} (3x10^{-4} M, dashed line) and glucose (1800 mg/dL).

As a result of this dissociation, nonradiative deactivation pathways are removed leading to a relative increase in fluorescence with increasing sugar concentration. This viologen carries two positive charges at physiological pH of 7.4. In this cationic state, the boron substituents are trigonal and neutral and the viologen forms a non-fluorescent ground state complex with anionic fluorescent dye HPTS. Upon sugar binding, the pK_a of boron in its ester configuration is lowered, causing the boron to convert to its tetrahedral, anionic form in which it bears a charge of -1. This change, which has been confirmed with ^{11}B NMR and UV-visible absorbance spectra, causes the viologen quencher to become electronically neutral and results in dissociation of the complex. Thus, fluorescence is restored as the complex dissociates and the quenching interaction is diminished. In this sensing system, signal transduction

derives from two separate, but interdependent, reversible reactions. The first is complexation of a fluorescent dye with a viologen, which quenches the fluorescence. The second is the binding of the sugar to the boronic acid receptor of the viologen, which causes the initial dye:quencher complex to dissociate and fluorescence emission to recover.

1.6.1 Variations in the Viologen Quencher-Bipyridinium Quenchers

We prepared a series of boronic acid-modified viologen quenchers to examine the effects of boronic acid positioning, quencher charge, and quencher-to-dye ratio on fluorescence quenching and glucose sensing. The quenchers are simple, symmetrical dicationic viologens with two boronic acid receptor groups arranged in the *ortho*, *meta*, and *para* positions (4,4'-*o*-BBV^{2+}, 4,4'-*m*-BBV^{2+} and 4,4'-*p*-BBV^{2+}) as shown in Figure 1.15.

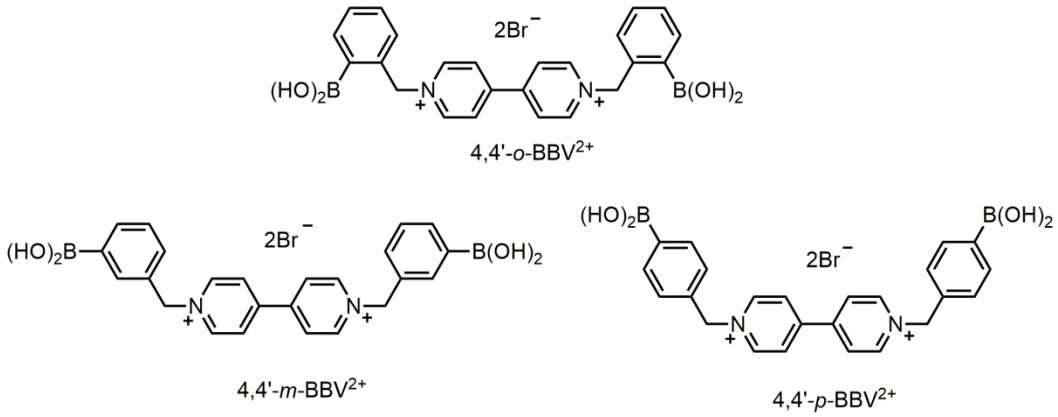

Figure 1.15. Symmetrically substituted boronic acid-modified violgen quenchers.

We were interested in how the position of the boronic acid groups on the benzyl ring would affect fluorescence quenching and glucose sensing, and hypothesized that the signal magnitude and saccharide selectivity might be affected. After our initial work with *o*-BBV^{2+}, we evaluated the ability of *m*-BBV^{2+} and *p*-BBV^{2+} to quench HPTS fluorescence (Figure 1.16.).

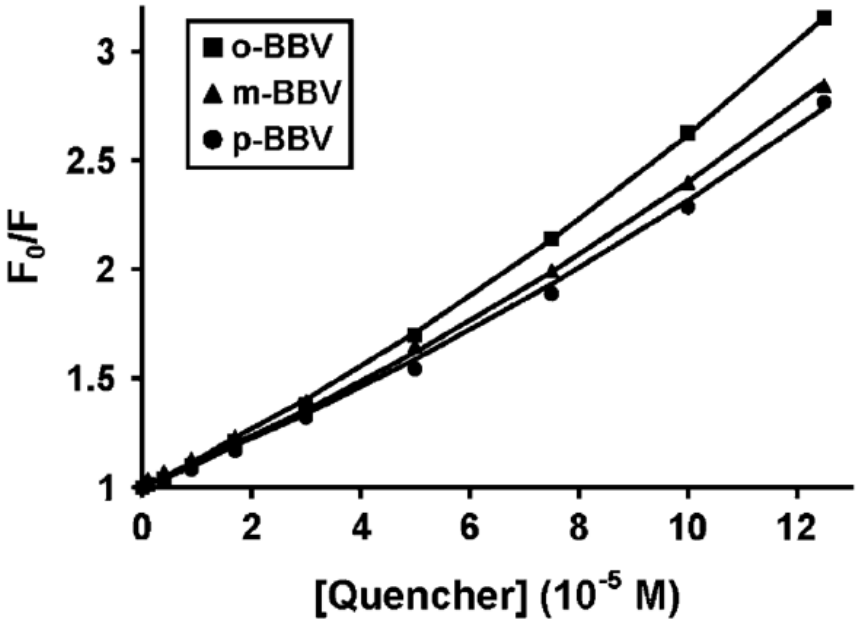

Figure 1.16. Stem-Volmer plots of HPTS ($4x10^{-6}$ M) with increasing concentration of 4,4'-*o*-BBV^{2+} (square), 4,4'-*m*-BBV^{2+}(triangle), 4,4'-*p*-BBV^{2+} (circle) in pH 7.4 buffer, λ_{ex} = 460nm and λ_{em} = 510nm; F_o = original fluorescence; F= fluorescence after addition of quencher.

As indicated in Figure 1.16, we found only minor differences in quenching efficacy for these three bipyridinium quenchers with the *ortho*-substiuted viologen providing the best results followed by *meta*- and then *para*-substituted BBVs.

1.6.2. Glucose Binding Studies with 4,4'-*o*-BBV^{2+}, 4,4'-*m*-BBV^{2+}, 4,4'-*p*-BBV^{2+}

When these three compounds were tested for their response to glucose we found a fair degree of variation in the results, with o-BBV^{2+} giving the greatest signal. We first carried out a set of optimization experiments to determine the effects of quencher-to-dye ratio on glucose sensing. Initial work established that good sugar sensing results could be obtained after first substantially quenching the HPTS with a 30:1 quencher-to-dye ratio. When the three viologens were tested for their response to glucose at this 30:1 ratio, we observed *o*-BBV^{2+} to give the greatest signal. Significantly, this was the compound that had provided the weakest quenching among the three. We suspect that this may be a consequence of a unique charge-neutralization interaction that can occur in *o*-BBV^{2+} between the boron and the positively charged nitrogen of the viologen.[47] The *meta*- and *para*-substituted viologens gave a smaller, but still significant response in the physiological range. The superimposed relative fluorescence increase of all three quenchers is shown for comparison in Figure 1.17.

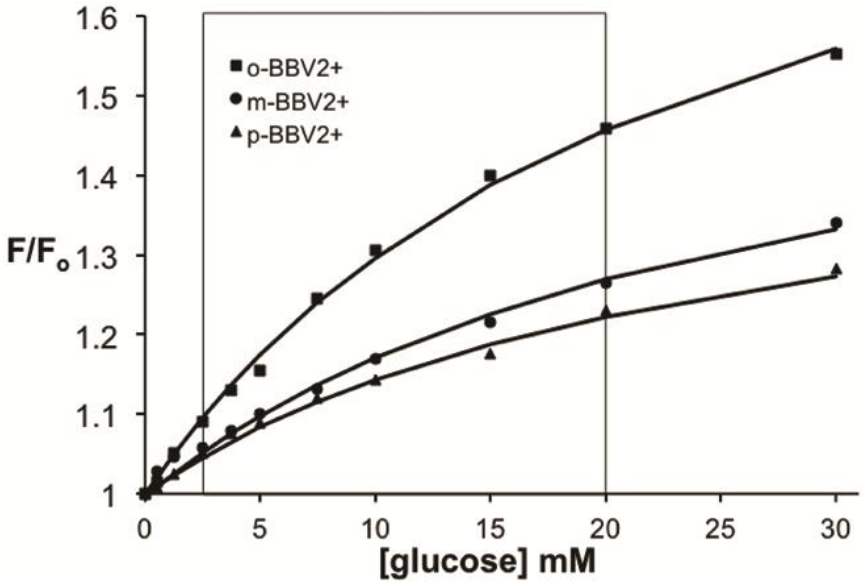

Figure 1.17. Glucose response of *o*-, *m*-, and *p*-BBV^{2+} in combination with HPTS (4 x 10^{-6} M) at the same quencher:dye of ratio of 30:1 in pH 7.4 aqueous solution. Human physiological glucose range is boxed. λ_{ex} = 460 nm, λ_{em} = 510 nm. F_o = quenched fluorescence; F= fluorescence after addition of glucose.

In our study of viologens and related quenchers we also looked at the effect of solution pH. We studied the behavior of the quenchers at pH 3, 7.4, and 10 in combination with HPTS. At pH 3, addition of each of the viologen quenchers caused significant changes in the UV spectra of HPTS that were consistent with the ground state complex formation between dye and quencher. At pH 10, however, only the non-functionalized benzyl viologens BV^{+2} appeared to form a complex with HPTS. This is consistent with a model of charge induced sensing as depicted in Scheme 1.17. That is, at pH 3 all the BBV quenchers are expected to have a net charge of 2+ and thus maintain an electrostatic attraction for the anionic dye. When the pH is raised to

10, however, the boronic acids convert to their anionic "ate" configuration. Thus at pH 10, boronic acid substituted quenchers such as the bipyridinium 4,4'-*o*-BBV^{+2} would exist in their neutral, zwitterionic form. In this state they do not appear to possess a strong enough attraction for anionic HPTS to form a ground state complex, as evidenced by the unchanged absorbance spectra during titration.[43]

Several important observations emerged from these initial quenching and sugar response experiments. First, in comparing structurally and electronically similar viologen-receptors, we realized that the best quencher in a series is not necessarily expected to have the best response to changes in saccharide concentration. In this study of *ortho*-, *meta*-, and *para*-substituted compounds there was actually an inverse correlation between quenching efficacy and glucose sensing ability. Secondly, because the quenching and sugar sensing interactions are interdependent by virtue of their dependence on quencher concentration, the ratio of quencher-to-dye is a critical parameter. Consequently, the optimization of the ratio between quencher and dye was among several areas of active research in the early studies in our labs.[45, 46] Monosaccharide binding studies were carried out using fructose and galactose as well, but they all demonstrated essentially the same fructose >> galactose > glucose selectivity as that observed for simple phenylboronic acid. These early results suggested that achieving glucose selectivity in our system might be overly difficult given the limitations of the 4,4'-bipyridinium structure at the core of our receptor. Additional experimentation with mixed boronic acid substitution patterns based on

the 4,4'-bipyridinium failed to provide any significant deviations from the aforementioned selectivity. However, systematic exploration of new receptor structures resulted in the identification of quenchers based on 4,7-phenanthroline that showed greater selectiviey. This led to the development of a viologen quencher based on 3,3'-bipyridine that showed both good signal response and a remarkable and rarely observed selectivity for glucose over fructose and a number of other carbohydrates.[50]

1.6.3. Variations of Boronic Acid-Modified Viologens

After some time, a modest library of over twenty structurally unique, boronic acid-modified viologens was prepared. These included variously substituted viologens based on the 3,3'-, 3,4'-, and 4,4'-bipyridinium cores and a series of interesting bis-viologens in which two bipyridinium units were combined in a single compound.[67-69] While the positioning of boronic acids clearly has a major effect on the sugar sensing and quenching ability, we were also curious about the effects of viologen charge on the sensing properties of the system. The major structural elements of the viologens are the bipyridyl core and the benzyl boronic acid group. Established reaction schemes and readily available starting materials were used to access the viologen structures. Structural variables include the position of nitrogens in bipyridyl rings and position of boronic acid moieties on the benzyl ring (Figure 1.18).

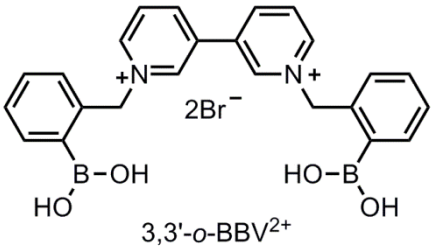

Figure 1.18. Structure of the glucose-selective sensor component 3,3'-*o*-BBV^{2+}.

In addition to the commercially available 4,4'-bipyridine, gram quantities of 3,4'- and 3,3'-bipyridines have also made by cross-coupling reactions.[68] Bromomethyl phenylboronic acid or benzyl bromide was reacted in dimethylformamide with the corresponding bipyridines to obtain the desired viologens. Isolation of the products was achieved by precipitation from acetone (Figure 1.19).

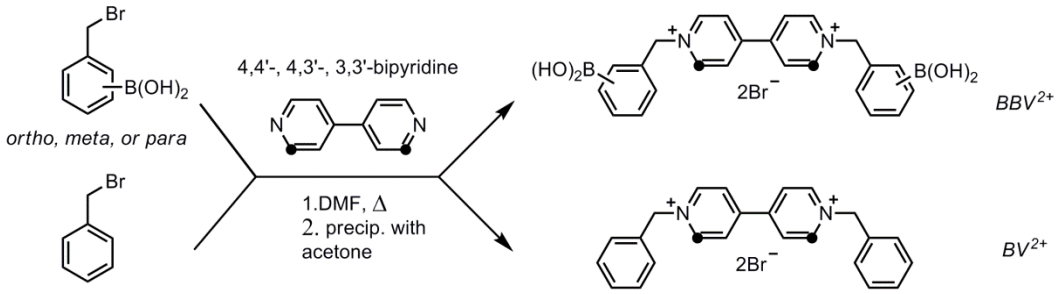

Figure 1.19. Synthesis of BBVs and BVs as controls (dots indicate variable positions of the nitrogen in bipyridyl rings)

The quenching characteristics for each of the receptors with HPTS were established by titration of the fluorescent dye with the corresponding viologens. The calculated Stern−Volmer constants,[70] K_s and *V*, indicating the degree of static and dynamic quenching, respectively, are summarized in Table 1. The quenching efficiencies of

the boronic acid appended bipyridinium salts were found to be of the order: 4,4‘-BBVs > 3,4‘-BBVs > 3,3‘-BBVs. A similar trend was shown with the benzyl bipyridinium salts. Variation of the position of nitrogen bipyridyl rings from 4,4’ to 3,3’ was accompanied with a loss in quenching ability.

Table 1.1. Quenching constants for BBVs and BV compounds.

Quencher	K_s (10^3 M^{-1})	V (10^3 M^{-1})
4,4‘-*o*-BBV	8.9 ± 0.2	2.9 ± 0.1
4,4‘-*m*-BBV	8.1 ± 0.1	3.0 ± 0.1
4,4‘-BV	15.0 ± 1.0	2.3 ± 0.2
3,4‘-*o*-BBV	6.6 ± 0.2	1.7 ± 0.1
3,4‘-*m*-BBV	7.5 ± 0.2	1.7 ± 0.1
3,4‘-BV	9.5 ± 0.5	2.8 ± 0.3
3,3‘-*o*-BBV	4.3 ± 0.2	0.14 ± 0.03
3,3‘-*m*-BBV	5.0 ± 0.1	0.70 ± 0.05
3,3‘-BV	7.4 ± 0.3	2.2 ± 0.2

Table 1.1. Static (K_s) and dynamic (V) quenching constants for BBVs with HPTS (4×10^{-6} M in pH 7.4 phosphate buffer)

Another family of boronic acid-appended viologen quenchers was synthesized containing two viologen subunits in a single quencher moiety. Relative to the single viologen-based quenchers, the bis-viologen ortho-boronic acid (BOB) compounds, in

combination with the fluorescent dye, HPTS, display greatly enhanced Stern–Volmer quenching constants and much greater signal modulation in response to glucose.[69] Superior performance is realized at lower quencher-to-dye ratios than are required for the single-viologen systems. The improved performance was attributed both to the increased positive charge on the BOBs and greater electron affinity. Polymeric viologens comprising two or more 4,4'-dipyridinium units are widely reported in the literature.[44, 59, 71, 72] They characteristically exhibit more positive reduction potentials than the mono-viologens.

In addition to working with bipyridinium viologen quenchers, the extended conjugated viologen 4,7-phenanthrolinium (4,7-$PBBV^{2+}$) attracted our interest because of its electron accepting ability. The enhanced ability of the 4, 7-phenanthrolinium quenchers to accept electrons prompted us to study their quenching ability and compare them to bipyridyl quenchers. Since they are better electron acceptors, we anticipated greater quenching. Identical behavior had been observed with *o*-BBV^{2+}, but the difference in quenching efficiency between *o*-$PBBV^{2+}$ with and without glucose present was considerably larger than in the case of *o*-BBV^{2+}. Similarly to the BOB quenchers, the $PBBV^{2+}$ required a lower quencher-to-dye ratio to obtain a significant signal in response to changes in glucose concentration across the physiological range.[43]

1.6.4. Effects of Quencher Charge

As the proposed mechanism suggests, the quenching process appears heavily dependent on the degree of electrostatic attraction between the cationic viologen quencher and anionic fluorescent dye. All of our earlier studies had demonstrated the importance of charge interactions in our sensing system and suggested that the number of charges on the viologen quencher/receptor play a major role in determining quenching and sugar sensing behavior. So, a series of experiments was conducted to carefully examine the effects of viologen charge on the sensing system.[73] Initial work was done to prepare a set of variously charged, but structurally similar boronic acid-modified viologen quenchers (Figure 1.20).

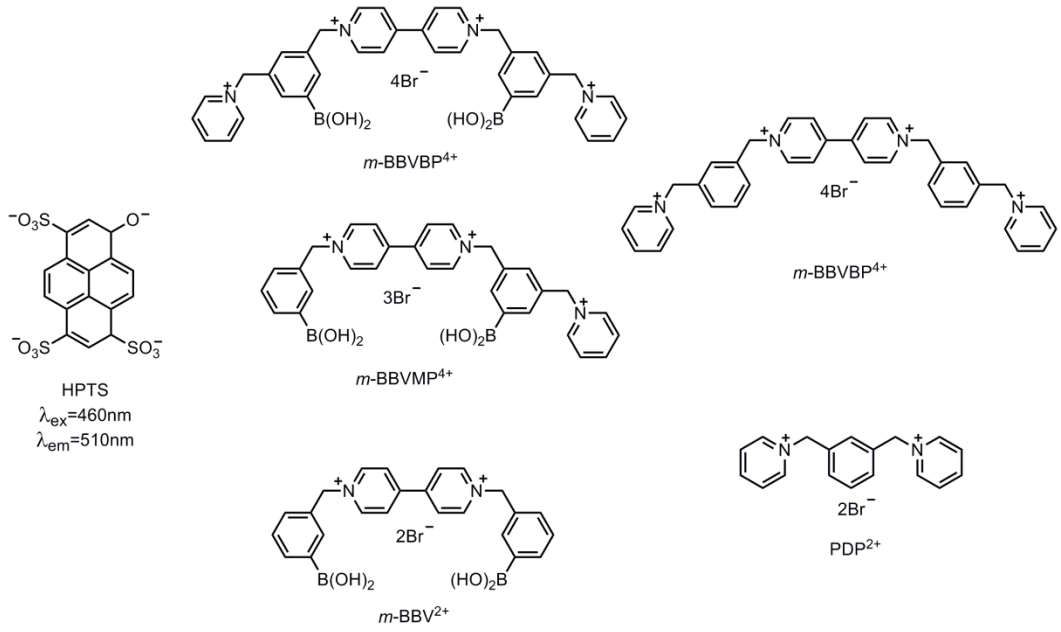

Figure 1.20. Structures of HPTS and some of the viologen quenchers used in the study.

In the first of these studies, the boronic acid-substituted viologens were used to quench the fluorescence of HPTS. Results are shown in Figure 1.21.

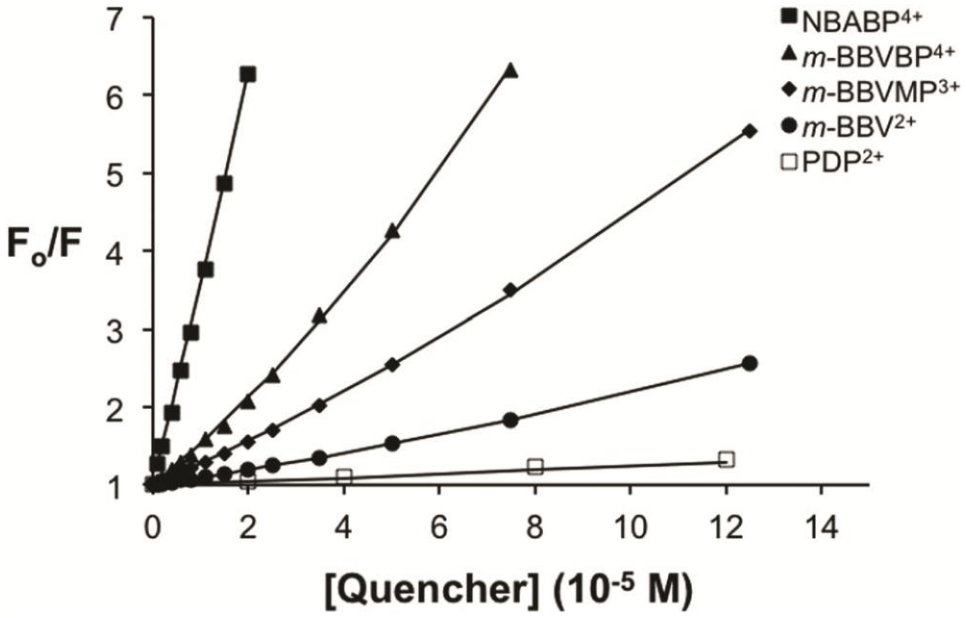

Figure 1.21. Stern-Volmer plot of fluorescence quenching of HPTS (4 x 10^{-6} M) by quenchers at pH 7.4 with charges indicated. Studies conducted at 20 ^{o}C, λ_{ex} = 460 nm, λ_{em} = 510 nm; F_o = original fluorescence; F= fluorescence after addition of quencher.

It appears that more positively charged viologens have either greater electron affinity or a stronger electrostatic attraction through which they can bind HPTS in a non-fluorescent quencher/dye complex, or both. That our system operates via static and not dynamic quenching was confirmed with temperature experiments and through absorbance studies, the latter of which provided binding constants in good agreement with those obtained from the fluorescence quenching studies. A considerable benefit of the two-component system is the ability to vary the ratio of quencher-to-dye in

order to optimize both the magnitude of the sensor response and its sensitivity in the concentration range of interest. When the ratio between quencher and dye is steadily increased for each in a series of glucose titrations, a pattern emerges in which the point at which the system saturates steadily shifts to higher glucose concentrations. This makes the binding isotherm more linear in the low concentration range and is illustrated in Figure 1.22.

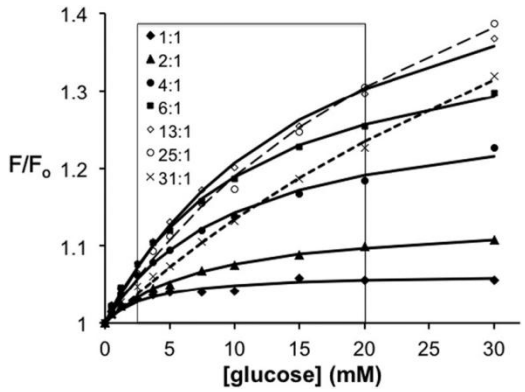

Figure 1.22. Binding isotherms for different quencher:dye ratios from fluorescence data for addition of glucose to a sample of HPTS (4 x 10^{-6} M) quenched by *m*-$BBVBP^{4+}$ at pH 7.4. Physiological glucose range is boxed.

As is evident in Figure 1.22, the low quencher-to-dye ratios such as 1:1 and 2:1 give weak signals and relatively saturated responses in the physiological range of glucose concentration (2.5 mM to 20 mM). Higher quencher-to-dye ratios, however, provide an isotherm that is increasingly linear in the physiological range of interest. At 25:1 and 31:1, the signal response in the physiological range drops from a maximum reached at 13:1, but the linearity is improved across the same region. All of the quenchers studied displayed similar behavior with respect to quencher-to-dye

ratios.

For glucose sensor applications, a dynamic, but linear response across the physiological glucose range is highly desirable so that a fluorescence change can be easily correlated with changes in glucose concentration. The ability to tune the signal response for a particular concentration range circumvents a common problem of many fluorescence-based systems in which there may be excellent sensitivity at low concentrations, but the signal response is too rapidly saturated before physiological glucose concentrations are even reached. For this reason, we adjusted quencher-to-dye ratios for each of the quencher-dye combinations in order to obtain a linear response across the physiological range. We found that *m*-BBVBP^{4+} gave optimal results with HPTS at a quencher-to-dye ratio of 31:1, while *m*-BBVMP^{3+} and *m*-BBV^{2+} worked best at a ratio of 125:1. The apparent glucose binding constants for *m*-BBV^{2+}, *m*-BBVMP^{3+}, *m*-BBVBP^{4+} determined from the fluorescence data at the optimized ratios were, respectively, 11±3, 12±2, and 27±6 M^{-1}. The optimized apparent glucose binding isotherms for these viologens are shown in Figure 1.23.

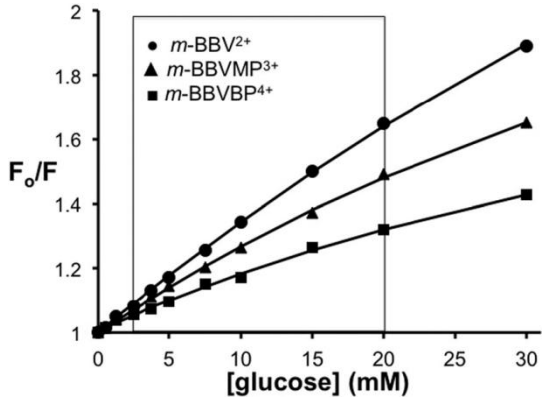

Figure 1.23. Glucose response of viologens with HPTS (4 x 10^{-6} M) at pH 7.4. Optimized quencher-to-dye ratios for *m*-BBV^{2+}, *m*-$BBVMP^{3+}$, and *m*-$BBVBP^{4+}$ with HPTS were, respectively, 31:1; 125:1; and 125:1.

A number of additional studies were carried out under exploring a wide variety of quenchers based on variously substituted bipyridinium[67-69] and phenanthrolinium[43] species. Together, with the work described above, these studies demonstrate the considerable versatility possible with respect to the receptor component in this system.

1.7. Conclusion

Inspired to pursue a new area of research with the well-developed two component system, the proceeding chapters described herein utilized this system to ultimately develop a high-throughput assay for measuring gastrointestinal permeability. Through this work, exploration of boronic acid binding was pursued by analyzing binding characteristics and patterns of binding from various sugar alcohols and sugar acids (chapters 2), a novel method for measuring sucralose (chapter 3), a chemical modification approach to improve boronic acid binding for low-binding aldoses (chapter 3), and lastly, an array based system was developed for discriminating between low and increased small intestinal permeability (chapter 4).

1.8. References

1. Kobata, A., Glycobiology - An expanding research area in carbohydrate-chemistry. *Acc. Chem. Res.* **1993,** *26*, 319-324.

2. Bidon, N.; Brichory, F.; Bourguet, P.; Le Pennec, J.-P.; Dazord, L., Galectin-8: a complex sub-family of galectins. *Int. J. Mol. Med.* **2001,** *8*, 245-250.

3. Fukuda, M., Carbohydrate-dependent cell adhesion. *Biorg. Med. Chem.* **1995,** *3*, 207-215.

4. Poirier, F.; Kimber, S., Cell surface carbohydrates and lectins in early development. *Mol. Hum. Reprod.* **1997,** *3*, 907-918.

5. vandenBerghe, G., Disorders of gluconeogenesis. *J. Inh. Metabol. Dis.* **1996,** *19*, 470-477.

6. Fuchs, M.; Hoekstra, J. B. L.; Mudde, A. H., Glucose and cardiovascular risk. *Nether. J. Med.* **2002,** *60*, 192-199.

7. Renard, E., Monitoring glycemic control: the importance of self-monitoring of blood glucose. *Am. J. of Med.* **2005,** *118*, 12S-19S.

8. Yoo, E. H.; Lee, S. Y., Glucose Biosensors: An Overview of Use in Clinical Practice. *Sensors* **2010,** *10*, 4558-4576.

9. McShane, M. J., Potential for glucose monitoring with nanoengineered fluorescent biosensors. *Diabetes Technol. Ther.* **2002,** *4*, 533-538.

10. Lakowicz, J. R., *Principles of Fluorescence Spectroscopy*. 3rd ed.; Springer: New York, 2006; 954.

11. Frank, J. M.; Vavilov, S. I., Effective spheres in the extinction process in fluorescent liquids. *Z. Phys.* **1931,** *69*, 100-10.

12. Wang, D.; Wang, J.; Moses, D.; Bazan, G. C.; Heeger, A. J., Photoluminescence Quenching of Conjugated Macromolecules by Bipyridinium Derivatives in Aqueous Media: Charge Depen dence. *Langmuir* **2001,** *17*, 1262-1266.

13. Kuivila, H. G.; Keough, A. H.; Soboczenski, E. J., Areneboronates from diols and polyols. *J. Org. Chem.* **1954,** *19*, 780-783.

14. Lorand, J. P.; Edwards, J. O., Polyol complexes and structure of the bezeneboronate ion. *J. Org. Chem.* **1959,** *24*, 769-774.

15. Yan, J.; Fang, H.; Wang, B. H., Boronolectins and fluorescent boronolectins: An examination of the detailed chemistry issues important for the design. *Med. Res. Rev.* **2005,** *25*, 490-520.

16. Springsteen, G.; Wang, B., A detailed examination of boronic acid-diol complexation. *Tetrahedron* **2002,** *58*, 5291-5300.

17. Yan, J.; Springsteen, G.; Deeter, S.; Wang, B. H., The relationship among pK(a),pH, and binding constants in the interactions between boronic acids and diols - it is not as simple as it appears. *Tetrahedron* **2004,** *60*, 11205-11209.

18. Russell, A. P. Photometric method and means involving dyes for detecting vicinal polyhydroxyl compounds. WO9104488A1, **1991**.

19. Yoon, J.; Czarnik, A. W., Fluorescent Chemosensors of Carbohydrates - a Means of Chemically Communicating the Binding of Polyols in Water Based on Chelation-Enhanced Quenching. *J Am. Chem. Soc.* **1992,** *114*, 5874-5875.

20. Nagai, Y.; Kobayashi, K.; Toi, H.; Aoyama, Y., Stabilization of sugar-boronic esters of indolylboronic acid in water via sugar indole interaction-a notable selectivity in oligosaccharides. *Bull. Chem. Soc. Japan* **1993,** *66*, 2965-2971.

21. Suenaga, H.; Mikami, M.; Sandanayake, K.; Shinkai, S., Screening of fluorescent boronic acids for sugar sensing which show a large fluorescence change. *Tetrahedron Lett.* **1995,** *36*, 4825-4828.

22. DiCesare, N.; Lakowicz, J. R., Spectral properties of fluorophores combining the boronic acid group with electron donor or withdrawing groups. Implication in the development of fluorescence probes for saccharides. *J. Phys. Chem. A* **2001,** *105*, 6834-6840.

23. Di Cesare, N.; Lakowicz, J. R., Wavelength-ratiometric probes for saccharides based on donor-acceptor diphenylpolyenes. *J. Photochem. and Photobiol. a-Chem.* **2001,** *143*, 39-47.

24. Yang, W.; Yan, J.; Springsteen, G.; Deeter, S.; Wang, B., A novel type of fluorescent boronic acid that shows large fluorescence intensity changes upon binding

with a carbohydrate in aqueous solution at physiological pH. *Bioorg. Med. Chem. Lett.* **2003,** *13*, 1019-1022.

25. Yang, W.; Lin, L.; Wang, B., A new type of boronic acid fluorescent reporter compound for sugar recognition. *Tetrahedron Lett.* **2005,** *46*, 7981-7984.

26. James, T. D.; Sandanayake, K. R. A. S.; Shinkai, S., A glucose-specific molecular fluorescence sensor. *Angew. Chem.* **1994,** *106*, 2287-9.

27. James, T. D.; Sandanayake, K.; Iguchi, R.; Shinkai, S., Novel Saccharide-Photoinduced Electron-Transfer Sensors Based on the Interaction of Boronic Acid and Amine. *J. Am. Chem. Soc.* **1995,** *117*, 8982-8987.

28. Burgemeister, T.; Grobe-Einsler, R.; Grotstollen, R.; Mannschreck, A.; Wulff, G., Fast Thermal Breaking and Formation of a B–N Bond in 2-(Aminomethyl)benzeneboronates1). *Chemis. Berich.* **1981,** *114*, 3403-3411.

29. Wulff, G., Selective Binding to Polymers Via Covalent Bonds- The Construction of Chiral Cavities as Specific Receptor-Sites.. *Pure Appl. Chem.* **1982,** *54*, 2093-2102.

30. James, T. D.; Sandanayake, K.; Shinkai, S., Saccharide sensing with molecular receptors based on boronic acid. *Angew. Chem.-Intl. Ed. Engl.* **1996,** *35*, 1911-1922.

31. Liang, X.; James, T. D.; Zhao, J., 6,6 '-Bis-substituted BINOL boronic acids as enantio selective and chemoselective fluorescent chemosensors for D-sorbitol. *Tetrahedron* **2008,** *64*, 1309-1315.

32. Van den Berghe, G.; Wilmer, A.; Hermans, G.; Meersseman, W.; Wouters, P. J.; Milants, I.; Van Wijngaerden, E.; Bobbaers, H.; Bouillon, R., Intensive insulin therapy in the medical ICU. *New Eng. J. Med.* **2006,** *354*, 449-461.

33. Van den Berghe, G.; Wouters, P.; Weekers, F.; Verwaest, C.; Bruyninckx, F.; Schetz, M.; Vlasselaers, D.; Ferdinande, P.; Lauwers, P.; Bouillon, R., Intensive insulin therapy in critically ill patients. *New Eng. J. Med.* **2001,** *345*, 1359-1367.

34. Shiomi, Y.; Saisho, M.; Tsukagoshi, K.; Shinkai, S., Specific complexation of glucose with a diphenylmethane-3,3'-diboronic acid derivative: correlation between the absolute configuration of mono- and disaccharides and the circular dichroic-activity of the complex. *J. Chem. Soc., Perkin Trans. 1* **1993,** 2111-17.

35. Norrild, J. C.; Eggert, H., Evidence for Mono- and Bisdentate Boronate Complexes of Glucose in the Furanose Form. Application of 1JC-C Coupling Constants as a Structural Probe. *J. Am. Chem. Soc.* **1995,** *117*, 1479-84.

36. Yang, W.; He, H.; Drueckhammer, D. G., Computer-guided design in molecular recognition: design and synthesis of a glucopyranose receptor. *Angew. Chem., Int. Ed.* **2001,** *40*, 1714-1718.

37. Wiskur, S. L.; Ait-Haddou, H.; Lavigne, J. J.; Anslyn, E. V., Teaching old indicators new tricks. *Acc. Chem. Res.* **2001,** *34*, 963-972.

38. Anslyn, E. V., Supramolecular Analytical Chemistry. *J. Org. Chem.* **2007,** *72*, 687-699.

39. Nguyen, B. T.; Anslyn, E. V., Indicator-displacement assays. *Coord. Chem. Rev.* **2006,** *250*, 3118-3127.

40. Shabbir, S. H.; Regan, C. J.; Anslyn, E. V., A general protocol for creating high-throughput screening assays for reaction yield and enantiomeric excess applied to hydrobenzoin. *Proc.Nalt. Acad. Sci.U.S.A.* **2009,** *106*, 10487-10492.

41. Camara, J. N.; Suri, J. T.; Cappuccio, F. E.; Wessling, R. A.; Singaram, B., Boronic acid substituted viologen based optical sugar sensors: modulated quenching with viologen as a method for monosaccharide detection. *Tetrahedron Lett.* **2002,** *43*, 1139-1141.

42. Suri, J. T.; Cordes, D. B.; Cappuccio, F. E.; Wessling, R. A.; Singaram, B., Continuous glucose sensing with a fluorescent thin-film hydrogel. *Angew. Chem., Int. Ed.* **2003,** *42*, 5857-5859.

43. Suri, J. T.; Cordes, D. B.; Cappuccio, F. E.; Wessling, R. A.; Singaram, B., Monosaccharide detection with 4,7-phenanthrolinium salts: Charge-induced fluorescence sensing. *Langmuir* **2003,** *19*, 5145-5152.

44. Cappuccio, F. E.; Suri, J. T.; Cordes, D. B.; Wessling, R. A.; Singaram, B., Evaluation of Pyranine Derivatives in Boronic Acid Based Saccharide Sensing: Significance of Charge Interaction Between Dye and Quencher in Solution and Hydrogel. *J. Fluoresc.* **2004,** *14*, 521-533.

45. Cordes, D. B.; Gamsey, S.; Sharrett, Z.; Miller, A.; Thoniyot, P.; Wessling, R. A.; Singaram, B., The interaction of boronic acid-substituted viologens with pyranine: The effects of quencher charge on fluorescence quenching and glucose response. *Langmuir* **2005,** *21*, 6540-6547.

46. Cordes, D. B.; Miller, A.; Gamsey, S.; Sharrett, Z.; Thoniyot, P.; Wessling, R.; Singaram, B., Optical glucose detection across the visible spectrum using anionic fluorescent dyes and a viologen quencher in a two-component saccharide sensing system. *Org. Biomol.Chem.* **2005,** *3*,1708-1713.

47. Gamsey, S.; Baxter, N. A.; Sharrett, Z.; Cordes, D. B.; Olmstead, M. M.; Wessling, R. A.; Singaram, B., The effect of boronic acid-positioning in an optical glucose-sensing ensemble. *Tetrahedron* **2006,** *62*, 6321-6331.

48. Gamsey, S.; Suri, J. T.; Wessling, R. A.; Singaram, B., Continuous Glucose Detection Using Boronic Acid-Substituted Viologens in Fluorescent Hydrogels: Linker Effects and Extension to Fiber Optics. *Langmuir* **2006,** *22*, 9067-9074.

49. Thoniyot, P.; Cappuccio, F. E.; Gamsey, S.; Cordes, D. B.; Wessling, R. A.; Singaram, B., Continuous glucose sensing with fluorescent thin-film hydrogels. 2.

Fiber optic sensor fabrication and in vitro testing. *Diabetes Technol. Ther.* **2006,** *8*, 279-287.

50. Gamsey, S.; Miller, A.; Olmstead, M. M.; Beavers, C. M.; Hirayama, L. C.; Pradhan, S.; Wessling, R. A.; Singaram, B., Boronic acid-based bipyridinium salts as tunable receptors for monosaccharides and alpha-hydroxycarboxylates. *J. Am. Chem. Soc.* **2007,** *129*, 1278-1286.

51. Sharrett, Z.; Gamsey, S.; Fat, J.; Cunningham-Bryant, D.; Wessling, R. A.; Singaram, B., The effect of boronic acid acidity on performance of viologen-based boronic acids in a two-component optical glucose-sensing system. *Tetrahedron Lett.* **2007,** *48*, 5125-5129.

52. Sharrett, Z.; Gamsey, S.; Levine, P.; Cunningham-Bryant, D.; Vilozny, B.; Schiller, A.; Wessling, R. A.; Singaram, B., Boronic acid-appended bis-viologens as a new family of viologen quenchers for glucose sensing. *Tetrahedron Lett.* **2008,** *49*, 300-304.

53. Vilozny, B.; Schiller, A.; Wessling, R. A.; Singaram, B., Enzyme assays with boronic acid appended bipyridinium salts. *Anal. Chim. Acta* **2009,** *649*, 246-251.

54. Dickert, F. L., The Viologens. Physicochemical properties, synthesis and applications of the salts of 4,4'-bipyridine. by P. M. S. Monk. *Angew. Chem., Int. Ed.* **1999,** *38*, 2456-2457.

55. Summers, L. A. In *Chemical constitution and activity of bipyridinium herbicides*, Pergamon: 1979; 244-7.

56. Summers, L. A., The Bipyridines. In *Advances in Heterocyclic Chemistry*, Alan, R. K., Ed. Academic Press: 1984; Vol. Volume 35, 281-374.

57. Bard, A. J.; Ledwith, A.; Shine, H. J., Formation, properties and reactions of cation radicals in solution. *Adv. Phys. Org. Chem.* **1976,** *13*, 155-278.

58. Bird, C. L.; Kuhn, A. T., Electrochemistry of the Viologens. *Chem.Soc. Rev.* **1981,** *10*, 49-82.

59. De Borba, E. B.; Amaral, C. L. C.; Politi, M. J.; Villalobos, R.; Baptista, M. S., Photophysical and Photochemical Properties of Pyranine/Methyl Viologen Complexes in Solution and in Supramolecular Aggregates: A Switchable Complex. *Langmuir* **2000,** *16*, 5900-5907.

60. Nakashima, K.; Kido, N., Fluorescence quenching of 1-pyrenemethanol by methylviologen in polystyrene latex dispersions. *J. Photochem. Photobiol.* **1996,** *64*, 296-302.

61. Zhao, Z.; Shen, T.; Xu, H., Photoinduced interaction between eosine and viologen. *J. Photochem. Photobiol., A* **1990,** *52*, 47-53.

62. Gaylord, B. S.; Wang, S. J.; Heeger, A. J.; Bazan, G. C., Water-soluble conjugated oligomers: Effect of chain length and aggregation on photoluminescence-quenching efficiencies. *J. Am. Chem. Soc.***2001**, *123*, 6417-6418.

2001, *123*, 6417-6418.

63. Wang, D. L.; Gong, X.; Heeger, P. S.; Rininsland, F.; Bazan, G. C.; Heeger, A. J., Biosensors from conjugated polyelectrolyte complexes. *Proc.Nalt. Acad. Sci.U.S.A.* **2002,** *99*, 49-53.

64. DiCesare, N.; Pinto, M. R.; Schanze, K. S.; Lakowicz, J. R., Saccharide detection based on the amplified fluorescence quenching of a water-soluble poly(phenylene ethynylene) by a boronic acid functionalized benzyl viologen derivative. *Langmuir* **2002,** *18*, 7785-7787.

65. Chen, L. H.; McBranch, D. W.; Wang, H. L.; Helgeson, R.; Wudl, F.; Whitten, D. G., Highly sensitive biological and chemical sensors based on reversible fluorescence quenching in a conjugated polymer. *Proc.Nalt. Acad. Sci.U.S.A.***1999,** *96*, 12287-12292.

66. McPhie, P., Principles of Fluorescence Spectroscopy, Second ed. Joseph R. Lakowicz. *Anal. Biochem.* **2000,** *287*, 353-354.

67. Gamsey, S.; Baxter, N. A.; Sharrett, Z.; Cordes, D. B.; Olmstead, M. M.; Wessling, R. A.; Singaram, B., The effect of boronic acid-positioning in an optical glucose-sensing ensemble. *Tetrahedron* **2006,** *62*, 6321-6331.

68. Gamsey, S.; Miller, A.; Olmstead, M. M.; Beavers, C. M.; Hirayama, L. C.; Pradhan, S.; Wessling, R. A.; Singaram, B., Boronic acid-based bipyridinium salts as

tunable receptors for monosaccharides and alpha-hydroxycarboxylates. *J. Am. Chem. Soc.* **2007,** *129*, 1278-1286.

69. Sharrett, Z.; Gamsey, S.; Levine, P.; Cunningham-Bryant, D.; Vilozny, B.; Schiller, A.; Wessling, R. A.; Singaram, B., Boronic acid-appended bis-viologens as a new family of viologen quenchers for glucose sensing. *Tetrahedron Lett.* **2008,** *49*, 300-304.

70. Buryak, A.; Severin, K., A chemosensor array for the colorimetric identification of 20 natural amino acids. *J. Am. Chem. Soc.***2005,** *127*, 3700-3701.

71. Mohr, G. J.; Werner, T.; Wolfbeis, O. S., Application of a novel lipophilized fluorescent dye in an optical nitrate sensor. *J. Fluoresc.* **1995,** *5*, 135-8.

72. Hui, H. K.; Soonkap, H.; Bankert, C. S. Optical-fiber pH microsensor and method of manufacture. EP481740A2, 1992.

73. Cordes, D. B.; Gamsey, S.; Sharrett, Z.; Miller, A.; Thoniyot, P.; Wessling, R. A.; Singaram, B., The interaction of boronic acid-substituted viologens with pyranine: The effects of quencher charge on fluorescence quenching and glucose response. *Langmuir* **2005,** *21*, 6540-6547.

CHAPTER 2

Molecular Recognition of Sugar Alcohols and Sugar Acids: Synthesis of Mono- and Bis-Boronic Acid Appended Viologens (BBVs) for the Discrimination of these Sugar Derivatives

2.1. Introduction

Monosaccharides (ex. glucose, galactose fructose etc.) and sugar alcohols (reduced form) are widely distributed in nature, being found in plants, animals, and micro-organisms. Monosaccharides can be classified into triose, tetrose, pentose, hexose, etc. according to the number of carbon atoms in the molecule. For example, xylose ($C_5H_{10}O_5$) is a pentose, glucose ($C_6H_{12}O_6$) is a hexose, and rhamnose ($C_6H_{12}O_5$) is a deoxyhexose. These monosaccharides are monomeric repeat units of polysaccharides or glycoconjugates (i.e. glycoproteins or glycolipids) and are difficult to hydrolyze to simpler compounds. Within monosaccharides, there exist the polyhydroxyl aldehydes (aldoses) or ketones (ketoses) and, as reducing sugars, exist exclusively as cyclic hemiacetals. The hemiacetals that are formed in saccharides stems from the intramolecular reaction between the aldehyde/ketone and the hydroxyl group as shown in Scheme 2.1.

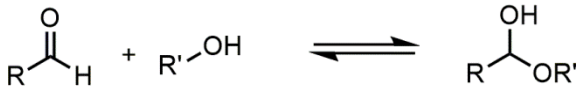

Scheme 2.1. Formation of a hemiacetal I n aldoses from an aldehyde and hydroxyl group.

Due to the hemiacetal formation in aldoses, sugars in solution are present in both five-membered (furanose) and six-membered (pyranose) forms. These furanose and pyranose forms can also exist in two anomeric forms, α and β (anomeric carbon at C-1 in the case of aldoses and C-2 for ketoses). This epimerization arises from the rapid

equilibrium between themselves and the intermediate acyclic form as demonstrated in Scheme 2.2 for D-glucose for which this sugar majority exists in the pyranose form.

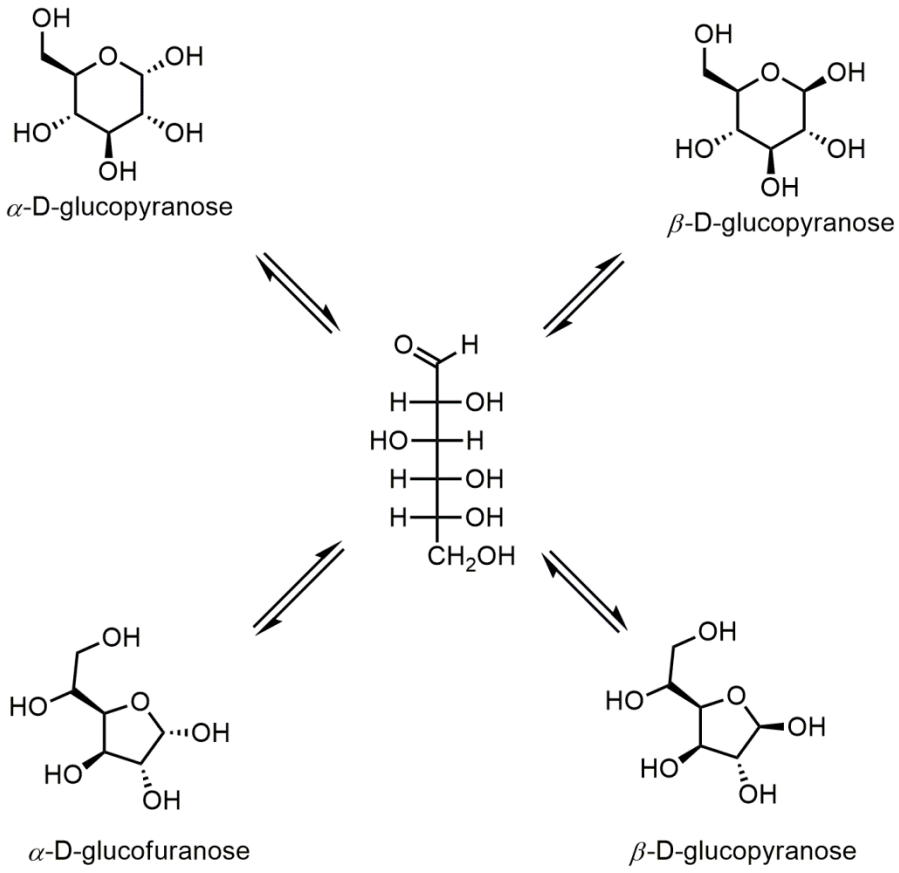

Scheme 2.2. The equilibrium process for D-glucose between the acyclic and possible cyclic forms.

Based on the Haworth projection, the pyranose ring is formed by hemiacetal formation between the hydroxyl group on C-5 and the aldehyde. Similarly, the furanose ring is formed through forming the hemiacetal between the hydroxyl group

on C-4 and the aldehyde. The structures of commonly found monosaccharides and the established names are shown in Scheme 2.3.

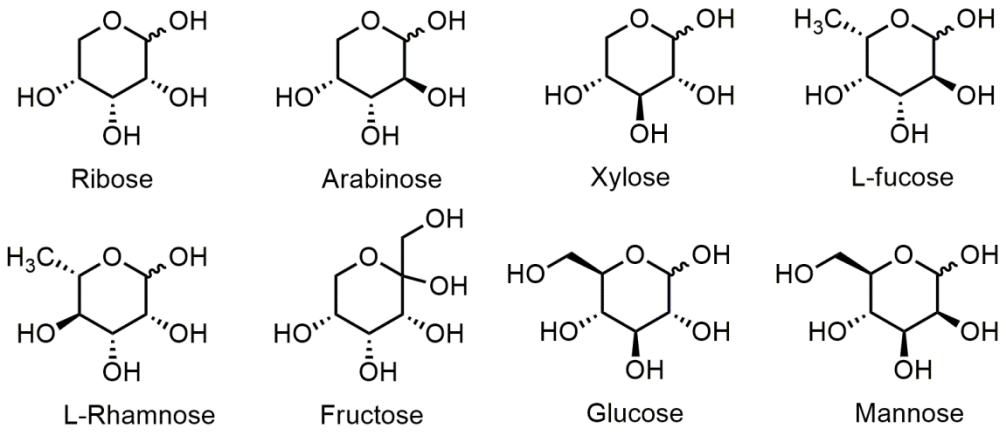

Scheme 2.3. Common monosaccharide structures in the pyranose form.

These monosaccharides are known to include modifications via the introduction of functional groups, such as acetamide (acetylneuraminic acid), carboxylic acid (uronic acid), and phosphate (sugar-phosphate).[1]

2.1.1. Sugar Alcohols

Sugar alcohols are compounds obtained from the reduction of the carbonyl group of a monosaccharide to the corresponding hydroxyl group providing the acyclic polyol structure. The sugar alcohols derived from aldoses are referred to as alditols. More common alditols, such as sorbitol (D-glucitol), mannitol (D-mannitol), ribitol, D-galactitol (dulcitol), are the reduced forms of glucose, mannose, ribose, and

galactose respectively (Scheme 2.4). Few of these sugar alcohols have a plane of symmetry and are optically inactive meso compounds.[2]

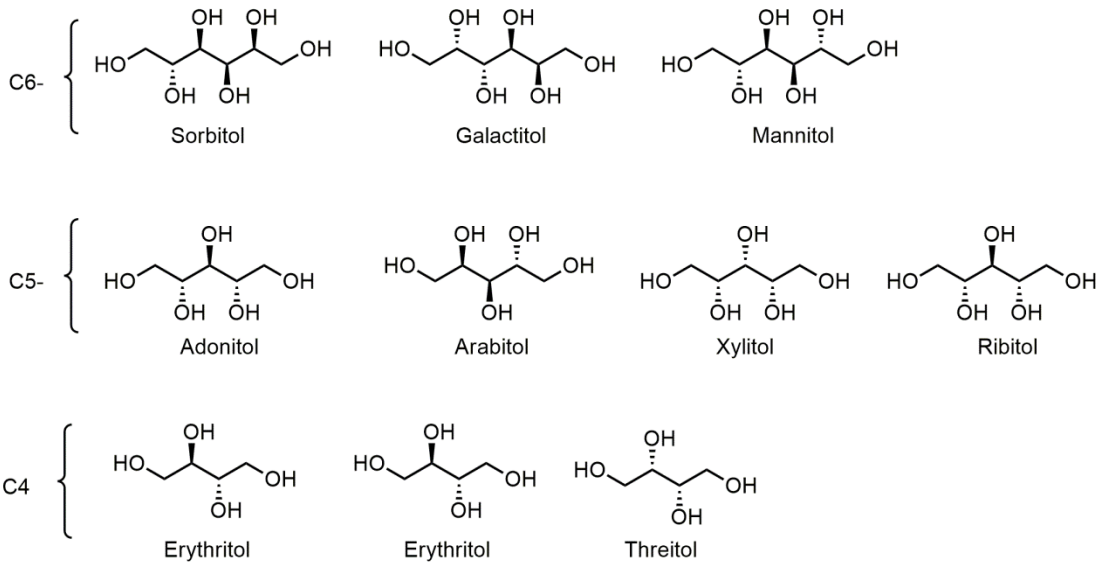

Scheme 2.4. Structures of common alditols separated by their carbon chain length.

Examples of these meso compounds include meso-erythritol, ribitol, galactitol, xylitol, and allitol. These polyols were first discovered in plants and later were found to be useful as alternatives for sucrose and glucose as sweeteners.[3] The distribution of these sugar alcohols are also found in animals, fungi, and microbial sources, but those from plants have been studied in greater details.[4, 5] The sugar alcohols that have been isolated from plants are sorbitol (glucitol), galactitol, and mannitol. In higher plants, it is believed that the main site of sugar alcohol formation is in the leaf where they arise as end products of photosynthesis. From the leaf, some of the products are translocated to the root, stem, fruit, and seed compartments.[5]

2.1.2. Sugar Acids

Uronic and aldonic acids are the derivatives of sugars where the C-1 aldehyde (aldonic acids) or the C-6 primary alcohol (uronic acids) group has been oxidized to the corresponding carboxylic acid group. There are examples where both of these have been oxidized and these types are known to be aldaric acids with the exception of C-4 or C-3 α-hydroxy acids (Scheme 2.5).

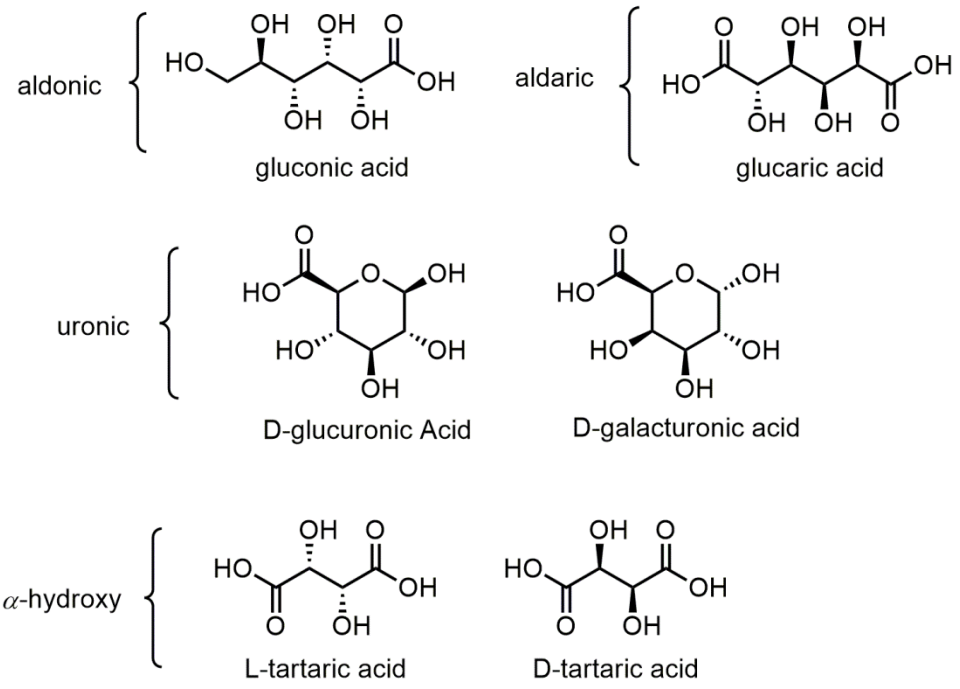

Scheme 2.5. Structures of aldonic, uronic, aldaric, and α-hydroxy acids.

The α-hydroxy acids L- or D- tartaric acid being the popular sugar acids obtained from the wine industry as a byproduct during fermentation. Since tartaric acid is usually an indicator of quality of the wine, there is high interest in developing rapid

sensing methodologies for this α-hydroxy acid.[6, 7] Of the sugar acids listed, glucaric acid (D-glucarate) is a biologically active carbohydrate derivative that is present in human serum, vegetables, and fruits.[8, 9] There have been attempts to use this sugar acid as a chemopreventive agent in certain cancers.[10-12] Additionally, the glucaric acid metabolic pathway in microbial organisms has been studied extensively.[13, 14]

Since sugars alcohols and sugar acids remain as biologically relevant molecules, methods for quick and cost-effective analysis of these compounds has been in the focus of molecular receptor design field. In the standard method, analysis of these sugar alcohols relies heavily on chromatographic methods, such as gas chromatography, high-performance liquid chromatography, and mass spectrometry, which can be costly and labor intensive. There remains an unmet need for developing alternative analytical methods for the quantification and detection of these sugar alcohols and sugar acids in a cost effective and timely manner. To improve on current methods, researchers have used their efforts to design sensor and assay based systems using boronic acid based methodology that rely on fluorescence as an signal output for high sensitivity, quick response time, remote detection abilities, and multiple sensing modes in aqueous or complex media.[15, 16]

2.1.3. Design of Boronic Acid Receptors for the Recognition of Sugar Alcohols and Sugar Acids

Since the seminal work of boronic acid complexation with polyol compounds by Lorand and Edwards, boronic acid recognition for different types of polyol or cis diol containing compounds has vastly evolved into an area of research for the molecular recognition by boronic acids. Lorand and Edward's early work involved studying the complexing equilibria of aqueous benzeneboronate ion with several polyols and compared the association constants to that of borate.[17] Early elucidation of this type of complexation was reported by Lorand and Edwards in 1955 and provided elucidation of the structure of the borate ion in aqueous medium.[18] This was the first quantitative evaluation of saccharide-boronic acid interaction and observed a level of selectivity to the saccharides that were analyzed (Table 2.1).[17]

Table 2.1. Stability constants (log K_a) of polyol complex with phenyl boronic acid

Polyol	Phenyl Boronic Acid (log K_a)
D-fructose	3.64
D-galactose	2.44
D-mannose	2.23
D-glucose	2.04
Ethylene glycol	0.44

D-fructose provided the highest association constant while ethylene glycol gave almost a negligible constant. It can be deduced from this that the adjacent rigid cis diols present in saccharides can from stronger cyclic esters than simple acyclic diols such as ethylene glycol. But, with saccharides there is a level of complexity because of the rapid isomerization between pyranose and furanose. Consequently, the design

and synthesis of selective boronic acid receptors continue to be a challenge and since Lorand and Edwards's quantitative work, there have been only few examples that demonstrate selectivity towards saccharides, sugar alcohols, and sugar acids.

Several fluorescent probes based on boronic acid recognition for sugar alcohols have been developed and demonstrated to be effective. Most notable and popular ones pertain to the one component classification system that utilizes an internal charge transfer mechanism for signal generation. Taking advantage of the various fluorophores that are amenable for boronic acid tethering, an anthracene,[19] napthalene,[20] naphthalimide,[21, 22] indol,[23] and benzo-thiophene[24] have been reported to measure sugar alcohols in aqueous media. Similarly, fluorescent boronic acid based receptors have been developed for various sugar acid derivatives, such as tartaric acid,[6, 25] D-glucuronic acid,[26, 27] and D-glucaric acid[28] have been reported. Additionally, boronic acid based colorimetric based indicator displacement assay for α-hydroxy acid.[29] Unfortunately, there are few examples that utilize chiral receptors for selective recognition of sugar alcohols and sugar acids by fluorescent boronic acid based receptors. In collaboration with Jianzhang Zhao, Tony D. James reported the first enantioselective fluorescent chemosensor for the sugar alcohol mannitol based on boronic acids.[30] This involved developing a chiral receptor to be inherently more selective for the chiral mannitol by introducing a chiral center near the boronic acid binding site (Scheme 2.6). Through initial reductive amination with phenyl ethyl amine (**1**) and 9-anthracenecarboxaldehyde (**2**) followed by alkylation with 2-2-(2-

bromobenzyl)-1,3,2-dioxaborinane (**3**) to provided the R,R- or S,S- bidentate receptor (**4**) .

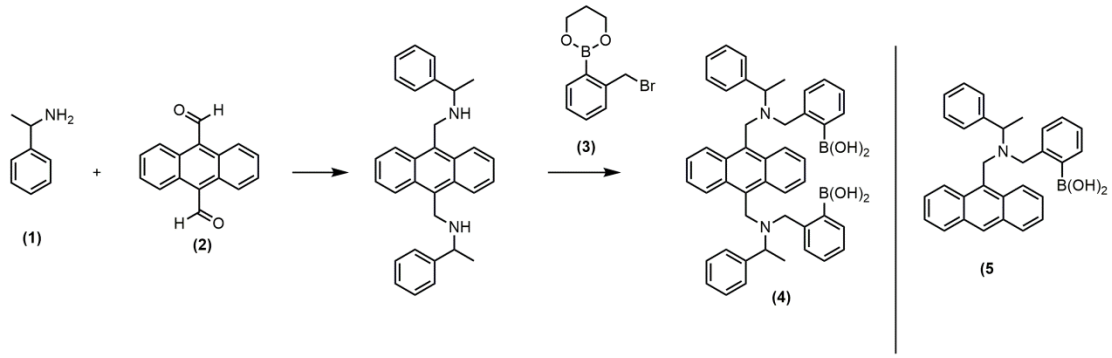

Scheme 2.6. Synthesis of R,R or S,S-bidentate (**4**) and monodentate receptor (**5**).

Initial studies demonstrated that fluorescence enhancement of S,S-receptor and R,R-receptor (**4**) showed similar binding for D-glucose but had significantly different responses for D-mannitol. The S,S-receptor provided a 6-fold difference in relative fluorescence response over the R,R-receptor and gave a 2000-fold increase in binding constant (Figure 2.1).

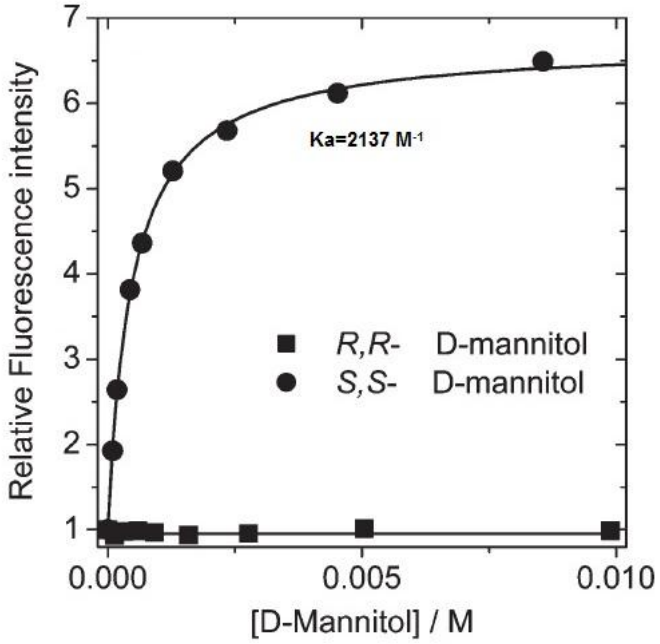

Figure 2.1. Relative fluorescence intensity in the presence of D-mannitol with the R,R- or S,S- bidentate receptor (**4**) in 0.05 M NaCl solution (52 wt % methanol solution), pH 8.3, Fluorescence measurements taken at λ_{ex}= 365nm, λ_{em}= 429nm. Image used with permission.[30]

Compared to the monodentate form of the R,R or S,S (**5**), the binding constants for 6-carbon sugar alcohols (D-mannitol, D-sorbitol, D-galactitol) were slightly lower than the bidentate form (**4**) and provided enantioselective binding. On the contrary, the monodentate receptor (**5**) gave higher binding constants for C-5 sugar alcohols but unable to demonstrate selective recognition for the sugar alcohols compared to the bidentate receptor (Table 2.2).

Table 2.2. Association binding constants (K_a) for each R,R or S,S-bidentate and monodentate receptor with each sugar alcohol.

Sugar alcohol	**R,R (4) (K, M^{-1})**	**S,S (4) (K, M^{-1})**
Mannitol	--	2137
Sorbitol	85	1995
Galactitol	10,965	11,149
Arabitol	334	42
Xylitol	72	79
Adonitol	40	51
	R (5)	**S (5)**
Mannitol	398	295
Sorbitol	4,165	2,290
Galactitol	676	724
Arabitol	426	269
Xylitol	525	513
Adonitol	53	59

It is interesting that the binding constants are higher for the monodentate (**5**) receptor compared to bidentate receptor (**4**) because there is usually favorable binding with bidentate receptors which can form 1:1 cooperative binding. This can be attributed to the rigid linker and the sterically demanding binding pocket of the bidentate receptor (**4**). With this demanding pocket in place, it is possible to prefer a 2:1 complex with certain sugar alcohols, such as the 5-membered carbon (arabitol, xylitol, and adonitol). Usually, when there is a significantly high binding constant for a bidentate receptor compared to the monodentate, this is indicative of a cooperative 1:1 complex formation. Illustration of the possible 1:1 cooperative binding and 2:1 complex is shown in Figure 2.2.

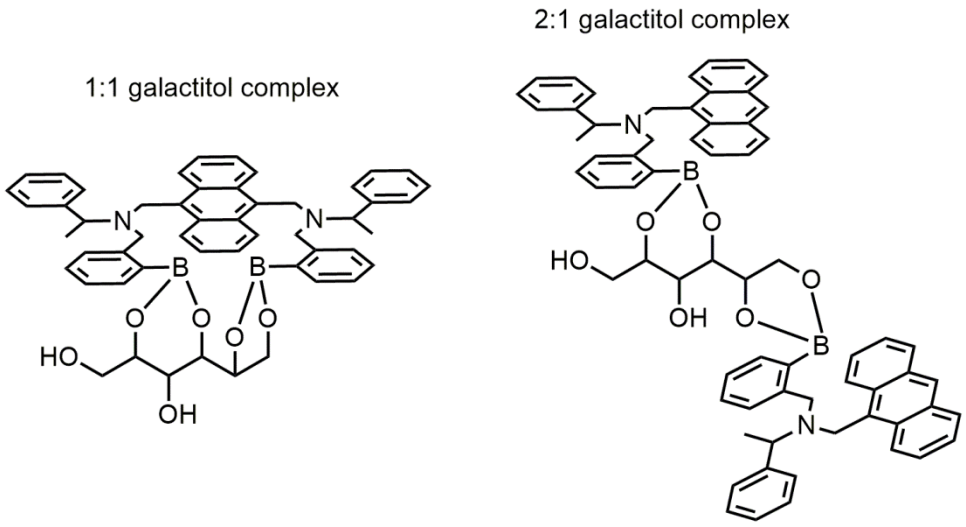

Figure 2.2. Possible cooperative 1:1 binding complex and 2:1 complex with each receptor and galactitol.

The same napthalene based chiral receptor was utilized to study the binding to a series of sugar acids such as, D-glucaric acid, D-gluconic acid, D-glucuronic acid, D-galacturonic acid, and D- or L- tartaric acid.[31] Of the six sugar acids examined, enantioselective recognition by the R,R- and S,S-bidentate boronic acid receptor (**4**) was achieved only for tartaric acid, while no enantioselectivity was observed for the monodentate receptor (**5**) as shown in Figure 2.3 (data not shown for monodentate receptor).

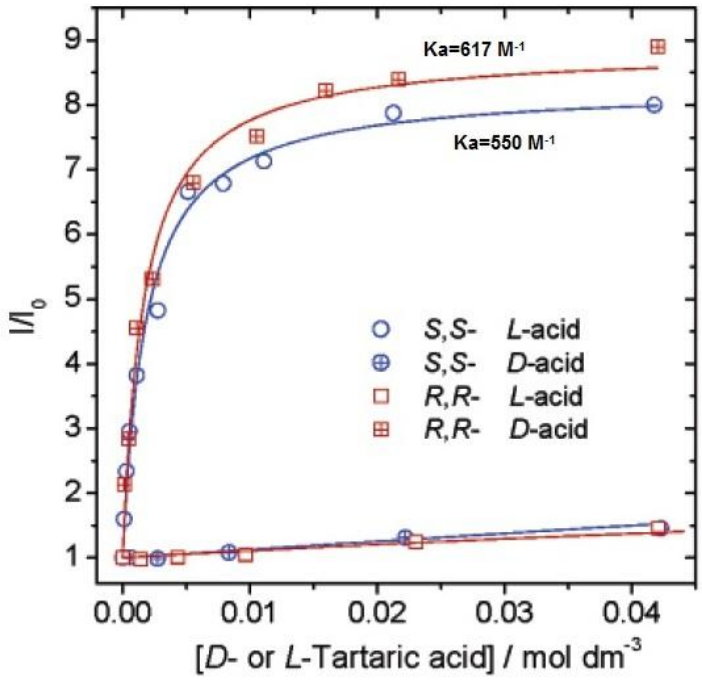

Figure 2.3. Enantioselective recognition of D- or L-tartaric acid by bidentate receptor (**4**) in 0.05 M NaCl ionic buffer pH 8.3. Image used with permission.[31]

The fluorescence response for the R,R-bidentate receptor binding to D-tartaric acid mirrored that of S,S-bidentate binding to L-tartaric acid. This demonstrated the ability to discriminate the D- from L-tartaric using one of the receptors give by the significantly different binding constants for each receptor. For example, the R,R bidentate receptor (**4**) for D-tartaric acid provided a binding constant of 617 ± 0.12 M^{-1} while its binding constant with L-tartaric acid was undetermined due to the small fluorescence change (Table 2.3).

Table 2.3. Association binding constants (K_a) for each R,R or S,S-bidentate and monodentate receptor with each sugar acid in pH 8.3 and 5.6.

Sugar Acid	@ pH 8.3 R,R (4)	@ pH 8.3 S,S (4)
L-tartaric acid	617	--
D-tartaric acid	--	550
D-glucaric acid	204	479
D-gluconic acid	257	851
D-glucuronic acid	724	1,023
D-galacturonic acid	--	--
	@ pH 5.6 R,R (4)	**@ pH 5.6 S,S (4)**
L-tartaric acid	831,763	10,000
D-tartaric acid	8,511	575,439
D-glucaric acid	57,543	53,703
D-gluconic acid	12,303	53,703
D-glucuronic acid	3,311	6,457
D-galacturonic acid	1,047	851

As the stability constants and fluorescence of the R,R and S,S bidentate receptors are highly enantioselective for D- or L-tartaric acid, the enantiomeric excess were able to be determined from a mixture of D and L-tartaric acid. In this particular system, the pH can be used to its advantage to provide high sensitivity for these sugar acids over the sugar alcohol sorbitol. The best selectivity that was demonstrated was for the R,R bidentate receptor between D-tartaric acid/D-sorbitol, 7.2:1 (at pH 8.3) and 11,000:1 (at pH 5.6). These selectivity enhancements and the ability to switch through pH changes is highly desirable which can allow for the concentration of D-tartaric acid in mixtures to be determined. Using the R- or S- monodentate receptor (**5**) no enantioselectivity was achieved for these sugar acids eluding to the fact that 1:1 complex formation is preferred for the R,R- or S,S- bidentate receptor (**4**) with the sugar acids and is strongly pH dependent.

2.2. Background and Rationale

Given the literature precedence on the ability of boronic acid binding for bidentate compared to monodentate receptors for sugar alcohols and sugar acids, there is an interest to use a monodentate boronic acid receptor for the discrimination of sugar alcohols. Monodentate receptors have been demonstrated to have high sensitivity to sorbitol over other sugar alcohols.[19,32, 33] Based on our previous studies with the bidentate receptor 4,4'-*o*-BBV (**6**) and 3,3'-*o*-BBV (**7**) were efficient at providing high selectivity and sensitivity for aldoses such as, fructose and glucose.[34] This was attributed to the potential 1:1 favorable complex formation between the monosaccharide and the bidentate receptor. This prompted us to synthesize the monodentate receptors (**8** & **9**) to study the sensitivity and possible selectivity for sugar alcohol of interest (Scheme 2.7).

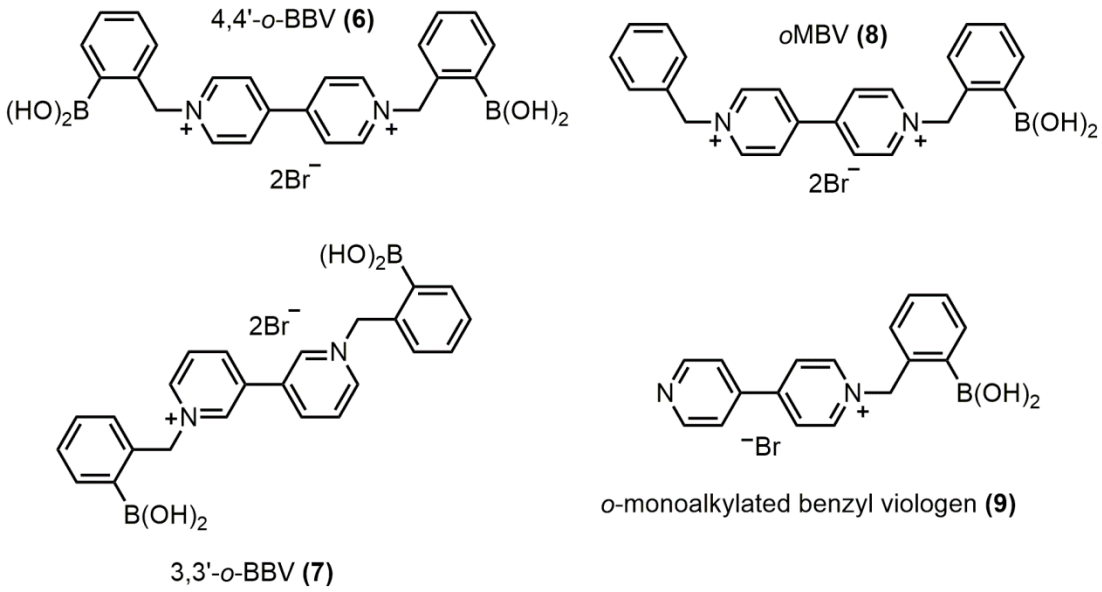

Scheme 2.7. Structures of mono- and bidentate receptors used in the Singaram-Wessling two component system to study sugar alcohol and sugar acid binding.

2.3. Results

Sugar alcohols are the reduction products from aldoses or ketoses. Few of these sugar alcohols, such as meso-erythritol, xylitol, and galactitol, are achiral, difficult to detect in aqueous solution, and challenging to separate chromatographically. Due to their acyclic nature, they tend to adopt different conformations when binding to boronic acid derivatives as compared with cyclic aldoses or ketoses.[35] Consequently, designing selective boronic acid receptors for these alcohols poses a difficult challenge. Because these sugar alcohols are important metabolic intermediates, designing sensitive and selective sensors for sugar alcohols has attracted considerable attention in the field of sensor design. To circumvent the selectivity challenge, boronic acid arrays can be utilized to provide semi-specific binding to these acyclic

sugars generating fingerprints for each sugar alcohol. Before coming to this conclusion of array-based analysis, we pursued the possibility of designing a selective boronic acid receptor for the recognition and discrimination of sugar alcohols.

Using previous synthetic routes to the bidentate receptors 4,4'-*o*-BBV and 3,3'-*o*-BBV, attempts to design the synthesis with feasibility and economic efficiency was taken into account when synthesizing the bidentate receptor (**8** & **9**).

2.3.1. Preparation of Monodentate Receptors

The monodentate receptor (oMBV, **9**) was prepared using a one-step procedure by reacting a four-fold excess of the readily available 4,4'-bipyridyl with bromomethylphenyl boronic acid in acetone at 25°C for one hour. After this time, diethyl ether was added and the product precipitated from the reaction as an off-white solid. By performing the reaction at ambient temperature, this prevented the formation of the mixture of mono- or bi- alkylated products. The ortho-substituted was obtained within one hour, the meta- and para-substituted products needed to react for at least four hours to obtain good yields (Scheme 2.8).

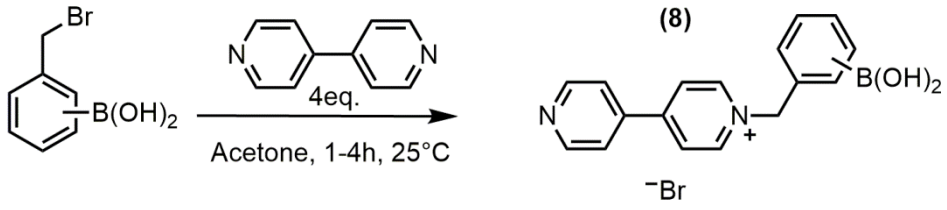

Scheme 2.8. Synthesis of *o*-, *m*-, or *p*-monoalkylated receptor (**8**)

Then, the unreacted quaternary nitrogen was alkylated with benzyl bromide to provide the bis-quarternized products (Scheme 2.9). Given that these monoalkylated receptors only have one positive charge, they were also investigated for their binding properties to the sugar alcohols of interest.

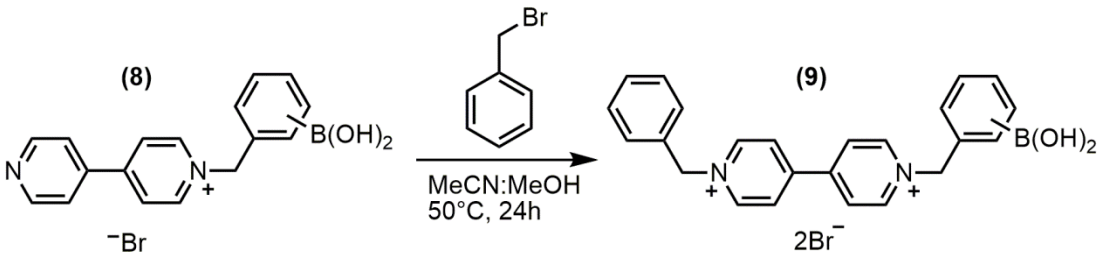

Scheme 2.9. Synthesis of *o*-, *m*-, and *p*-monodentate receptors (**9**).

Based on previous work, it was demonstrated that the 4,4'-*o*-BBV (**6**) bidentate receptor exhibited unique behavior due to the ortho substitution of the boronic acid motif. The boronic acid is in closer proximity to the quaternary nitrogen and able to participate in a favorable electrostatic interaction. This has been previously documented in work by Lakowicz and co-workers, where a similar interaction was proposed and characterized as a "charge neutralization stabilization mechanism"[36, 37] (Scheme 2.10).

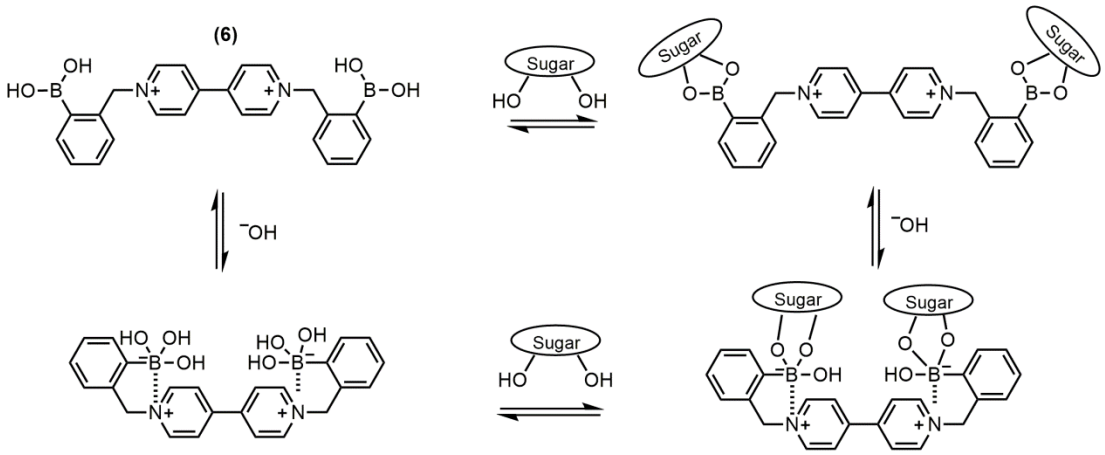

Scheme 2.10. Charge neutralization stabilization mechanism of 4,4'-*o*-BBV (**6**). The dashed lines represent the charge interactions between the boronate and positively charged quaternary nitrogen.

2.3.2. Quenching of Pyranine (HPTS) with Monodentate Receptors

To determine the relative quenching abilities of these boronic acid receptors, a solution of HPTS (1 μM in pH 7.4 sodium phosphate buffer) was titrated with increasing amounts of the ortho-monoalkylated receptor (**8**), o-monodentate receptor (**9**), and the 4,4'-o-BBV bidentate receptor (**6**). The quenching efficiencies for each one is compared by comparing the decrease in the fluorescence emission of HPTS (λ_{ex}=405, λ_{em}=535) upon addition of quencher/receptor as illustrated in Figure 2.4.

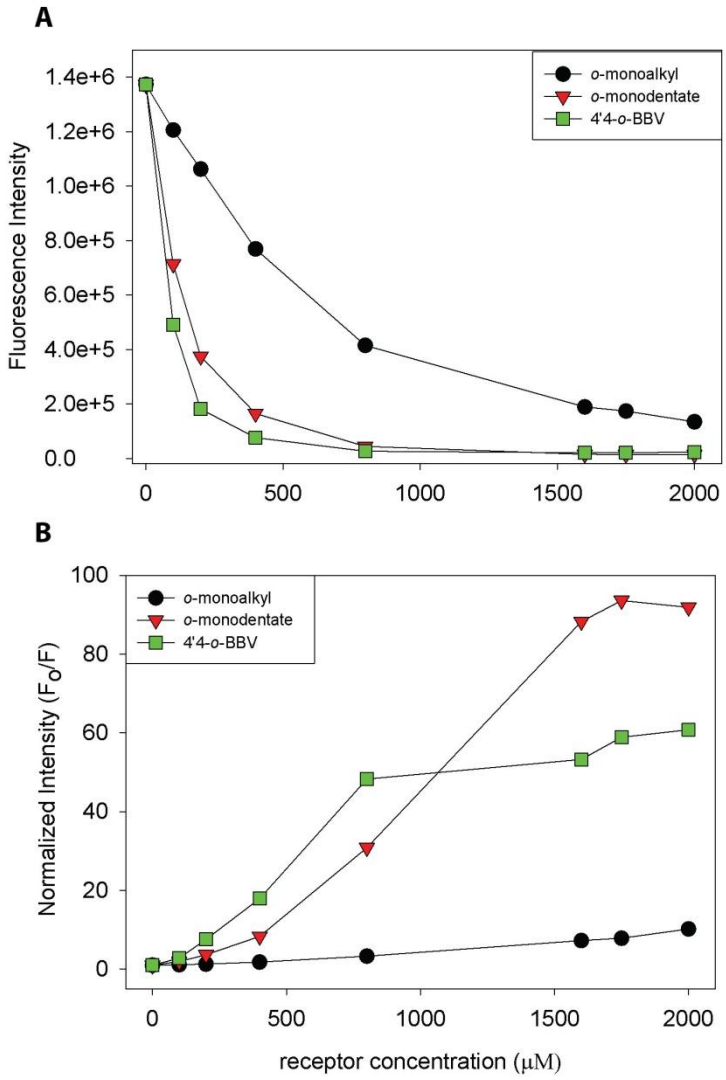

Figure 2.4. A. Fluorescence intensity of HPTS (1 μM in 0.1 M sodium phosphate buffer, pH 7.4, λ_{ex}=405, λ_{em}=535) with increasing concentration of boronic acid receptors. **B.** Stern-Volmer plots of the fluorescence intensity of HPTS where F=quenched fluorescence after addition of boronic acid receptor and F_o=initial fluorescence in the absence of boronic acid receptor under the same conditions.

As expected, the bidentate, the 4,4'-o-BBV receptor performed more effectively in quenching HPTS over the monodentate (oMBV, **8**) and the monoalkyl receptor (**9**). The correlation between the number of positive charge of the receptor has been well

documented by our group and have determined that with increasing number of positive charge on the boronic acid receptor, increase the overall quenching efficiency.[38] Although the 4,4'-*o*-BBV is effective at quenching HPTS at lower concentration than that of *o*MBV because it has a wider dynamic range of quenching and this can used to as an advantage when tuning the sensitivity of binding response to saccharides, sugar alcohols, and sugar acids of interest.

The Stern-Volmer plots are utilized to obtain quenching efficiencies from the fluorescence intensity data. From these plots, the static and dynamic quenching constants for each boronic acid receptors were calculated using equation (**1**) and are summarized in Table 2.4. At pH 7.4 the bidentate 4,4'-*o*-BBV (**6**) and monodentate *o*-MBV (**8**) receptor are quite effective quenchers, giving quenching constants for the static model of around K_s ~ 8000-28000 M^{-1}.

$$\frac{F_o}{F} = (1 + K_s[\mathrm{Q}])\, e^{V[Q]} \qquad (1)$$

Table 2.4. Static and Dynamic quenching constants.

Receptor	K_s (M^{-1})	V (M^{-1})
o-monoalkyl (**9**)	1248±43	1010±44
*o*MBV(**8**)	8965±220	1781±43
4,4'-*o*-BBV (**6**)	28,988±238	937±110

Table 2.4. Static (K_s) and dynamic (V) quenching constants for *o*-monoalkyl, monodentate (*o*MBV), and bidentate (4,4'-*o*-BBV) receptors with HPTS (1 μM) in 0.1 M sodium phosphate buffer pH 7.4.

When comparing each boronic acid receptor, the bidentate 4,4'-*o*-BBV (**6**) demonstrated to have higher quenching efficiency for HPTS followed by the monodentate receptor (**8**) and *o*-monoalkyl receptor (**9**). Given by the high static quenching constant, this further validates the mechanism of quenching which proceeds through the static quenching model resulting in the non-fluorescent ground state complex. Additionally, the high static quenching constant can be attributed to the increase in positive charge and increase the interaction to form the ground state complex driven by the coulombic attraction.

2.3.3. Recognition of Sugar Alcohols

To examine whether any selectivity can be achieved using the three unique receptors, we investigated the binding response of these boronic acid receptors against seven sugar alcohols (sorbitol, mannitol, galactitol, xylitol, arabitol, adonitol, and erythritol). Given that the naphthalene monodentate receptor (**5**) provided unique binding characteristics for sorbitol, we hypothesized that similar binding selectivity could be achieved with our monodentate receptor (*o*MBV, **8** or *o*-monoalkyl, **9**) to sorbitol.

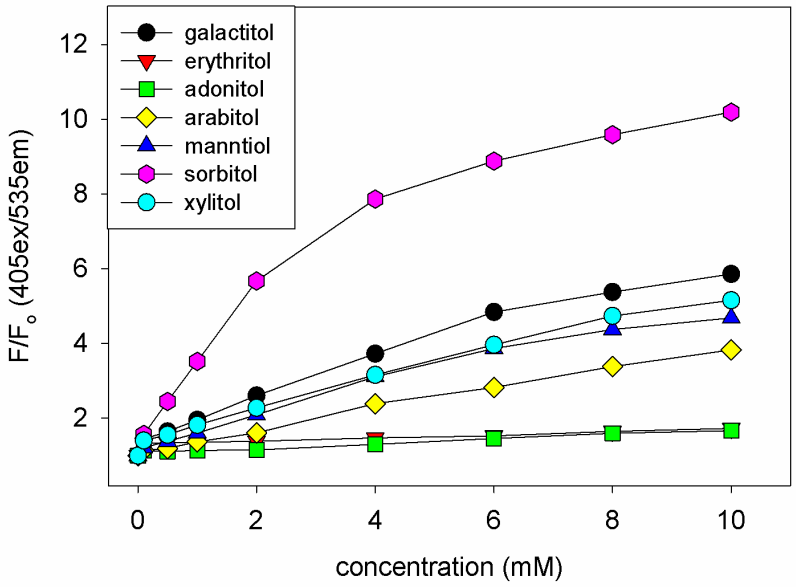

Figure 2.5. Normalized HPTS fluorescence response with each sugar alcohols against the bidentate receptor 4,4'-*o*-BBV (**6**) in 0.1M phosphate buffer solution, pH 7.4.

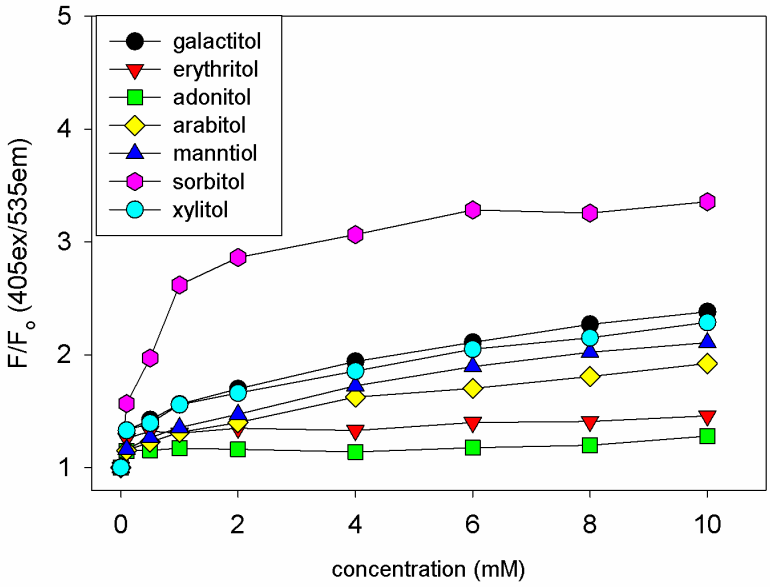

Figure 2.6. Normalized HPTS fluorescence response with each sugar alcohol against monodentate *o*-MBV (**8**) in 0.1M phosphate buffer solution, pH 7.4.

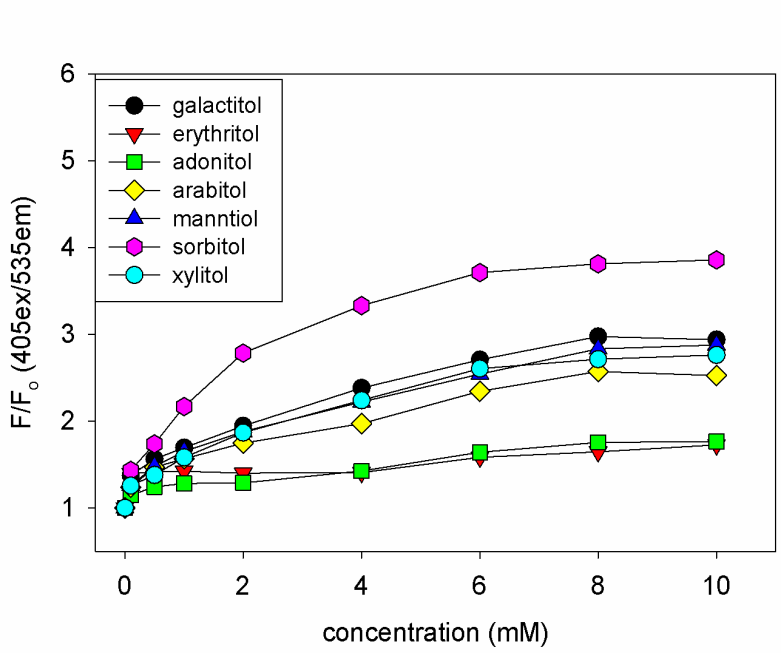

Figure 2.7. Normalized HPTS fluorescence response with each sugar alcohol against *o*-monoalkyl receptor (**9**) in 0.1M phosphate buffer solution, pH 7.4.

The monodentate receptor *o*-MBV (**8**) demonstrated to have good selectivity for sorbitol over two of the seven sugar alcohols examined. With moderate sensitivity of <100 μM and <500 μM limit of detection and quantification respectively, the *o*-MBV receptor can be useful for the recognition and discrimination of sorbitol against other sugar alcohols. Also, the *o*-MBV receptor had a modest distinction between the fluorescence recoveries for galactitol, mannitol, xylitol, and arabitol. This can be attributed to the small differences in the *o*-MBV binding mechanism. Similarly, the receptor that demonstrated superior fluorescence recovery for the majority of the sugar alcohols 4,'4-*o*-BBV (**6**) and provided great sensitivity with <100 μM and <500 μM limit of detection and quantification respectively. On the contrary, the o-

monoalkyl (**9**) receptor provided good selectivity for sorbitol compared to the bidentate receptor 4,'4-*o*-BBV (**6**), but lacked sensitivity for the sugar alcohols >1 mM limit of detection and quantification (Figure 2.5-2.7). There was significant overlap of fluorescence recovery between galactitol, arabitol, mannitol, and xylitol which alludes to the possibility of the preferred binding conformation that the o-monoalkyl receptor participates in. Apparent association binding constants were determined by non-linear curve fitting using Equation 1 (Table 2.5).

$$\frac{F}{F_o} = \frac{\left(1 + \frac{F_{\max}}{F_o}\right) K_b[A]}{1 + K_b[A]} \tag{1}$$

where F_0 is the fluorescence intensity of the quenched dye, F is the fluorescence intensity after the addition of analyte, F_{max} is the fluorescence intensity at which no further signal is obtained with further analyte addition, K_b is the apparent stability constant, and [A] is analyte concentration. K_b was solved using OriginLab software (Originlab Corp, Northampton, MA, USA)

Table 2.5. Apparent association binding association constants ($K_{b,}$ M^{-1}) for 4,4'-*o*-BBV (**6**), *o*-MBV (**8**), and *o*-monoalkyl (**9**) receptors and the seven sugar alcohols

Sugar alcohol	4,4'-*o*-BBV(**6**)	*o*-MBV (**8**)	*o*-monoalkyl (**9**)
Galactitol	111±21	54±8	37±11
Erythritol	15±2	1.5±0.3	1.6±1.5
Adonitol	19±3	2.6±0.6	2.5±1.2
Arabitol	29±5	1.6±1.5	26±6
Mannitol	88±13	38±6	31±7
Sorbitol	290±19	169±16	552±29
Xylitol	82±22	61±9	32±6

To our surprise, the *o*-monoalkyl (**9**) demonstrated to have higher selectivity for sorbitol compared to the fully quarternized monodentate (**8**) with a 3:1 selectivity (*o*-monoalkyl:*o*MBV) for the six-membered sugar alcohol. Other notable examples that have moderate selectivity is the 4,4'-*o*-BBV receptor for galactitol, which provided a 3:1 selectivity (4,4'-*o*-BBV:*o*-monoalkyl). Although some selectivity was shown with the monodentate receptor, the level of selectivity achieved was not comparable to what other groups have shown.

2.3.4. Sugar Alcohol Binding Mechanism

Acyclic sugar alcohols, in general, have multiple syn-1,2- and/or syn-1,3-diol units, the latter being where boronate ester formation occurs preferentially. Similarly, the number of carbon atoms in the chain also influences boronic acid binding.[39] For example, erythritol (four carbons), adonitol, arabitol, and xylitol (five carbons) exhibit significantly different binding affinities. The stability constants for boronate ester formation for acyclic sugars are known to be proportional to the number of hydroxyl groups.[40] These structural differences are known to contribute to sugar alcohol binding affinities for boronic acid receptors. Upon boronate ester formation in *erythro*-1,2-diol, the neighboring substituents are transposed from a staggered to a sterically demanding eclipsed conformation. Conversely, in *threo*-1,2-diol there is minimal conformation change where the neighboring substituents remain in an energetically favorable staggered conformation (Scheme 2.11).[41]

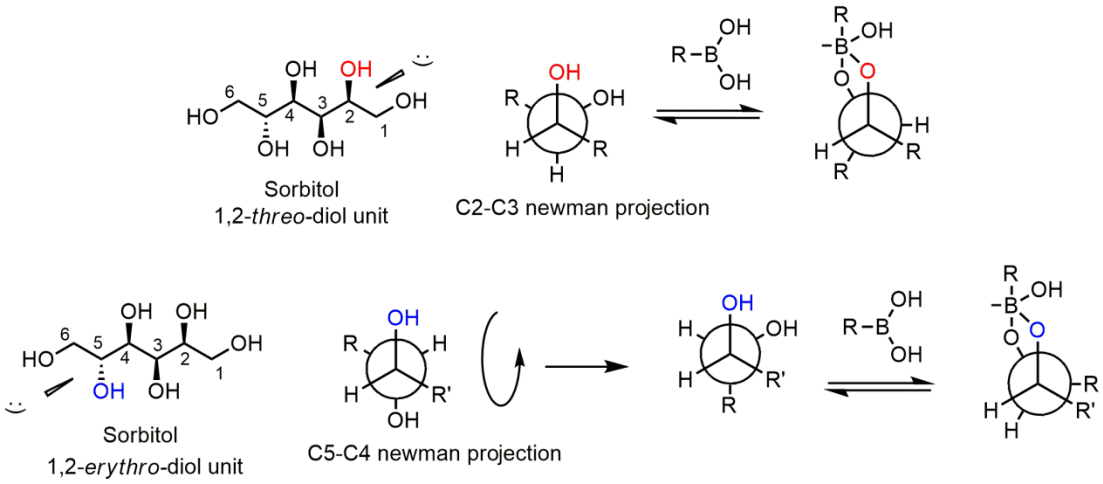

Scheme 2.11. Proposed preferred binding conformations between 1,2-*threo* or –*erythro*-diol units with boronic acid.

As such, acyclic sugar alcohols with a *threo*-1,2-diol motif have higher binding affinities compared with that of the *erythro*-1,2-diol motif. Similar observations have been made regarding other groups.[40, 42] Of the seven sugar alcohols analyzed in this study, sorbitol (two *threo*-1,2-diol units and one *syn*-1,3-diol unit) we predict will have an optimal binding for the majority of receptors tested and can easily be discriminated using our array. Binding preference for the 1,3-diol units stems for the boronate ester formation to form a chair-like transition state and the preferred diol will adapt a stable conformation. The diol unit that should adapt the most stable conformation is the *syn*-1,3-diol unit as shown in scheme 2.12.

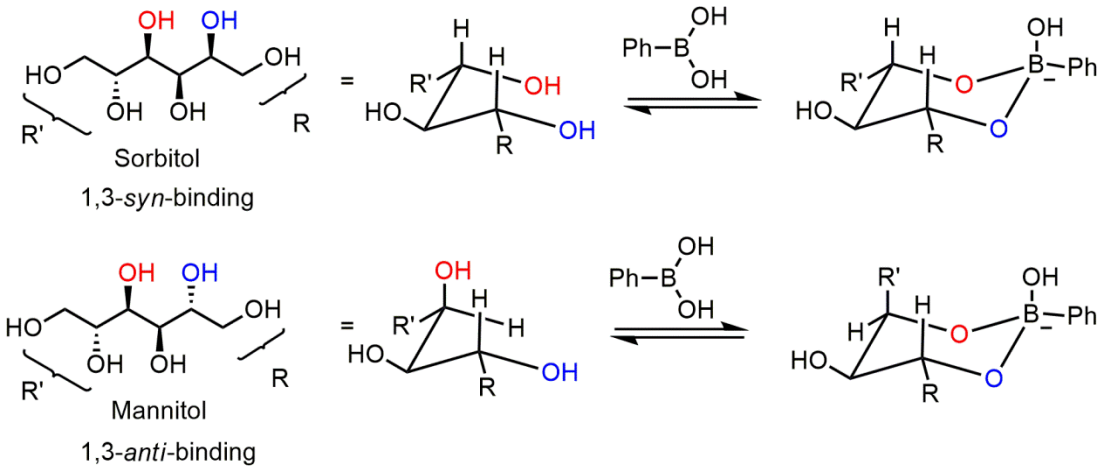

Scheme 2.12. Illustration between the different binding conformations for *syn*-1,3-diol or *anti*-1,3-diol in sorbitol and mannitol respectively with a phenylboronic acid model compound.

Boronate ester formation of *syn*-1,3-diols is generally more stable than those of *anti*-1,3-diols, most likely due to the destabilizing effects of the 1,3-diaxial steric interactions in the 6-membered chair-like transition state of the latter diols. Evans and co-workers have previously observed a pattern of stability where the order of 5-membered alditols the increasing order of stability: xylitol (2 *threo*-diol units) > arabitol (1 *threo*-diol unit) > ribitol (no *threo*-diol unit).[39] Additionally, a factor that can have a significant effect on the ability of the BBV receptors to bind differentially is due to the intramolecular distance between the two boron atoms is also important for achieving cooperative binding of boronic acids to sugar alcohols containing diols in the *threo* configuration.

2.3.5. Discrimination of Sugar Alcohols by a Multiwell Based Array

Since an overarching goal of this work is to develop a high-throughput assay utilizing the Singaram-Wessling two component system, using these types of viologen receptors provides synthetic and economic advantages compared to other systems. With this in mind, we decided to pursue other bidentate receptors that previous members of the Singaram group have worked with to discriminate sugar alcohols and sugar acids through a pattern-based recognition approach by an array of boronic acid receptors. Five other receptors were synthesized to assemble the array to discriminate between the sugar alcohols used in the previous study (Figure 2.8). We hypothesized to assemble the array containing receptors with varying the intramolecular distance between the boronic acid motif as well as the positioning could provide discriminatory power to the sugar alcohols of interest (Description of differential based recognition is discussed in section 4.1.2.)

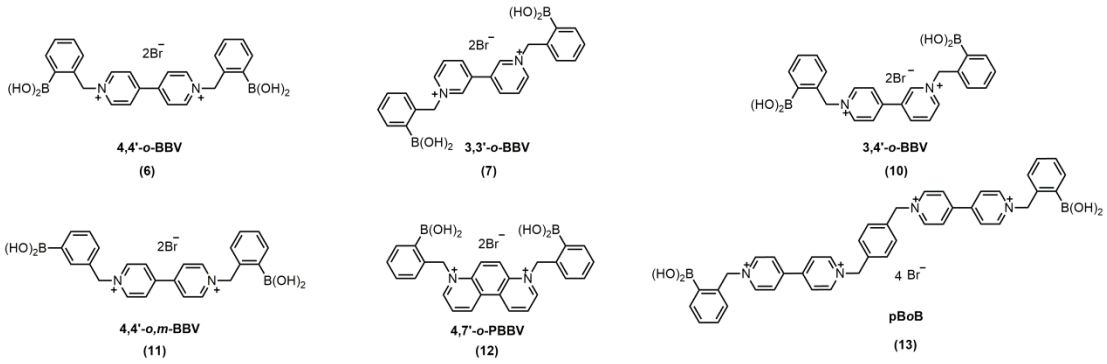

Figure 2.8. Structures of the boronic acid array composed of six unique boronic acid-appended benzyl viologens with corresponding abbreviations and numbering.

The dye and quencher are two discrete entities can provide better selectivity and sensitivity over saccharides of interest. This also allows the quencher to be readily modified without altering the photophysical properties of the reporter dye. Because of the ionic nature of these receptors, they are water soluble at physiological pH even in the absence of sugar. In addition, varying ratios of receptor to reporter dye can be used to modulate fluorescence response. Several bipyridinium and phenanthrolinium based receptors have been synthesized previously and have been studied extensively for glucose binding.[43-47] From our library of receptors, six BBVs were chosen for this study based on the following criteria: a) at least one boronic acid motif must be in the ortho position; b) each receptor have varying intramolecular distance between boron atoms; c) the cationic charge of all receptors must be at minimum of 2+; and d) each receptor must be synthesized in no more than three steps (Figure 2.8).

The BBV array was utilized to discriminate these sugar alcohols. Boronic acid receptors were prepped as "probe" solutions separately, and the seven sugar alcohols were prepared in 0.1 M sodium phosphate buffer at pH 7.4 to afford a twofold concentration of each individual probe solution and each sugar alcohol. Because the quenching efficiency of BBVs are different, the quencher to dye ratio (Q:D) of each receptor was adjusted to provide at least 80% quenching of HPTS. For 4,4'-*o*-BBV (**6**), 3,3'-*o*-BBV (**7**), 3,4'-*o*-BBV (**10**), 4,4'-*o,m*-BBV (**11**) a Q:D ratio of 125:1 was used; for 4,7-*o*-PBBV (**12**) a Q:D ratio of 30:1; and for pBoB (**13**) a Q:D ratio of 3:1.

Sugar alcohol concentrations between 2 and 4 mM occupied the midpoint of the dynamic range for each receptor. This fit well within the range that is expected for these sugar alcohols to appear in urine during a permeability test. The boronic acid array provided a data matrix of 6 replicates x 6 receptors x 7 analytes. The fluorescence intensity (F) for each permutation was normalized against initial F without analyte (F_0) as the ratio (F/F_0). The resulting bar chart conveys a "fingerprint" of the differential responses (Figure 2.9).

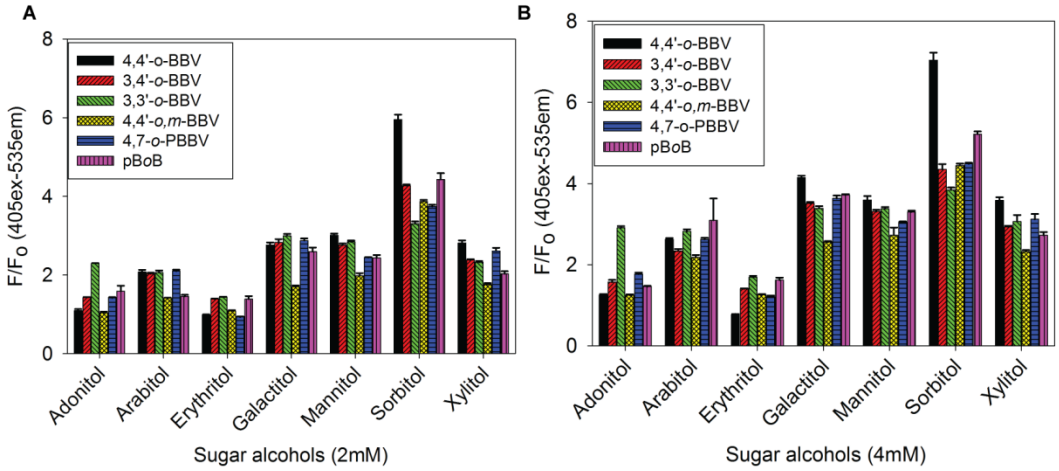

Figure 2.9. Normalized HPTS (4 µM final concentration) fluorescence responses (F_o=initial quenched fluorescence, F=recovered fluorescence) with each boronic acid receptor (4'-*o*-BBV (**6**), 3,3'-*o*-BBV (**7**), 3,4'-*o*-BBV (**10**), 4,4'-*o,m*-BBV (**11**), 4,7-*o*-PBBV (**12**), pB*o*B (**13**)) against 2 mM (A) and 4 mM (B) of each sugar alcohol in 0.1 M phosphate buffer solution, pH 7.4. Data points are mean ± SEM, n=6.

Due to the difficulty to discern the similarities and nuances of the fingerprint data, the data must be subjected to principle component (PCA) or linear discriminate analysis (LDA) to reduce the dimensionality of the data set to single points on a two-

dimensional plot. Doing so can allow identification and/or quantification of which sugar alcohol is present in solution. From the fingerprint data alone, it can be deduced that overall sorbitol provided high fluorescence recovery for all six receptors, while erythritol gave little to no recovery. Processing the data through the principle component analysis algorithm developed by XLSTAT®, the discriminatory power of these receptors for the seven sugar alcohols can be determined.[48] The two-dimensional PCA Plot obtained for the seven sugar alcohols using the array of six boronic receptors with HPTS as the fluorescence report is shown in Figure 2.10.

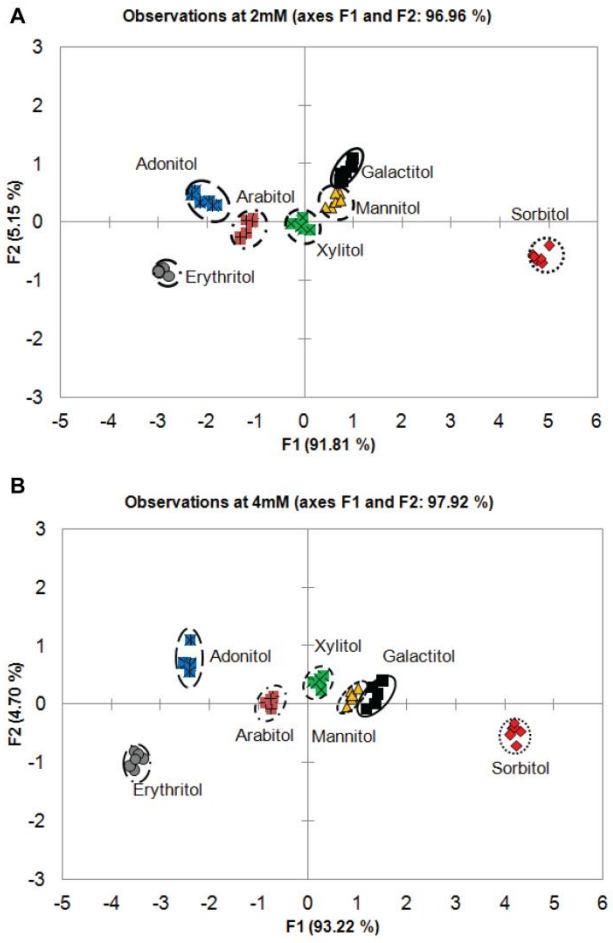

Figure 2.10. PCA plot with 97% variance for all seven sugar alcohols analyzed at 2mM (A) and 4mM (B) concentrations with six boronic acid receptors (4'-*o*-BBV (**6**), 3,3'-*o*-BBV (**7**), 3,4'-*o*-BBV (**10**), 4,4'-*o*,*m*-BBV (**11**), 4,7-*o*-PBBV (**12**), pBoB (**13**)). All of these studies were carried out in 0.1 M sodium phosphate buffer pH 7.4 at 25°C.

Using the six boronic acid array provided high variance (F1 and F2 >96%) for 2 mM and 4 mM sugar alcohols, with F1 being the significant contributor variance (92%). The F1 axis discriminates these sugar alcohols by their chain length; with six carbon sugar alcohols (galactitol, mannitol, and sorbitol) on the right quadrant and

five or four carbon sugars alcohols (adonitol, arabitol, xylitol, and erythritol) on the left quadrant. The basis of their separation stems from the differences in the conformations of boronate esters formed from the sugar alcohol. In addition to the favorable *threo*-1,2-diol, sugars with *syn*-1,3-diols displayed higher binding affinity over those with only *threo*-1,2-diol subunits. The PCA plot shows a clear discrimination of majority of the sugar alcohols, with significant overlap between galactitol and mannitol indicating low discrimination between these sugar alcohols. Galactitol and mannitol (*syn*-1,2-diol and at least one *threo*-1,2-diol) have similar diol characteristics explaining their similar binding behavior. Boronate ester formation upon binding sugars with *threo*-1,2- or *syn*-1,3-diol was favored over those with *erythro*-1,2- or *syn*-1,2-diol units. Moreover, better cluster segregation is observed as the concentration of sugar alcohols increased to 4 mM. The five carbon sugar alcohols, such as xylitol and adonitol, segregate along the F1 axis with minor overlap between the xylitol, galactitol, mannitol, and arabitol cluster in near proximity. This concentration effect decreases the spatial resolution between the clusters and the clusters migrate towards the positive side along the F1 axis with increasing analyte concentration. Because of the overlap observed in the PCA plot with mannitol, galactitol and xylitol are not suitable mannitol substitutes as GI markers. However, adonitol and erythritol show promise as GI markers, because they are well-separated from mannitol. Overall, sorbitol remained farther apart from the rest of the sugar alcohols.

Using this array of boronic acid receptors provided a rapid screening of multiple sugar alcohols in a short period of time. This fingerprint generating assay technique is similar to the high-throughput screening of chemical libraries for identifying drug targets and is less labor-intensive than designing selective boronic acids for binding sugar alcohols. The sugar alcohols examined here were of interest because of their potential to be utilized as a substitute for mannitol or use in applications other than gut permeability tests (Chapter 4).

2.3.6. DFT Analysis of Boronic Acid Binding to Sugar Alcohols

The binding pattern that was observed in section 2.3.5 for sugar alcohol binding by the array of boronic acid receptors was further validated by performing density functional theory calculation carried out at B3LYP/6-31+G* level in the gas phase. The *threo*-1,2- versus *erythro*-1,2- preference was studied with borane esters of threitol and erythritol, where the latter is 1.89 kcal/mol higher in energy. Upon tetrahedral anionic borate formation, the energy further raised to 2.24 kcal/mol. This validates the previous observation that *threo*-1,2-diol units adapt a more energetically favorable conformation upon boronate ester formation.[30] Similarly, the difference between *syn*-1,3- and *anti*-1,3- were computationally studied with sorbitol and mannitol. It was found that *syn*-1,3- ester is 3.55 kcal/mol lower in energy than the corresponding *anti*-1,3- ester (Figure 2.11).

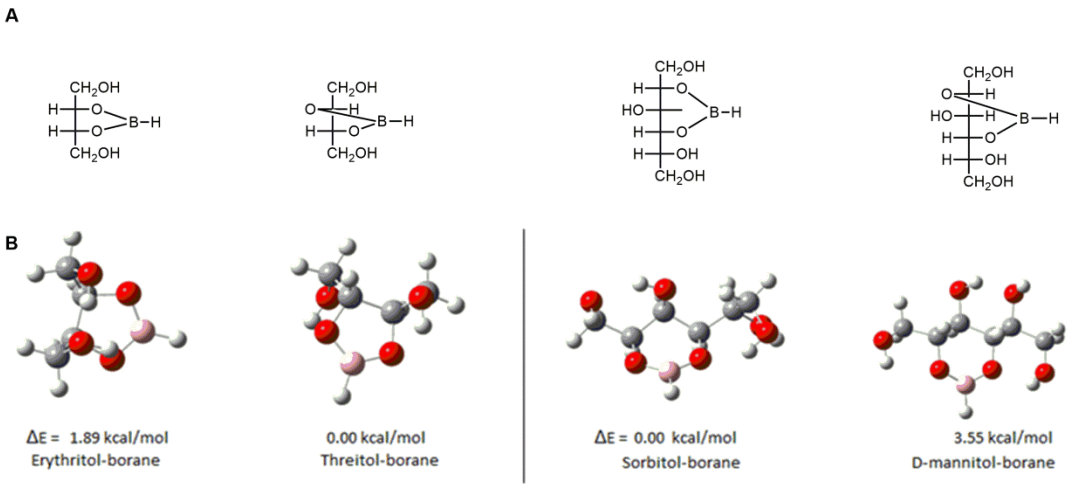

Figure 2.11. A. Fisher projections of the *erythro*-1,2- and *threo*-1,2 with borane (left side) and the *syn*-1,3- and *anti*-1,3- borane diol interaction (right side) **B.** Optimized molecular models of those interactions with each sugar alcohol and borane.

Experimental results showed that the 4,7-*o*-PBBV receptor had a positive correlation with the calculated predictions of preferred binding between threitol over erythritol, while the other five receptors showed no significant differences (Figure 2.12).

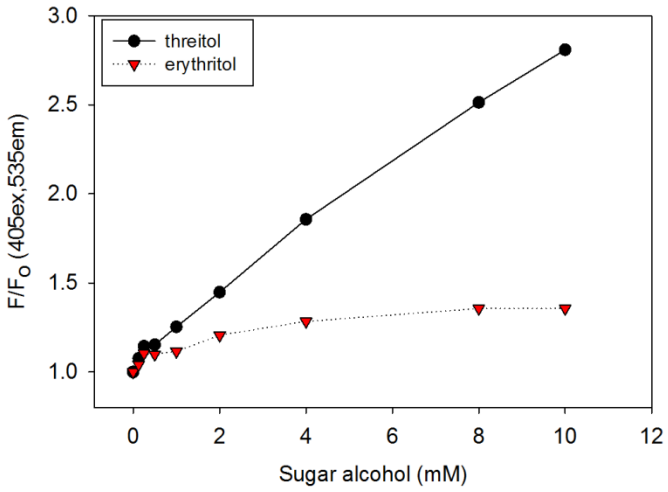

Figure 2.12. Binding isotherm of erythritol and threitol with the 4,7-o-PBBV (12) boronic acid receptor in sodium phosphate buffer pH 7.4. Normalized HPTS (4 µM final concentration) fluorescence responses (F_o=initial quenched fluorescence, F=recovered fluorescence).

Despite erythritol and threitol are 1.89 kcal/mol different their conversion to borate is equally feasible (differed by only 0.35 kcal/mol). In contrast, sorbitol-borane is preferred over mannitol-borane, but the borate is preferred for Mannitol. Further, there is an additional ~8 kcal/mol lowering from erythritol/ threitol (5 member ring) to Sorbitol (6 member ring). An additional ~4 kcal/mol advantage for mannitol, as the tetrahedral boron, relieves the steric strain. This demonstrates and confirms the preferred binding of 1,2-*threo* diol over 1,2-*erythro* diol units.

2.3.7. Recognition of Sugar Acids

Aldonic and aldaric acids are interesting sugar derivatives because of the carboxyl functional present now which can have considerable effects for the boronic acid-diol interaction through stabilization or destabilization by the ionized carboxyl group. The α-hydroxycarboxylic acid function in these sugar acids contains in its non-dissociated state a *vicinal* diol function and can be responsible for interaction with boronic acids. Stabilities for the boronate ester formation have been previously reported to be much higher than those for certain sugar alcohols. This can be attributed to electronic and ring strain effects of the carbonyl function.[49] But, the affinity of the boronic acid for the neighboring vicinal diol in these sugar acids can be lower than sugar alcohol affinities since the ester formation is usually formed when the pH > pKa of the boronic acid-diol complex. This complex can be destabilized or stabilized by repulsion between the negatively charged boron and the carboxylate group.[50] Work by Peters J.A. and co-workers demonstrated this effect further with a phenylboronic acid binding to erythronic and threonic acid (each 1:1 mixture) as a function of pH.[51] Below pH 9, the boron chemical shift of the bound species is δ= -10 ppm, which is typically observed for the phenylboronic acid-glycolate system. It can be deduced that the α-hydroxy carboxylate ester and boronate ester moiety bound to C-1 and C-2 is the predominant ester in the pH range of 2-9 (Scheme 2.13).

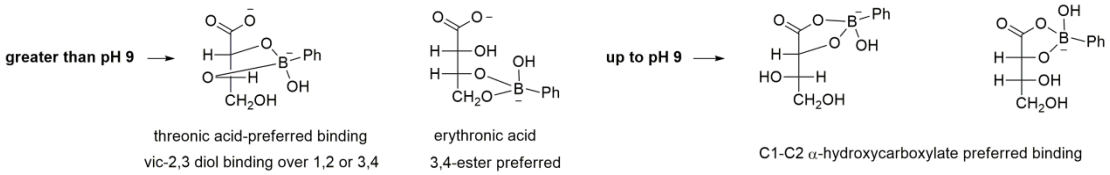

Scheme 2.13. Preferred binding of phenylboronic acid with erythronic at pH > 7.4.

Above pH 9, there was an increase in shift indicating the disruption of the interaction at C-1 and C-2 and boronate ester formation occurs at the 2,3-threo-diol unit and 3,4-ester for threonic and erythronic acid, respectively.

Given the ability of our bidentate boronic acid receptors, we decided to pursue binding studies for these receptors and their ability to discriminate between various sugar acids (D-tartaric, L-tartaric, galacturonic, gluconic, glucuronic, and L-malic acid) at physiological pH. Glucuronic acid was of high interest due to recent work by Janda and co-workers who demonstrated the potential of using a glucuronic acid derivative (N-acetyltyramine-O,*β*-glucuronide, NATOG) as a host specific biomarker for the tropical disease onchocerciasis progression, which is also known as river blindness.[52]

With the established quencher to dye ratios that were used in the sugar alcohol study (see section 2.3.3.), initial studies involved look at the binding profiles for each bidentate receptors against the six sugar acids and α-hydroxyacids (Figure 2.13).

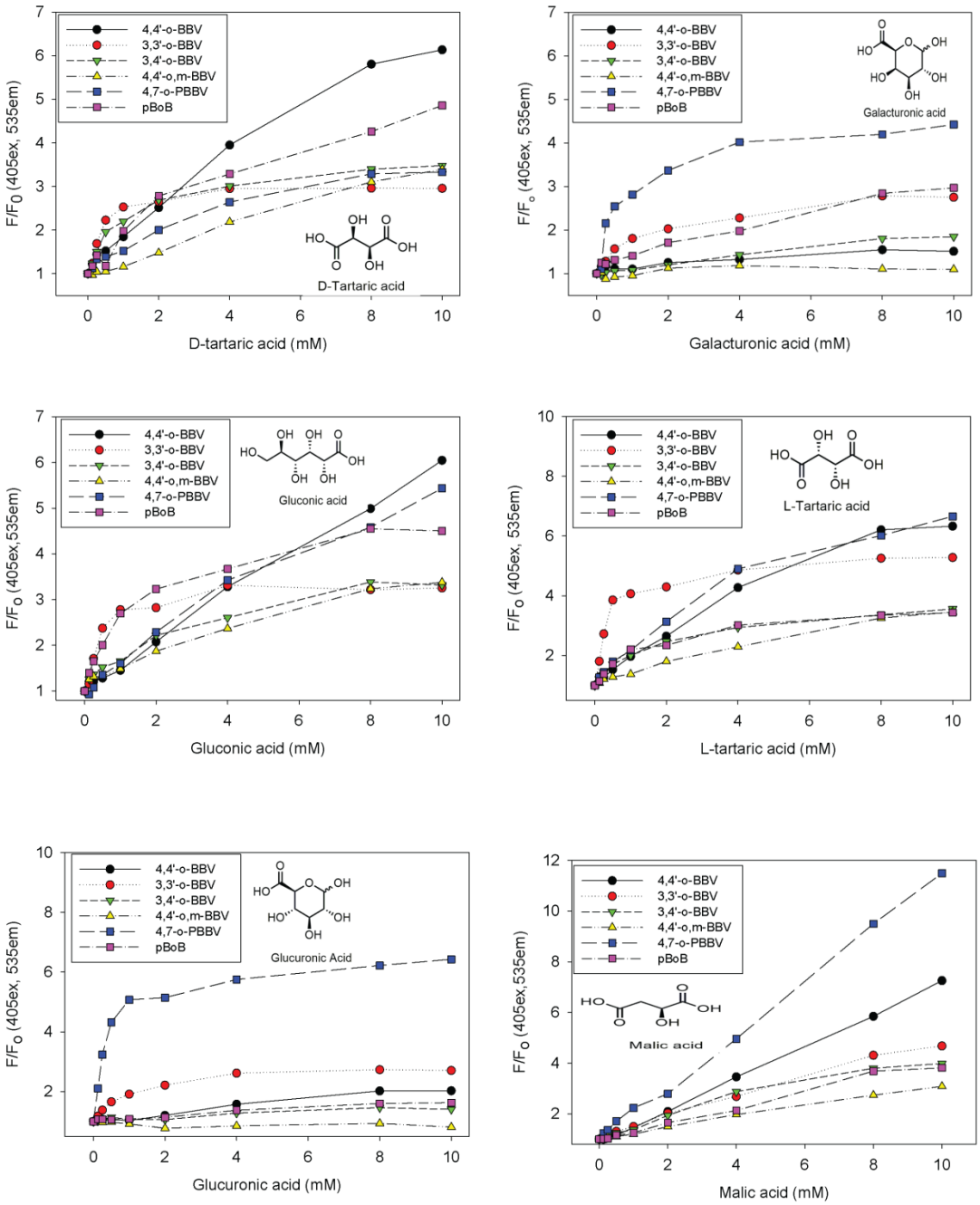

Figure 2.13. Binding isotherms for each sugar acid against each corresponding bidentate boronic acid receptor in 0.1 M sodium phosphate buffer pH 7.4.

The binding recognition patterns for the α-hydroxyacids (L-malic acid, L- or D-tartaric acid) for each receptor provided modest to excellent fluorescence recovery with little preference amongst the six receptors examined. The 3,3'-*o*-BBV (**7**) exhibited rapid saturation with good sensitivity for D-tartaric acid as previously observed. Additionally, L-malic acid provided high fluorescence recovery for the 4,7-*o*-PBBV (**12**) and 4,'4-*o*-BBV (**6**) receptors with linear characteristics. For the sugar acids, the binding profiles for glucuronic acid and galacturonic acid demonstrated to have selective binding for the 4,7-o-PBBV (**12**) over the other five receptors examined. A 3-fold difference in binding was observed for this receptor for glucuronic and galacturonic acid. This shows the potential to use the 4,7-o-PBBV (**12**) to selectively detect these sugar acids in the presence of others.

2.3.8. Discrimination of Sugar Acids by a Probe Array of BBVs

A fingerprint for these sugar acids was generated using the six receptor array at 2 mM and 4 mM concentration in sodium phosphate buffer. This was the mid-point of the dynamic range for each receptor. The boronic acid array provided a data matrix of 6 replicates × 6 receptors × 6 sugar acids. The fluorescence intensity (F) was normalized against initial fluorescence intensity (F_o) without sugar acid as the ratio (F/F_o). The resulting bar graph illustrates the "fingerprint" of the differential responses (Figure 2.14).

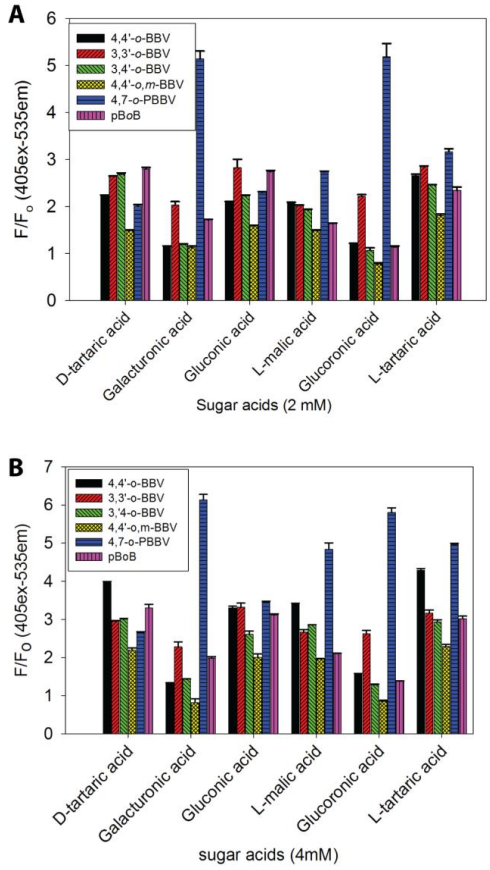

Figure 2.14. Normalized HPTS (4 μM final concentration) fluorescence responses (F_o=initial quenched fluorescence, F=recovered fluorescence) with each boronic acid receptor (4'-*o*-BBV (**6**), 3,3'-*o*-BBV (**7**), 3,4'-*o*-BBV (**10**), 4,4'-*o,m*-BBV (**11**), 4,7-*o*-PBBV (**12**), pBoB (**13**)) against 2 mM (A) and 4 mM (B) of each sugar acid in 0.1 M phosphate buffer solution, pH 7.4. Data points are mean ± SEM, n=6.

From the fingerprint analysis, the 4,7-*o*-PBBV (**12**) provided good discrimination for galacturonic, L-malic, and glucuronic acid with good fluorescence recovery. This receptor provided significant differences in the fluorescence recovery for 2 mM and 4 mM concentration for the three sugar acids.

Using the six boronic acid array provided high variance (F1 and F2 of 91%) for 2 mM and 4 mM sugar acids, with F1 being the significant contributor variance (81%). The F1 axis discriminates these sugar acids by their acid type (aldonic and uronic acids, and α-hydroxy acids); with the α-hydroxy acids (L-tartaric, D-tartaric, and L-malic acid) on the right quadrant and uronic acids (glucuronic and galacturonic acid) on the left quadrant. The basis of their separation stems from the differences in the conformations of boronate esters formed from the sugar acids (Figure 2.15).

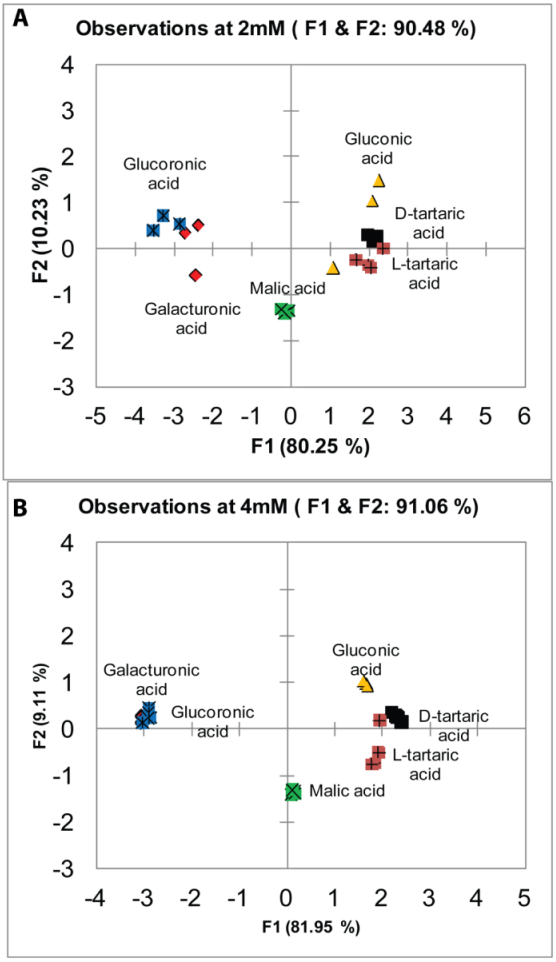

Figure 15. PCA plot with up to 91% variance for all seven sugar alcohols analyzed at 2mM (A) and 4mM (B) concentrations with six boronic acid receptors (4'-*o*-BBV (**6**), 3,3'-*o*-BBV (**7**), 3,4'-*o*-BBV (**10**), 4,4'-*o,m*-BBV (**11**), 4,7-*o*-PBBV (**12**), pBoB (**13**)). All of these studies were carried out in 0.1 M sodium phosphate buffer pH 7.4 at 25°C.

With increasing concentration from 2 to 4 mM of these sugar acids, gluconic acid clusters efficiently improving the overall resolution of discrimination for all sugar acids. On the contrary, there is indistinguishable discrimination between galacturonic and glucuronic acid at 4 mM concentration with complete overlap on the left quadrant and clusters nearly overlapping for L- and D-tartaric acid. Overall, there was effective

discrimination between L-malic and gluconic acid along the F2 axis as they appear on opposite quadrants. This could be attributed to the difference in binding, where L-malic acid would bind to the C1-C2 position forming the hydroxy carboxylate complex with the boronic acid motif. While the boronic acid motif binds gluconic acid preferentially through the vicinal C2-C3 *threo*-1,2-diol or the *syn*-1,3-diol units.

2.3.9. Recognition of a Glucuronide Derivative

Among the six boronic acid receptors examined for glucuronic acid, the 4,7-*o*-PBBV (**12**) provided superior binding which contributed to the overall discrimination power of the boronic acid array. Due to this, the 4,7-o-PBBV (**12**) appear to be an excellent candidate to pursue studies to measure the glucuronic acid derivative N-acetyltyramine-O,*β*-glucuronide, NATOG. Since this derivative has biological implications in utilizing the NATOG as a potential biomarker for river blindness disease, we deemed it to examine the ability of (**12**) to recognize this biomarker and the sensitivity or selectivity properties.

For this two-component system to be of any use, the sensitivity for NATOG detection must be within the range that NATOG would be present in biological samples. From previous work by Janda and co-workers, examined blood and urine samples from individuals who were affected with Onchocerciasis observed NATOG in the mid-nanomolar to sub-micromolar ranges.[52] The sensitivity of the two-component system examined with glucuronic acid since NATOG is a derivative of

this biomarker. Given that the 4,7-*o*-PBBV (12) receptor provided remarkable fluorescence recovery in our earlier work, we decided to examine its limit of detection and quantification for glucuronic acid (Figure 2.16).

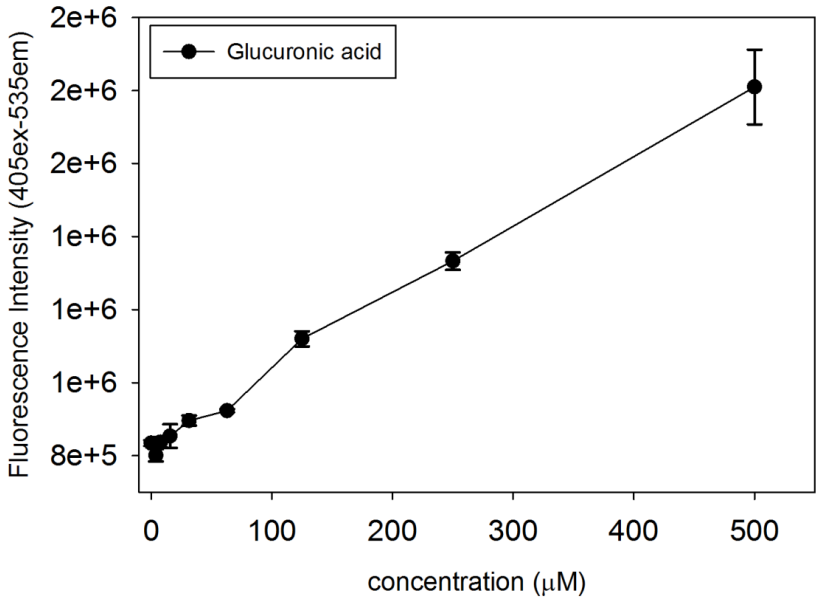

Figure 2.16. Binding isotherm of glucuronic acid with 4,7-*o*-PBBV in 0.1 M sodium phosphate buffer pH 7.4. Data points are mean ± SEM, n=3.

The 4,7-*o*-PBBV (**12**) receptor provided an excellent linear response with linearity R^2 of 0.99 and with a limit of detection (LOD) and limit of quantification (LOQ) of 40 and 170 μM. Although the 4,7-*o*-PBBV (**12**) receptor was able to detect glucuronic acid with excellent sensitivity, it was still not in the range that would render this receptor highly effective for actual samples from infected individuals (30-40 μM, observed by Janda et al.). Further investigation is required to increase the sensitivity of 4,7-o-PBBV for glucuronic acid.

Furthermore, to determine whether or not (**12**) would be capable of detecting the NATOG biomarker, *p*-tolyl glucuronide was used as a model compound for the biomarker, as the *p*-tolyl glucuronide is also a derivative of glucuronic acid where the C1-hydroxy group is participating in a β-glycosidic bond. The fluorescence recovery with 4,7-*o*-PBBV against p-tolyl glucuronide and compared to glucuronic acid was investigated in 0.1 M sodium phosphate buffer at pH 7.4 (Figure 2.17).

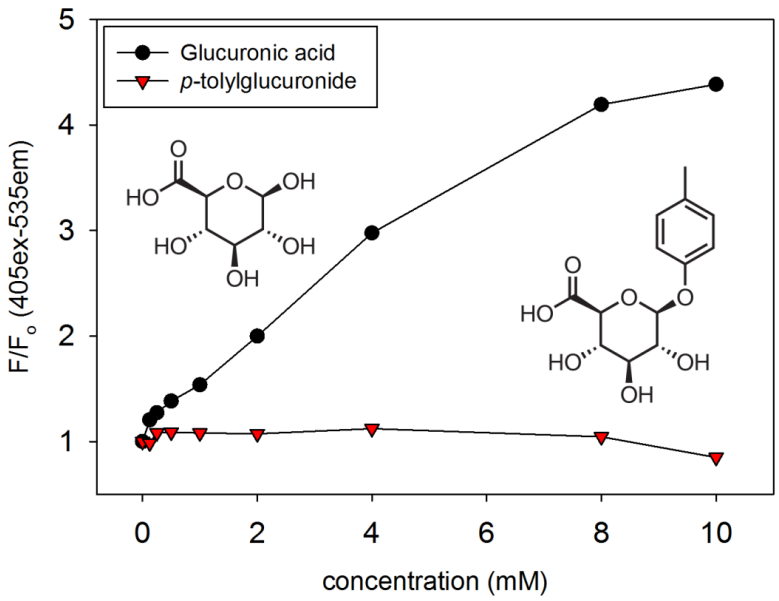

Figure 2.17. Binding isotherms of 4,7-*o*-PBBV (12) against glucuronic acid and *p*-tolyl glucuronide in 0.1 M sodium phosphate buffer pH 7.4. The fluorescence responses are normalized where F_o=initial quenched fluorescence, F=recovered fluorescence.

Unfortunately, the 4,7-*o*-PBBV (**12**) coupled to HPTS was unable to obtain a fluorescence response indicative of no boronic acid binding to the p-tolyl glucuronide (NATO derivative). Initially, we had speculated that binding would be low or none at

all based on our previous work from attempting to detect non-reducing sugars with our two-component system.[53] This phenomenon continues to hold true, the boronic acid appended viologen receptors does not observe any binding affinity (low to no fluorescence response) for non-reducing sugar and sugar derivatives such as, sucrose, sucralose, glucose 1-phosphate and now *p*-tolyl glucuronide.

2.4. Conclusion

This chapter describes the utility of the two-component system for the recognition of sugar alcohols and sugar acids and its ability to discriminate amongst these classes of sugars by assembling an array of boronic acid appended viologen receptors (BBVs, minimum of 6). Additionally, the binding mechanism was elucidated by examining the discrimination pattern of the six BBV receptors and determined the preferred binding mode based on which sugar alcohols discriminated the most. The preferred binding mode for the two-component system was determined to have a preference for *syn*-1,3 diol and *threo*-1,2 diol units and with increasing number of these units on the backbone, there was an increase in fluorescence recovery for this system. Although no structural evidence was provided, this was a rapid way to gain an insight on the binding based on the discrimination patterns these BBVs provided, demonstrating an effective way to study binding characteristics. The discriminatory power of the array of BBVs was also examined for sugar acids including the biologically relevant glucuronic acid, which is a main structural motif for river blindness biomarker.

2.6. Experimental

General. All reagents and chemicals were of at least analytical grade. Reactions were performed using standard syringe techniques and were carried out in oven-dried glassware under an argon atmosphere. Ultra pure water (> 14 MΩ cm) obtained from a Millipore water system was used for each analysis unless otherwise stated. All saccharides and sugars were used as received.

2.5.1 Synthesis

Synthesis of ortho-monoalkylated dipyridyl-(1-(2-boronic acid-benzyl)-[4-4'] bipyridyl – 1-ium bromide

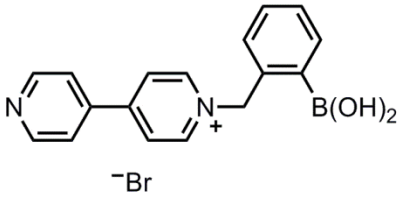

To a solution of 2-bromomethyl phenyl boronic acid (0.405 g, 1.86 mmol) in dry acetone (50 mL) was added 4,4'-dipyridyl (1.16g, 7.4 mmol), the reaction was stirred at 25°C for 1 h. After the reaction went to completion, the solution was decanted onto a 100 mL round bottom flask and diethyl ether (100 mL) was added. The off-white precipitate was collected by centrifugation, washed with acetone several times, and then dried under a stream of argon (0.5 g, 72% yield). ^{1}H-NMR (500 MHz, d_2o) δ 8.91 (d, J=5.0 Hz, 2H), 8.74 (d, J=5.0Hz, 2H), 8.60 (d, J=5.0Hz, 2H), 8.32 (d, J=5.0Hz, 2H), 7.86 (d, J=5.0Hz, 1H), 7.78 (d, J=5.0Hz, 1H), 7.72 (d, J=5.0Hz, 1H), 7.56 (m ,1H), 6.02 (s, 2H). ^{13}C-NMR (D_2O, 125MHz) δ 155.20, 151.45, 146.39,

143.74, 137.34, 136.46, 132.61, 123.49, 130.92, 127.02, 123.84, 65.69; ^{11}B-NMR (160MHz, D_2O) δ= +28.2

Synthesis of para- Monoalkylated dipyridyl (1-(2-boronic acid-benzyl)-[4-4'] bipyridyl – 1-ium bromide

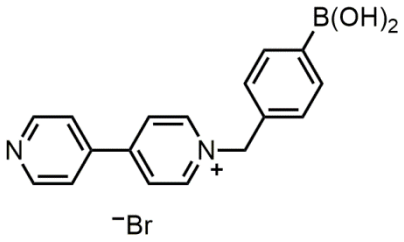

To a solution of 4-bromomethyl phenyl boronic acid (0.405 g, 1.86 mmol) in dry acetone (50 mL) was added 4,4'-dipyridyl (1.16 g, 7.4 mmol), the reaction was stirred at 25°C for 4 h. After the reaction went to completion, the solution was decanted onto a 100 mL round bottom flask and diethyl ether (100 mL) was added. The off-white precipitate was collected by centrifugation, washed with acetone several times, and then dried under a stream of argon (0.43 g, 69% yield). ^{1}H NMR (600 MHz, D_2O) δ 9.04 (d, J=6Hz, 2H), 8.78 (d, J=6Hz, 2H), 8.63 (d, J=6Hz, 2H), 8.42 (d, J=6Hz, 2H), 7.86 (dd, J=6Hz, 10Hz, 4H), 5.91 (s, 2H); ^{11}B-NMR (160MHz, D_2O) δ= +28.2.

Synthesis of para- Monoalkylated dipyridyl (1-(2-boronic acid-benzyl)-[4-4'] bipyridyl – 1-ium bromide

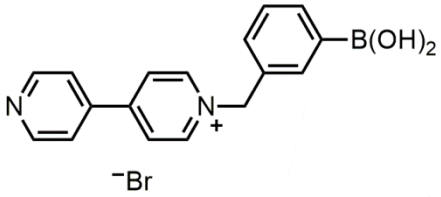

To a solution of 3-bromomethyl phenyl boronic acid (0.405 g, 1.86 mmol) in dry acetone (50 mL) was added 4,4'-dipyridyl (1.16 g, 7.4 mmol), the reaction was stirred at 25°C for 4 h. After the reaction went to completion, the solution was decanted onto a 100 mL round bottom flask and diethyl ether (100 mL) was added. The off-white precipitate was collected by centrifugation, washed with acetone several times, and then dried under a stream of argon (0.399 g, 57% yield). ^{1}H NMR (500 MHz, D_2O) δ 9.03 (d, J=5Hz, 2H), 8.78 (d, J=5Hz, 2H), 8.65 (d, J=5Hz, 2H), 8.41 (d, J=6Hz, 2H), 7.91 (m, 1H), 7.87 (m, 1H), 7.79(m, 1H), 7.56 (m, 1H), 5.91 (s, 2H); ^{11}B-NMR (160MHz, D_2O) δ= +28.2

Synthesis of 1-benzyl-1'-(2-boronobenzyl)-4,4'-bipyridine-1,1'-dium (oMBV)

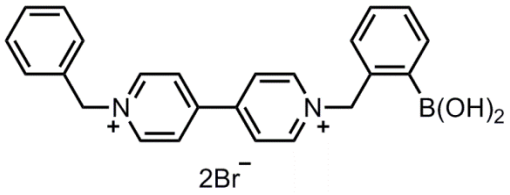

To a solution of 4, 4'-monoalkylated bipyridyl boronic acid salt (0.275 g, 0.74 mmol) in MeCN (10 mL) was added MeOH (0.65 mL) dropwise. The reaction stirred for 10 minutes, benzyl bromide (0.130 mL, 1.1 mmol) was added and the reaction stirred at 50°C for 24 h. The resulting orange solution was cooled to room temperature and diluted with acetone (30 mL) to precipitate out the product as a pale yellow solid. The solution was stored at 4^{o}C for 1 h to induce further precipitation. The precipitate was collected by centrifugation, washed with acetone, and dried under a stream of argon to give a pale yellow solid (0.270 g, 66%). ^{1}H NMR (500 MHz, D_2O) δ 9.16 (d, J=10.0Hz, 2H), 9.07(d, J=5 Hz, 2H), 8.49 (dd, J=5, 10Hz, 4H), 7.79 (d, J=5, 1H), 7.55 (m, 5H), 6.10 (s, 2H), 5.95 (s, 2H); ^{13}C NMR (126 MHz, D_2O) δ 151.55, 146.73, 136.37, 133.47, 132.42, 131.42, 130.94, 130.58, 127.89, 66.08; ^{11}B NMR (160 MHz, D_2O) δ +29.83.

Synthesis of 1-benzyl-1'-(3-boronobenzyl)-4,4'-bipyridine-1,1'-diium (mMBV)

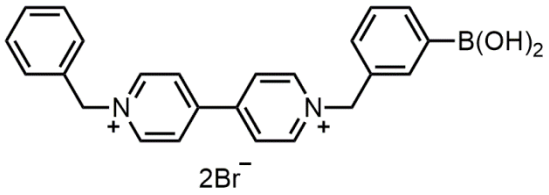

To a solution of 4,4'-monoalkylated bipyridyl boronic acid salt (0.275 g, 0.74 mmol) in MeCN (10 mL)was added MeOH(~0.65 mL) dropwise. The reaction stirred for 10 minutes, benzyl bromide (0.130 mL, 1.1 mmol) was added and the reaction was stirred at 50°C for 24 h. The resulting orange solution was cooled to room temperature and diluted with acetone (30 mL) to precipitate out the product as a pale yellow solid. The solution was stored at 4^{o}C for ~1 hour. The precipitate was collected by centrifugation, washed with diethyl ether, and dried under a stream of argon. ^{1}H-NMR (D_2O, 500 MHz) δ 9.18 (d, J=10Hz, 2H), 9.08 (d, J=5Hz, 2H), 8.55 (dd, J=5Hz, 20, 4H), 7.80(d, J=5Hz, 1H), 7.65 (m, 8H), 6.10 (s, 2H), 5.95 (s, 2H). ^{13}C-NMR (D_2O, 126 MHz) δ 151.55, 146.92, 136.75, 136.37, 133.47, 132.42, 131.42, 130.94, 130.58, 128.36, 127.89, 66.08. ^{11}B-NMR (160MHz, D_2O) δ= +28.2

Synthesis of 1-benzyl-1'-(4-boronobenzyl)-4,4'-bipyridine-1,1'-diium (pMBV)

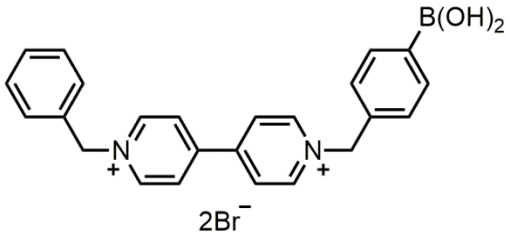

To a solution of 4,4'-monoalkylated bipyridyl boronic acid salt (0.275 g, 0.74 mmol) in MeCN (10 mL)was added MeOH (~0.65 mL) dropwise. The reaction stirred for 10 minutes, benzyl bromide (0.130 mL, 1.1 mmol) was added and the reaction was stirred at 25°C for 24 h. The resulting orange solution was cooled to room temperature and diluted with diethyl ether (30 mL) to precipitate out the product as a pale yellow solid. The solution was stored at 4^{o}C for ~1 hour. The precipitate was collected by centrifugation, washed with diethyl ether, and dried under a stream of argon. ^{1}H-NMR (D_2O, 500 MHz) δ 9.18, 9.17, 8.55, 8.54, 7.85, 7.84, 7.55, 7.53, 5.96, 5.95.

2.5.2. Multiwell Fluorescence Measurements

Construction of boronic acid array for sugar alcohol or sugar acid analysis

The boronic acid array was pipetted onto a 96-well (Fisherbrand®, flat-bottom, clear polystyrene, non-sterile) by preparing a stock "probe" solution of each boronic acid receptor at its respective quencher: dye ratio prepared as a twofold concentration in 0.1M NaH_2PO_4/Na_2HPO_4 pH 7.4 buffer. For 4, 4'-, 3, 4'-, 3, 3'-*o*-BBV and 4, 4'-*o*, *m*-BBV a ratio of 125:1 was used. For 4, 7-*o*-PBBV a ratio of 30:1 was used. For pBoB a ratio of 3:1 was used. To each receptor, solution was added HPTS (8 μM) to complete the probe solution. Blank wells were given 40 μL of the sodium phosphate buffer. Baseline fluorescence ("probe") wells were given 20 μL of the probe and sodium phosphate buffer. The rest of the wells received 20 μL of probe and analyte.

	1	2	3	4	5	6	7	8	9	10	11	12
A		Sugar 1 →			Sugar 2 →			Sugar 3 →			Sugar 4 →	
B		Sugar 5 →			Sugar 6 →			Sugar 7 →			Sugar 8 →	
C		Sugar 9 →			Sugar 10 →			Sugar 11 →			Sugar 12 →	
D		Sugar 13 →			Sugar 14 →			Sugar 15 →			Sugar 16 →	
E		Sugar 17 →			Sugar 18 →			Sugar 19 →			Sugar 20 →	
F		Sugar 21 →			Sugar 22 →			Sugar 23 →			Sugar 24 →	
G		Sugar 25 →			Sugar 26 →			Sugar 27 →			Sugar 28 →	
H		Sugar 29 →			Sugar 30 →			"blank" →			"probe" →	

Figure 2.18. Map of the multi-well plate for sugar alcohol and sugar acid study that outlines the location of each sugar and probe used.

Analysis of Sugar Alcohols

Serial dilutions of each sugar alcohol or permeability marker were prepared as a twofold concentration in 0.1M NaH_2PO_4/Na_2HPO_4 pH 7.4 buffer to obtain eight data points for each analyte. Each data point was then measured with each receptor and the fluorescence recovery was obtained. Upon running assays, each well received 20 μL of probe solution and 20 μL of analyte solution. Blank wells received 40 μL of sodium phosphate buffer. The fluorescence recovery of HPTS was read using a 96-well plate on a 2103 Envision Multilabel Perkin Elmer reader (excitation filter: 405 nm, emission filter: 535 nm). After background (blank) subtraction, the relative fluorescence increase F/F_o for each receptor/analyte combination was calculated, resulting in an individual recognition pattern for each analyte and receptor.

2.5.3. DFT Analysis of Sugar Alcohol Binding

B3LYP/6-31+G* minimized structures of the lowest energy conformers described in the text

Trigonal Erythritol Borane **(*Erythro*-1-2-)**

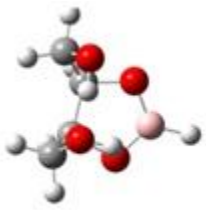

Energy = -483.677523 hartree

C	-0.837779	0.243774	0.855190
C	0.281655	-0.842778	0.742574
H	-1.215614	0.274388	1.884532
H	0.201453	-1.519054	1.604801
O	-1.891157	-0.281671	0.015831
O	-0.070143	-1.601973	-0.438144
B	-1.363236	-1.260858	-0.772279
H	-1.957883	-1.791512	-1.651682
C	-0.525465	1.687537	0.442927
H	0.212862	2.102989	1.150215
H	-1.449074	2.263678	0.558178
C	1.750715	-0.428990	0.629292
H	2.008454	0.307934	1.396016
H	2.375438	-1.317406	0.790625
O	-0.115127	1.854122	-0.897470
H	0.777973	1.464859	-0.984290
O	2.075839	0.161308	-0.629316
H	1.852521	-0.493146	-1.314093

Trigonal Threitol Borane **(*Threo*-1-2-)**

Energy = -483.6805357 hartree

C	-0.473153	-0.239611	-0.613717
C	0.473142	-0.239648	0.613729
H	0.049678	-0.590882	-1.511336
O	-0.804147	1.158767	-0.818805
O	0.804208	1.158719	0.818840
B	0.000060	1.905705	0.000010
C	-1.762809	-1.032144	-0.430122
H	-1.524633	-2.082298	-0.227633
H	-2.345503	-0.990317	-1.361384
O	-2.532870	-0.577680	0.674071
H	-2.806838	0.334972	0.486548
H	-0.049684	-0.590892	1.511356
C	1.762791	-1.032208	0.430103
H	2.345494	-0.990431	1.361365
H	1.524626	-2.082353	0.227554
O	2.532806	-0.577706	-0.674087
H	2.806640	0.334991	-0.486598
H	0.000129	3.093543	-0.000026

Tetrahedral Erythritol Borate ester **(*Erythro*-1-2-)**

Energy = -559.5865407 hartree

C	-0.608907	-1.000068	0.573992
C	0.114234	0.194360	1.277833
H	-0.708971	-1.794887	1.346342
H	-0.128117	0.198013	2.356032
O	0.275984	-1.423313	-0.430429
O	1.482332	-0.115575	1.112474
B	1.632827	-0.856727	-0.158117
C	-2.041600	-0.796899	0.061262
H	-2.664815	-0.495269	0.926730
H	-2.411759	-1.775653	-0.276037
C	-0.200407	1.610393	0.767067
H	-1.232937	1.886959	1.025634
H	0.479007	2.304921	1.287325
O	-2.236739	0.111702	-1.011099
H	-1.456723	0.712790	-1.067881
O	-0.077890	1.773309	-0.644599
H	0.741963	1.276226	-0.944575
H	2.499314	-1.725401	-0.096982
O	1.970432	0.145849	-1.244765
H	1.826034	-0.286548	-2.099568

Tetrahedral Threitol Borate ester **(*Threo*-1-2-)**

Energy = -559.5901149 hartree

C	-0.786590	-0.378628	-0.288439
C	0.309563	-0.868041	0.701529
H	-0.650189	-0.820102	-1.288330
O	-0.651852	1.030312	-0.364776
O	0.739503	0.293963	1.378903
B	0.493645	1.459242	0.513640
C	-2.207001	-0.680674	0.207847
H	-2.270223	-0.452416	1.284839
H	-2.470224	-1.736282	0.056742
O	-3.159223	0.103302	-0.512444
H	-2.689596	0.954159	-0.631514
H	0.210520	2.473669	1.141946
O	1.720844	1.675180	-0.337834
H	1.469862	2.229566	-1.091040
H	-0.122112	-1.567638	1.443458
C	1.472420	-1.620485	0.032829
H	2.209696	-1.854148	0.822296
H	1.096394	-2.576689	-0.366177
O	2.090685	-0.939305	-1.043141
H	2.097646	0.033038	-0.828690

Sorbitol Boronate Ester **(*Syn*-1-3-)**

Energy = -712.747835 hartree

C	0.656660	-0.772771	-0.428955
C	-0.653414	-0.054123	-0.769877
C	1.837604	0.140514	-0.803851
H	-0.686360	0.099973	-1.855082
H	0.717242	-1.678192	-1.056367
H	1.813544	0.299716	-1.891802
B	0.480139	1.908503	0.158575
O	-0.679096	1.257296	-0.148624
O	1.720786	1.419081	-0.154589
C	3.215126	-0.417914	-0.449037
H	3.989846	0.264027	-0.822556
H	3.357252	-1.395585	-0.920016
C	-1.933807	-0.836650	-0.403739
H	-1.705769	-1.903936	-0.516650
O	0.640011	-1.122966	0.947813
H	1.563032	-1.238693	1.247607
O	3.373727	-0.627873	0.957997
H	3.356387	0.243991	1.387801
O	-2.968165	-0.540609	-1.337887
H	-3.513839	0.155922	-0.925680
C	-2.449510	-0.583852	1.024675
H	-1.630251	-0.632956	1.747782
H	-3.194646	-1.344398	1.274026
O	-3.142468	0.667184	1.091638
H	-2.475708	1.362034	0.952022
H	0.414248	2.957453	0.719949

D-mannitol Boronate ester **(*Anti*-1-3-)**

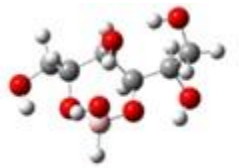

Energy = -712.7421689 hartree

C	0.654279	0.723500	0.834816
C	-0.801644	0.207077	0.804946
C	1.513762	0.003566	-0.213836
H	-1.332906	0.624202	1.667984
H	1.052786	0.463942	1.825755
O	-0.801109	-1.225565	0.972293
O	1.360464	-1.430749	-0.068944
C	-1.618403	0.533494	-0.461659
H	-1.123039	0.104828	-1.344615
O	0.759363	2.130735	0.721785
H	0.041056	2.447444	0.141476
O	-1.644252	1.969970	-0.555281
H	-2.074956	2.233488	-1.384007
C	-3.058362	-0.010222	-0.394950
H	-3.643470	0.457902	-1.195643
H	-3.514453	0.283895	0.563319
O	-3.149161	-1.406086	-0.615868
H	-2.628229	-1.846920	0.076577
H	1.193204	0.266436	-1.230214
C	3.003117	0.304765	-0.082872
H	3.173567	1.373611	-0.227828
H	3.342412	0.030158	0.928600
O	3.761177	-0.371682	-1.075099
H	3.571174	-1.320933	-0.992578
C	0.259487	-1.973639	0.515491
H	0.197060	-3.155910	0.643963

2.6. References

1. Robbins, G. B.; Upson, F. W., Some Fully Acetylated Sugar Acids and their Derivatives. *J. Am. Chem. Soc.* **1940,** *62,* 1074-1076.

2. Sturgeon, R. J., 1 - Monosaccharides. In *Methods in Plant Biochemistry*, P.M, D. E. Y., Ed. Academic Press: 1990; vol. 2,1-37.

3. Lewis, D. H.; Smith, D. C., Sugar alcohols (polyols) in fungi and green plants in distribution physiology and metabolism. *New Phyto.* **1967,** *66,* 143.

4. Beck, E.; Hopf, H., 7 - Branched-chain Sugars and Sugar Alcohols. In *Methods in Plant Biochemistry*, P.M, D. E. Y., Ed. Academic Press: 1990; Vol. 2, 235-289.

5. Bieleski, R. L., Sugar Alcohols. In *Plant Carbohydrates I: Intracellular Carbohydrates*, Loewus, F. A.; Tanner, W., Eds. Springer Berlin Heidelberg: Berlin, Heidelberg, 1982;158-192.

6. Lavigne, J. J.; Anslyn, E. V., Teaching Old Indicators New Tricks: A Colorimetric Chemosensing Ensemble for Tartrate/Malate in Beverages. *Angew. Chem.-Intl. Ed.* **1999,** *38,* 3666-3669.

7. Boulton, R., Relationships Between Total Acidity, Titratable Acidity and pH in Wine. *Am. J. Enol. Viticul.* **1980,** *31,* 76-80.

8. Dwivedi, C.; Heck, W. J.; Downie, A. A.; Larroya, S.; Webb, T. E., Effect of calcium glucarate on beta-glucuronidase activity and glucarate content of certain vegetables and fruits. *Biochem. Med. Metabol. Biol.* **1990,** *43*, 83-92.

9. Blumenthal, H. J.; Lucuta, V. L.; Blumenthal, D. C., Specific enzymatic assay for D-glucarate in human serum. *Anal. Biochem.* **1990,** *185*, 286-293.

10. Walaszek, Z.; Szemraj, J.; Narog, M.; Adams, A. K.; Kilgore, J.; Sherman, U.; Hanausek, M., Metabolism, uptake, and excretion of a D-glucaric acid salt and its potential use in cancer prevention. *Cancer Det. Prev.* **1997,** *21*, 178-190.

11. Heerdt, A. S.; Young, C. W.; Borgen, P. I., Calcium glucarate as a chemopreventive agent in breast-cancer. *Israel J. Med. Sci.* **1995,** *31*, 101-105.

12. Abouissa, H.; Dwivedi, C.; Curley, R. W.; Kirkpatrick, R.; Koolemansbeynen, A.; Engineer, F. N.; Humphries, K. A.; Elmasry, W.; Webb, T. E., Basis for the antitumor and chemopreventive activities of glucarate and the glucarate-retinoid combination. *Anticancer Res.* **1993,** *13*, 395-399.

13. Palmer, D. R. J.; Gerit, J. A., Evolution of enzymatic activities: Multiple pathways for generating and partitioning a common enolic intermediate by glucarate dehydratase from Pseudomonas putida. *J. Am. Chem. Soc.***1996,** *118*, 10323-10324.

14. Trudgill, P. W.; Widdus, R., D-glucarate catabolism by pseudomonadaceae and enterobacteriaceae. *Nature* **1966,** *211*, 1097.

15. Miron, C. E.; Petitjean, A., Sugar Recognition: Designing Artificial Receptors for Applications in Biological Diagnostics and Imaging. *Chembiochem* **2015,** *16*, 365-379.

16. Wright, A. T.; Anslyn, E. V., Differential receptor arrays and assays for solution-based molecular recognition. *Chem.Soc. Rev.***2006,** *35*, 14-28.

17. Lorand, J. P.; Edwards, J. O., Polyol complexes and structure of the benzeneboronate ion. *J. Org. Chem.***1959,** *24* , 769-774.

18. Lorand, E. J.; Edwards, E. I., Para-methylbenzyl hydroperoxide. *J. Am. Chem. Soc.* **1955,** *77*, 4035-4037.

19. Swamy, K. M. K.; Jang, Y. J.; Park, M. S.; Koh, H. S.; Lee, S. K.; Yoon, Y. J.; Yoon, J., A sorbitol-selective fluorescence sensor. *Tetrahedron Lett.* **2005,** *46*, 3453-3456.

20. Gao, X. M.; Zhang, Y. L.; Wang, B. H., New boronic acid fluorescent reporter compounds. 2. A naphthalene-based on-off sensor functional at physiological pH. *Org. Lett.* **2003,** *5*, 4615-4618.

21. Wang, J. F.; Jin, S.; Akay, S.; Wang, B. H., Design and synthesis of long-wavelength fluorescent boronic acid reporter compounds. *Eur. J. Org.Chem.* **2007,** 2091-2099.

22. Liu, S.; Bai, H.; Sun, Q.; Zhang, W.; Qian, J., Naphthalimide-based fluorescent photoinduced electron transfer sensors for saccharides. *RSC Adv.* **2015,** *5*, 2837-2843.

23. Wang, J. F.; Jin, S.; Lin, N.; Wang, B. H., Fluorescent indolylboronic acids that are useful reporters for the synthesis of boronolectins. *Chem. Biol. & Drug Design* **2006,** *67*, 137-144.

24. Akay, S.; Yang, W. Q.; Wang, J. F.; Lin, L.; Wang, B. H., Synthesis and evaluation of dual wavelength fluorescent benzo b thiophene boronic acid derivatives for sugar sensing. *Chem. Biol. & Drug Design gn* **2007,** *70*, 279-289.

25. Gray, C. W.; Houston, T. A., Boronic acid receptors for alpha-hydroxycarboxylates: High affinity of Shinkai's glucose receptor for tartrate *J. Org. Chem.* **2002,** *67*, 5426-5428.

26. Takeuchi, M.; Yamamoto, M.; Shinkai, S., Fluorescent sensing of uronic acids based on a cooperative action of boronic acid and metal chelate. *Chem. Comm.* **1997,** 1731-1732.

27. Yamamoto, M.; Takeuchi, M.; Shinkai, S., Molecular design of a PET-based chemosensor for uronic acids and sialic acids utilizing a cooperative action of boronic acid and metal chelate. *Tetrahedron* **1998,** *54*, 3125-3140.

28. Yang, W. Q.; Yan, J.; Fang, H.; Wang, B. H., The first fluorescent sensor for D-glucarate based on the cooperative action of boronic acid and guanidinium groups. *Chem. Comm.* **2003,** 792-793.

29. Zhu, L.; Anslyn, E. V., Facile quantification of enantiomeric excess and concentration with indicator-displacement assays: An example in the analyses of alpha-hydroxyacids. *J. Am. Chem. Soc.***2004,** *126*, 3676-3677.

30. Jianzhang, Z.; James, T. D., Chemoselective and enantioselective fluorescent recognition of sugar alcohols by a bisboronic acid receptor. *J. Mat. Chem.* **2005,** *15*, 2896-901.

31. Zhao, J. Z.; Davidson, M. G.; Mahon, M. F.; Kociok-Kohn, G.; James, T. D., An enantioselective fluorescent sensor for sugar acids. *J. Am. Chem. Soc.* **2004,** *126*, 16179-16186.

32. Hosseinzadeh, R.; Mohadjerani, M.; Pooryousef, M., A new selective fluorene-based fluorescent internal charge transfer (ICT) sensor for sugar alcohols in aqueous solution. *Anal. Bioanal. Chem.* **2016,** *408*, 1901-1908.

33. Jin, S.; Zhu, C. Y.; Cheng, Y. F.; Li, M. Y.; Wang, B. H., Synthesis and carbohydrate binding studies of fluorescent alpha-amidoboronic acids and the corresponding bisboronic acids. *Bioorg.Med. Chem.* **2010,** *18*, 1449-1455.

34. Gamsey, S.; Miller, A.; Olmstead, M. M.; Beavers, C. M.; Hirayama, L. C.; Pradhan, S.; Wessling, R. A.; Singaram, B., Boronic acid-based bipyridinium salts as

tunable receptors for monosaccharides and alpha-hydroxycarboxylates. *J. Am. Chem. Soc.* **2007,** *129*, 1278-1286.

35. Norrild, J. C., An illusive chiral aminoalkylferroceneboronic acid. Structural assignment of a strong 1 [ratio] 1 sorbitol complex and new insight into boronate-polyol interactions. *J. Chem. Soc., Perkin Trans. 2* **2001,** 719-726.

36. Badugu, R.; Lakowicz, J. R.; Geddes, C. D., Fluorescence sensors for monosaccharides based on the 6-methylquinolinium nucleus and boronic acid moiety: potential application to ophthalmic diagnostics. *Talanta* **2005,** *65*, 762-768.

37. Arimori, S.; Murakami, H.; Takeuchi, M.; Shinkai, S., Sugar-Controlled Association and Photoinduced Electron-Transfer in Boronic-Acid-Appended Porphyrins. *J. Chem. Soc., Chem. Commun.*, **1995,** 961-962.

38. Sharrett, Z.; Gamsey, S.; Levine, P.; Cunningham-Bryant, D.; Vilozny, B.; Schiller, A.; Wessling, R. A.; Singaram, B., Boronic acid-appended bis-viologens as a new family of viologen quenchers for glucose sensing. *Tetrahedron Lett.* **2008,** *49*, 300-304.

39. Evans, W. J.; McCourtney, E. J.; Carney, W. B., A comparative analysis of the interaction of borate ion with various polyols. *Anal. Biochem.* **1979,** *95*, 383-386.

40. Van Duin, M.; Peters, J. A.; Kieboom, A. P. G.; Van Bekkum, H., Studies on borate esters II11For part I see reference 7. *Tetrahedron* **1985,** *41*, 3411-3421.

41. Peters, J. A., Interactions between boric acid derivatives and saccharides in aqueous media: Structures and stabilities of resulting esters. *Coord. Chem.Rev.* **2014,** *268*, 1-22.

42. Liang, X.; James, T. D.; Zhao, J., 6,6 '-Bis-substituted BINOL boronic acids as enantio selective and chemoselective fluorescent chemosensors for D-sorbitol. *Tetrahedron* **2008,** *64*, 1309-1315.

43. Cordes, D. B.; Singaram, B., A unique, two-component sensing system for fluorescence detection of glucose and other carbohydrates. *Pure Appl. Chem.* **2012,** *84*, 2183-2202.

44. Gamsey, S.; Baxter, N. A.; Sharrett, Z.; Cordes, D. B.; Olmstead, M. M.; Wessling, R. A.; Singaram, B., The effect of boronic acid-positioning in an optical glucose-sensing ensemble. *Tetrahedron* **2006,** *62*, 6321-6331.

45. Sharrett, Z.; Gamsey, S.; Fat, J.; Cunningham-Bryant, D.; Wessling, R. A.; Singaram, B., The effect of boronic acid acidity on performance of viologen-based boronic acids in a two-component optical glucose-sensing system. *Tetrahedron Lett.* **2007,** *48*, 5125-5129.

46. Suri, J. T.; Cordes, D. B.; Cappuccio, F. E.; Wessling, R. A.; Singaram, B., Monosaccharide detection with 4,7-phenanthrolinium salts: Charge-induced fluorescence sensing. *Langmuir* **2003**, *19*, 5145-5152.

47. Gamsey, S.; Suri, J. T.; Wessling, R. A.; Singaram, B., Continuous Glucose Detection Using Boronic Acid-Substituted Viologens in Fluorescent Hydrogels: Linker Effects and Extension to Fiber Optics. *Langmuir* **2006,** *22*, 9067-9074.

48. Jurs, P. C.; Bakken, G. A.; McClelland, H. E., Computational methods for the analysis of chemical sensor array data from volatile analytes. *Chem. Rev.* **2000,** *100*, 2649-2678.

49. Vanduin, M.; Peters, J. A.; Kieboom, A. P. G.; Vanbekkum, H., The pH-dependence of the stability esters of boronic-acid and borate in aqueous-medium studied by B-11 NMR. *Tetrahedron* **1984,** *40*, 2901-2911.

50. Vanduin, M.; Peters, J. A.; Kieboom, A. P. G.; Vanbekkum, H., Studies on borate esters. Synergic coordination of calcium in borate polyhydroxycarboxylate systems. *Carb. Res.***1987,** *162*, 65-78.

51. Djanashvili, K.; Frullano, L.; Peters, J. A., Molecular recognition of sialic acid end groups by phenylboronates. *Chem.-a Eur. J.* **2005,** *11*, 4010-4018.

52. Globisch, D.; Moreno, A. Y.; Hixon, M. S.; Nunes, A. A. K.; Denery, J. R.; Specht, S.; Hoerauf, A.; Janda, K. D., Onchocerca volvulus-neurotransmitter tyramine is a biomarker for river blindness. *Proc. Nalt. Acad. Sci.U.S.A.* **2013,** *110*, 4218-4223.

53. Schiller, A.; Vilozny, B.; Wessling, R. A.; Singaram, B., Recognition of phospho sugars and nucleotides with an array of boronic acid appended bipyridinium salts. *Anal. Chim. Acta* **2008,** *627*, 203-211.

CHAPTER 3

Improving Boronic Acid Recognition of Carbohydrates via Reduction of Aldoses and Dechlorination of Sucralose

3.1. Introduction

Analysis of carbohydrates in solution continues to be an important aspect of several areas of research for the environmental,[1] food,[2] pharmaceutical,[3] and petrochemical[4] industries. The wide diversity of carbohydrates continues to create a challenge: these targets can exist as simple monosaccharides or complex branched oligomers in nature. Carbohydrates (also referred to as saccharides or sugars) not only provide nutritional value to cells, but also have roles as structural material in plants (cellulose); participate in cell–cell recognition through interactions of glycoproteins or glycolipids; and are also part of the genetic makeup of cells as being a major component in nucleotides.[5] This wide range of applicability has prompted researchers to develop a range of analytical tools for carbohydrates and their derivatives.

3.1.1 Analytical Methodologies for Carbohydrate Analysis

Methodologies developed over the years can be categorized as enzymatic or non-enzymatic. The former can be specific, depending on the target analyte, and the latter usually are chromatographic methods (HPLC, GC, or CE). Derivatization of reducing sugars is often performed by reductive amination using an amine and strong chromophores or fluorophores, such as 4-aminobenzoic acid ethyl ester,[6] 2-aminobenzoic acid,[7] 4-aminobenzoic acid,[8,9] 4-aminobenzonitrile,[10] 2-aminopyridine,[11] and S-(-)-1-phenylethylamine.[12]

Although effective, there are some drawbacks that accompany chromatography. For instance, carbohydrates have no intrinsic chromophore, therefore a tag for labeling is added as the basis for detection and characterization (Scheme 3.1).[13-15]

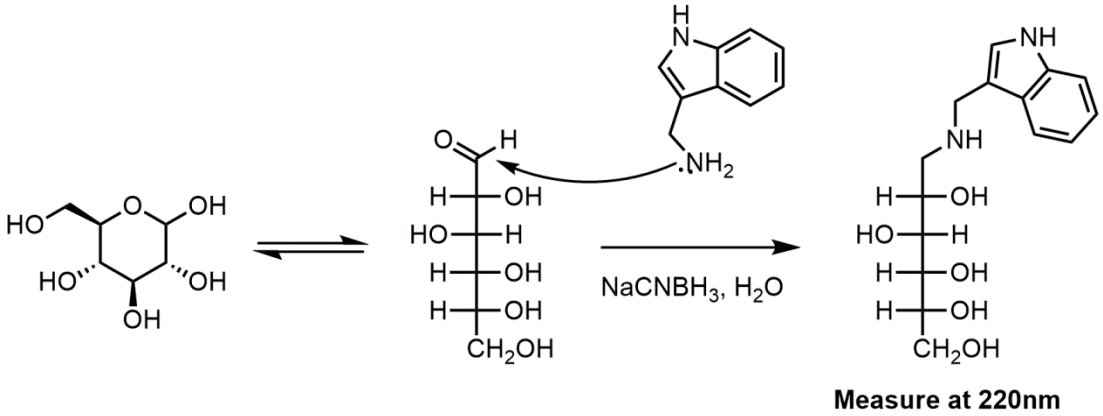

Scheme 3.1. Labeling of D-glucose with tryptamine followed by reductive amination.[15]

After being derived from a source, individual saccharides must be separated if the sample contained a mixture of sugars. Analyses of twelve carbohydrates were conducted through micellar electrokinetic capillary chromatography to determining their concentrations in sample mixtures. A multitude of sugars were analyzed: three pentoses (D-ribose, L-arabinose, and D-xylose); three hexoses (D-glucose, D-mannose, and D-galactose); two deoxy sugars (L-rhamnose and L-fucose; two uronic acids (D-glucuronic acid and D-galacturonic acid); and two disaccharides (cellobiose and melibiose) using D-thyminose as the internal standard. This chromatographic method allowed analysis within one hour with excellent sensitivity in the picomolar range and good linearity in the 25–2500 μM range. Upon derivatization, separation

through capillary electrophoresis allowed good differentiation among the sugars examined (Figure 3.1).

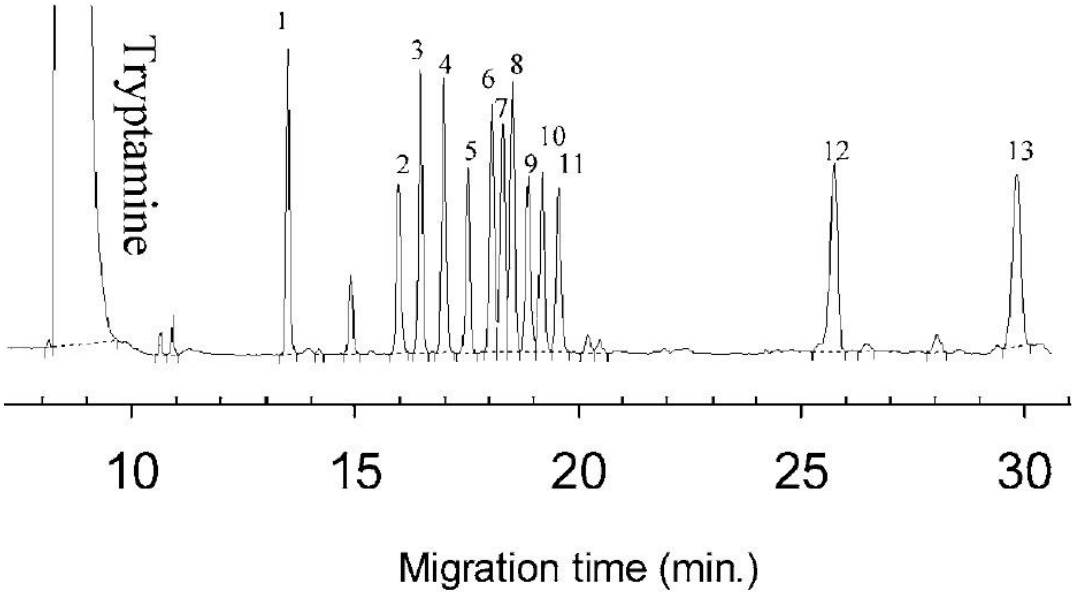

Figure 3.1. Electropherogram of tryptaminated carbohydrates using a pH 9.7 buffer post-derivatization. Reproduced with permission from Ref.[15]

It is important to separate target analytes from potential interfering species before analysis of derivatized carbohydrates using tryptamine, because proteins and other biomolecules containing tryptophan will interfere with the derivatized carbohydrate product. Tryptamine has absorption peak maxima at λ = 197, 220, and 276 nm, with the 220-nm detection providing high sensitivity and minimizes interference from other compounds. Optimal separation conditions for the present study required 35 mM cholate, 100 mM borate, and 2% propanol, adjusted to pH 9.7. Migration is assisted by the carbohydrate-borate complex, which can greatly affect migration time and signal response. Although effective separation and high sensitivity can be

achieved using this chromatographic method, there are limitations, as there are with any analytical method. One major drawback is the costly and time-consuming process for the analysis of multiple samples at a given time.

3.1.2. Non-chromatographic Recognition of Carbohydrates

From the drawbacks of chromatographic methods, non-enzymatic methods have been developed that take advantage of other chemistries such as supramolecular and boronic acid chemistries, which have become a major research area focused on developing glucose sensors,[16,17] and chemoreceptors for other carbohydrate targets.[18] Supramolecular chemistry takes advantage of a host–guest type interaction through intermolecular forces (i.e., hydrogen bonding, ion pair, hydrophobic, cation-π, anion-π, or π-π interactions; see Scheme 3.2). Upon interaction, the system produces a detectable signal change.[19]

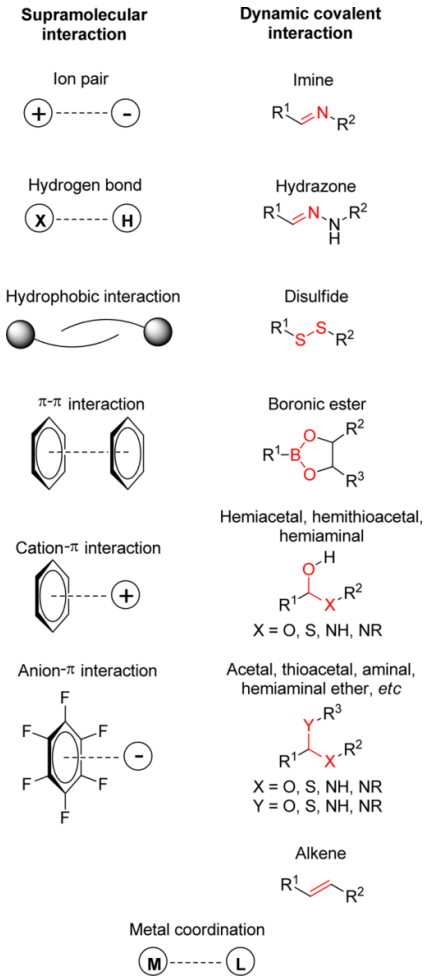

Scheme 3.2. Types of molecular interactions in supramolecular noncovalent and covalent interactions. Reproduced with permission from Ref.[20] Copyright 2015 American Chemical Society

Among the noncovalent interaction systems described over the years, one notable example is de Silva's pioneering work of crown ether-based receptors (or sensors) for alkaline metal ions: the interactions in this system are ion-dipole interactions.[21] In this system, the metal bond interaction has a more covalent character (Figure 3.2).

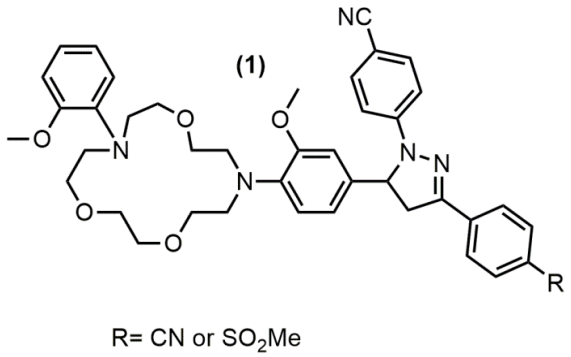

Figure 3.2. Structure of A. Prasanna de Silva's crown ether (**1**)

In the absence of the Na^+ ion, the crown ether unit participates in the photo-induced electron (PET) transfer of the fluorophore moiety, quenching the fluorescence. The fluorescence emission of the diazo crown ether sensor (**1**) displayed large Na^+-induced change. Upon forming the Na^+ complex, the receptor adopts a conformation with the methoxy groups in the axial position that deconjugates the nitrogen electron pair from the rest of the π-system, disrupting the PET mechanism. This receptor allows for selective recognition of Na^+ over K^+ with a 13-fold increase in fluorescence demonstrating one of the first examples of selective ion recognition.

On the other end of the spectrum, there exists a vast area of research that utilizes covalent interactions to construct receptor–guest assemblies through reversible or irreversible interactions.[22] This has grown into the field of "dynamic covalent chemistry" where constructs utilize the covalent interactions that include imine formation and exchange, hydrazone formation,[23] disulfide exchange,[24] olefin metathesis,[25] Diels-Alder,[26] acetal,[27] and hemiacetal formation.[20] The interaction that our two-component system exploits is the reversible boronic acid hemiacetal

formation upon interaction with diols, which is the foundation of boronic acid-based receptor–guest assemblies.

Although previously most assemblies have relied on noncovalent interactions for the recognition event between analyte and receptor, boronic acid methodology for the recognition of saccharides exploits the reversible covalent bonding of diols found in saccharides.[17,28] The advantage of using boronic acid-based chemistry for designing receptors is that it allows these chemoreceptors to be readily synthesized, to operate in range of pHs, and to have a plethora of possible host-reporter recognition systems.[29]

3.1.3. Signal Amplification for Analysis of a Sugar Analyte

Signal amplification in analytical method development is a way to increase signal modulation during analyte recognition. This is a useful strategy in immunoassay development when sensitivity for analyte detection is insufficient. Typically, concepts of signal amplification have been utilized for developing ultrasensitive biosensors or immunosensors using nanomaterial-based bioamplification strategies that can significantly improve sensitivity.[30-32] These methods rely on a nanomaterial such as gold nanoparticles (AuNPs), as a host for signal-generating labels for enhancement or as biosensors.[33-37] For example, Wang and coworkers developed a quartz crystal microbalance (QCM) sensor surface to measure carbohydrates with an increase in sensitivity of at least a 20-fold in the detection limit.[38] This was achieved by first self-assembling carbohydrates to AuNPs, which can then be used to amplify the mass of

the carbohydrate-boronic acid complex on the QCM surface. Quartz crystal microbalance measures only those materials that are acoustically coupled to the sensor surface. It is a binding-based detection rather than a proximity-based detection (e.g., Surface Plasmon Resonance, SPR) and requires the host-analyte complex to be rigid. Because the measurement relies on mass changes, the higher the molecular weight of the target and the higher density of recognition elements immobilized, the increase in mass produces a larger signal.

Mono- and disaccharides have relatively small mass (<1kDa) and due to the large mass requirement for QCM measurements, to measure carbohydrates of interest with high sensitivity an increase of mass is needed. Carbohydrates of interest were conjugated to AuNPs to assemble a larger "payload", as illustrated in Figure 3.3, and characterized by UV-Vis spectroscopy based on the unusual dependence of the optical and electronic properties of the AuNPs size and shape.

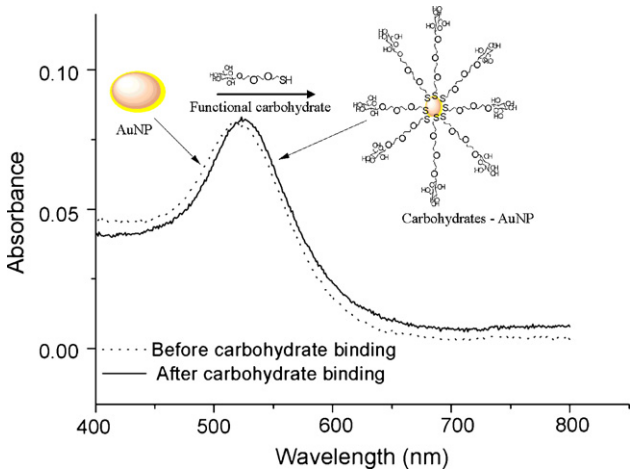

Figure 3.3. Self-assembly formation of carbohydrate-AuNPs, before (dot line) and after carbohydrate addition (solid line). Reproduced with permission from Ref.[38]

Assembly of carbohydrates on the AuNP surface provided a shift in the plasmon absorption peak shift from 520 nm to 526 nm, indicative of carbohydrate binding. Having this carbohydrate-AuNP assembly will provide a larger mass that can enhance the signal on the QCM sensor platform. Because QCM relies on the interfacial mass changes for the binding between the host (that is conjugated on the gold surface) and a ligand (analyte) that results in changes in the QCM oscillation frequency, the measurement is highly dependent on mass. Then, these self-assembled carbohydrate-AuNPs were analyzed against a boropolymer containing a cyanate group as a reactive chemical hand that would provide immobilization on an Au surface (Scheme 3.3).[38]

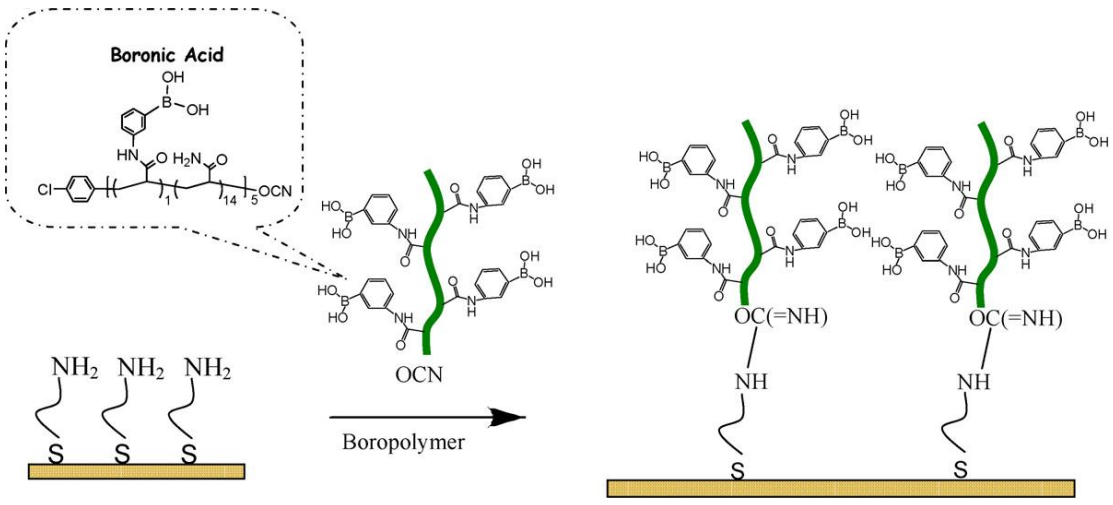

Scheme 3.3. Representation of the QCM sensor by immobilization of a boropolymer onto cysteamine-functionalized Au electrode. Reproduced with permission from Ref.[38]

Following the change of frequency of the Au surface allows the number of molecules interacting at that surface to be determined. By comparing the differences

in the change of frequency of carbohydrates without the added payload versus carbohydrate-assembled AuNPs can determine how significantly the added AuNPs increased the sensitivity of the measurement. Compared to the frequency of the baseline (curve b, of sensor surface only), the initial frequency decrease was only about 7 Hz when free mannose was added to the boropolymer-modified Au sensor (upper region of curve a in Figure 3.4).

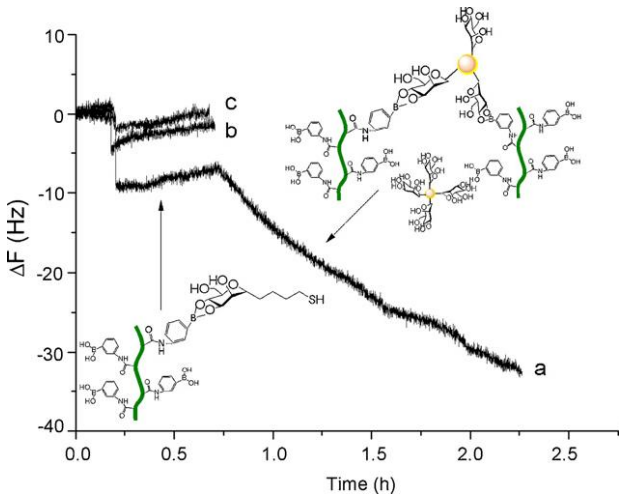

Figure 3.4. The frequency change versus time of the boropolymer-cysteamine modified Au surface exposed to mannose-thiol (upper part of a) and mannose-conjugated AuNPs (lower part of a).

However, when treating the sensor surface with carbohydrate-assembled AuNPs, the sensor yielded a frequency decrease of about 32 Hz (lower part of curve a), indicating that the mannose conjugated to AuNPs offered an amplification of signal change from the carbohydrate-boronic acid binding event. Overall, this sensor increased the sensitivity by 20-fold providing a detection and quantification limit of 2 μM and 50 μM, respectively. Although this technique is a fluorophore-free method,

there are drawbacks for purposes of practicality in analyzing complex mixtures and samples, such as those in blood, urine, or saliva. Analysis of these samples will require isolation of the target of interest to synthesize the AuNP assembly for increasing the payload of the target.

An example of signal amplification with fluorescent-based boronic acid chemoreceptor for signal enhancement has been reported by James and Jiang and coworkers, wherein an amphiphilic monoboronic acid that is highly selective for glucose undergoes an excimer emission enhancement upon aggregation.[39] The amphiphilic mono-boronic acid described by James and co-workers displayed a selective ratiometric fluorescent response toward glucose. This amphiphilic mono-boronic acid was assembled by conjugating a pyrene fluorophore moiety through a pyridinium amide linkage (Figure 3.5).

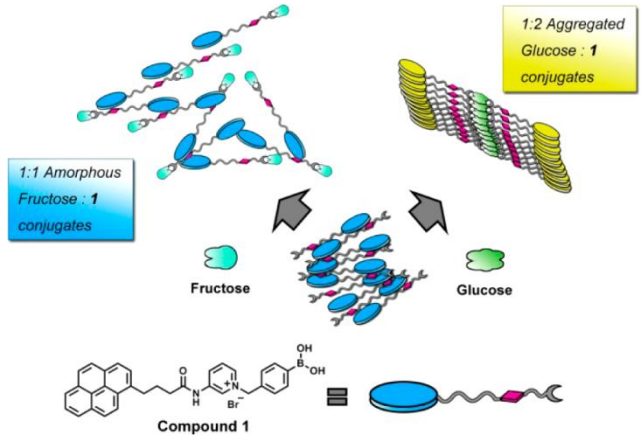

Figure 3.5. Illustration of the amphiphilic mono boronic acid and the formation of a 1:1 fructose complex compared to the 1:2 glucose aggregate complex. Reproduced with permission from ref.[39] Copyright 2013 American Chemical Society.

Having the cationic pyridinium group appended to the phenyl boronic would allow for a cation-π interaction that would quench the fluorescence of the pyrene monomer.[40] The amphiphilic compound **1** exhibited monomer fluorescence around 390 nm, whereas in the presence of glucose it led to the development of an excimer emission at 510 nm that increases in intensity as glucose concentration increases (Figure 3.6a). Compared to fructose, there is no excimer emission at 510 nm (Figure 3.6b), which demonstrates that excimer emission is depended on glucose binding to establish a selective detection of glucose in the presence of fructose.

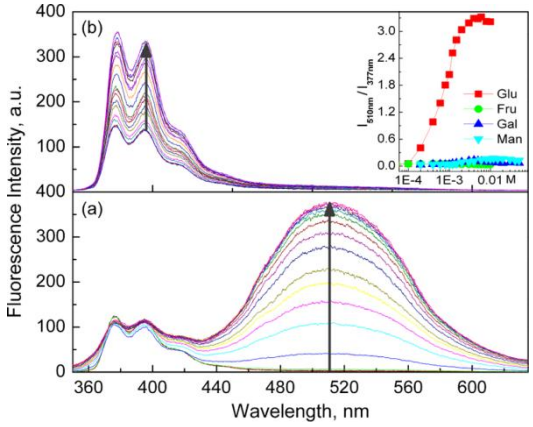

Figure 3.6. Fluorescence spectra of the amphiphilic compound in pH 10.00 carbonate buffer in the presence of D-glucose (a) and D-fructose (b) over 0–10 mM. The inset demonstrates the selectivity of the excimer (λ_{em}= 510 nm): monomer (λ_{em}= 377 nm) intensity ratio with increasing carbohydrate concentration. The excitation wavelength is λ_{ex}= 328 nm. Reproduced with permission from ref.[39] Copyright 2013 American Chemical Society.

The formation of this aggregate is pH independent; because phenyl boronic forms the boronate anion at pH > 9.5, no excimer was observed with increasing pH but only with increasing glucose. The aggregation formation with increasing glucose

correlated well with formation of relatively large particles. These pyridinium-pi interactions are a strong driving force for the aggregation for the amphiphilic compound in the presence of glucose over fructose, increasing its sensitivity with detection limits of 10 μM. For this reason, it was hypothesized based on binding and absorbance data that the amphiphilic compound forms a 1:2 (glucose:amphiphilic compound) complex in large aggregates, producing the excimer emission from the resulting stacking of pyrene moiety. Overall, this ratiometric fluorescent chemosensor based on an amphiphilic mono-boronic acid receptor compound provided excellent selectivity and sensitivity.

To date, indirect signal amplification for saccharides using boronic acid-based chemosensor detection system has not been utilized to measure chemically modified saccharides. With the interest of utilizing our two-component system for the recognition of saccharides with low binding affinities toward boronic acids, we aim to develop a method to increase the binding affinity to these saccharides that are of interest for use as permeability markers, such as fucose, L-rhamnose, xylose, and sucralose. Traditionally, these saccharides and sugar derivatives have given low binding constants to boronic acid receptor systems; the aim of this chapter is to demonstrate a way to improve boronic acid binding through chemical modification of these targets.

3.2. Background and Rationale

In general, boronic acids can lack specificity and/or selectivity for the alcohol groups on carbohydrates, in particular certain aldoses (i.e., mannose, L-rhamnose, xylose, and fucose), but can have high affinity to sorbitol, the reduced form of glucose.[41] Sugar alcohols can have multiple *threo*-1,2- and/or *syn*-1,3-diol units, usually the latter units are where boronate ester formation occurs preferentially.[41] Certain acyclic sugar alcohols can have a higher binding affinity toward boronic acids compared with its aldose form (Table 3.1).

Table 3.1. Association Constants of Phenylboronate.

Aldose*	**Log (Ka)**
Mannose [42]	1.69
Mannitol [42]	3.32
D-glucose [43]	1.81
Glucitol [41]	2.20
Xylose [43]	2.20
Xylitol [41]	3.38

Table 3.1. Association constants of phenylboronate to the corresponding aldoses and alditols. *Reference to the study.

If boronic acid recognition systems were to be used as an alternative approach for measuring these aldoses in solution, an increase in binding affinity through chemical modification is of interest. Additionally, increasing the binding affinity for these aldoses would provide a method of detection that can be make these aldoses useful as markers for gastrointestinal permeability (see section 4.1.4).

3.3. Results

With the aim of developing a rapid method for the analysis of sugar and sugar derivatives that usually provide low binding affinity to boronic acids, we sought to explore a gentle, simple, and effective way to increase the binding affinity through a chemical transformation. This transformation of the sugar target would indirectly allow an increase in the fluorescent signal from the increase in binding affinity of the boronic acid moiety to the modified sugar target (scheme 3.4).

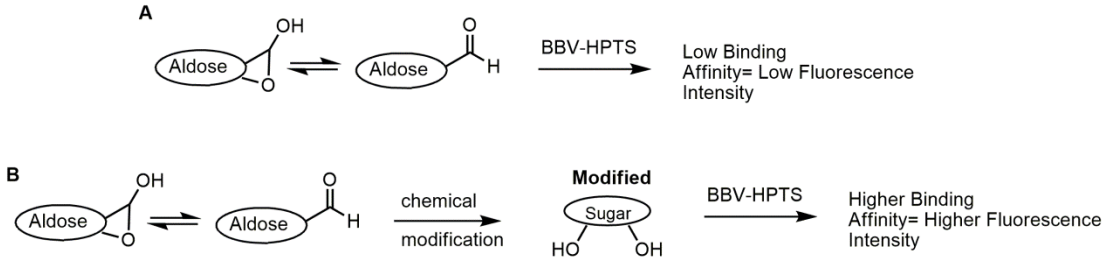

Scheme 3.4. Strategy to improve boronic acid recognition for aldoses and sugar derivatives that usually have low binding affinity (A) by chemical modification to a higher binding sugar derivative "modified sugar" to increase fluorescence intensity of two-component fluorescent probe (B).

3.3.1 Reduction of Aldoses for Improving Boronic Acid Recognition

Chemical modification for analysis of a specific compound/analyte has been widely used for amplification of the signal, detection of an analyte, or to remove unwanted species. Because boronic acid binding relies on *cis*-1,2 or 1,3-diol motifs for moderate binding affinity, certain saccharides or sugar derivatives cannot be recognized with high affinity based on the structural motifs that are present in "challenging" saccharides or sugar derivatives. Modification of these challenging

saccharides can improve boronic acid binding and be used to quantify these saccharides in solution. Reduction of these saccharides to their corresponding sugar alcohol would render them recognizable by boronic acid binding. Previous studies have shown that acyclic sugar alcohols can have higher binding affinity compared with its aldose (e.g., mannitol and mannose).[44] In acyclic sugar alcohols that contain *syn*-1,3- or *threo*-1,2-diol motifs, boronic acid binding is preferred.

The first report of carbohydrate reduction by sodium borohydride by Hamilton and Smith demonstrated the effectiveness of using this mild reducing agent for the reduction of mannose.[45] Decades later, Sturgeon and coworkers demonstrated the utility of using aqueous sodium borohydride for the reduction of various oligo- and polysaccharides to the corresponding reduced form. These reduced forms were then analyzed by enzymatic methods to determine the liberated alditols: one capable of measuring sorbitol in the presence of mannitol, and the other to measure mannitol in the presence of sorbitol.[46, 47] Overall, successful generation of the alditol species were produced and measured enzymatically. Herein, we report a method to detect aldoses and saccharides such as sucralose that are not amenable to recognition or have low binding affinity via boronic acid recognition after they have been subjected to sodium borohydride reduction.

$NaBH_4$ is a reagent that is widely used in organic synthesis and in a variety of solvent systems. We envisioned a way to develop a simple method that would allow quantification of aldoses that are traditionally not amenable to recognition by boronic

acid-based systems because of their lack of binding affinity. To increase the binding affinity of boronic acids to aldoses that are known to have low affinity, these aldoses of interest (e.g., fucose, L-rhamnose, and xylose) were subjected to reduction by $NaBH_4$ in neutral buffer under ambient conditions; the fluorescence recovery of these products was then compared to the aldose form. Aldoses are known to be in equilibrium with their cyclic and acyclic forms, exposing the aldehyde functionality to reactive groups (Scheme 3.5).

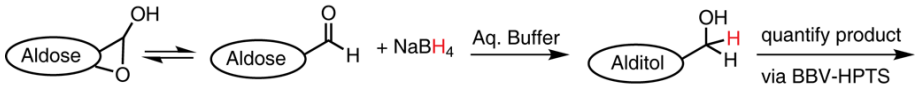

Scheme 3.5. Reaction scheme for the reduction of aldoses and quantified by the BBV-HPTS probe

The initial investigation measured the reduction capabilities of each aldose of interest with $NaBH_4$ in the presence of aqueous methanol. Using $NaBH_4$ in an aqueous system can create an alkaline solution. For our two-component fluorescent probe, the boronic acid is susceptible to changes in pH, which can provide a false positive signal in pH > 8. The pKa value of 8.0 for the 4,4'-*o*-BBV receptor has been previously reported.[48] Therefore, it is important to ensure that the reaction is maintained at a pH close to neutral to prevent false positive signals during fluorescence measurements.

3.3.2 Reaction Optimization for the Reduction of Aldoses

The primary objective of this reduction reaction was to determine the optimal buffer conditions to perform the borohydride reduction that would allow obtaining a confident signal from the reaction product. Fucose was subjected to 3 equivalents of sodium borohydride and methanol, and then mixed for one hour at 0° C in 0.1M sodium phosphate aqueous buffer. Additionally, a 1:1 mixture (Aldose/$NaBH_4$) was used to determine the optimal conditions for fucose reduction (scheme 3.6).

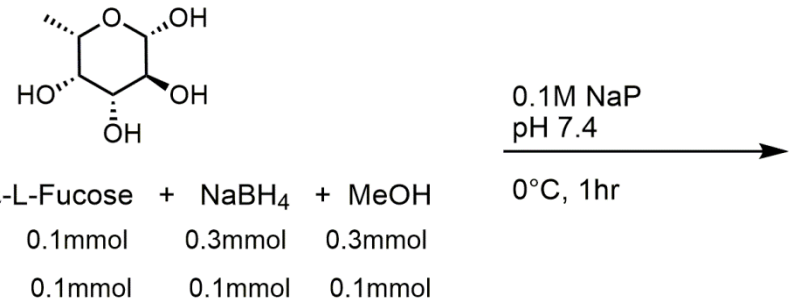

Scheme 3.6. Reaction optimization scheme for the reduction fucose in sodium phosphate buffer pH 7.4.

A probe solution of 4,4'-o-BBV and HPTS was used to analyze the fluorescence recovery of the 1:3 and 1:1 reaction conditions and to compare them to control reaction conditions in which no fucose was present (Figure 3.7).

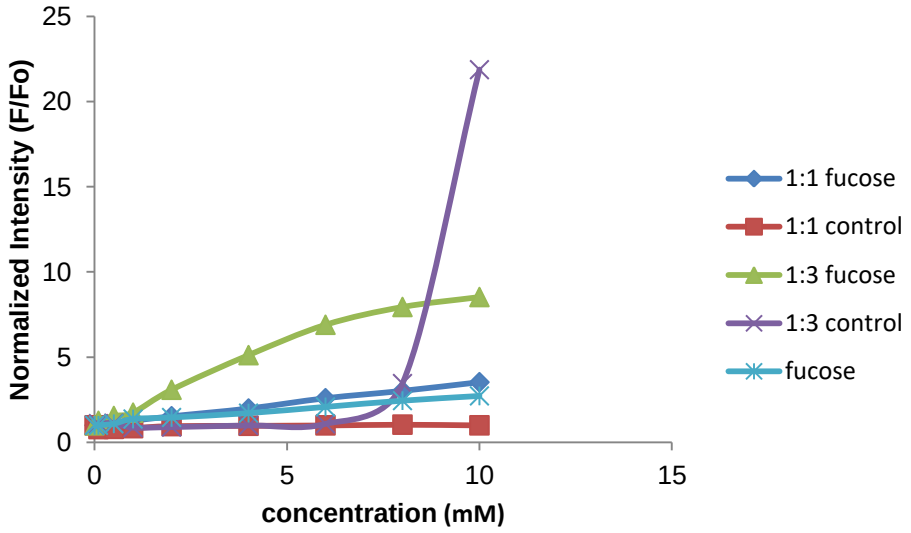

Figure 3.7. Reaction optimization of NaBH4/MeOH reduction of fucose. Quantified by 4,4-o-BBV (500μM) and HPTS (4μM) in 0.1M sodium phosphate buffer pH 7.4

Based on the fluorescence recovery using 4,4-o-BBV as the receptor, the 1:1 reaction provided minimal difference in signal from unreacted fucose but the reaction control gave no false positive signal. On the contrary, the 1:3 reaction gave a 4-fold change compared with unreacted fucose, but the 1:3 reaction control gave a significant false positive after the 8mM concentration data point. It was speculated that this reaction condition (1:3) could be causing a pH change in the buffer media, which would lead to a false positive because the boronic acid motif can become negatively charged with increasing pH. To verify if this might be the case, a stronger buffer was used and the same reaction conditions were conducted in 0.1M sodium phosphate and HEPES buffer pH 7.4; the same equivalences were used for

$NaBH_4$/MeOH (3 equivalence) to reduce fucose (1 equivalence) as illustrated in Figure 3.8.

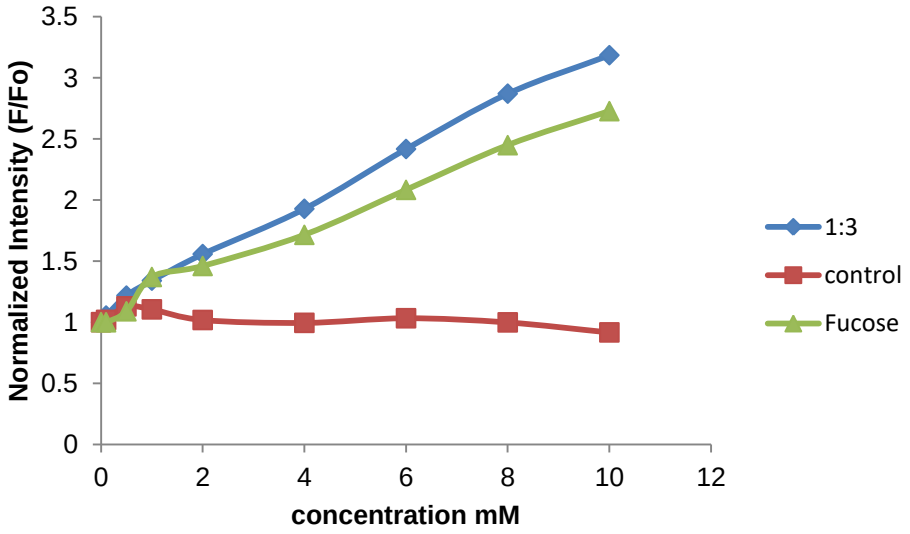

Figure 3.8. Fucose reduction by NaBH4/MeOH in 0.1M sodium phosphate/HEPES buffer pH 7.4. Reaction product measured by 4,4'-*o*-BBV/HPTS.

Using the 0.1 M sodium phosphate-HEPES buffer as the reaction medium provided no false positive as observed in the red line in Figure 3.8. While the 1:3 reaction conditions to reduce fucose gave only modest fluorescence recovery compared to unreacted fucose (0.5-fold change). Based on this small change of fluorescence of reacted fucose compared with unreacted fucose, it was hypothesized that the salt concentration of HEPES or sodium phosphate could be an interfering component. The salt concentration was decreased to 0.05 M sodium phosphate-HEPES and re-examined (Figure 3.9).

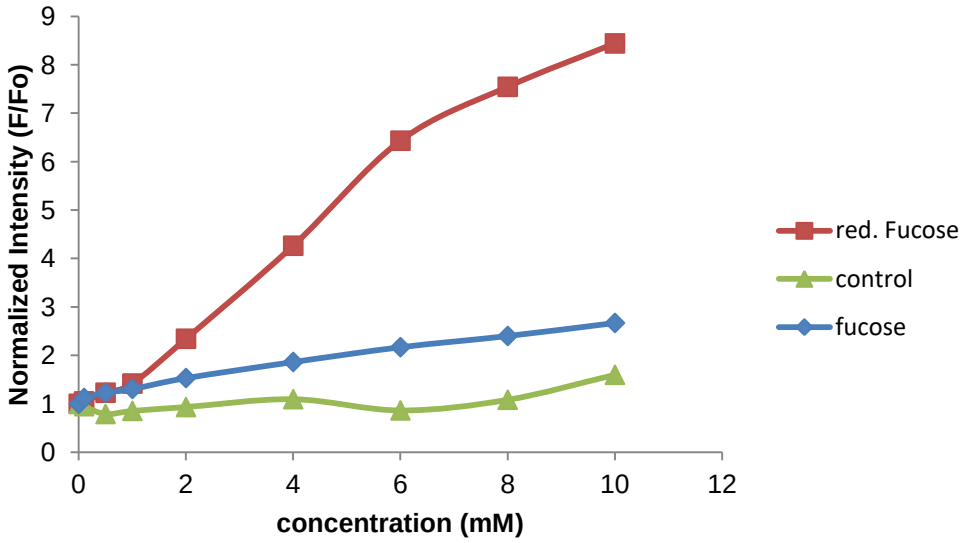

Figure 3.9. Fucose reduction by $NaBH_4$/MeOH in 0.05 M sodium phosphate/HEPES buffer pH 7.4. Reaction product measured by 4,4'-o-BBV/HPTS.

This change of salt concentration demonstrated that the reduction of fucose can be achieved using a stronger buffer in the presence of $NaBH_4$/MeOH; it was quantified by the 4,4'-o-BBV/HPTS method. Using a 1:3 ratio of fucose to $NaBH_4$/MeOH, the reduced form of fucose (fucitol) was obtained with a good fluorescence recovery of ~2-fold change (red line) compared to unreacted fucose (blue line, Figure 3.9).

After examination of the ^{11}B NMR of the reaction mixtures containing $NaBH_4$ under different conditions (i.e., MeOH, NaP/HEPES or H_2O, 0°C or 25°C), it was determined that the prominent species present is the BH_4 (δ = -40 ppm), and this species was likely responsible for the reduction and not the $NaBH_3(OH)$ (δ = -12 ppm)although present in small amounts (Figure 3.10A & 3.10B).

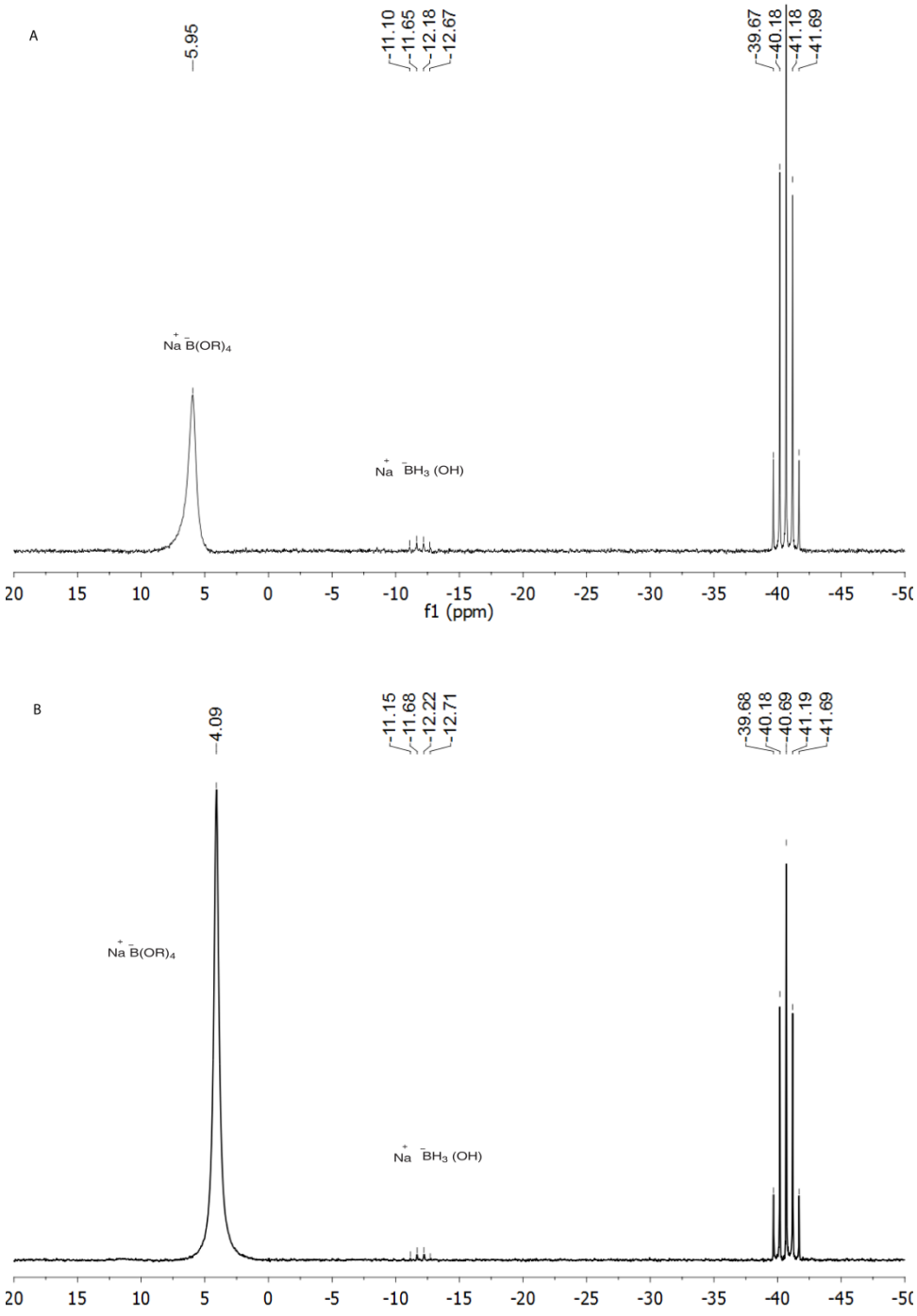

Figure 3.10. A. ^{11}B NMR of $NaBH_4$ and MeOH in NaP/HEPES at 0 °C **B.** $NaBH_4$ in NaP/HEPES at 25 °C.

This led us to utilize $NaBH_4$ in excess in the presence of NaP/HEPES buffer media to reduce the corresponding aldoses—fucose, rhamnose, and xylose—to improve boronic acid binding. To demonstrate any difference in fluorescence recovery using 4,4'-*o*-BBV-HPTS, a comparative analysis of each reaction condition was conducted for fucose, rhamnose, and xylose (Figure 3.11).

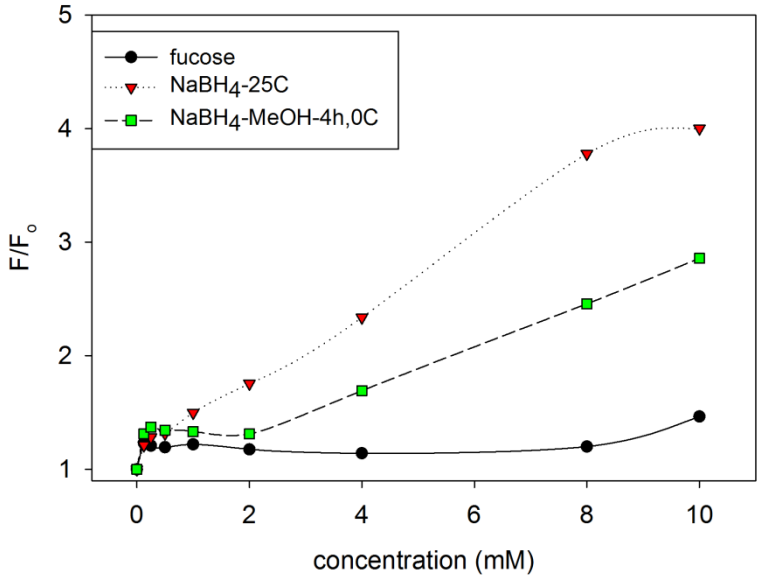

A.

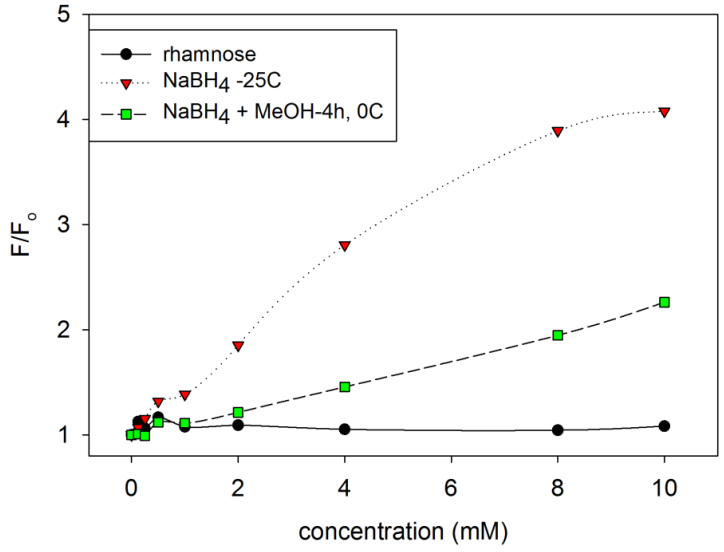

B.

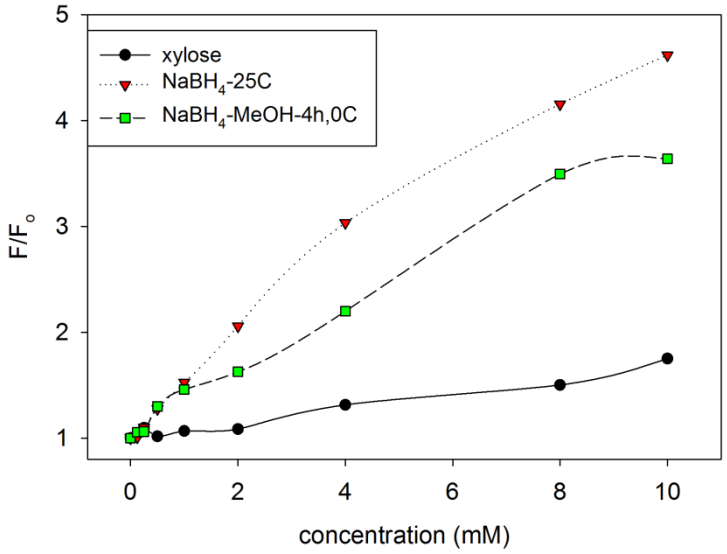

C.

Figure 3.11. Fluorescence recovery of 4,4'-*o*-BBV-HPTS after reduction of **A.** fucose, **B.** L-rhamnose, and **C.** xylose in $NaBH_4$-NaP/HEPES at 25 °C (red triangle) or in $NaBH_4$/MeOH-NaP/HEPES at 0 °C.

When subjecting each sugar to $NaBH_4$-MeOH at 0 °C, a modest recovery was achieved compared to unreacted aldose. However, using $NaBH_4$ alone provided a higher recovery with only one hour of reaction time. Control reactions were also conducted in the absence of sugar to demonstrate that a false positive signal is not observed for either set of reaction conditions (data not shown). Additionally, an improvement of the binding affinities was observed when each aldose was subjected to $NaBH_4$ alone compared to unreduced aldose for 4,4'-o-BBV (Table 3.2).

Table 3.2. Binding constants for each aldose after NaBH4 reduction compared to untreated aldose.

4,4'-*o*-BBV	**Binding constant (Reduced. Aldose) M^{-1}**	**Binding constant (aldose) M^{-1}**
Fucose	39.89 ± 2.6	5.2± 2.0
Rhamnose	74.5± 16.2	9.5± 1.5
Xylose	72.69± 8.5	2.08± 0.4

It was determined that using three equivalents of $NaBH_4$ to the aldose sugar in 0.05M sodium phosphate-HEPES buffer was the optimal reaction condition to achieve fluorescent recovery with no false positive signal arising from the reaction conditions. Compared to unreacted aldose, reduced aldoses provided significant fluorescent recovery with at least a 2-fold difference for fucose and up to 4-fold difference for reduced L-rhamnose at 10 mM concentration (Figure 3.12A & 3.12B).

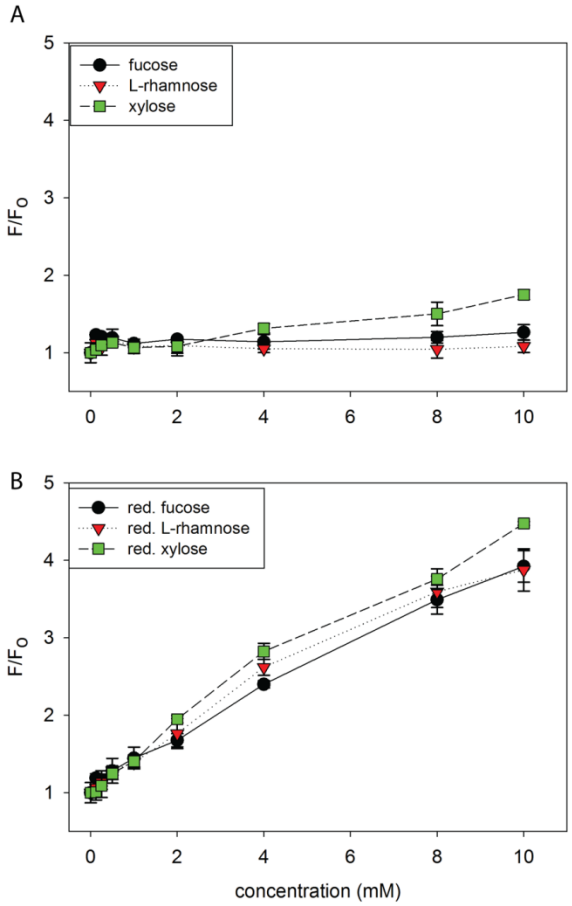

Figure 3.12. Normalized HPTS (4 μM final concentration) fluorescence recovery (F=initial quenched fluorescence, F_o=recovered fluorescence) with 4,4'-*o*-BBV as the boronic acid receptor. **A.** non-reduced **B.** reduced aldoses fucose, L-rhamnose, and xylose in 0.05M sodium phosphate-HEPES buffer solution, pH 7.4. Error bars represents standard deviation of triplicate responses.

Similarly, the binding constants for each aldose versus reduced aldose (alditols) provided a significant difference. Apparent binding constants for reduced aldoses was 4, 7, and 25 times higher than for reduced fucose, L-rhamnose, and xylose, respectively (Table 3.2).

The preceding investigation demonstrates that the reduced form of each aldose has a higher binding affinity for the boronic acid receptor 4,4'-*o*-BBV, following the general relationship that sugar alcohols have higher binding affinities compared to their aldose form. When comparing diastereomeric fucose and L-rhamnose, we speculated that binding affinities would be significantly different. The following order of apparent binding affinities was obtained for the aldoses upon reduction: L-rhamnose > xylose > fucose. In addition, the sensitivity for each sugar improved upon reduction, where the detection limits (signal to noise ratio greater than 3 and 10 standard deviations) improved by at least 2-fold compared to unreacted aldose (Table 3.3).

Table 3.3. Limit of detection and quantification for reduced aldose versus unreacted aldose with 4,4'-*o*-BBV.

4,4'-*o*-BBV	**Reduced Aldose (LOD, LOQ μM)**	**Aldose (LOD, LOQ mM)**
Fucose	175,560	ND
L-rhamnose	250,550	ND
Xylose	260, 475	4, 6

ND: not determined because there was no increase in fluorescence throughout the standard curve.

Since reduction is carried out at ambient temperature and near neutral pH, we suspected that epimerization of each glycitol was unlikely. Since xylitol is readily available, the fluorescent recovery for commercially available xylitol and reduced xylose can be compared. This will be useful to determine whether the reduced xylose that is produced is not an epimerized form and can provide a different pattern the

fluorescence recovery. The reduction of xylose was performed under the same conditions as described previously; commercially available xylitol was used to compare the fluorescence recovery for both standard sugar alcohol solutions using 4,4'-*o*-BBV as the boronic acid receptor (Figure 3.13).

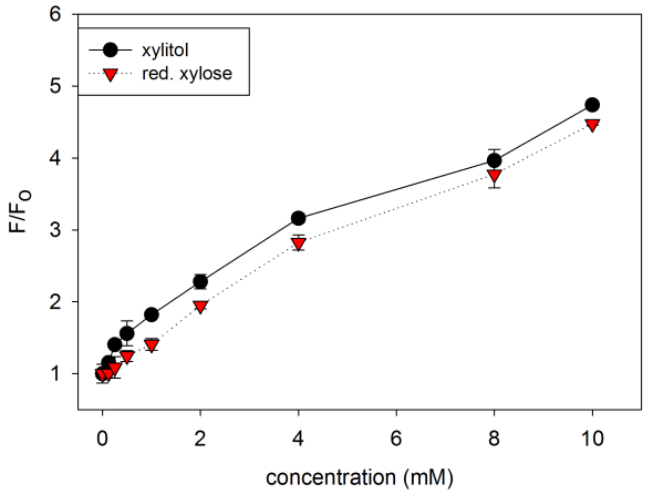

Figure 3.13. Normalized HPTS (4 µM final concentration) fluorescence recovery (F=initial quenched fluorescence, F_o=recovered fluorescence) with 4,4'-*o*-BBV as the boronic acid receptor comparing commercially available xylitol (black) to reduced xylose (red) in 0.05M sodium phosphate-HEPES buffer, pH 7.4. Error bars represent the standard deviation of triplicate responses.

The fluorescence recovery for commercially available xylitol gave up to 5-fold recovery at 10 mM, and reduced xylose (i.e., xylitol product) provided a similar recovery. Similarly, when fitting a non-linear curve to the data to obtain the apparent binding constant for each standard curve, 65.9 ± 8.6 and 52.3 ± 12.2M^{-1} constants were observed for xylitol and reduced xylose, respectively. Based on the fluorescence recovery data, it appears that epimerization is unlikely to occur during the reduction,

and that the reaction is only reducing the aldehyde to the primary alcohol with negligible side products. This demonstrates that $NaBH_4$ is an effective mild reducing agent for converting aldoses to their glycitol form under ambient conditions, and that the glycitol product can be readily quantified using boronic acid-based detection systems—such as our two-component fluorescent probe (4,4'-*o*-BBV-HPTS).

3.3.3 Determination of Alditol Produced from $NaBH_4$ Reduction

To ensure that the product being analyzed by the two-component fluorescent probe is most of the alditol that is produced, a spectroscopic method was utilized to determine the yield of the reaction for each aldose reduction. Phenylhydrazine is a useful labeling compound for analyzing aldehydes of interest that do not have an intrinsic chromophore, as it readily reacts with sugars at their reducing end to form the phenylhydrazone adduct. This method is traditionally used for post-column labeling for UV enhancement or mass spectrometry detection.[49,50] Here, phenylhydrazine was used to quantify the presence of unreacted aldose after $NaBH_4$ reduction by measuring the formation of the phenylhydrazone/osazone adducts through UV-Vis absorbance at 285 nm (Scheme 3.7).

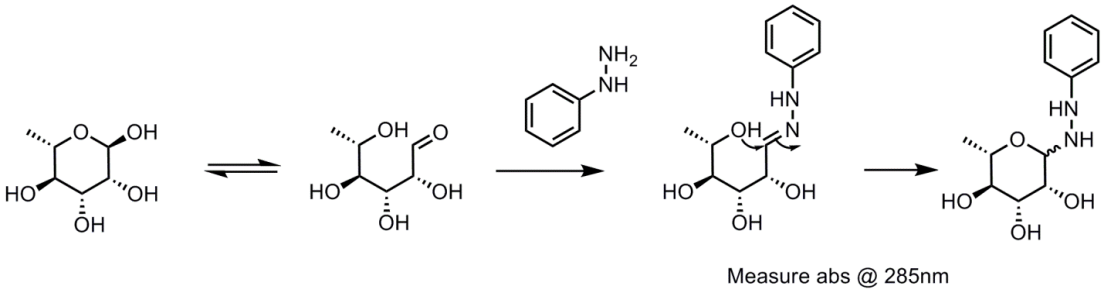

Scheme 3.7. Labeling of rhamnose with phenylhydrazine.

Two reactions (reactions A and B) were run simultaneously for reduction of each aldose. The sample mixture (reaction A) contained the aldose of interest, $NaBH_4$, and phenylhydrazine to form the phenylhydrazone adduct from unreacted aldose. The standard mixture (reaction B) contained the aldose of interest and phenylhydrazine to quantify the phenylhydrazone adduct in reaction A. The reduction was performed as previously described, and after 1 h of reaction time, a slight excess of phenylhydrazine was added to each reaction and stirred for another hour at 80 °C. Upon completion, excess phenylhydrazine was removed by $CHCl_3$ extraction (Scheme 3.8).

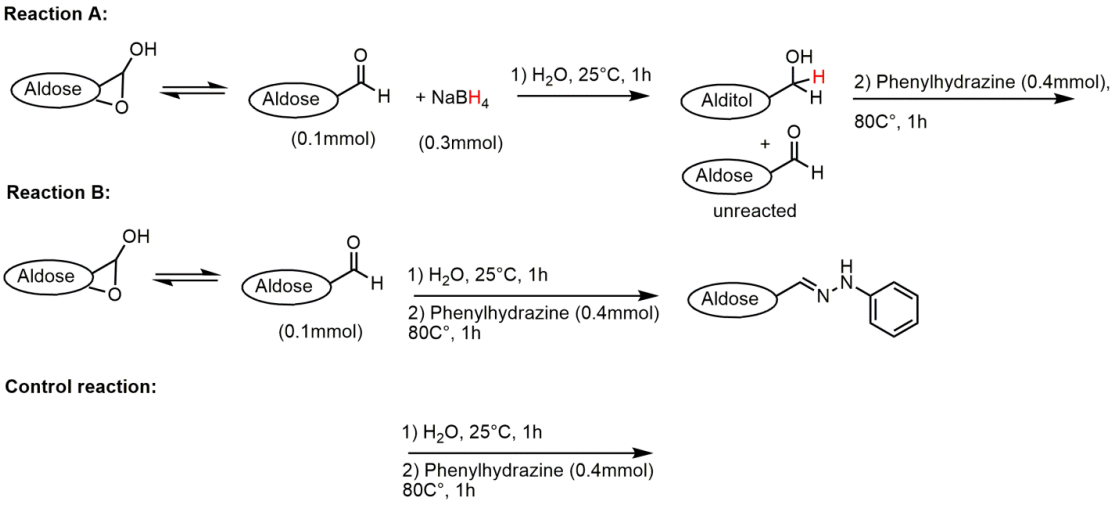

Scheme 3.8. Illustration of the reactions conducted for the determination of unreacted aldose.

For the standard mixture (reaction B), excellent linearity was obtained with $R^2 >$ 0.99. By measuring the presence of the phenylhydrazone adducts after each aldose

was reduced, equation (1) was used to determine the yield of reduced product for each aldose reduction reaction:

$$\%\,yield = \left(\frac{Aldose\ present}{Aldose\ used} \right) - 1 * 100 \quad (1)$$

Each aldose reduction reaction provided good to excellent yields, with about 90% or greater in the reduced form measured by the BBV-HPTS probe. This further demonstrated the effectiveness $NaBH_4$ as a mild reducing agent in aqueous systems (Table 3.4).

Table 3.4. Yields of glycitol obtained after labeling unreacted aldose with phenylhydrazine.

Aldose	**% of reduced product**
L-rhamnose	89.1
Fucose	93.7
Xylose	96.8

Each reaction with $NaBH_4$ provided excellent yields of >85%, demonstrating that what is measured with the BBV-HPTS is mostly the sugar alcohol form.

3.2.5 Indirect Sucralose Quantification by Dechlorination

Sucralose is one of the most widely used artificial sweeteners in the food industry: it has low caloric content but is 600-times sweeter than sucrose. When consumed by humans, being resistant to metabolic pathways means it is absorbed and excreted intact into the environment. It survives the wastewater treatment process.[51] which is increasingly becoming an environmental concern: there is a need to elucidate potential effects it may have on aquatic life.[52] Demand for the development of rapid, cost-effective, and reliable analytical methods that allow for in-field analysis for sucralose will therefore continue to grow. Analysis of sucralose by boronic acid-based detection methods can provide low-cost, feasible, and rapid analysis compared to conventional methods. Because sucralose is a sugar derivative, with three chlorine atoms substituted for its hydroxyl groups, our group envisioned the conversion of sucralose to a hydroxylated product that is amenable for recognition by boronic acids through in situ-generated reactive oxygen and hydroxide intermediates.

Sucralose is a non-reducing sugar; based on our earlier studies we have shown that the hemiacetal (or hemiketal) in reducing sugars is critical for boronic acid recognition. Sucralose was subjected to chemical modification by reactive oxygen intermediates generated in situ by the Fenton reaction, using ferrous iron and hydrogen peroxide as the oxidant. Hydrogen peroxide is reduced and generates the reactive hydroxyl or hydroperoxyl radical and hydroxide intermediates (Scheme 3.9).[53-55]

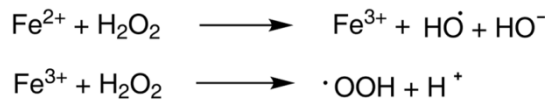

Scheme 3.9. Reaction scheme for the Fenton reaction and its possible reactive intermediates.

Sucralose was dechlorinated using iron sulfate heptahydrate and 30% w/w hydrogen peroxide in water at ambient conditions for longer than an hour to obtain the hydroxylated product. Initially, liberated chloride was verified by a qualitative $AgNO_3$ test after one hour of reaction time by AgCl precipitate observation. After the reaction conditions were optimized (1:1:0.5, sucralose:H_2O_2:$FeSO_4$), the reaction was then repeated along with a control reaction (absence of sucralose); when the reaction was completed, appropriate dilutions were made to measure the fluorescent recovery of the 4,4'-*o*-BBV-HPTS probe (Scheme 3.10).

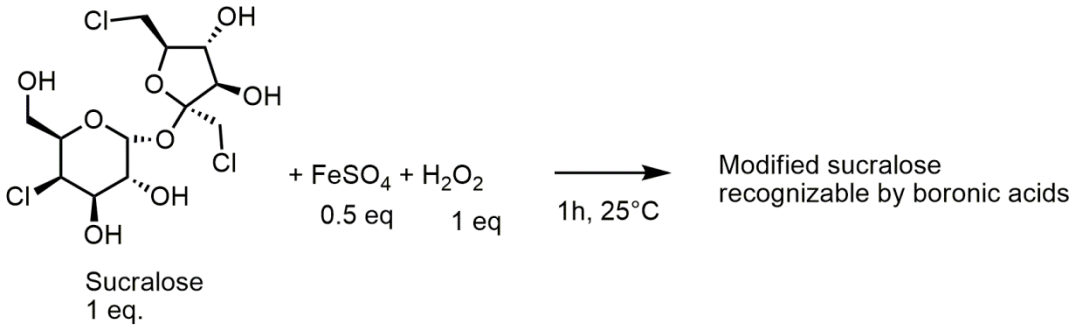

Scheme 3.10. Dechlorination of sucralose by reactive oxygen intermediates generated by a Fenton reaction.

The fluorescence recovery for dechlorinated sucralose was compared to unreacted sucralose and the control reaction. The control reaction was useful to rule out the possibility of a false positive signal resulting from cross reaction with the 4,4'-*o*-BBV-HPTS probe (Figure 3.14).

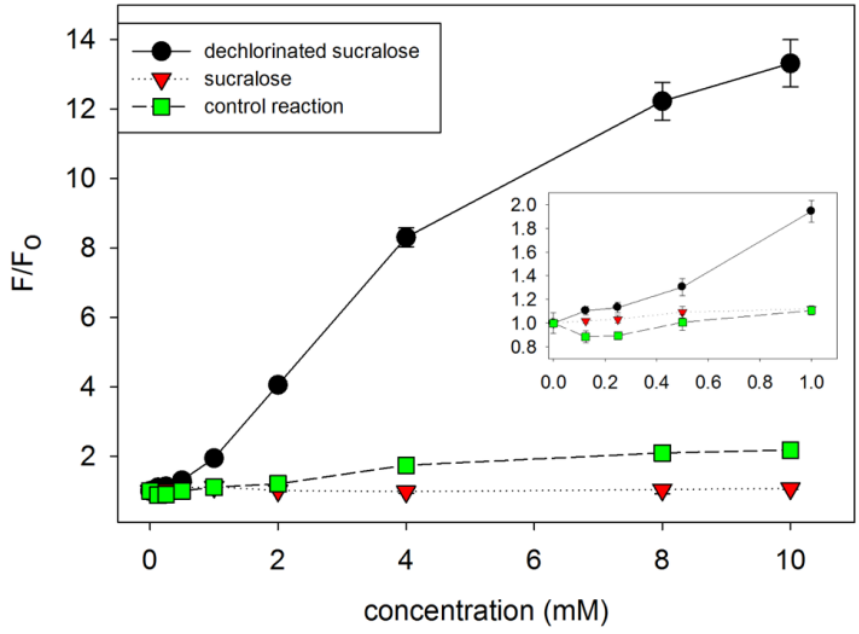

Figure 3.14. Normalized HPTS (4 µM final concentration) fluorescence recovery (F=initial quenched fluorescence, F_o=recovered fluorescence) with 4,4'-*o*-BBV as the boronic acid receptor comparing solution containing dechlorinated sucralose (black), sucralose (red), and control reaction (green) in 0.05M sodium phosphate-HEPES pH 7.4 buffer. Inset is the fluorescence recovery in the lower concentration range. Error bars represent the standard deviation of triplicate responses.

For the dechlorination of sucralose reaction mixture, there was significant fluorescence recovery with up to 13-fold increase at 10 mM concentration and with an apparent binding constant of 52.5 ± 4.3 M^{-1}. Because unreacted sucralose produced almost no change in fluorescence recovery, the binding affinity was

assumed to be zero. Compared to the reaction conditions (absence of sucralose), there was a slight fluorescence change above 4 mM concentration. Linden and coworkers have previously demonstrated the modification of sucralose by photooxidation in water and showed the presence of the intermediates by mass spectrometry.[56, 57]

Two dominant products were detected: isomers from dechlorination of the C-1 primary alkyl chloride carbon bond and dechlorination of the C-4 secondary alkyl chloride carbon bond, yielding the products with a product with m/z of 379 and 381, respectively (Figure 3.15).

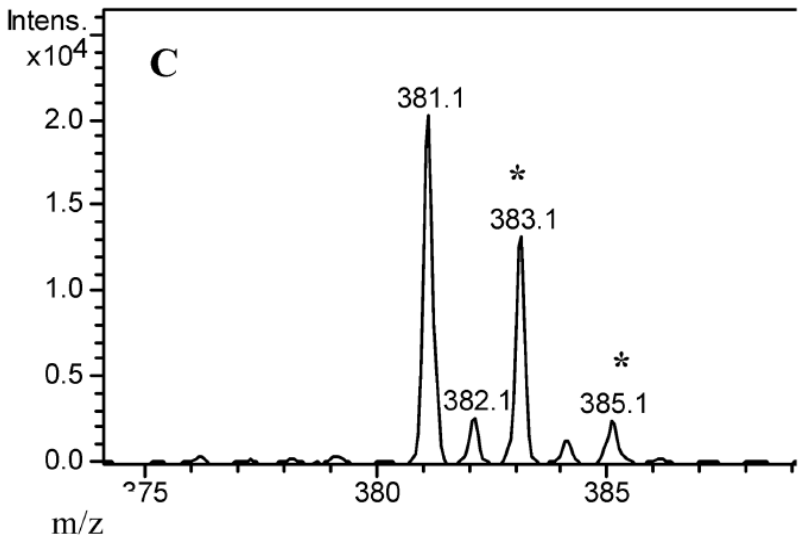

Figure 3.15. Chromatogram of products after advanced oxidation of sucralose after separation by liquid chromatography. *Isotope peaks of chlorine. Reproduced with permission.[57] Copyright 2013 American Chemical Society.

Because this chemical modification reaction generates similar reactive intermediates, we anticipated that the reaction would also lead to more than one

product. The yield of the reaction was determined based on per mole of H_2O_2 forming at least two reactive intermediates; that and could dechlorinate at two positions per sucralose. The number of moles of chloride liberated after modification were determined using Mohr titration to obtain a semi-quantitative yield. Accounting for 1 mole of Cl per sucralose, a yield of 89% was obtained. Given the significant fluorescence recovery, it is plausible that a sugar alcohol derivative is generated from the hydroxide or reacts with the secondary chlorine. Further structural elucidation of the intermediates formed in this reaction is necessary to determine whether the product causes such a high fluorescence recovery.

3.4. Conclusions

Aldoses have a low binding affinity for the two-component fluorescent probe based on a boronic acid-appended viologen (4,4'-*o*-BBV-HPTS); these sugars can be converted to their glycitol form amenable for recognition by a simple transformation via a $NaBH_4$ reduction under ambient conditions. That reaction provided good-to-excellent yields determined by the phenylhydrazone adduct produced by the unreacted aldose. Using the 4,4'-*o*-BBV-HPTS probe, glycitols were measured by monitoring the fluorescence recovery of the probe and provided excellent apparent binding affinities compared to unreacted fucose, L-rhamnose, and xylose. This further demonstrated that some sugar alcohols can have higher binding affinities for boronic acid receptors as compared to the aldose form. Similarly, sucralose was modified by in situ-generated reactive oxygen and hydroxide intermediates by the Fenton reaction. Compared to sucralose, significant fluorescence recovery was observed, with good apparent binding affinity. When utilizing boronic acid-based detection methods for measuring aldose or sugar derivatives such as sucralose, simple chemical transformations can be used to eliminate the need to use conventional chromatographic methods for quantification of these sugars.

3.5. Experimental

General

All reagents and saccharides were purchased from Sigma Aldrich Co. TCI Chemicals for sucralose were used as received. Hydrogen peroxide (H_2O_2, 30% w/w) purchased from Fisher Scientific International. All solvents were at least HPLC grade. MeCN was obtained from a solvent purification system, moved to an ampule under argon, and stored no more than 4 weeks before use. Ultra-pure water (>14 MΩ cm) obtained from a Millipore water system was used for each analysis unless otherwise stated.

3.5.1. Instrumentation

The 4,4'-*o*-BBV receptor was characterized through nuclear magnetic resonance (NMR) spectroscopy measured in ppm and was obtained on a 500 MHz spectrometer using D_2O (δ=4.80) as an internal standard for ^{1}H NMR, 126 MHz for ^{13}C spectra, and 160 MHz using BF_3:Et_2O (δ=0) as an external standard for ^{11}B spectra. NMR data are reported as s = singlet; d = doublet; t = triplet; q = quartet; m = multiplet; br = broad; dd = doublet of doublet. Coupling constants (*J*) are given in Hertz (Hz). For multi-well fluorescence measurements, the fluorescence plate reader Envision 2103 Multilabel reader from PerkinElmer® was used (excitation filter, 405 nm; emission filter, 535 nm; emission aperture normal; measurement height from the bottom 6.5 mm; number of flashes; 10). Absorption spectra were measured on a UV-1800 Shimadzu spectrophotometer to determine phenylhydrazone adducts.

3.5.2. $NaBH_4$ Reduction of Aldoses

To a round-bottom flask (10 mL), the aldose sugar (0.1 mmol) and 0.05 M sodium phosphate-HEPES buffer (5 mL) were was added; the solution (20 mM aldose) was stirred for 5 min. After stirring, $NaBH_4$ (0.0111 g, 0.3 mmol) was added and the reaction mixture stirred for 1 h at 25°C. After reaction , the solution was serially diluted with sodium phosphate-HEPES buffer to produce the desired concentration points (10 mM–0.1 mM) for fluorescence measurements.

3.5.3. Reaction Optimization

The optimal reaction time for the reduction of fucose, rhamnose, and xylose was determined by subjecting each sugar to $NaBH_4$ and MeOH in water, and after each hour an aliquot of the reaction mixture was removed and treated with concentrated sulfuric acid to convert any unreacted aldose to its corresponding furfural derivative. The absorbance of each furfural derivative was measured at 315 nm for each aliquot and compared to a standard curve of unreacted aldose (fucose, rhamnose, and xylose).

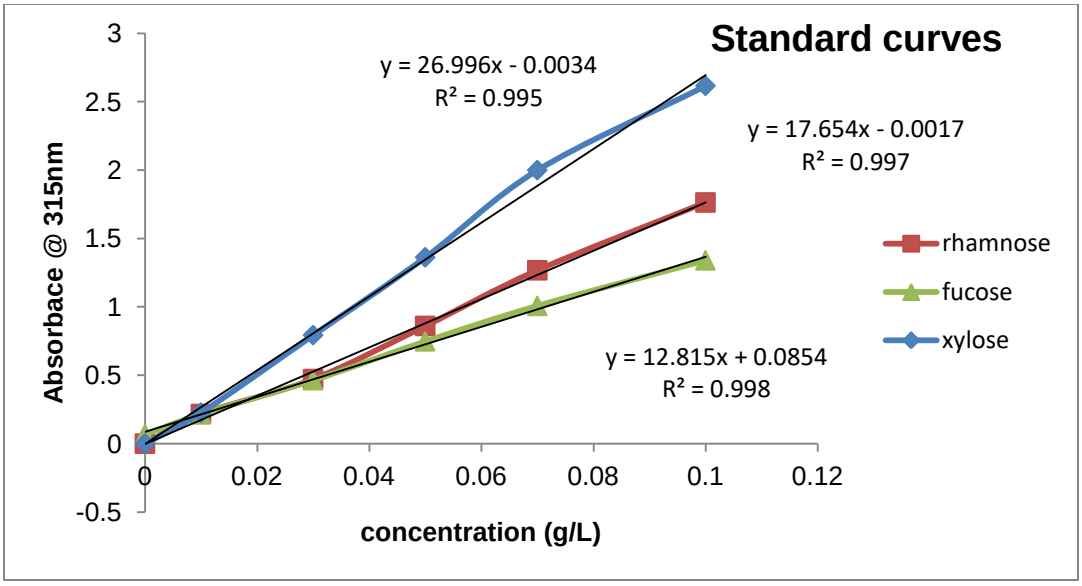

Figure 3.16. Absorbance response for each aldose saccharide without $NaBH_4$ reduction. Rhamnose (red), fucose (green), and xylose (blue) and their corresponding linear regression plots.

The absorbance responses for each saccharide after treating with sulfuric acid provided excellent linearity (R^2>0.990), which is comparable to reported valuesThis demonstrates that the UV-sulfuric acid method also works well with these saccharides.

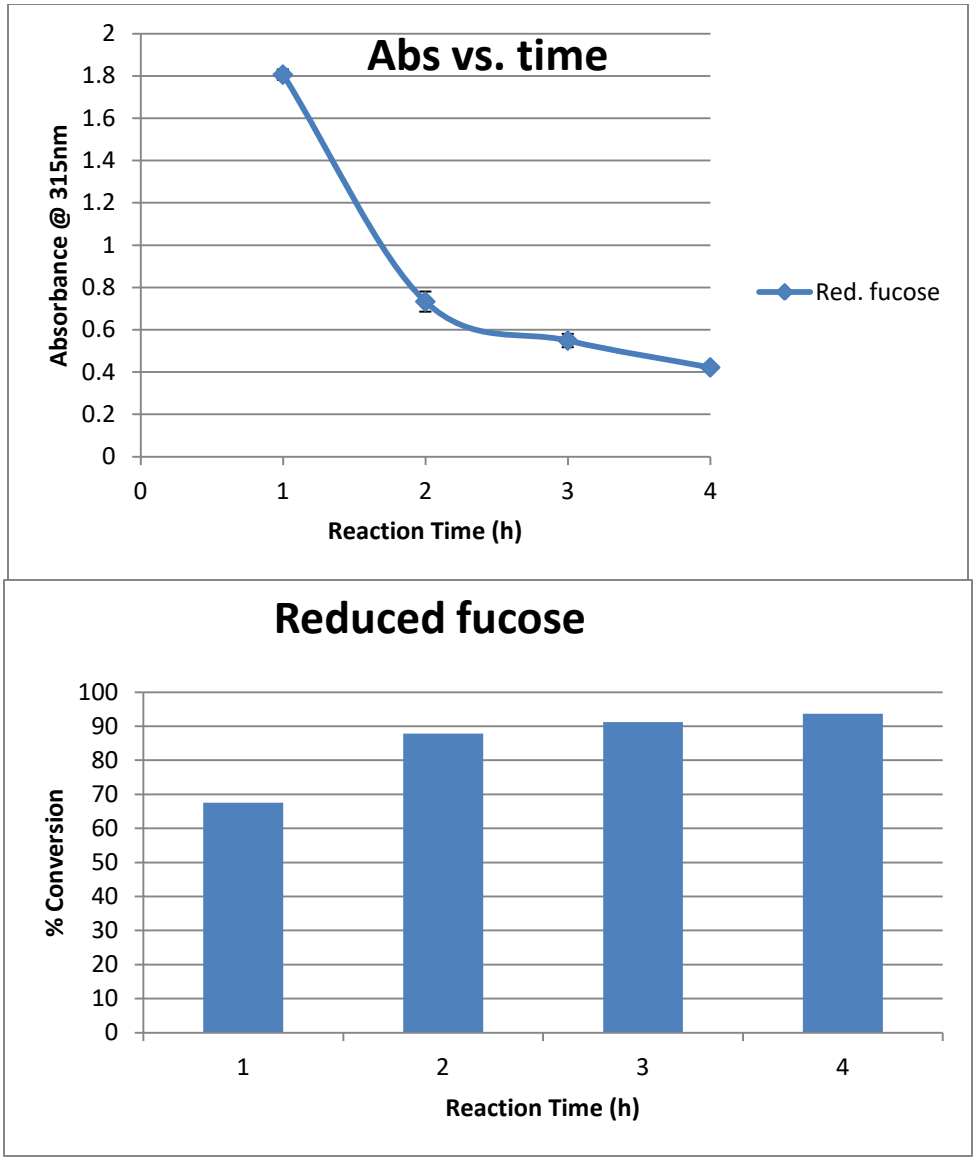

Figure 3.17. Monitoring the reduction of fucose over 4 hours. Top: absorbance response with respect to time of the aliquot mixture at each time point. Bottom: Percent conversion (1-(Final conc./Initial conc.)*100) of each aliquot mixture.

To determine the optimal reaction time for subjecting each saccharide to NaBH4: MeOH, an aliquot of the reaction for fucose reduction was removed at 1-hour increments and then treated with concentrated sulfuric acid. That measures the

presence of any unreacted aldose at each time point. Taking an aliquot of the reaction mixture at four different instances provided a decay of absorbance with respect to time while the reaction went to completion (Figure 18, top). Because the absorbance of the converted furfural derivative measures the presence of aldose, the data was then converted to determine the percent of product formed; this data showed that after 2 hours, there was 90% conversion of an aldose to its alditol product, which reached 94% at 4 hours for fucose reduction.

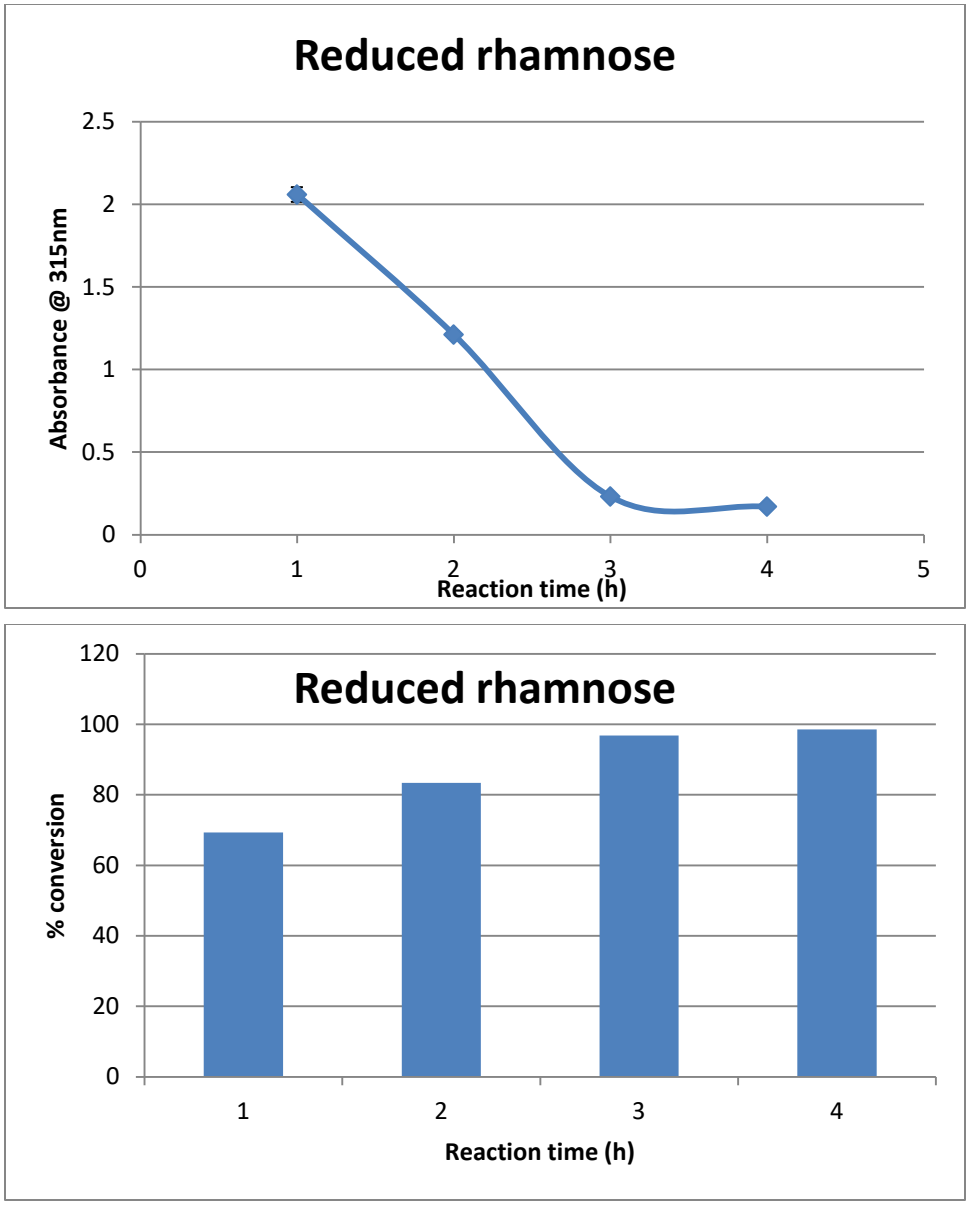

Figure 3.18. Monitoring the reduction of rhamnose over 4 hours. Top: absorbance response with respect to time of the aliquot mixture at each time point. Bottom: Percent conversion (1-(Final conc./Initial conc.)*100) of each aliquot mixture.

Rhamnose was then subjected to the same conditions; aliquots were removed at different time points and treated with concentrated sulfuric acid to measure the

absorbance of the furfural derivative. For the rhamnose reduction, after 1 hour only 70% conversion was obtained, which approached 95% conversion only after 3 hours.

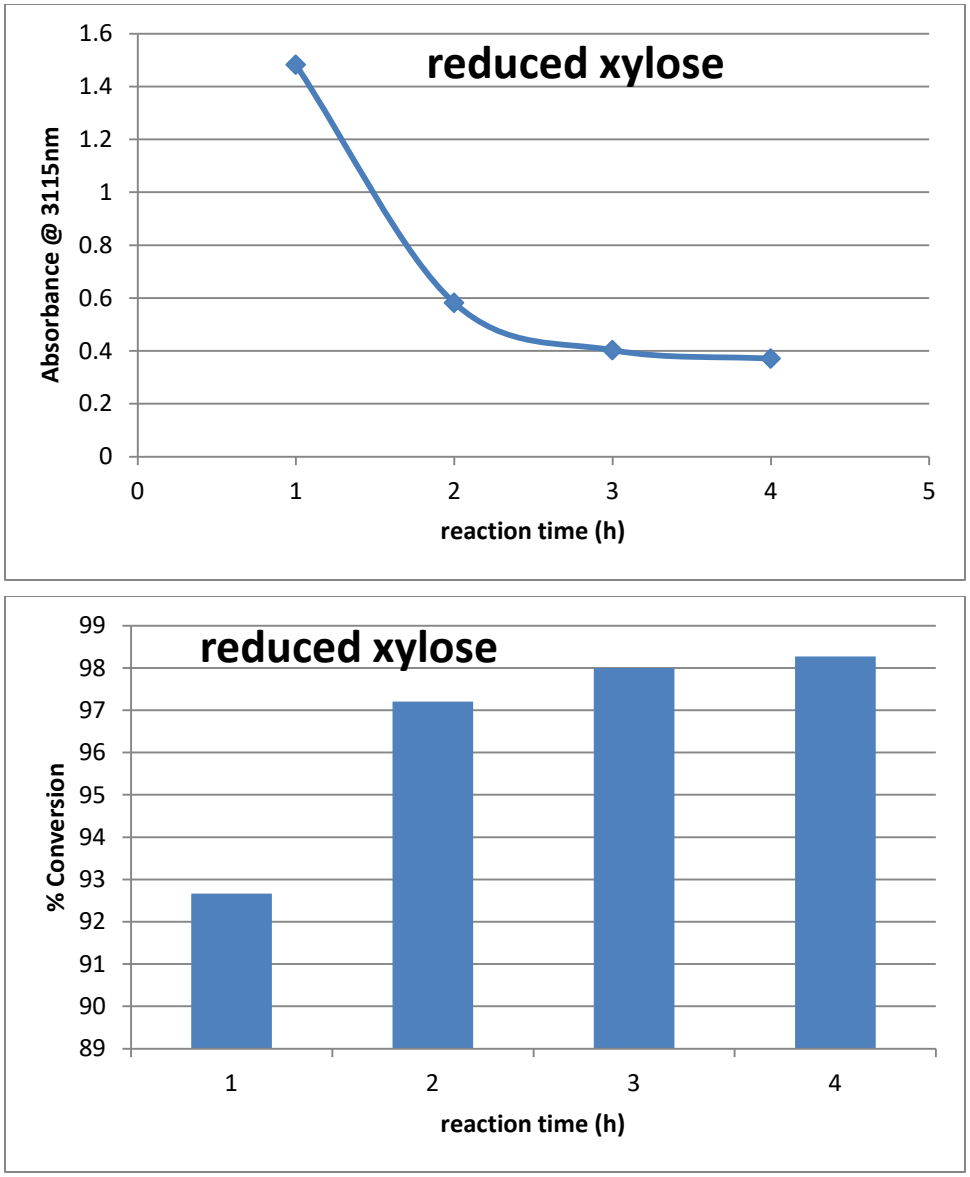

Figure 3.19. Monitoring the reduction of xylose over 4 hours. Top: absorbance response with respect to time of the aliquot mixture at each time point. Bottom: Percent conversion (1-(Final conc./Initial conc.)*100) of each aliquot mixture.

Surprisingly, with the reduction of xylose, at the 1-hour time point, the reaction was >90% conversion and reached 98% after 2 hours of reaction time. Clearly, this

highlights the difference in reactivity for each of these aldoses. It can be concluded that the reactivity is attributable to the equilibrium of these aldoses. The dominant species present in solution (open-chain form versus closed chain-form) dictates the reactivity for the reduction of their carbonyl group.

Saccharide	**Optimal Reaction time (h)**
Rhamnose	3
Fucose	2
xylose	2

Table 3.5. Optimal reaction time for the reduction of each saccharide

Reduction of aldose by $NaBH_4$/MeOH:

To an oven-dried round-bottom flask (10 mL) purged with argon was added L-rhamnose (0.0165 g, 0.1mmol) and 0.05M sodium phosphate/HEPES buffer (5 mL); the solution (20 mM rhamnose) was cooled to 0°C. After stirring for 10 min, $NaBH_4$ (0.0111 g, 0.3 mmol) and MeOH (15 μL, 0.3 mmol) were added and the reaction mixture stirred for 1 h at 0°C. After reaction , the rhamnose solution was then serially diluted to make the various concentration levels (10 mM–0.1 mM), of which 30 μL was then subjected to the boronic acid viologen probe solution (10 μL) in a 96-well plate; fluorescence was read on a Perkin-Elmer plate reader (405 nm excitation–535 nm emission).

3.5.4. Determination of Aldose Present:

A stock solution (0.005 g, 0.1 g/L) of the sugar of interest was prepared in 50 mL of milliQ H_2O; four concentration points were prepared from this stock (0.07, 0.05, 0.03, 0.01 g/L) to generate a standard curve. Using a 10-mL testtube,1 mL at each concentration point was removed. concentrated H_2SO_4 (3 mL, 56.28 mmol, ~500 equiv.);to each was added and the solution was vortexed rapidly for 30 s. The temperature of the mixture rises sharply within 10–15 s; the solution was cooled in an ice bath for 2 min and allowed to sit at room temperature for 10 min. UV light absorption was read at 315 nm using a UV spectrophotometer. **Note:** concentration of sugar solution was diluted by 4-fold in a test tube and the actual sample will have to be diluted accordingly if absorption becomes saturated even with the initial 4-fold dilution. 10-fold dilution or 2-fold dilution has been used. Standard *eg*., (cuvette x 4-fold → initial conc.) Sample eg. (cuvette concentration = x 10-fold→test tube x 4-fold →initial conc.)

Time-dependent study:

To an oven dried round-bottom flask (10 mL) purged with argon, was added L-rhamnose (0.0165 g, 0.1 mmol) and milliQ H_2O (5 mL);the solution (20 mM rhamnose) was cooled to 0° C. After stirring for 10 min, $NaBH_4$ (0.0111 g, 0.3 mmol) and MeOH (15 μL, 0.3 mmol) were added, and the reaction mixture was stirred for 1–4 h at 0 °C. A blank standard was prepared by starting with milliQ H_2O (5 mL) that was cooled to 0° C. After stirring for 10 min, $NaBH_4$ (0.0111 g, 0.3 mmol) and MeOH (15 μL, 0.3 mmol) were added; the solution was stirred for 1–4 h. An aliquot (1 mL) of each mixture was taken at each hour increment and treated with 3 mL of concentrated sulfuric acid in a 10-mL test tube. The mixtures were rapidly vortexed for 30 sec and cooled in an ice bath for 2 min and allowed to sit at room temperature for 10 min before reading absorbance.

Determination of Unreacted Aldose by phenylhydrazine:

Two reactions were run simultaneously (reaction A and B): reaction A (sample mixture) contained the aldose of interest, $NaBH_4$, and phenylhydrazine; Reaction B (standard mixture) contained aldose and phenylhydrazine. Reaction A: To a round bottom flask (10 mL) L-rhamnose (0.0165 g, 0.1 mmol), H_2O (5 mL) and $NaBH_4$ (0.0111 g, 0.3 mmmol) were added, and the mixture stirred for 1 h at 25 °C. Phenylhydrazine (40 μL, 0.4 mmol) was then added and the reaction stirred for 1 h at 70–80 °C. Reaction B: To a round bottom flask (10 mL) L-rhamnose (0.0165 g, 0.1

mmol) and H_2O (5 mL) were added and the mixture was stirred for 1 h at 25 °C. Phenylhydrazine (40 μL, 0.4 mmol) was then added and the reaction stirred for 1 h at 70–80 °C. Upon completion of each reaction, excess phenylhydrazine was removed by washing the aqueous layer with $CHCl_3$ (3 x 2 mL), and the aqueous layer for each reaction was collected. For Reaction A, a 4-fold dilution was performed to obtain an absorbance. For Reaction B, the following concentrations were used to generate the standard curve: 0.6, 0.3, 0.15, 0.075, or 0.0375 mM ; the absorbance was measured at 285 nm.

UV-Vis absorbance measurements:

An absorbance scan of Reaction B and the control reaction was conducted to determine the amount of background noise present when having excess phenylhydrazine present in the mixture. Reaction B and the control reaction were diluted 100-fold (0.2 mM fraction), and an absorbance scan was performed from 200 to 400 nm (Figure 3.20).

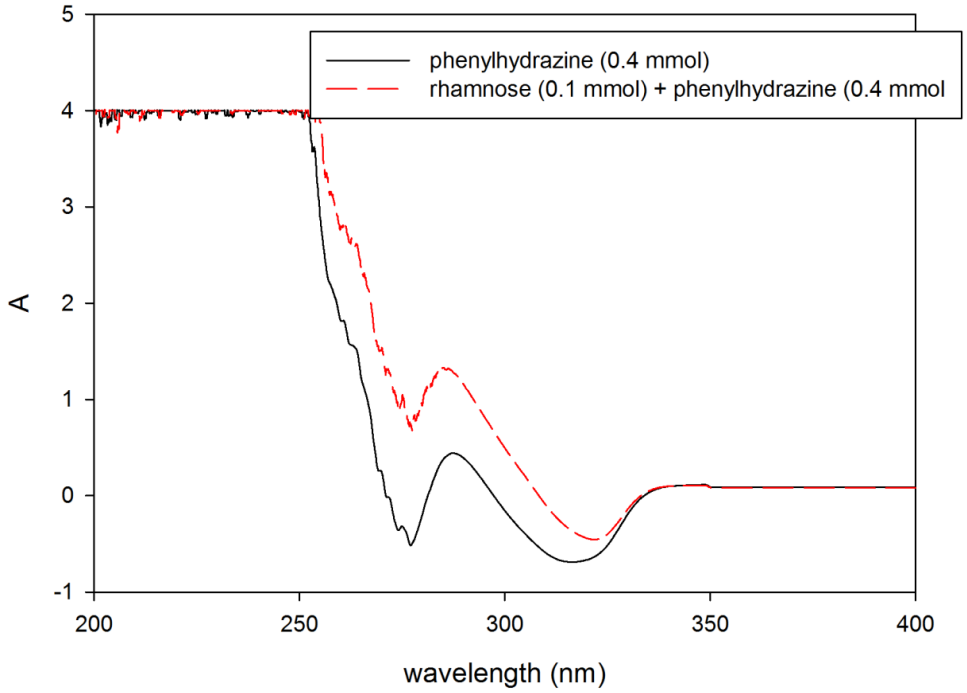

Figure 3.20. Absorbance scans of reaction B (red) and control reaction (black) in milliQ H_2O after stirring for 1h at 80 °C.

An absorbance maxima were observed at 285 for Reaction B while 287 nm was observed for phenylhydrazine alone (slight red-shifted) with absorbance values of 1.32 and 0.452, respectively. If all rhamnose was converted to the hydrazone adduct, then there would be an excess of 0. 3mmol remaining; this would give a high background absorbance, as indicated in Figure 3.20. Therefore, the excess phenylhydrazine would need to be removed by organic extraction to avoid this level of background noise. Excess phenylhydrazine was removed by organic extraction with $CHCl_3$, and absorbance measurements were conducted on Reactions A and B. After 1 h reaction time, excess phenylhydrazine was removed by washing the

mixtures with $CHCl_3$ (2 mL x 3) for Reactions A and B. For Reaction B, the following concentrations were used to generate a standard curve: 0.6, 0.3, 0.15, 0.075, or 0.0375 mM. The absorbance was then read at 285 nm.

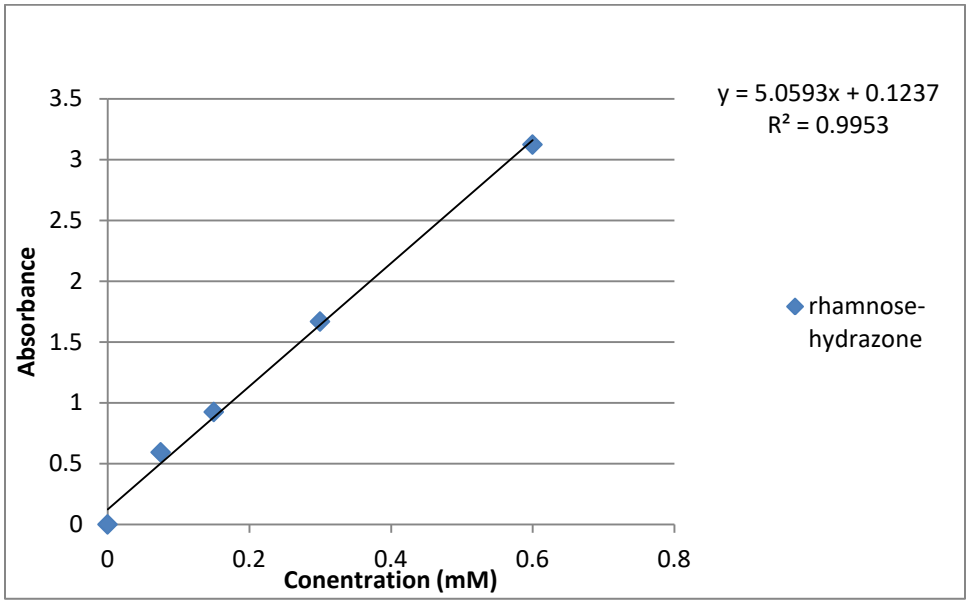

Figure 3.21. Reaction B (rhamnose + phenylhydrazine) in milliQ H_2O standard curve. R^2=0.995.

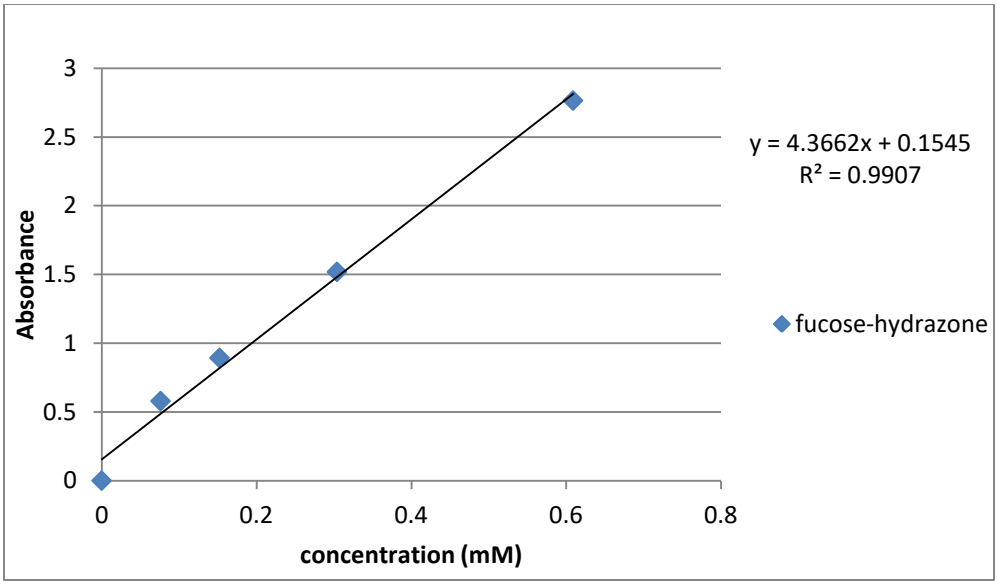

Figure 3.22. Reaction B (fucose + phenylhydrazine) in milliQ H_20 standard curve. R^2=0.99.

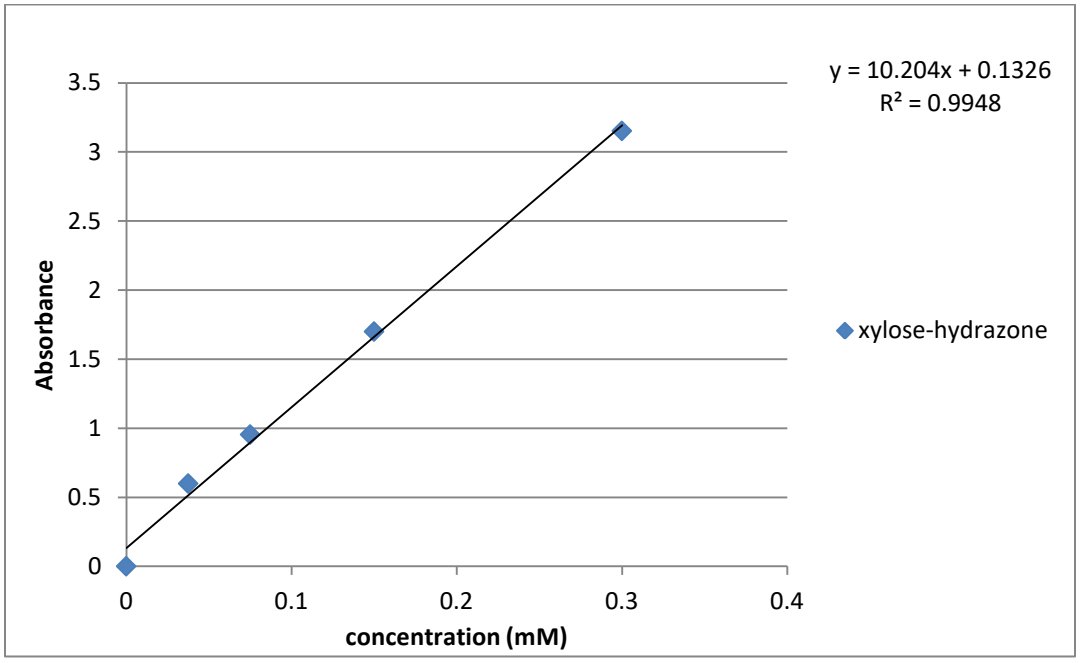

Figure 3.23. Reaction B (xylose + phenylhydrazine) in milliQ H_20 standard curve. R^2=0.99.

Successful removal of excess phenylhydrazine provided negligible absorbance and linear responses for each standard reaction, with excellent linearity R^2>0.99 (Reaction B) for on each aldose. To determine the amount of unreacted aldose present after $NaBH_4$ treatment, to Reaction A, phenylhydrazine was added to generate the phenylhydrazone adduct and any excess was removed by $CHCl_3$ extraction; then the absorbance was read. For Reaction A (sample), a 4-fold dilution was performed and the absorbance was read at 285 nm.

Table 3.6. Reduced product percent yields determined by measuring unreacted aldose. Mean ± SD (n=2).

Aldose	Absorbance	Concentration (mM)	% unreacted present	% reduced product
Rhamnose	2.90±0.021	2.19	14.7	85.3
Fucose	1.52 ±0.0070	1.25	6.3	93.7
Xylose	1.77±0.056	0.64	3.2	96.8

3.5.5. Dechlorination of Sucralose

To a (25 mL) round bottom flask, sucralose (0.0795 g, 0.2 mmol), $FeSO_4 \bullet 7H_2O$ (0.0278 g, 0.1 mmol), and deionized H_2O (9.979 mL) were added and allowed to stir for 5 min. After stirring, (21 μL, 0.2 mmol) of a 30% w/w solution of H_2O_2 (9.79 M) was added to the reaction mixture, producing a translucent bronze color; the mixture stirred for 1 h at 25 °C. After the reaction went to completion, the sugar solution was serially diluted to make the desired concentration points (10–0.1 mM) in 0.1 M sodium phosphate buffer, pH 7.4. Standard samples were centrifuged at 10,000 rpm for 5 min before adding to a 96-well plate.

Determination of Cl

A 50-mL buret was loaded with a solution of AgNO3 (0.1 M, 0.85 g) to titrate an unknown solution (10 mL) containing 50 uL of Na2CrO4 (0.1 M) to determine the number of moles of Cl present.

3.5.6. Fluorescence Recovery Measurements

A stock "probe" solution of the 4,4'-*o*-BBV receptor was prepared as a 2-fold concentration in 0.05 M sodium phosphate-HEPES pH 7.4 buffer with an initial concentration of 1 mM. To the receptor, the solution was added HPTS (8 μM) to complete the probe solution. Blank wells were given 40 μL of the sodium phosphate-HEPES buffer. To the quenched baseline fluorescence (F_o) wells, 20 μL of the probe and buffer were added; to the other wells, 20 μL of probe and analyte solution were added. The fluorescence recovery of HPTS was read using a 96-well plate on a 2103 Envision Multilabel Perkin Elmer reader. After blank subtraction, the relative fluorescence increase F/F_o for each analyte was calculated.

Data Analysis

Apparent binding constants were determined by non-linear curve fitting using the following equation.

$$\frac{F}{F_o} = \frac{\left(1 + \frac{F_{\max}}{F_o}\right) K_b[A]}{1 + K_b[A]} \quad (1)$$

where F_0 is the fluorescence intensity of the quenched dye; F is the fluorescence intensity after the addition of analyte; F_{max} is the fluorescence intensity at which no further signal is obtained with further analyte addition; K_b is the apparent stability constant; and [A] is analyte concentration. K_b was solved using OriginLab software (Originlab Corp, Northampton, MA, USA).

3.6. References

1. Fukasawa, Y.; Tateno, O.; Hagiwara, Y.; Hirose, D.; Osono, T., Fungal succession and decomposition of beech cupule litter. *Ecol. Res.* **2012,** *27*, 735-743.

2. Golovchenko, V. V.; Khramova, D. S.; Ovodova, R. G.; Shashkov, A. S.; Ovodov, Y. S., Structure of pectic polysaccharides isolated from onion Allium cepa L. using a simulated gastric medium and their effect on intestinal absorption. *Food Chem.* **2012,** *134*, 1813-1822.

3. da Cunha, A. L.; de Oliveira, L. G.; Maia, L. F.; de Oliveira, L. F. C.; Michelacci, Y. M.; de Aguiar, J. A. K., Pharmaceutical grade chondroitin sulfate: Structural analysis and identification of contaminants in different commercial preparations. *Carbohydr. Poly.* **2015,** *134*, 300-308.

4. Fujieda, T.; Kitamura, Y.; Yamasaki, H.; Furuishi, A.; Motobayashi, K., An experimental study on whole paddy saccharification and fermentation for rice ethanol production. *Biomass Bioener.* **2012,** *44*, 135-141.

5. Varki, A., Essentials of glycobiology. *Essentials of glycobiology* **1999**, 653.

6. Bao, L. G.; Ma, S. W.; van Huystee, R. B., Glycosylation of the cationic peanut peroxidase gene expressed in transgenic tobacco. *Plant Sci.* **2000,** *156*, 55-63.

7. Anumula, K. R., Quantitative-determination of monosaccharides in glycoproteins by high-performance liquid-chromatography with highly sensitive fluorescence detection. *Anal. Biochem.* **1994,** *220*, 275-283.

8. Grill, E.; Huber, C.; Oefner, P.; Vorndran, A.; Bonn, G., Capillary zone of electrophoresis of p-aminobenzoic acid-derivatives of aldoses, ketoses, and uronic-acids. *Electrophoresis* **1993,** *14*, 1004-1010.

9. Vorndran, A. E.; Grill, E.; Huber, C.; Oefner, P. J.; Bonn, G. K., Capillary zone of electrophoresis of aldoses, ketoses and uronic-acids derivatized with ethyl para-aminobenzoate. *Chromatographia* **1992,** *34*, 109-114.

10. Schwaiger, H.; Oefner, P. J.; Huber, C.; Grill, E.; Bonn, G. K., Capillary zone of electrophoresis and micellar electrokinetic chromatography of 4-aminobenzonitrile carbohydrate derivatives.*Electrophoresis* **1994,** *15*, 941-952.

11. Honda, S.; Akao, E.; Suzuki, S.; Okuda, M.; Kakehi, K.; Nakamura, J., High-performance liquid chromatography of reducing carbohydrates as strongly ultraviolet-absorbing and electrochemically sensitive 1-phenyl-3-methyl-5-pyrazolone derivatives. *Anal. Biochem.***1989,** *180*, 351-357.

12. Noe, C. R.; Freissmuth, J., Capillary zone electrophoresis of aldose enantiomers-separation after derivatization with S-(-)-1-phenylethylamine. *J.Chromat. A.* **1995,** *704*, 503-512.

13. Lamari, F.; Theocharis, A.; Hjerpe, A.; Karamanos, N. K., Ultrasensitive capillary electrophoresis of sulfated disaccharides in chondroitin dermatan sulfates by laser-induced fluorescence after derivatization with 2-aminoacridone. *J. Chromat. B* **1999,** *730*, 129-133.

14. Anumula, K. R., Single tag for total carbohydrate analysis. *Anal. Biochem.* **2014,** *457*, 31-37.

15. Andersen, K. E.; Bjergegaard, C.; Sorensen, H., Analysis of reducing carbohydrates by reductive tryptamine derivatization prior to micellar electrokinetic capillary chromatography. *J. Agri. Food Chem.* **2003,** *51*, 7234-7239.

16. Hansen, J. S.; Christensen, J. B., Recent Advances in Fluorescent Arylboronic Acids for Glucose Sensing. *Biosensors* **2012,** *3*, 400-418.

17. Zhai, W. L.; Sun, X. L.; James, T. D.; Fossey, J. S., Boronic Acid-Based Carbohydrate Sensing. *Chem. Asian J.* **2015,** *10*, 1836-1848.

18. Taylor, M. S., Catalysis Based on Reversible Covalent Interactions of Organoboron Compounds. *Acc. Chem. Res.***2015,** *48*, 295-305.

19. James, T. D.; Shinkai, S., Artificial receptors as chemosensors for carbohydrates. *Host-Guest Chemistry: Mimetic Approaches to Study Carbohydrate Recognition* **2002,** *218*, 159-200.

20. You, L.; Zha, D. J.; Anslyn, E. V., Recent Advances in Supramolecular Analytical Chemistry Using Optical Sensing. *Chem. Rev.* **2015,** *115*, 7840-7892.

21. de Silva, A. P.; Gunaratne, H. Q. N.; Gunnlaugsson, T.; Nieuwenhuizen, M., Fluorescent switches with high selectivity towards sodium ions: Correlation of ion-induced conformation switching with fluorescence function. *Chem. Commun.***1996,** 1967-1968.

22. Corbett, P. T.; Leclaire, J.; Vial, L.; West, K. R.; Wietor, J. L.; Sanders, J. K. M.; Otto, S., Dynamic combinatorial chemistry. *Chem. Rev.* **2006,** *106*, 3652-3711.

23. Bhat, V. T.; Caniard, A. M.; Luksch, T.; Brenk, R.; Campopiano, D. J.; Greaney, M. F., Nucleophilic catalysis of acylhydrazone equilibration for protein-directed dynamic covalent chemistry. *Nat. Chem.* **2010,** *2*, 490-497.

24. Otto, S.; Furlan, R. L. E.; Sanders, J. K. M., Dynamic combinatorial libraries of macrocyclic disulfides in water. *J. Am. Chem. Soc.***2000,** *122*, 12063-12064.

25. Vougioukalakis, G. C.; Grubbs, R. H., Ruthenium-Based Heterocyclic Carbene-Coordinated Olefin Metathesis Catalysts. *Chem. Rev.* **2010,** *110*, 1746-1787.

26. Boul, P. J.; Reutenauer, P.; Lehn, J. M., Reversible Diels-Alder reactions for the generation of dynamic combinatorial libraries. *Org. Lett.* **2005,** *7*, 15-18.

27. Cacciapaglia, R.; Di Stefano, S.; Mandolini, L., Metathesis reaction of formaldehyde acetals: An easy entry into the dynamic covalent chemistry of cyclophane formation. *J. Am. Chem. Soc.***2005,** *127*, 13666-13671.

28. Bull, S. D.; Davidson, M. G.; Van den Elsen, J. M. H.; Fossey, J. S.; Jenkins, A. T. A.; Jiang, Y.-B.; Kubo, Y.; Marken, F.; Sakurai, K.; Zhao, J.; James, T. D., Exploiting the Reversible Covalent Bonding of Boronic Acids: Recognition, Sensing, and Assembly. *Acc. Chem. Res.***2013,** *46*, 312-326.

29. Cao, H. S.; Heagy, M. D., Fluorescent chemosensors for carbohydrates: A decade's worth of bright spies for saccharides in review. *J. Fluores.* **2004,** *14*, 569-584.

30. Yu, X.; Munge, B.; Patel, V.; Jensen, G.; Bhirde, A.; Gong, J. D.; Kim, S. N.; Gillespie, J.; Gutkind, J. S.; Papadimitrakopoulos, F.; Rusling, J. F., Carbon nanotube amplification strategies for highly sensitive immunodetection of cancer biomarkers. *J. Am. Chem. Soc.***2006,** *128*, 11199-11205.

31. Wang, J.; Liu, G. D.; Jan, M. R., Ultrasensitive electrical biosensing of proteins and DNA: Carbon-nanotube derived amplification of the recognition and transduction events. *J. Am. Chem. Soc.***2004,** *126*, 3010-3011.

32. Alivisatos, P., The use of nanocrystals in biological detection. *Nat. Biotechnol.* **2004,** *22*, 47-52.

33. Chen, Y.; Xianyu, Y.; Jiang, X., Surface Modification of Gold Nanoparticles with Small Molecules for Biochemical Analysis. *Acc. Chem. Res.* **2017,** *50*, 310-319.

34. Wang, P.; Lin, Z.; Su, X.; Tang, Z., Application of Au based nanomaterials in analytical science. *Nano Today* **2017,** *12*, 64-97.

35. Liu, J. W.; Lu, Y., Colorimetric biosensors based on DNAzyme-assembled gold nanoparticles. *J. Fluores.* **2004,** *14*, 343-354.

36. Aslan, K.; Zhang, J.; Lakowicz, J. R.; Geddes, C. D., Saccharide sensing using gold and silver nanoparticles - A review. *J. Fluores.* **2004,** *14*, 391-400.

37. Luo, X. L.; Morrin, A.; Killard, A. J.; Smyth, M. R., Application of nanoparticles in electrochemical sensors and biosensors. *Electroanal.***2006,** *18*, 319-326.

38. Wang, Y.; Chalagalla, S.; Li, T.; Sun, X.-l.; Zhao, W.; Wang, P. G.; Zeng, X., Multivalent interaction-based carbohydrate biosensors for signal amplification. *Biosens. Bioelectron.* **2010,** *26*, 996-1001.

39. Huang, Y. J.; Ouyang, W. J.; Wu, X.; Li, Z.; Fossey, J. S.; James, T. D.; Jiang, Y. B., Glucose Sensing via Aggregation and the Use of "Knock-Out" Binding To Improve Selectivity. *J. Am. Chem. Soc.***2013,** *135*, 1700-1703.

40. Chen, W. B.; Elfeky, S. A.; Nonne, Y.; Male, L.; Ahmed, K.; Amiable, C.; Axe, P.; Yamada, S.; James, T. D.; Bull, S. D.; Fossey, J. S., A pyridinium cation-pi interaction sensor for the fluorescent detection of alkyl halides. *Chem. Commun.* **2011,** *47*, 253-255.

41. Evans, W. J.; McCourtney, E. J.; Carney, W. B., A comparative analysis of the interaction of borate ion with various polyols. *Anal. Biochem.* **1979,** *95*,383-386.

42. Lorand, J. P.; Edwards, J. O., Polyol complexes and structure of the benzeneboronate ion . *J. Org. Chem.***1959,** *24*, 769-774.

43. van den Berg, R.; Peters, J. A.; van, B. H., The structure and (local) stability constants of borate esters of mono- and disaccharides as studied by 11B and 13C NMR spectroscopy. *Carbohydr. Res.* **1994,** *253*, 1-12.

44. Van Duin, M.; Peters, J. A.; Kieboom, A. P. G.; Van Bekkum, H., Studies on borate esters II11For part I see reference 7. *Tetrahedron* **1985,** *41*, 3411-3421.

45. Abdelakher, M.; Hamilton, J. K.; Smith, F., The reduction of sugars with sodium borohydride. *J. Am. Chem. Soc.***1951,** *73*, 4691-4692.

46. Sturgeon, R. J., A reinvestigation of the borohydride reduction of carbohydrates. *Carbohydr. Res.* **1992,** *227*, 375-377.

47. Berezenko, S.; Sturgeon, R. J., The enzymatic determination of D-mannitol with dehydrogenase from agaricus-bisporus. *Carbohydr. Res.* **1991,** *216*, 505-509.

48. Gamsey, S.; Baxter, N. A.; Sharrett, Z.; Cordes, D. B.; Olmstead, M. M.; Wessling, R. A.; Singaram, B., The effect of boronic acid-positioning in an optical glucose-sensing ensemble. *Tetrahedron* **2006,** *62*, 6321-6331.

49. Lattova, E.; Perreault, H., Labelling saccharides with phenylhydrazine for electrospray and matrix-assisted laser desorption-ionization mass spectrometry. *J.Chromat. B-Anal. Technol. in the Biomed. Life Sci.* **2003,** *79*, 167-179.

50. Suzuki, H.; Kato, E.; Matsuzaki, A.; Ishikawa, M.; Harada, Y.; Tanikawa, K.; Nakagawa, H., Analysis of Saccharides Possessing Post-translational Protein Modifications by Phenylhydrazine Labeling Using High-Performance Liquid Chromatography. *Anal. Sci.* **2009,** *25*, 1039-1042.

51. Torres, C. I.; Ramakrishna, S.; Chiu, C.-A.; Nelson, K. G.; Westerhoff, P.; Krajmalnik-Brown, R., Fate of Sucralose During Wastewater Treatment. *Environ. Eng. Sci.***2011,** *28*, 325-331.

52. Wiklund, A.-K. E.; Breitholtz, M.; Bengtsson, B.-E.; Adolfsson-Erici, M., Sucralose - An ecotoxicological challenger? *Chemosphere* **2012,** *86*, 50-55.

53. Fenton, H. J. H.; Jones, H. O., The oxidation of organic acids in presence of ferrous iron Part I. *J. Am. Chem. Soc.***1900,** *77*, 69-76.

54. Fenton, H. J. H.; Gostling, M., The action of hydrogen bromide on carbohydrates. *J. Am. Chem. Soc.***1901,** *79*, 361-365.

CHAPTER 4

Development of a High-Throughput Assay for Evaluation of Gastrointestinal Permeability through Recognition of Permeability Markers

4.1. Introduction

The design and synthesis of synthetic molecular receptors for biologically important molecules have developed into a major research area. Progress has been driven by advances in the analytical capabilities of biologists and chemists as well as from medical professionals whose practices lay increasing emphasis on accurately monitoring a patient's biochemical balance. Since the coupling of boronic acids and a fluorescent molecule by Czarnik[1] and Shinkai and coworkers[2] for the detection of glucose, the field has become vastly transformed from detecting simple monosaccharides to the recognition of cell surface carbohydrate biomarkers.[3] Various research groups have developed molecular receptors for the detection of simple to complex saccharides.[4, 5] Although these receptors show potential, there still remains an open avenue for the development of sensors that utilize boronic acid receptors. Measurement of glucose concentration by boronic acid based recognition systems has been the driving force of majority of research.[6-9] An area of research that utilizes sugars as markers for non-invasive assessment of intestinal health is gastrointestinal permeability measurements (see section 4.1.4.).

Boronic acid–based methods have been developed for sensing glucose in biological fluids,[10] as well as for other assays for a variety of sugars.[11] Saccharide recognition by boronic acid derivatives has grown into a major field, taking advantage of the intrinsic affinity of boronic acids for 1,2-cis and/or 1,3-cis diols.[12-15] Largely in relation to diabetes, development of fluorescent-based glucose sensors has

been the focus of much of this research. However, there is a renewed interest in measuring other sugars in biological fluids, such as in blood serum and urine.[7,8,15] For biomedical application, these boronic acid–based sensors must operate in aqueous media at physiological pH around 7.4 and be free from endogenous fluorescence interference. Traditional molecular recognition by boronic acid based system and others have utilized a single receptor-single analyte approach that can dependent on a "lock and key" principle inspired from the concept enzyme-substrate recognition (Figure 4.1).[16]

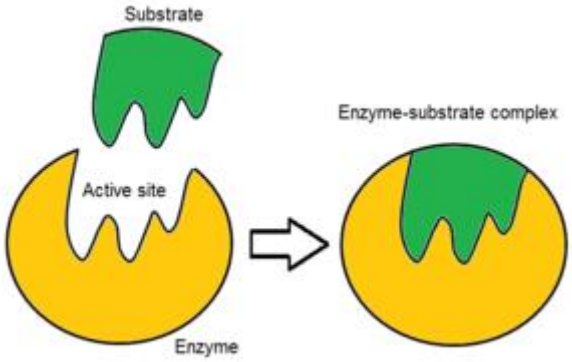

Figure 4.1. Lock and key principle used in enzyme-substrate binding mechanisms

Taking from biological inspirations of specific molecular recognition in enzymes or antibodies, many molecular receptor systems have been developed for single analyte sensing especially for glucose recognition by boronic acids.[6, 13, 15] When designing molecular receptors it is important to have high selectivity for the analyte of interest among multiple analytes that may be present. To achieve this, the receptor has to be systemically designed to prevent unwanted interactions with the

surrounding environment. An arduous task to achieve can come with several limitations and drawbacks. This is a major limitation of selectively designing a receptor for an analyte over other structurally similar analytes (*i.e.* in the case of sugars). With this comes a synthetic challenge and from a practical point of view, it can be an overwhelming synthetic task to design such a selective receptor. Secondly, the rational design of receptors for unknown biomolecular analytes is impossible. Lastly, when dealing with complex mixtures, having one single receptor is not ideal as other components in the mixture can subtly interact with the recognition system.

To circumvent these challenges associated with designing selective receptors, differential based recognition/sensing has been utilized as an alternative approach for the recognition of multiple analytes with multiple (array of) receptors. Array-based systems have been developed for the recognition and discrimination of various analytes,[17] such as metal ions,[18] volatile organic compounds,[19] warfare agents,[20] aromatic amines,[21] amino acids,[22] glycerides,[23] carbohydrates,[24] proteins,[25] bacteria,[26] as well as cancerous cells.[27] The various fingerprints that can be generated using an array of receptors allow for the identification and discrimination of target analytes in complex mixtures whose structure or components may be unknown.

4.1.1. Differential Based Recognition

Differential based recognition relies on the principles to that of human olfactory and gustatory systems.[28] Inspired by these systems, chemical-nose based sensor array approaches have exploited the differential receptor-analyte binding interactions.[29-33] Rather than having a single receptor with a binding affinity for a single analyte, recognition of that analyte can be achieved by the composite response of the analyte to an entire array of receptors (Scheme 4.1).

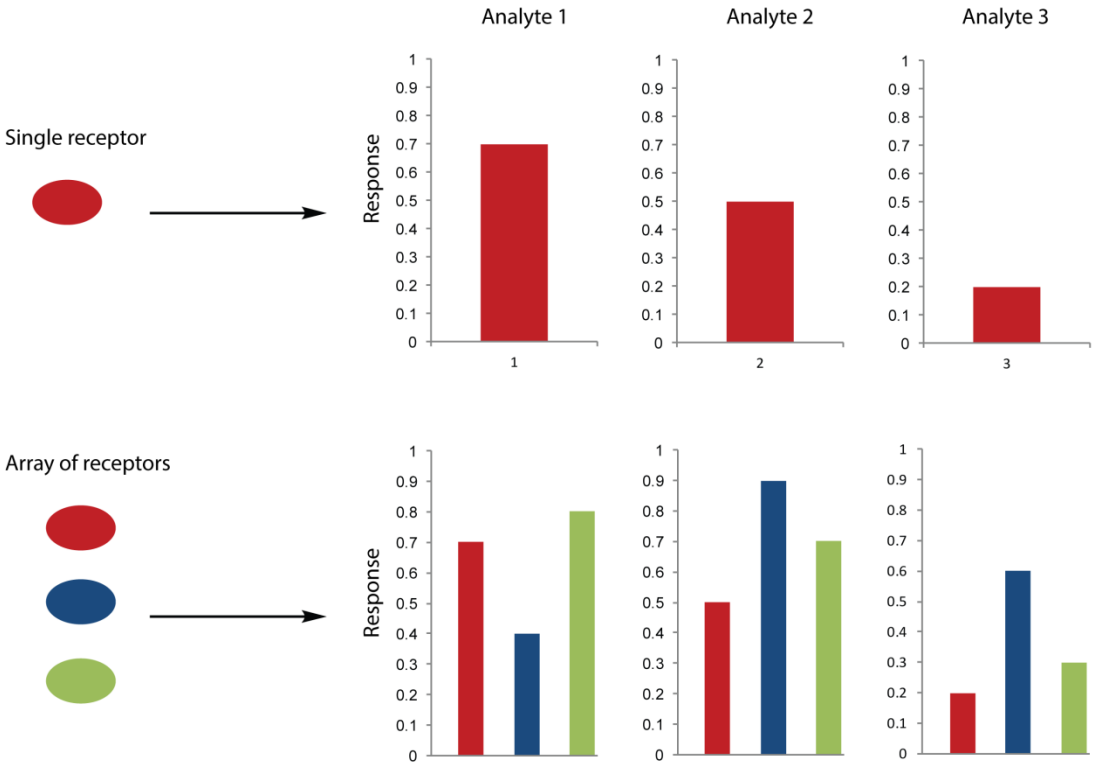

Scheme 4.1. Illustration of single analyte recognition (top) compared to differential recognition by an array of receptors (bottom).

From this, indicator displacement assays were used for developing differential sensing systems because of their flexibility to pick and choose a multitude of receptors or indicators. Each receptor shown in the bottom of Scheme 1 may bind to each analyte differently with varying extents generating a fingerprint. The resulting fingerprint provides a characteristic pattern for the individual analyte or even mixtures of them comprised of multiple analytes. As a result, these non-specific receptors are differential rather than highly specific. These arrays can be used to generate a fingerprint response for a mixture of analytes which can then be analyzed through statistical analysis, such as linear discriminant analysis (LDA) or principle component analysis (PCA).[34] Such statistical methods were devised early on during the developments of "electronic noses/tongues" that generate a differential response and then deconvoluting the response by pattern based recognition algorithms to determine the analytes that are present.

4.1.2. Differential Based Sensing with Indicator Displacement Assays

Indicator displacement assays (IDA) have been utilized as competitive binding assays where the receptor and indicator (or reporter) units are two discrete entities and can provide several advantages over direct sensing (*i.e.* one-component systems, see 1.5.1. for definition). Indicator displacement assay has a reporter unit bound to the receptor unit first, creating a sensing ensemble. Upon interaction with the analyte and receptor unit, the indicator is displaced from the sensing ensemble creating a

measurable change that directly proportional to analyte concentration (Scheme 4.2A). Innovative IDAs have been described by the Anslyn group[35-38] and Severin et al.[24, 39-41] Compared to our two-component approach, in a standard IDA, the indicator in our system is displaced by the analyte from an allosteric interaction, wherein the analyte does not compete at the same binding site with the indicator. In contrast, it binds at another site, inducing a decrease in the affinity of the indicator for the receptor. We have called this type of system as an "allosteric indicator displacement assay" (AIDA) (Scheme 4.2B).

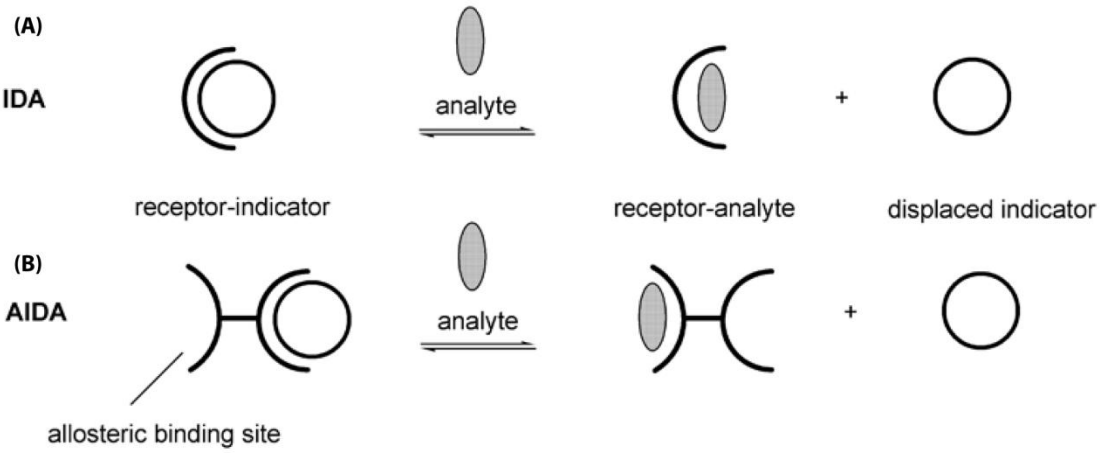

Scheme 4.2. A. Illustration of indicator displacement assay where the analyte competes for the receptor-indicator interaction. **B.** Allosteric indicator displacement assay where the analyte binds at an allosteric site.

These types of systems alleviate the synthetic challenge that is associated with one-component systems, where the receptor and indicator moieties exist as covalently linked entities. This allows for flexibility in the design and development of receptor and allows for screening of indicators to modulate sensitivity or selectivity. In

addition, because of the almost infinite combinations of the receptor and indicator, IDAs and AIDAs offer adaptability to array based sensing (*i.e.* differential sensing).

Compared to single-receptor single-analyte sensing, array-based sensing takes advantage of receptors with low binding or selectivity to enhance the cross-reactivity of the array to provide a differential response. Having these receptors with varied selectivity and affinity, more information could be extracted and be used to accurately identify analytes of interest. Similar to the single analyte systems, a measurable signal is generated upon the introduction of analytes to the array. The signals are collected and analyzed by chemometric analysis, such as PCA or LDA (Figure 4.2).[34, 42]

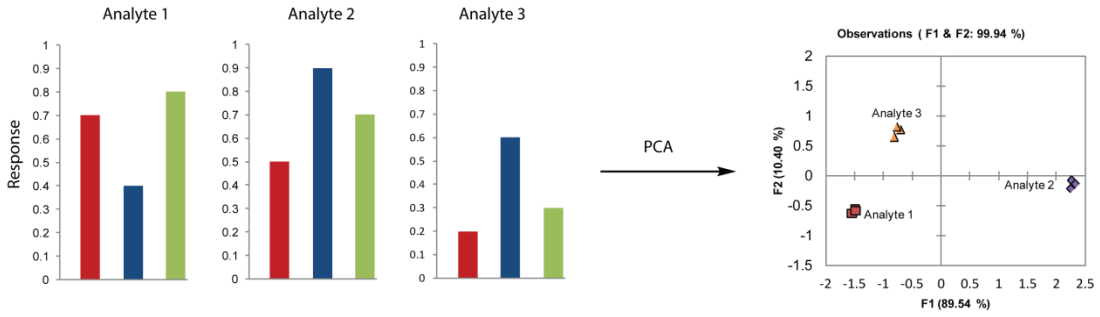

Figure 4.2. Illustration of data acquisition with an array of (3) receptors against 3 analytes. From the generation of a fingerprint response (left) to deconvoluting the dataset by chemometric analysis such as principle component analysis (right) where n=3.

Both PCA and LDA methods produce score plots that can display two, three or more dimensional coordinate system to best discriminate the analytes. Also, both methods decompose the raw data by a matrix technique, in which eigenvectors of the matrix produce axes in the coordinate system that measure the level of discrimination

within the dataset. Principle component analysis reduces the dimensionality of the dataset, with the magnitudes of the eigenvalues representing the variances in the data, which are displayed in the score plot as principle component (PC 1 or PC 2) axes. As a user, the level of discrimination can be simply judged by inspecting the score plots. In a plot with good discrimination, there will be close clustering between repetitions of the same analyte class and good separation between the different analyte classes that are present (*i.e.* analyte 1, analyte 2, and analyte 3 in Figure 4.2). The main difference between LDA and PCA is that with PCA there is no bias placed on finding the greatest variance between analytes. This indicates that the replicates of the same analyte are treated identically as different sets of analytes. In LDA, the mathematics place a bias toward clustering repetitive analytes (*i.e.* class) and separating them from repetitions of a different set of analytes (*i.e.* a different class). Additionally, LDA is a supervised method used for the classification of data as well as the assignment of unknown analytes to their appropriate classes. Linear discriminant analysis is useful for identifying an unknown analyte by assigning the unknown analyte to one of the classes after comparing its response to those in the dataset (training-set).

4.1.3. Boronic Acid Array Based Recognition

Indicator displacement assay or AIDAs are well suited for differential sensing because an array can be constructed by the combination of multiple receptors and/or with multiple indicators without needing additional synthetic steps. Utilization of boronic acids for developing displacement assay can be advantageous because of their robustness, ease of handling, and short syntheses for generating an array of these receptors. Many groups have taken advantage of the boronic acid-diol recognition property to assemble arrays of receptor-indicator for the differential recognition of various types of analytes. Anslyn and coworkers demonstrated the use of three chiral boronic acid receptors and three indicators to identify and determine enantiomeric excess and concentration of eight chiral vicinal diols.[43] Using chiral pyrrolidine linked to a phenylboronic acid moiety, three receptors were synthesized with readily available starting materials by reductive amination (Scheme 4.3, top left). Through an absorbance study, it was determined that the bromo pyrogallol red, 4-methyl esculetin, and pyrocatechol violet indicators (Scheme 4.2, top right) provided optimal discrimination for the four different types of vicinal diols showing an absorbance change of at least $\Delta Abs > 0.05$. Others, such as alizarin, alizarin complex one dihydrate, and pyrogallol red, provided low discrimination between the vicinal diols and were not incorporated into the array. These four different diols that were chosen had different electron withdrawing character. For example, diol **3** contains two phenyl

groups while diol **6** contains none and between diol **4** and **5** is a ketone or ester group (Scheme 4.3 bottom).

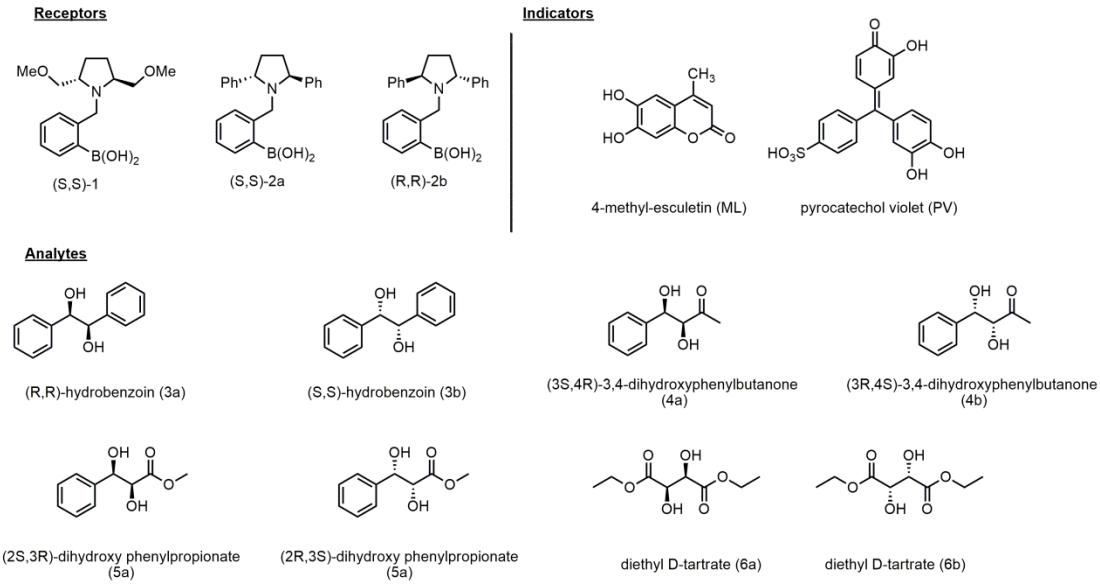

Scheme 4.3. Top left: Structures of chiral boronic acid receptors used. Top right: Indicators used. Bottom: chiral vicinal diols used for study

Using the three receptor-indicator array combinations, the ability to enantioselectivity discriminate amongst these chiral vicinal diols was investigated. This allowed the array to generate a dataset of 3 receptors × 8 vicinal diols × 2 indicators × 4 replicates matrix totaling192 data points. Each diol (5 mM) was treated with each receptor-indicator combination and the absorbance change was monitored at three different wavelengths for each indicator: 496, 500, and 516 nm for (S,S)-1–pyrocatechol violet (PV), 362, 366, and 374 nm for (R,R)-2–methyl esculetin (ML),

and 496, 500, and 516 nm for (S,S)-2–pyrocatechol violet (PV). Taking the absorbance data and subjecting it to chemometric analysis such as PCA provided a score plot for the eight vicinal diols and three receptor-indicator array. There was good separation and clustering within each diol analyzed and excellent discrimination amongst the different diol (Figure 4.3).

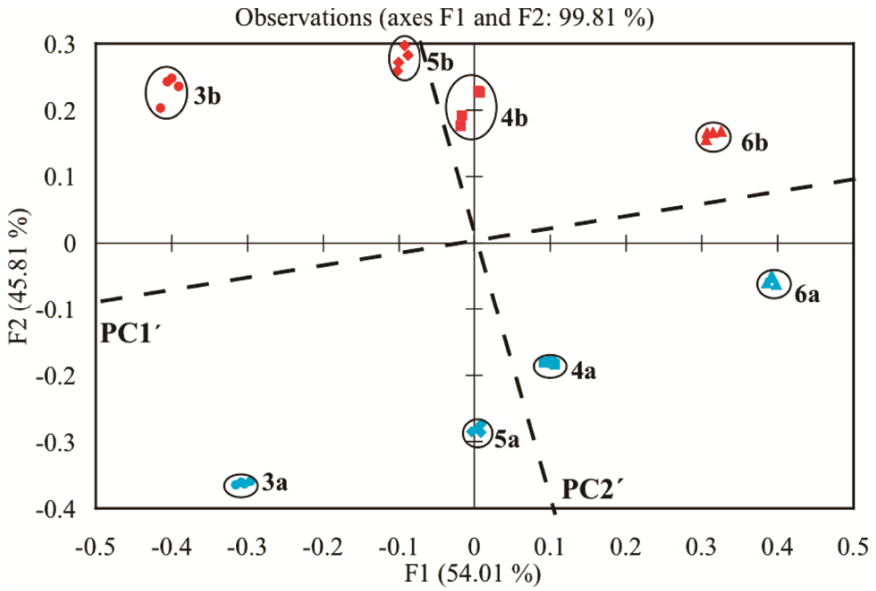

Figure 4.3. PCA plot of the different vicinal diols with the three-receptor indicator array: (S,S)-1–pyrocatechol violet (PV), (R,R)-2–methyl esculetin (ML), and (S,S)-2–pyrocatechol violet (PV). Image used with permission.[43]

Rotation of the X and Y axis by few degrees in the counterclockwise direction, this illustrated the ability of the three-receptor indicator array to discriminate chemoselectively amongst the diols along the PC1' axis. Diols with two aryls groups and one aryl and ester group (**3** & **5**) separated in the negative direction along the PC1' axis. In the positive direction along PC1', there was a good separation of diols with one aryl and ketone group and aliphatic ester diols (**4** & **6**). Additionally, there

was discrimination of the enantiomers of each vicinal diols along the PC2' axis. Diols with S configuration near the phenyl group were separated in the positive direction along PC2' and diols with R configuration separated in the negative direction along PC2'. Lastly, the biaryl diols (**3a** & **3b**) were farthest apart from the rest of the clustering groups which is usually a good indicator of the discriminatory power of this receptor-indicator array for the enantiomers of diol **3**.

Other approaches have been made by other groups such as Suslick and coworkers who have worked extensively on colorimetric sensor array based on boronic acids. This group has developed a boronic sensor array with various colorimetric indicators for the identification and discrimination of monosaccharides, disaccharides, and artificial sweeteners.[44] This immobilized sensor array was comprised of 16 different pH dependent indicators, five commercially available aryl boronic acids (phenyl-, o-hydroxymethyl phenyl-, 2,5-difluorophenyl-, 2,4,5-trifluorophenyl-, and 3-nitrophenyl- boronic acid), to analyze D-glucose. Using a multitude of indicators and boronic acids provided an array with unique composites for each sugar that is being analyzed. Initial difference maps were generated with D-glucose at 25 mM and the change in the RGB values for each indicator was calculated (Figure 4.4).

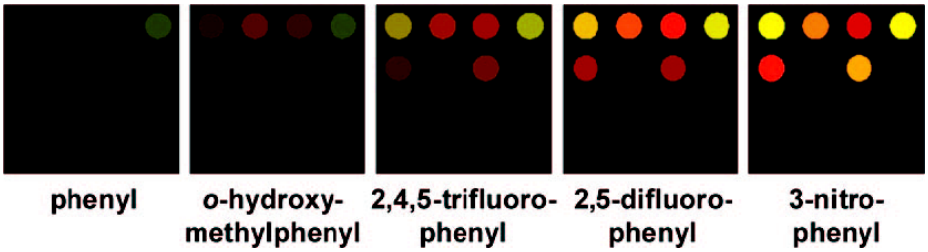

Figure 4.4. The average difference color map generated for each boronic acid-indicator combination with 25 mM D-glucose in phosphate buffer pH 7.4. Imaging of before and after addition of D-glucose and the difference is calculated and shown. Image used with permission.[44]

D-glucose generates a unique colored fingerprint for each boronic acid-indicator combination and this information can be used to generate a score plot using chemometric analysis. It was determined that the 3-nitrophenyl boronic acid had a distinctive response from the 16 indicators used and was then used for other 14 sugars (Figure 4.5).

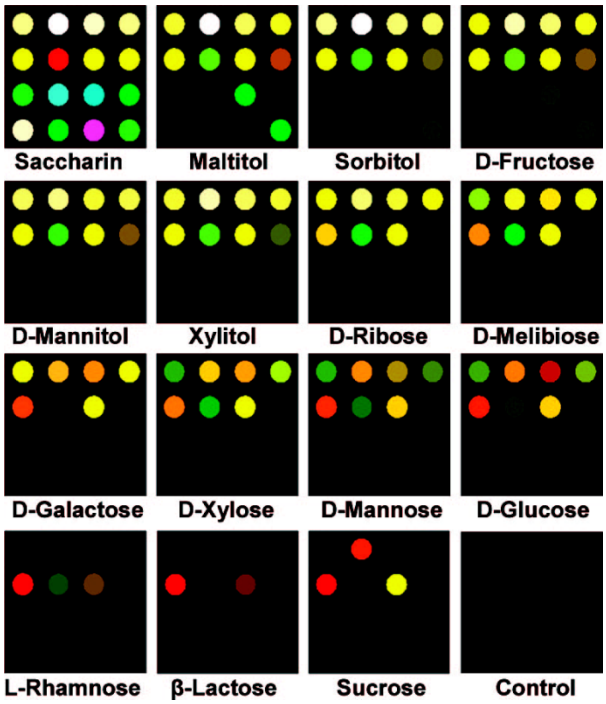

Figure 4.5. 3-nitrophneyl boronic-indicator difference maps for each sugar and sweeteners tested after equilibration at 25 mM concentration. Except for sucrose at 150 mM. Image used with permission.[44]

The 3-nitrophenyl boronic-indicator combinations provided unique fingerprint responses for all 15 sugars and sweeteners being analyzed. However, there was a minimal response (or changes) from three sugars such as L-rhamnose, β-lactose, and sucrose. Sucrose required at least 150 mM to establish some change in the color difference. This alludes to the low affinity that boronic acids have to non-reducing sugars a phenomenon our group has dealt with. In this boronic acid-indicator combination array, it is generally assumed that the resulting changes that are being monitored are predominantly due to only pH changes. From examining the principle component analysis and linear discriminant analysis of the color profile changes,

Suslick and coworkers determined that there was a much higher dimensionality for this colorimetric array. This would indicate that the resulting changes to generate the color differences are not just a result of pH change but through other non-specific interactions such as hydrogen bonding. One drawback that can limit array based sensing is their ability to distinguish between different concentrations of analyte. Surprisingly, this array was able to discriminate between different concentrations of D-glucose from 1, 5, 10, and 25 mM concentrations (Figure 4.6).

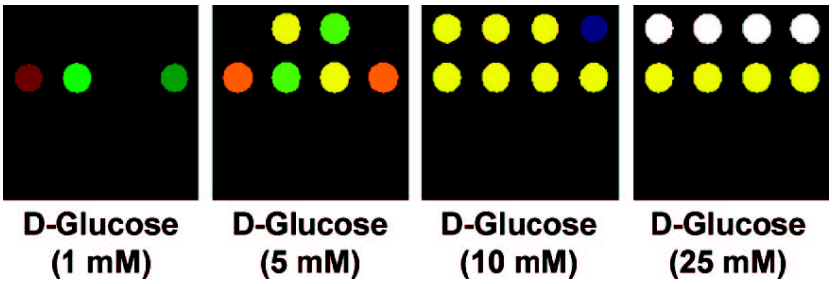

Figure 4.6. The difference in color response from the 3-nitrophenylboronic acid-indicator combination array with varying D-glucose. Image used with permission.[44]

An array with good sensitivity will make it versatile and practical for applications in monitoring changes of glucose in samples that are biologically relevant. The limit of detection where the signal to noise ratio is 3 times the standard deviation of the baseline signal, is <1 mM. For utilization of this array for diabetic applications, the range that is most relevant is between 1-10 mM glucose concentrations, although the colorimetric array was able to distinguish between the three concentrations (1, 5 and 10 mM). The ability to detect small changes in between these concentrations points

was not shown which is important for actual measurements and can limit the applicability of this array if unable to demonstrate this.

4.1.4. Noninvasive Assessment of Gastrointestinal Permeability

Measurement of sugars and sugar alcohols in biological fluids is increasingly important in clinical practice and research. For example, assessment of *in vivo* gastrointestinal (GI) permeability uses oral ingestion and subsequent analysis of combinations of sugar and sugar alcohol markers in urine. Performing GI permeability assessment provides an alternative approach to screening for malnutrition and several gastrointestinal diseases.[45] For example, it has been used to detect mucosal damage in humans and animals in studies connected with inflammatory bowel disease (IBD),[46, 47] celiac disease,[48] and type 1 diabetes.[49] Classically, small intestinal GI permeability is quantified by measuring urinary excretion of orally administered lactulose and mannitol by HPLC analysis in combination with an evaporative light scatter detector or mass spectrometry.[50]

Over the past decades, there has been an increasing recognition of an association between disrupted intestinal barrier function and the development of autoimmune and inflammatory diseases. Aside from permeability testing to be used to assess the presence of GI mucosal injury in diseases,[51] it has also been demonstrated to be an effective research tool to investigate the role of increased permeability in feeding intolerance in preterm infants and environmental enteric dysfunction.[52] Intestinal permeability plays a vital role in maintaining overall gut health by the regulation of transport and absorption of nutrients across the luminal side to the basolateral side

(circulation). How this is achieved is through the intestinal epithelium layer of cells lining the gut lumen acting as a barrier to prevent passage of harmful intraluminal antigens, microorganisms, and other toxins. Additionally, it acts as a selective filter that allows the translocation of necessary nutrients, electrolytes, and water. There are two known pathways that are known for molecules and entities to cross the epithelial barrier; transcellular or paracellular pathways (Figure 4.7).[53]

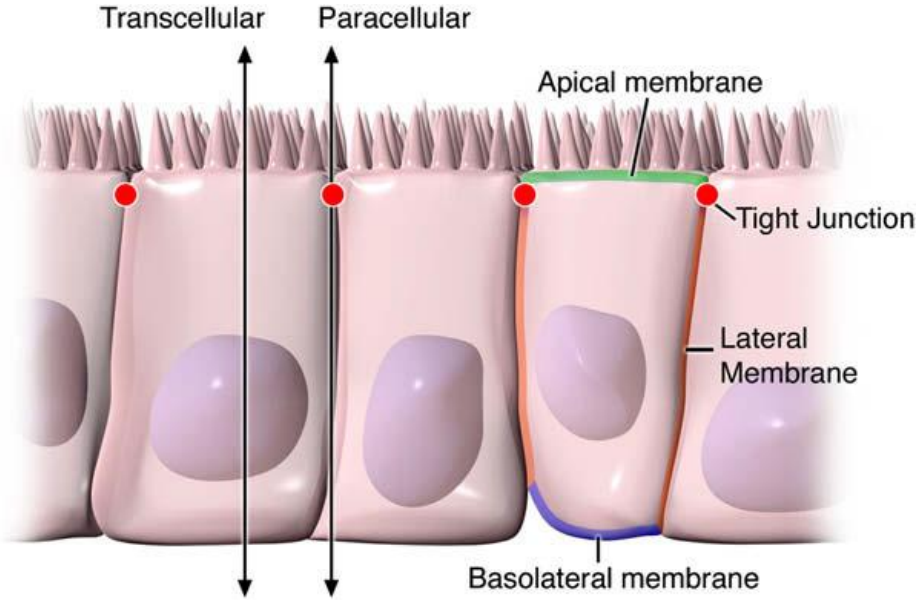

Figure 4.7. An intestinal epithelial layer of cells. Apical membrane (luminal) and basolateral (circulation) membrane shown. Arrows indicate different pathways of transport for nutrients. Image used with permission.[53]

The transcellular pathway is usually associated with solute transport through the epithelial cells and is regulated by selective protein transporters for amino acids, short-chain fatty acids, and sugars.[54, 55] Paracellular is considered the inactive transport of solutes through the space between epithelial cells which is regulated by intercellular protein complexes localized at the apical-lateral membrane junction and

along the lateral membrane.[56] Contact between these epithelial cells includes three major components that are identified as desmosomes, adheren junctions (AJs), and tight junctions (TJs). This adhesive complex matrix consists of transmembrane proteins that link adjacent cells to the actin cytoskeleton through cytoplasmic scaffolding proteins (Figure 4.8).[57]

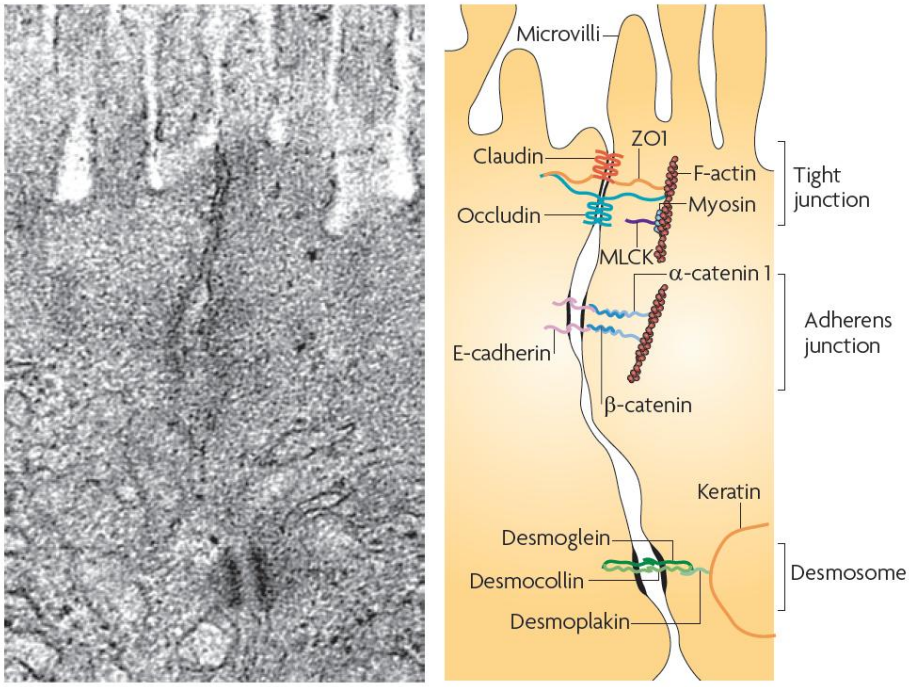

Figure 4.8. Electron micrograph of epithelial cells (left). Cartoon illustration of epithelial cells linked by the three major components (right). Reproduced with permission.[58]

Additionally, there are other architectural features along with these protein complexes. The small intestinal epithelium contains a gradient of pore sizes within the villi and microvilli as noted in Figure 8. The smallest being on the villus tip (4-5

Å), and the largest being in the crypt (> 20 Å) followed by an intermediate pore size along the villus base (Figure 4.9).[51]

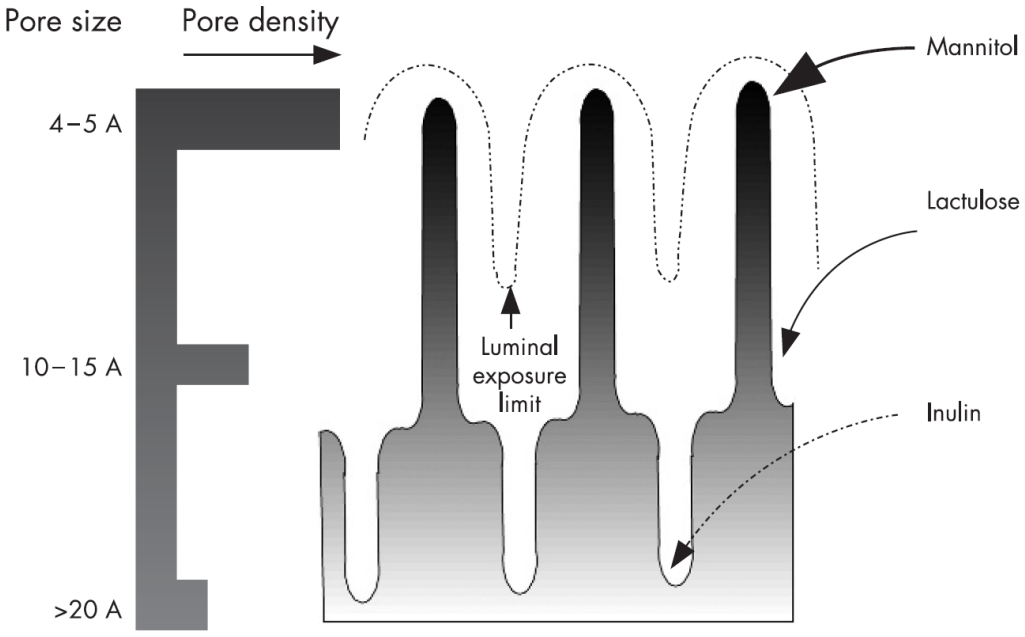

Figure 4.9. Illustration of the crypt-villus axis where the broken line is represented as the luminal exposure limit to which solvent drag effects are noticeable. The scale on left is a qualitative estimate of increasing pore size along the crypt-villus axis with a horizontal bar providing an estimate of the number of each size pore.

Small molecules such as mannitol are able to traverse the small pores on the villus tip, while larger molecules such as the disaccharide lactulose can only move through larger pores in the villus base or crypts. Consequently, mannitol serves as a marker of epithelial surface area, whereas the ability of lactulose to permeate through the pores depends on their extent of "leakiness". [59, 60] Once these markers have been absorbed, the markers enter the bloodstream and are excreted in the urine unmetabolized in the same amount and ratio as they permeate the mucosa.[61-63] If GI permeability becomes compromised, the ratio of lactulose to mannitol (lactulose/mannitol) found in the

urine will be greater than baseline permeability. Lactulose and mannitol measurements are strictly for small intestinal permeability as both sugars will be metabolized by the microbiota in the ileum or colon segments. In addition, other markers can be used to provide insight into the gastric permeability (sucrose), the intestinal absorptive function (xylose and 3-O-methyl-D-glucose).[59] To obtain assessment of colon permeability, sucralose has been utilized because of its unusual structure; it goes unrecognized by the body's and micro biota's metabolism remaining completely intact in urine (Figure 4.10).[64]

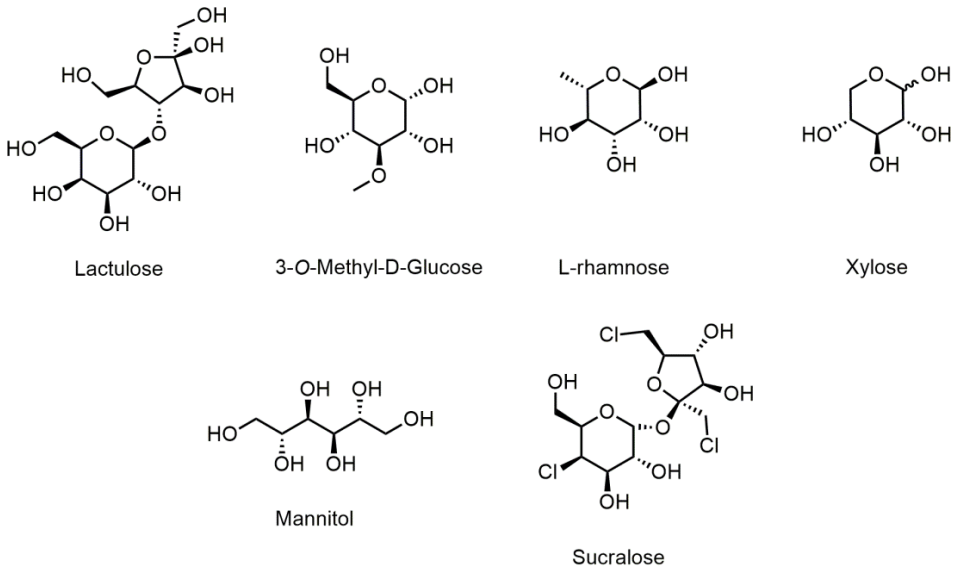

Figure 4.10. Structures of markers used for permeability assessment.

Each of these permeability markers lacks an intrinsic chromophore, consequently, analytical methods are needed to quantify these markers in urine samples when conducting the permeability test. Additionally, chromatographic separation is needed to obtain quantification values of each permeability marker to determine ratios of

lactulose/mannitol or lactulose/rhamnose for small intestinal permeability and sucralose for colon permeability. Alternatively, NAD(P)H-coupled enzyme assays are used but require considerable time and cost.[65, 66]

4.2. Background and Rationale

Due to the nature of our modular two-component system (BBV-HPTS), where the dye and quencher are two discrete entities, this can provide better selectivity and sensitivity over markers of interest. The quencher can be readily modified without altering the photophysical properties of the reporter dye. Because of the ionic nature of these receptors, they are water-soluble at physiological pH even in the absence of sugar. For the development of this assay, several boronic acid receptors were synthesized in pursuit of a sensitive and selective receptor for lactulose compared to mannitol. This would enable our BBV-HPTS assay to be used for lactulose/mannitol determination in permeability samples. Given the ease of synthesis, two boronic acid receptors were initially used for lactulose and mannitol studies. The bis-boronic acid receptor was compared to the mono boronic acid appended viologen receptor (Scheme 4.4).

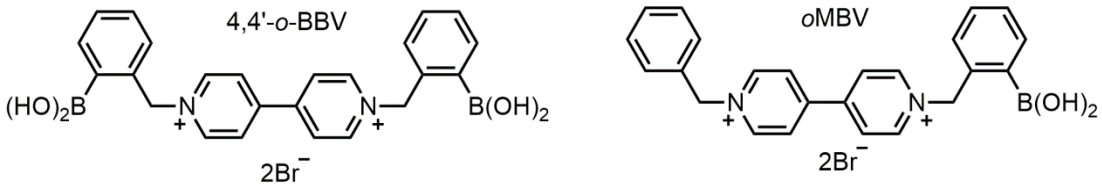

Scheme 4.4. Structures of bis-(4,4'-*o*-BBV) and mono- (*o*MBV) boronic acid appended viologen.

4.3. Results

Although HPLC-MS are sensitive analytical methods, the labor-intensive nature of these methods and cost per analysis hinder the use of this method in large-scale studies that require analysis of multiple samples per day. For permeability testing to advance to routine use, more rapid and cost-effective analyses of sugars and sugar alcohols in biological buffers, urine and blood are desirable and would facilitate other lines of biomedical research where sugars and sugar alcohols need to be measured. Herein, we report the utilization of our developed two-component system for the recognition and quantification of these permeability markers to provide an alternative analytical approach for permeability testing (Scheme 4.5).

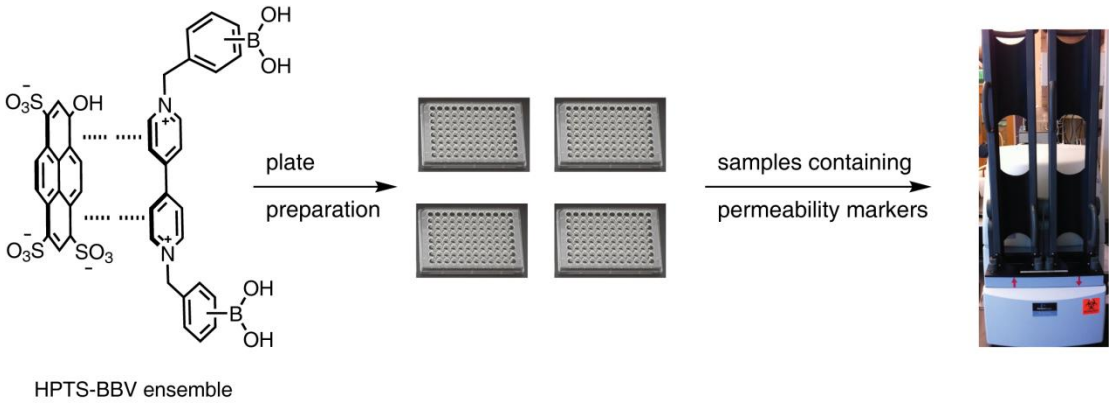

Scheme 4.5. Assembly of a high-throughput assay for quantification of permeability markers used in permeability test.

Assembling the BBV-HPTS ensemble onto 96- or 384-well plates would allow for rapid analysis of single permeability marker at a time. We envisioned that this assay would increase throughput analysis of permeability samples from 1-10 per day (standard analytical methods) to 100-1000 per day using the BBV-HPTS assay.

4.3.1. Recognition of Lactulose and Mannitol by Boronic Acid Appended Viologen Receptors

To quickly determine whether or not we can utilize our two-component assay for determining small intestinal permeability by measuring the classical lactulose/mannitol mixture, binding studies using the two boronic acids appended viologen receptors, such as 4,4'-*o*-BBV and *o*MBV were studied. An initial comparison between the binding affinity and/or selective of the selected boronic acid appended viologen receptors for lactulose and mannitol was conducted. This binding study was performed in sodium phosphate buffer and the fluorescence recovery of each receptor for each permeability marker was measured (Figure 4.11).

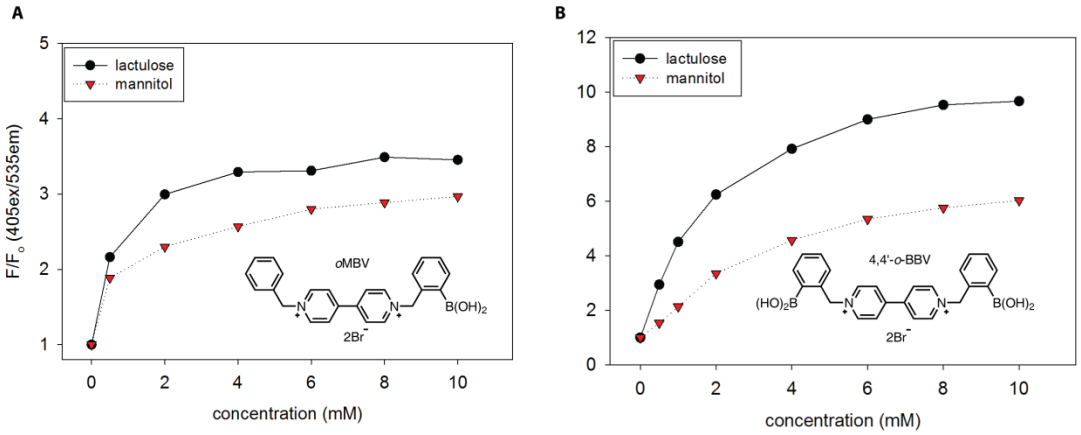

Figure 4.11. Normalized HPTS (4 μM final concentration) fluorescence responses (F_o=initial quenched fluorescence, F=recovered fluorescence) with each boronic acid receptor *o*MBV (**A**) and 4,4'-*o*-BBV (**B**) against lactulose and mannitol in 0.1 M sodium phosphate buffer, pH 7.4.

The mono-boronic acid appended viologen receptor (*o*MBV) provided moderate recovery for lactulose and mannitol with low selectivity. On the contrary, the bis-receptor (4,4'-*o*-BBV) provided much higher fluorescence recovery with modestly improved selectivity between lactulose and mannitol. Based on our previous work with sugar alcohols, we initially hypothesized that that mannitol would provide much higher fluorescence recovery compared to lactulose. Due to its acyclic nature and mannitol having the critical *threo*-1,2-diol unit for optimal boronic acid recognition, was still not sufficient to have higher affinity over lactulose. Conversely, lactulose a disaccharide comprised of galactose and fructose provided at least a 2-fold increase in binding for 4,4'-o-BBV and at least 3-fold increase for *o*MBV (Table 4.1).

Table 4.1. Association constants (K_b) of boronic acid appended viologen receptor

Receptor	**Lactulose**	**Mannitol (K_b, M^{-1})**
***o*MBV**	354±14	89±19
4,4'-*o*-BBV	481±19	218±15

Based on the fact that boronic acids have higher binding constants for the furanose in fructose over other saccharides,[67, 68] the above data implies that the fructose moiety of lactulose is responsible for the strong boronic acid affinity observed for lactulose. With the moderate level of selectivity observed for lactulose over mannitol with each two-component receptor, analysis of each permeability marker can only be performed one at a time. The binding mechanism of boronic acids

to diols has been investigated for glucose and fructose.[67, 69] Analysis by ^{13}C-NMR demonstrated that phenylboronic acid forms the β-D-fructofuranose complex or β-D-fructopyranose at C2 and C3 under alkaline conditions similar to what we observed in our study. Since lactulose contains a fructose moiety in which hydroxyls at C2 and C3 are available binding, the BBVs were anticipated to interact at these carbons, with galactose ring of lactulose contributing to a lesser extent.

A limit of detection and quantification analysis was conducted to evaluate which boronic acid appended viologen receptor would be best suited for lactulose analysis in actual urine samples. Standard curves for each receptor were obtained with the highest data point at 4 mM and lowest at 30 μM in sodium phosphate buffer and then in human baseline urine (see 4.3.2 for definition). The 4,4'-*o*-BBV receptor gave a marked improvement of lower limit of detection and quantification compared to the *o*MBV receptor (Table 4.2).

Table 4.2. Limit of detection and quantification of lactulose for each receptor

Receptor	LOD (uM)	LOQ (uM)
***o*MBV**	110	700
4,4'-*o*-BBV	80	400

Table 4.2. The limits of detection (LOD) and quantification (LOQ) were defined as the analyte concentration in which the fluorescence intensity in the assay was 3 and 10 standard deviations above the mean baseline fluorescence. Values were obtained in human baseline urine.

The limit of detection and quantification for lactulose by 4,4'-*o*-BBV demonstrated to be effective for detecting lactulose in the expected concentrations ranges that healthy subjects (low absorption of lactulose) would have in permeability samples. Due to the lack of selectivity of lactulose over mannitol with each receptor, we envisioned using 4,4'-*o*-BBV to measure lactulose as a sole marker.

4.3.2 Re-defining the Lactulose-Mannitol Ratio for Small Intestinal Permeability

Given that our BBV-HPTS system is limited to quantifying one permeability marker at a time (*i.e.* lactulose or mannitol), we needed an alternative reference marker to determine small intestinal permeability. This reference marker should be readily quantified without interfering with the BBV-HPTS measurement of lactulose. The strategy to indirectly measure small intestinal permeability using a new reference marker by the BBV-HPTS system is two-fold: 1) obtain a lactulose/new reference marker value 2) obtain a mannitol/new reference marker value to subsequently provide the classical lactulose/mannitol through two separate measurements. We selected riboflavin as the new reference biomarker for our studies. Riboflavin has been found to be almost entirely absorbed through the type 2 riboflavin transporter (RFT2) at apical epithelial membranes in the small intestine (Figure 4.12).[70]

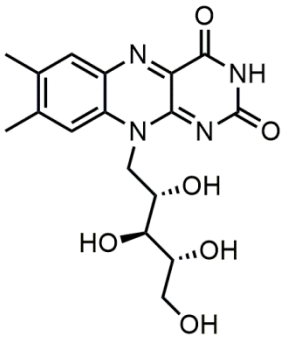

Riboflavin (Vitamin B2)

Figure 4.12. The structure of riboflavin.

Loss of RFT2 expression results in severe riboflavin deficiency.[71] Therefore, we hypothesized that the appearance of riboflavin in urine samples, during six hours after oral ingestion, reflects absorption of riboflavin at duodenum and jejunum. This profile is very similar to that observed for the absorption of mannitol. Riboflavin's intrinsic fluorescence was used to quantify it by measuring its fluorescence at 580 nm when excited at 450 nm (Figure 4.13).

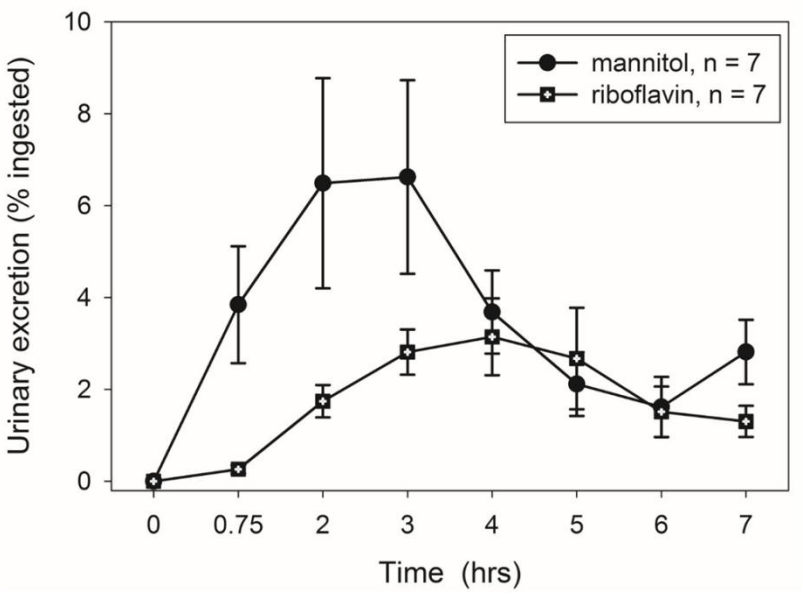

Figure 4.13. Percent ingested (urinary excretion) of mannitol or riboflavin in healthy volunteer subjects. Mannitol was measured using 4,4'-*o*-BBV-HPTS method and riboflavin by its intrinsic fluorescence (λ_{ex}=450, λ_{em}=580). Data points are mean ± SEM. Image reproduced with permission.[72]

Measuring small intestinal permeability was further simplified by replacing mannitol with riboflavin, after riboflavin measurement it can be easily removed by a C18 solid support, and our two-component system (BBV-HPTS) can be used to measure lactulose (Scheme 4.6). This will provide a lactulose/riboflavin measurement and after subsequent mannitol/riboflavin measurement, the classical lactulose/mannitol value can be obtained indirectly.

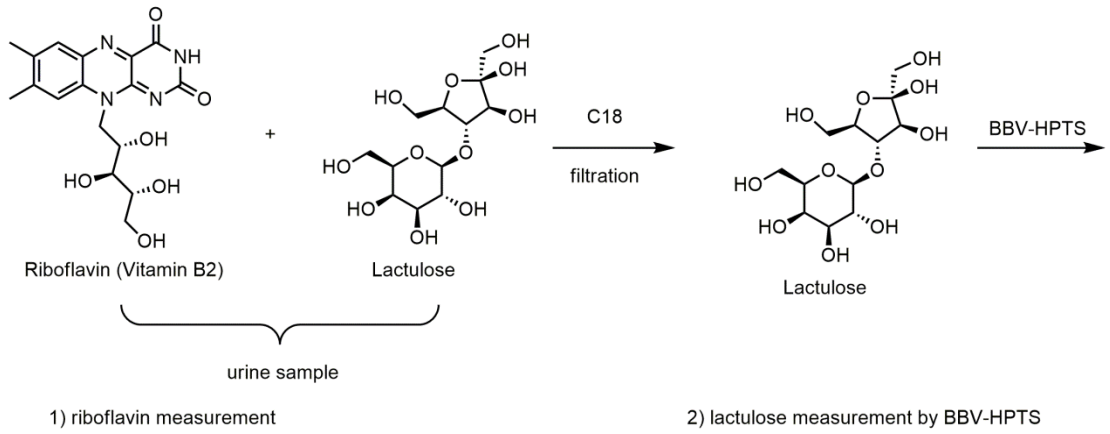

Scheme 4.6. Outline of using riboflavin and lactulose as the permeability markers and the methodological steps for the analysis of them.

In addition to riboflavin endogenously present in urine, there are other chromophores (*i.e.* bilirubin and urobilinogen) that we were aware of and their interference with HPTS wavelengths. Provided that these chromophores are moderately hydrophobic, the C18 solid phase extraction would likely remove the majority of these components. An absorbance study was conducted to demonstrate the effectiveness of the C18 solid phase extraction to urine samples provided by volunteer subjects (Figure 4.14).

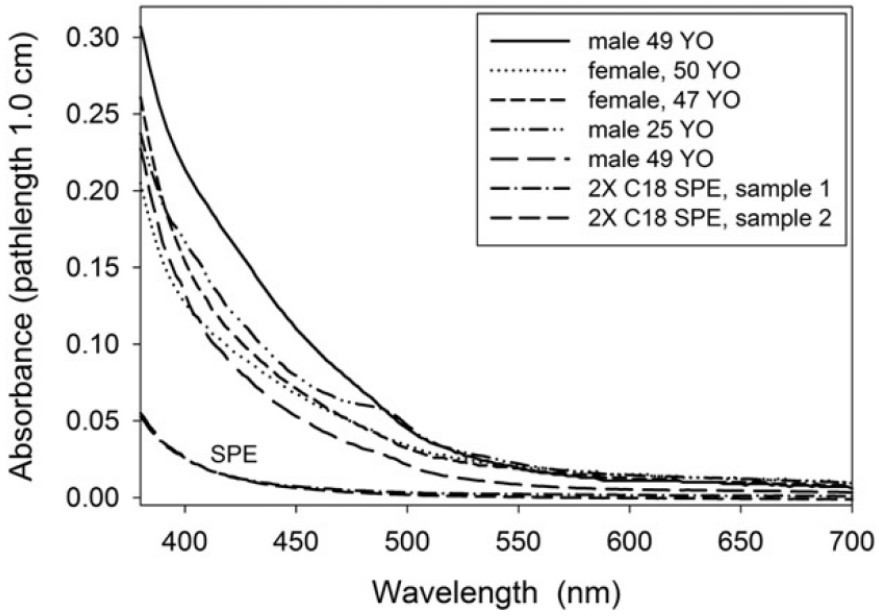

Figure 4.14. Absorbance spectra of urine from 5 volunteer subjects prior to ingesting the permeability markers. These baseline urine samples were used to show the effective removal of endogenous molecules that could interfere with HPTS. Reproduced with permission.[72]

Urine samples were collected prior to ingesting permeability markers and after having to drink large amounts of water before collection. This fraction of urine that is collected is defined to be the "baseline urine". The absorbance for samples that were treated or untreated with C18 was measured for background absorbance. All samples except the "2X C18 SPE" samples show the level of absorbance that is typical in untreated urine samples. After passing the urine samples through the C18 solid support twice, negligible absorbance was observed below 380 nm and above 700 nm. Additionally, this C18 treatment of urine reduced the background fluorescence to 20 times below quenched fluorescence of HPTS. Among the concerns in performing any light based assay on urine is interfering absorbance and fluorescence. For samples

destined for the viologen assay, the C18 SPE cleanup procedure proved sufficient to eliminate riboflavin as well as endogenous fluorescence to the extent of being negligible.

Having demonstrated the ability to remove unwanted background fluorescence with a simple C18 filtration step, the temporal profile of riboflavin was monitored and compared to mannitol. Each marker was analyzed hourly after ingestion, riboflavin measurement was conducted by its intrinsic fluorescence and mannitol by our two-component system assay (Figure 4.13).

Riboflavin consistently appeared later than mannitol. Both riboflavin and mannitol returned to baseline at about six hours, demonstrating six hours is an acceptable cutoff for studies of small intestinal permeability. Riboflavin, a true nutrient absorbed through RFT2 transport, should be able to replace mannitol and used as a surrogate marker for nutrient malabsorption.

Given that mannitol could be replaced by riboflavin to obtain an assessment of small intestinal permeability, 13 healthy volunteers (asymptomatic) were recruited to conduct the newly defined lactulose/riboflavin ratio for permeability testing. After oral ingestion of permeability markers (riboflavin and lactulose), urine was collected during a 0-6 hour time period and riboflavin was measured immediately. Urine was then processed through a C18 solid support and lactulose was measured by the two-component assay to obtain percent ingested by using the following equation (1).

$$\%\,\text{ingested} = \frac{concentration(g/mL) * urinevolume(mL)}{ingested(g)} * 100 \quad (1)$$

This can then be used to determine the lactulose/riboflavin ratio which provides level of permeability (i.e. "leakiness") of the small intestine. Amongst the 13 healthy volunteers that were evaluated, two subjects demonstrated to have high lactulose recovery with one being an obvious outlier (Figure 4.15).[72]

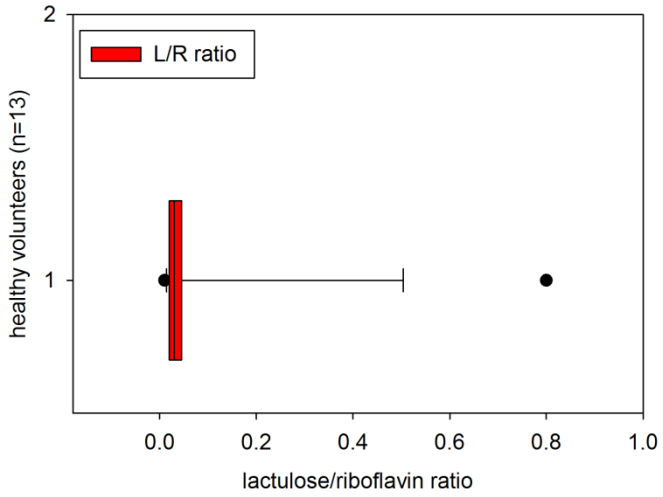

Figure 4.15. Box plot illustration of the various lactulose/riboflavin ratios obtained from 13 healthy volunteers.

Despite anticipated concerns for variation due to metabolism, *etc.*, riboflavin values in healthy subjects varied, if anything, less than mannitol. The delay in the appearance of riboflavin relative mannitol might reflect differences in where the initial uptake occurs. Riboflavin is confined to uptake through the RFT2 transporter and may more strongly correlate with the condition of villi tips of duodenum and

jejunum. Because RTF2 transport is down-regulated in some gastrointestinal diseases, riboflavin measurements should serve to identify such conditions. The range in riboflavin values obtained here suggests a narrow range of values in healthy individuals.

After further inspection of the subjects who participated in this study, it was determined that two volunteers had been taking NSAIDs for chronic pain, but were otherwise healthy. These two were outliers in the assays, presumably due to NSAID use, as noted in the box plot near the right enclosed box (0.05) and the outlier point on the far right (0.80 value). These identified outliers indicate the capacity to identify increased small intestinal permeability. The subject with unusually high lactulose/riboflavin value suggests detection of villi tip architectural damage.

To further demonstrate the effectiveness of our two-component assay for measuring the permeability marker lactulose, a comparative study was conducted between the ability of 4,4'-*o*-BBV to quantify lactulose and compared to the enzymatic method. A correlation plot between both of these methods was generated from 24 urine samples containing lactulose (Figure 4.16).

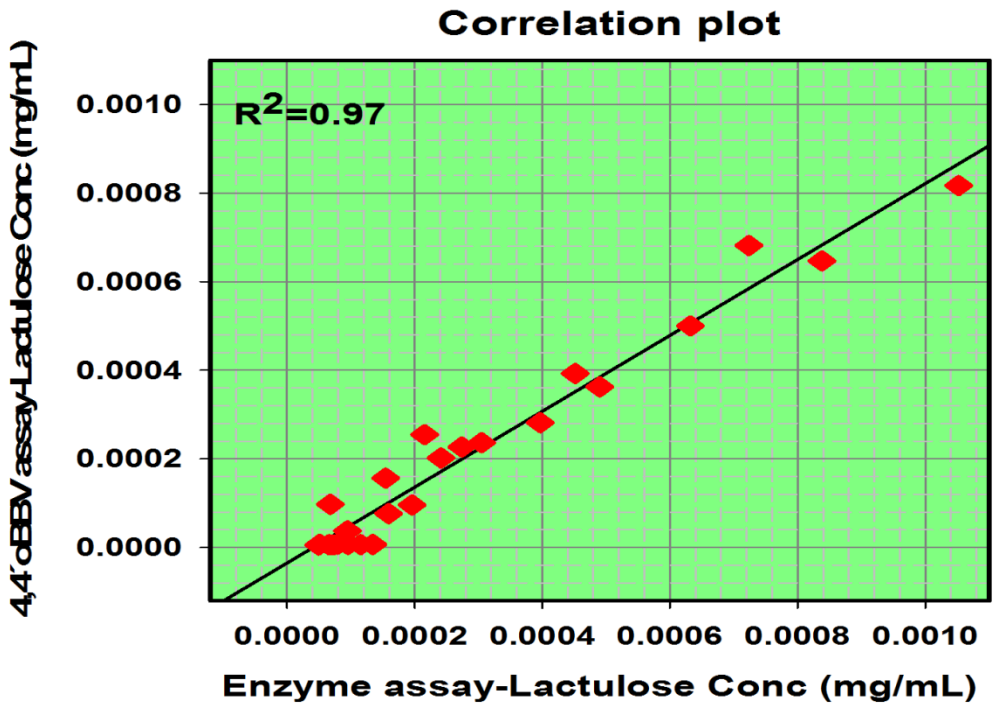

Figure 4.16. Correlation between the two-component assay using 4,4'-*o*-BBV and conventional enzyme assay. Two component assay was run in quadruplicates (CV=12%) while the enzyme assay was run in triplicates (CV=8%).

Using the two-component assay for lactulose measurements is advantageous by several-fold. The 4,4'-*o*-BBV-HPTS "probe" solution can be premixed and pipetted into a 96-well plate and stored for two weeks ready to be used. Ultimately increasing throughput and reducing cost compared to enzymatic means, this necessitates the utility of our two-component system for conducting small intestinal permeability measurements.

4.3.3. Development of a Florescent Probe Array for the Discrimination of Permeability Markers to Determine Level of Permeability

Having a modular two-component sensing system comprised of the HPTS dye and a boronic acid appended viologen (BBV), a small library of BBVs can be generated to assemble an array for the discrimination of permeability markers. The dye and quencher as two discrete entities can provide better selectivity and sensitivity over saccharides of interest. This also allows the quencher to be readily modified without altering the photophysical properties of the reporter dye. In addition, varying ratios of the receptor to reporter dye can be used to modulate fluorescence response. Several bipyridinium and phenanthrolinium based receptors have been synthesized previously and have been studied extensively for glucose binding.[73] From our library of receptors, six BBVs were chosen for this study based on the following criteria: a) at least one boronic acid motif must be in the ortho position; b) each receptor have varying intramolecular distance between boron atoms; c) the cationic charge of all receptors must be at minimum of 2+; and d) each receptor must be synthesized in no more than three steps (Scheme 4.7).

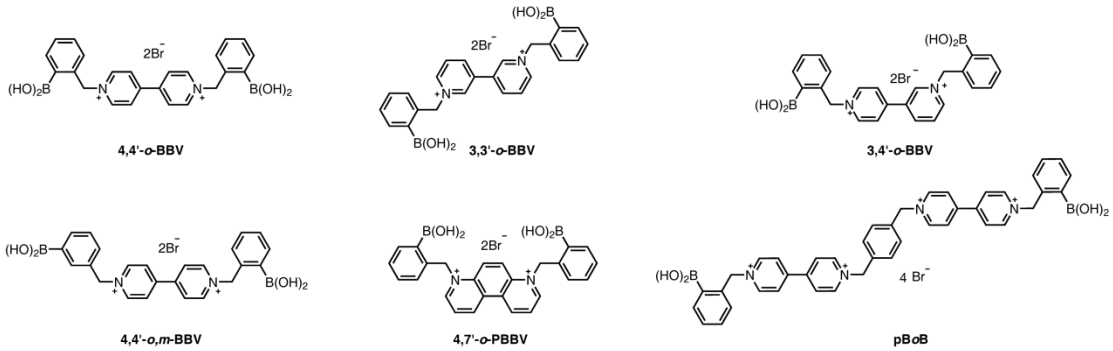

Scheme 4.7. Structures of boronic acid array composed of six unique boronic acid-appended benzyl viologens with corresponding abbreviations.

Using an array of boronic acid receptors provided a rapid screening of multiple sugar alcohols in a short period of time. This fingerprint generating assay technique is similar to the high-throughput screening of chemical libraries for identifying drug targets and alleviates the need for designing selective boronic acids for the recognition and discrimination of permeability markers.

In-vivo GI permeability assessment can be performed noninvasively by oral administration of sugar markers such as lactulose and mannitol. The transport of molecules from the intestinal lumen to the basolateral side can occur through two distinct mechanisms. Mannitol diffuses through the transcellular and paracellular pathway, whereas lactulose passes through a size-restricted, paracellular pathway.[60] Due to the current limitation of our two-component system to analyze one permeability marker at a time, we aimed to develop an array of boronic acid appended viologen receptors to discriminate between discriminate lactulose from

other sugar markers that are usually used as internal references in the permeability test.

From a range of permeability markers, we selected the markers lactulose, L-rhamnose, xylose, 3OMeGluc, erythritol, and mannitol for our investigation with the boronic acid array to obtain a fingerprint response. The goal of this analysis was to discriminate lactulose from the other sugar markers that are usually used as internal references in the permeability test. The concentration that would be regarded as low permeability, 100–500 µM, was chosen for all markers to identify the boronic acid receptors that are significant for fingerprint generation. For lactulose, the optimal fluorescent response is achieved with 4,4'-*o*-BBV, 4,7-*o*-PBBV, and pB*o*B receptors. For mannitol, 4,4'- and 3,3'-*o*-BBV provided a significant fluorescent response (Figure 4.17).

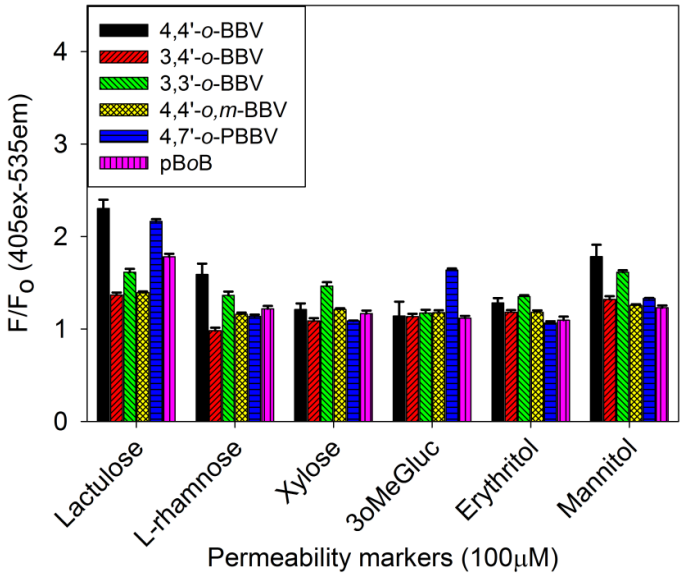

Figure 4.17. Normalized HPTS (4 μM) fluorescence responses with each boronic acid receptor against 100 μM of each individual permeability marker. Data points are mean ± SEM, n=6. F_o=initial quenched fluorescence, F=recovered fluorescence.

The benefit of having an array of up to six receptors is that the size of the array can be adjusted to find optimal discrimination pattern(s). Using all six receptors for the array was unnecessary and decided to reduce the size to three receptors. From the six receptors at our disposal, 20 different triad combinations can be generated using equation (2) and screened to determine optimal combination.

$$\frac{n!}{(n-r)!\,(r!)} \qquad (2)$$

Consequently, the fingerprint data obtained from just three receptors, 4,4'-*o*-BBV, 4,7-*o*-PBBV, and pB*o*B, was subjected to principle component analysis (PCA). A PCA plot was generated with 96% variance with F1 contributing the most. All the markers clustered and segregated with the exception of L-rhamnose and erythritol. The clusters for these two sugar markers overlapped; this was expected based on the fingerprint data (Figure 4.18).[74]

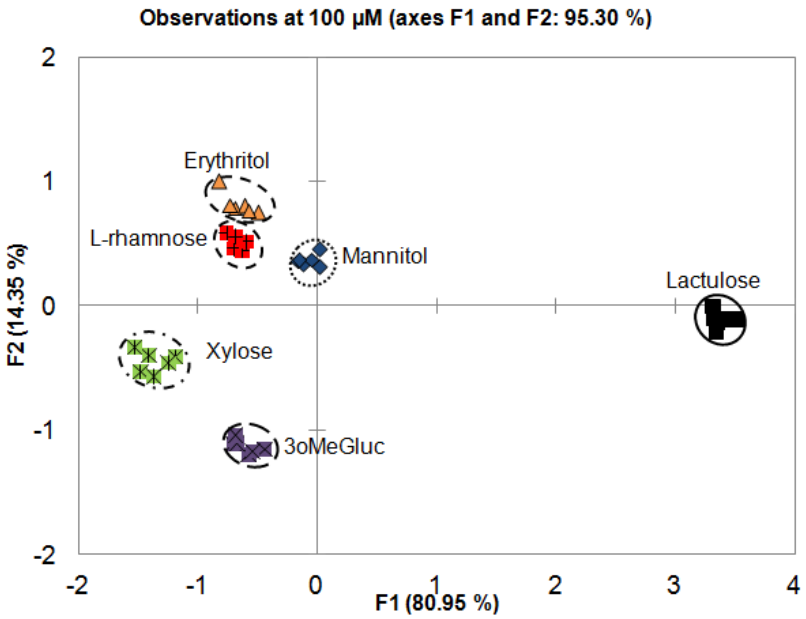

Figure 4.18. PCA plot with 100% variance for all permeability markers at 100 µM with 4,4'-*o*-BBV (500 µM) and 4,7'-*o*-PBBV (120 µM). Each study was carried out in 0.1 M sodium phosphate buffer solution, pH 7.4 at 25°C.

For monosaccharides, *cis*-1,2-diol is necessary for generating a fluorescent signal,[75] and for acyclic sugar alcohols, *threo*-1,2 and *syn*-1,3-diol binding are important for a signal generation.[76] Apparently, this binding motif is not optimal in L-rhamnose and

erythritol. The majority of the markers segregated onto the left quadrants, with xylose and 3oMeGluc in the left negative quadrant. Lactulose was discriminate along the F1 axis in the positive direction while the sugar alcohols (with the exception with L-rhamnose) segregated along the F2 axis in the positive direction. Overall, lactulose was well discriminated with just two receptors, which provided excellent segregation of the lactulose cluster from the other markers. We then turned our attention to evaluate the effectiveness of this boronic array to discriminate GI permeability markers of interest in human urine samples.

The optimal three receptors for lactulose were identified as 4,4'-*o*-BBV, 4,7-*o*-PBBV and pB*o*B. Using an array containing these three receptors, sensitivity parameters (LOD and LOQ) were determined for lactulose and mannitol in buffer and in human baseline urine (Figure 4.19).

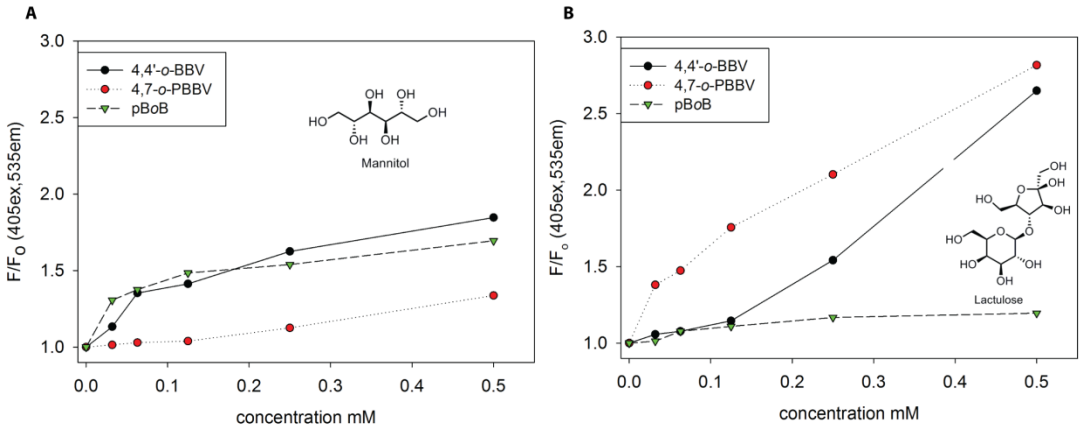

Figure 4.19. Binding isotherm of mannitol (**A**) and lactulose (**B**) with 4,4'-*o*-BBV, 4,7-*o*-PBBV, and pB*o*B in human baseline urine.

Our previous studies showed that 4,4'-*o*-BBV can detect lactulose in urine with LOD and LOQ of 90 and 364 µM and mannitol LOD and LOQ of 416 and 860 µM.[72] This study obtained similar values (Table 4.3).

Table 4.3. Measurement of limits of detection and quantification of lactulose and mannitol.

Receptor	LOD μM (urine, buffer)	LOQ μM (urine, buffer)
Lactulose:		
4,4'-*o*-BBV[a]	113, 88	450, 350
4,7-*o*-PBBV	40[b], 24[c]	72, 57
pBoB	275, 52	950, 225
Mannitol:		
4,4'-*o*-BBV[a]	560, 125	750, 300
4,7-*o*-PBBV	272[b], 190[c]	650, 400
pBoB	900, 650	1400, 1250

Table. 4.3. Each data point was obtained by generating a standard curve of lactulose in urine or buffer. All data points were measured in two separate runs.[a] Final 4,4'-o-BBV concentration is 400 μM (reproduced as in ref. 20.[b] Final 4,7-o-PBBV concentration is 200 μM, spiked into human urine after C18 SPE.[c] Final 4,7-o-PBBV concentration is 160 μM, spiked into phosphate/HEPES buffer.

In parallel measurements against 4,4'-*o*-BBV, 4,7-*o*-PBBV gave LOD and LOQ for lactulose of 40 and 72 μM, yielding 2.8 and 6.3 fold reductions compared to 4,4'-*o*-BBV. The LOD and LOQ of 4,7-*o*-PBBV for mannitol (272 and 650 μM) were not reduced to the extent relative 4,4'-*o*-BBV (2.1 and 1.1 fold). Hence, 4,7-*o*-PBBV offers sharper discrimination between lactulose and mannitol than 4,4'-*o*-BBV. The pB*o*B receptor demonstrated the highest LOD and LOQ values. For lactulose, LOD and LOQ were 2.4 and 2.1 fold higher than 4,4'-*o*-BBV. For mannitol, the values were 1.6 and 1.9 fold higher than 4,4'-*o*-BBV. The LOD and LOQ values obtained with 4,7-*o*-PBBV, in particular, are competitive with those reported for HPLC-MS. Overall, the data in Table 3 implies that discriminating different lactulose/mannitol

(L/M) ratios is feasible using an array of these three BBVs, and in turn, to differentiate low versus high GI permeability.

Lactulose is among the most used markers for small intestinal mucosal permeability tests. It is a measure of "leakiness" of the epithelium stemming from any loss of integrity in the tight junctional barrier. This marker is typically referenced against mannitol, which essentially has free diffusion through tight junctions by the paracellular as well as by the transcellular mechanism. With low permeability, lactulose levels are usually <500 μM (<1% ingested) and mannitol levels are between 700-2000 μM (5–10% ingested). These reference values were obtained from healthy subjects using enzyme assays.[61] With increased permeability, the level of lactulose in urine rises above 500 μM (>5% ingested). Consequently, in healthy humans, L/M ratios between 0.1 and 0.3 are common, whereas L/M ratios in the range of 0.5 or higher are common with moderate hyperpermeability. In extreme cases, L/M values can rise >1. Similar values of L/M ratios have been reported in studies involving non-human subject groups.[65, 77, 78] A higher L/M ratio is usually indicative of epithelial barrier damage stemming from maladies that affect the GI tract rooted from inflammation. To develop a routine, non-invasive, and user-friendly GI permeability test, new methodologies will be needed that do not involve specialized instruments, such as HPLC-ELSD and LC-MS, especially for use in low resource or high throughput settings. We were interested in applying our rapid and inexpensive assay

to measure lactulose/mannitol ratios in human urine samples using an array of boronic acid-appended viologens (BBVs).

However, the current limitation of utilizing boronic acid receptors to quantify small intestinal permeability results from their inability to discriminate lactulose from mannitol in a mixture. There are no prior reports of studies that measure L/M ratios using boronic acid receptors, as it is synthetically challenging to design a boronic acid that is selective for either lactulose or mannitol. One known boronic acid receptor that potently differentiates lactulose from mannitol has limited water solubility, limiting its use for analyzing lactulose in urine.[63] If boronic acids are not available to bind selectively to lactulose over mannitol, then it is limited to use one marker at a time in permeability tests. Fortunately, due to the semi-selective characteristics of our BBVs, it was possible to generate a fingerprint of the lactulose/mannitol mixtures at various analyte concentrations to discern L/M ratios that distinguish low from increased permeability.

To evaluate the contribution of an individual BBV receptor in discriminating various L/M mixtures, we utilized a combination of triads of *o*-BBVs. This resulted in twenty different BBV receptor arrays with varied L/M ratios. Twenty different triads of boronic acid receptors were prepared in 0.1 M sodium phosphate-HEPES buffer pH 7.4 containing 0.04% Triton X-100; the sugar GI marker (L/M) mixtures were prepared in the same buffer, with the exception that the salt concentration was decreased to 0.025 M. We observed that the triad of BBV receptors containing 4,4'-*o*-

BBV, 4,7-*o*-PBBV and pB*o*B generated relatively distinct chemometric patterns for the different L/M ratios (Figure 4.20).

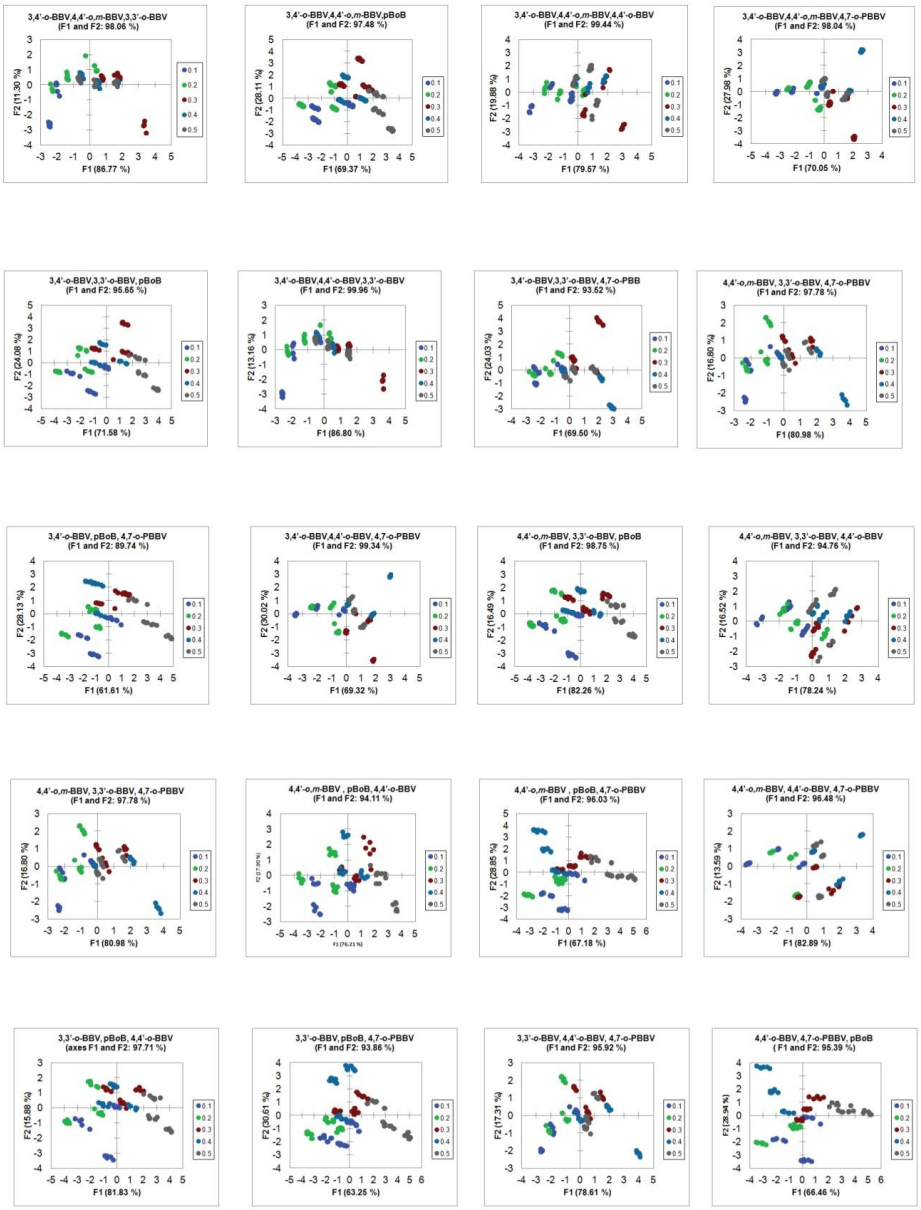

Figure 4.20. Linear discriminant analysis of L/M mixtures by 20 boronic acid receptor triads in 0.025 M sodium phosphate-HEPES buffer pH 7.4 containing 0.01 % Triton X-100 buffer.

After analysis in buffer, we then used the same triad of BBV receptors along with HPTS to generate fingerprints in human baseline urine of L/M ratios representing low and increased small intestinal permeability. The probe solutions were prepared in the same buffer as described previously. The various L/M mixtures were prepared by spiking human baseline urine obtained from healthy subjects. To obtain the lower range of L/M ratio of 0.1–0.2 used in the L1-L5 mixtures, 100–500 μM lactulose and 500–5,000 μM for mannitol were used (Table 4.4).

Table 4.4. Concentrations of L/M ratio representing low (L) or increased (I) gut permeability. Mixtures were prepared in human baseline urine or 1X buffer.

L/M Ratio	Subgroup	Concentration (lactulose/mannitol) μM
0.1	L1	100/100
	L2	200/2000
	L* (circled in Figure 22)	500/5000*
0.2	L3	100/500
	L4	200/1000
	L5	500/2500
0.3	I1	700/2300
	I2	1000/3333
	I3	2000/6000
0.4	I4	700/1750
	I5	1000/2500
	I6	2000/5000
0.5	I7	700/1400
	I8	1000/2000
	I9	2000/4000

The normalized fluorescence response of five low (L1-L5) and nine increased (I1-I9) L/M ratios of GI permeability mixtures added to human urine is shown in Figure 4.21A. The 4,4'-*o*-BBV gave an excellent fluorescence response, whereas 4,7-*o*-PBBV provided a modest response and pB*o*B a minimal fluorescence signal changes. However, the input from the pBoB receptor was essential to discriminate these L/M ratios. Together, these three receptors provided a wide varying range of binding affinities that yielded distinctively different fingerprints. The fluorescence data thus obtained were subjected to linear discriminant analysis (LDA) to generate the score plot (Figure 4.21B).[74]

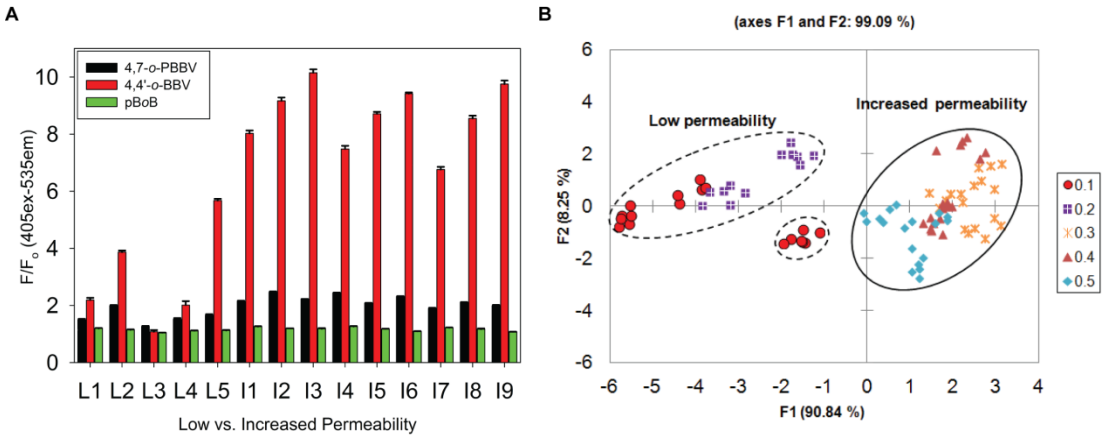

Figure 4.21. Discrimination between low and increased lactulose/mannitol (L/M) ratio. **A.** Normalized fluorescence response of various (L/M) ratios representative of normal or increased GI permeability. Low (L1–L5) and increased (I1–I9) L/M ratios were tested with 4,4'-*o*-BBV (400 μM), 4,7-*o*-PBBV (200 μM), and pB*o*B (16 μM) receptors and HPTS (4 μM). Concentrations are final values in plate wells. Data points are mean ± SEM, n= 6. **B.** LDA plot of normalized fluorescence response of various L/M ratios with 99% variance. Each measurement, in six replicates, was run in human urine. Probe solutions were prepared in sodium phosphate/HEPES buffer. Image used with permission.[74]

In the LDA plot resulting from the fluorescence data, there was 91% differentiation along the F1 axis and 8% along the F2 axis. The F1 axis separates the two clusters that represent the low L/M ratio of 0.1–0.2 and the increased (permeability) L/M ratio of 0.3–0.5. This array comprising only these three boronic acids (4,4'-*o*-BBV, 4,7-*o*-PBBV, and pB*o*B) was sufficient to discriminate between the low and increased permeability groups. Low values clustered into the left negative and positive quadrants whereas the increased L/M ratios clustered in the right quadrants. This provided unambiguous identification of the two major clusters without any significant overlap between them.

Confirmation of this training set was carried out using a cross-validation (re-substitution method) that is reported as a confusion matrix. In the cross-validation method, factor scores associated with each observation are submitted to the classification functions and assigned to a group. The numbers of correct and incorrect classifications are counted. In all cases, the LDA classification was validated and gave a 100% correct classification. The goal of this validation was to determine whether an unknown sample could be classified as indicating low or increased L/M ratio by segregating in the positive or negative quadrants along the F2 axis using this training set.

The discrimination of the different L/M ratios stem from increasing levels of mannitol; also, a false positive correlation can stem from >3 mM mannitol in the low permeability group (Figure 4.22).

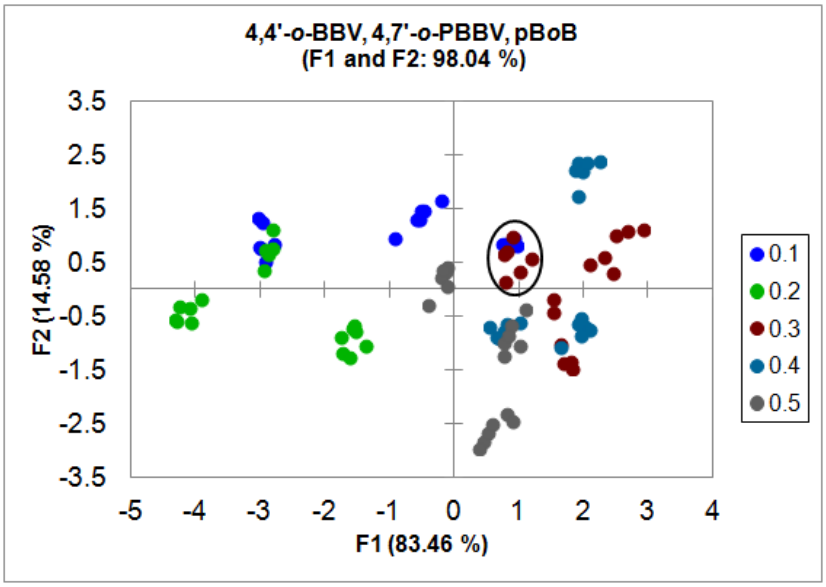

Figure 4.22. Linear discriminant analysis (LDA) of mixtures of lactulose and mannitol with low (L1-L5) and increased (I1-I9) L/M ratios by boronic acid receptor triads (4,4'-o-BBV, 4,7-o-PBBV, and pBoB) in 0.025 M sodium phosphate-HEPES buffer pH 7.4 containing 0.01 % Triton X-100 buffer.

With the aim of discerning between different sugar and sugar alcohols of biomedical relevance, such as gut permeability, arrays of two-component probes were assembled with up to six boronic acid–appended viologens (BBVs): 4,4'-*o*-BBV, 3,3'-*o*-BBV, 3,4'-*o*-BBV, 4,4'-*o,m*-BBV, 4,7'-*o*-PBBV and pB*o*B, each coupled to the fluorophore 8-hydroxypyrene, 1,3,6-trisulfonic acid trisodium salt (HPTS). Arrays

with only three BBVs sufficed to discriminate between sugars (*e.g.*, lactulose) and sugar alcohols (*e.g.*, mannitol), establishing a differential probe. Compared with 4,4'-*o*-BBV, twofold reductions in lower limits of detection (LOD) and quantification (LOQ) were achieved for lactulose with 4,7-*o*-PBBV (LOD 41 µM, LOQ 72 µM). Using a combination of 4,4'-*o*-BBV, 4,7-*o*-PBBV, and pB*o*B, LDA statistically segregated lactulose/mannitol (L/M) ratios from 0.1 to 0.5, consistent with values encountered in small intestinal permeability tests.

4.4. Conclusions

The versatility of this two-component system has been successfully demonstrated. A newly defined combination of markers (lactulose/riboflavin) was used for assessing small intestinal permeability in healthy subjects. This provided an alternative to using the classical lactulose/mannitol mixture which typically requires costly and time-consuming methodology (HPLC-MS or enzymatic method).

Furthermore, this study described a small array of three boronic acid receptors configured in a two-component fluorescence assay that was used to analyze GI markers lactulose and mannitol in connection with discerning normal from increased small intestinal permeability. In addition, discrimination of seven sugar alcohols and six GI permeability markers was achieved. This study revealed that sugar alcohols with *threo*-1,2 diol units have a higher preference for the boronic acid receptors over that of *erythro*-1,2 units. Our results demonstrate that it is possible to replace mannitol with other sugars, such as 3-O-methyl-D-glucose, as the reference GI marker. Using an array containing a triad of boronic acids receptors, such as, 4,4'-*o*-BBV, 4,7-*o*-PBBV, and pB*o*B, it was possible to discriminate between low and increased small intestinal permeability by analyzing various L/M ratios. Boronic acid arrays can provide an inexpensive, rapid, analytical tool that plays a central role in the high-throughput analysis in mixtures of sugars or sugar derivatives in complex media. For the first time, a boronic acid array has been used to rapidly identify different sugar and sugar alcohol ratios utilizing chemometric analysis for a biomedical

application. This technique alleviated the need to design a highly selective boronic acid receptor for lactulose or mannitol. The present triad receptor array demonstrates the feasibility of rapidly identifying changes in small intestinal permeability, and clearly, it may be applied in other biomedical applications. Lastly, this receptor array is continued to be demonstrated in baseline urine samples to show consistency, reproducibility, and confidence this model of discrimination will work in permeability test samples from individuals with basal or increased permeability.

4.5. Experimental

General. All reagents and chemicals were of at least analytical grade. Reactions were performed using standard syringe techniques and were carried out in oven-dried glassware under an argon atmosphere. Ultra pure water (> 14 MΩ cm) obtained from a Millipore water system was used for each analysis unless otherwise stated. All saccharides and sugars were used as received.

Statistics. The limits of detection (LOD) and quantification (LOQ) were defined as the analyte concentration in which the fluorescence intensity in the assay was 3 and 10 standard deviations above the mean baseline fluorescence. Results are given as mean ± SEM.

Instrumentation. For multi-well fluorescence measurements the fluorescence plate reader Envision 2103 Multilabel reader from PerkinElmer® was used (excitation filter: 405 nm, emission filter: 535 nm, emission aperture: normal, measurement height from the bottom: 6.5mm, number of flashes: 10).

4.5.1 Synthesis of Receptors (BBVs) used in Array

The syntheses of 4,4'-*o*-BBV, 4,4'-*o,m*-BBV, 3,4'-*o*-BBV, 3,3'-*o*-BBV, 4,7-*o*-PBBV, and pB*o*B boronic acid receptors were synthesized according to previously published procedures, with slight modifications.[79-82]

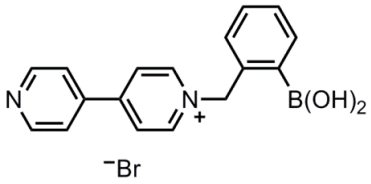

Preparation of monoalkylated bipyridyl boronic acid salt (1-(2-boronic acid-benzyl)-[4-4'] bipyridyl bromide). To a solution of 2-bromomethyl phenyl boronic acid (0.405g, 1.86 mmol) in dry acetone (50 mL) was added 4, 4'-bipyridyl (1.16g, 7.4 mmol). This reaction was stirred at 25°C for 1 h. After the reaction went to completion, the solution was decanted onto a 100 mL round bottom flask and diethyl ether (100 mL) was added. The off-white precipitate was collected by centrifugation, washed with acetone several times, and dried under a stream of argon (0.5 g, 72% yield). ^{1}H-NMR (500 MHz, d_2o) δ 8.91 (d, J=5.0 Hz, 2H), 8.74 (d, J=5.0Hz, 2H), 8.60 (d, J=5.0Hz, 2H), 8.32 (d, J=5.0Hz, 2H), 7.86 (d, J=5.0Hz, 1H), 7.78 (d, J=5.0Hz, 1H), 7.72 (d, J=5.0Hz, 1H), 7.56 (m ,1H), 6.02 (s, 2H). ^{13}C-NMR (D_2O, 125MHz) δ 155.20, 151.45, 146.39, 143.74, 137.34, 136.46, 132.61, 123.49, 130.92, 127.02, 123.84, 65.69; ^{11}B-NMR (160MHz, D_2O) δ= +28.2.

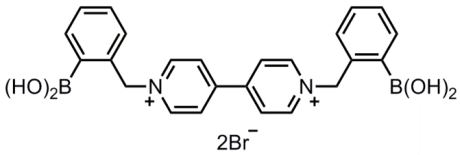

Preparation of 4,4'-*o*-BBV.[81] To a solution of 2-bromomethylphenyl boronic acid (0.77 g, 3.6 mmol) in dry MeCN (10 mL) was added MeOH (0.65 mL) drop wise , 4,4'-dipyridyl (0.23 g, 1.5 mmol), and the reaction was stirred at 55 °C for 48 hours. The reaction mixture was cooled to room temperature and acetone (10 mL) was added to induce further precipitation of a pale yellow solid. The precipitate was centrifuged, washed with acetone (2x 10mL) and dried under a stream of argon (0.85 g, 96%yield). ^{1}H NMR (500 MHz, D_2O) δ 9.06 (d, J=10 Hz, 4H), 8.47 (d, J=5 Hz, 4H), 7.79 (d, J=10Hz, 2H), 7.56 (m, 6H), 6.11 (s, 4H); ^{13}C NMR (126 MHz, D_2O) δ 146.72, 135.51, 132.80, 130.44, 128.35, 127.85, 66.13; ^{11}B NMR (160 MHz, D_2O) δ +29.83.

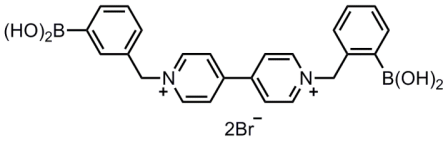

Preparation of 4,4'-*o,m*-BBV. To a solution of 4,4'-monoalkylated bipyridyl boronic acid salt (0.275 g, 0.74 mmol) in MeCN (10 mL) was added MeOH (0.65 mL) dropwise. The reaction stirred for 10 minutes, 3-bromomethyl phenyl boronic acid (0.191 g, 0.89 mmol) was added and the reaction stirred at 50 °C for 24 h. The resulting orange solution was cooled to room temperature and diluted with acetone (30 mL) to precipitate out the product as a pale yellow solid. The solution was stored

at 4 ^{o}C for 1 h to induce further precipitation. The precipitate was collected by centrifugation, washed with acetone, and dried under a stream of argon to give a pale yellow solid (0.390 g, 90%). ^{1}H NMR (500 MHz, D_2O) δ 9.18 (d, J=5Hz, 2H), 9.08 (d, J=5Hz, 2H), 8.55 (d, J=5Hz, 2H), 8.50 (d, J=5Hz, 2H) , 7.88 (m, 2H), 7.82 (d, J=5 Hz, 1H), 7.59 (m, 5H), 6.12 (s, 2H), 5.99 (s, 2H); ^{13}C NMR (126 MHz, D_2O) δ 146.72, 135.51, 132.80, 130.44, 128.35, 127.85, 66.13; ^{11}B NMR (160 MHz, D_2O) δ +30.48.

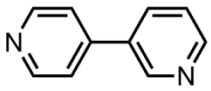

Preparation of 3,4' bipyridyl.[83] To a 25mL oven round bottom flask purged with argon, was added $Pd(OAc)_2$ (0.009 g, 0.04 mmol, 4 mol%), XPhos (0.023 g, 0.048 mmol, 4.8 mol%), 3-bromopyridine (0.096 mL, 1 mmol), 4-pyridinyl boronic acid (0.15 g, 1.2 mmol), and n-butanol (5.6 mL). After the mixture pre-stirred at 25 °C for 30 minutes, a degassed aqueous solution of NaOH (1.4 mL, 5.1 mmol, 1.2 M) was added to the mixture and vigorously stirred at 80 °C for 4 h. At the end of the reaction, the organics were extracted with ethyl acetate (10 mL x 2). The organic extracts were combined, dried over $MgSO_4$, and concentrated on a rotary evaporator. The resulting residue was purified by silica gel flash chromatography with MeOH:DCM (1:20) as eluent to give the title compound as a pale yellow oil (0.10 g, 70% yield). ^{1}H NMR (500 MHz, CDC_3) δ 8.89 (d, J=5Hz, 1H), 8.71 (d, J=5Hz, 2H), 8.69 (dd, J=5, 2Hz, 1H), 7.93 (dt, J=8, 2Hz, 1H), 7.54-7.52 (m, 2H), 7.43 (dd, J=5,

2Hz, 1H); ^{13}C NMR (126 MHz, $CDCl_3$) δ 150.60, 150.46, 150.10, 148.06, 145.19, 134.36, 133.78, 123.84, 121.56, 121.41, 62.35.

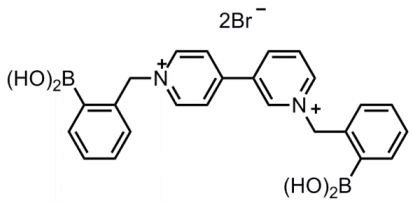

Preparation of 3,4'-o-BBV.[81] To a solution of 2-bromomethylphenyl boronic acid (0.3 g, 1.38 mmol) in DMF (10 mL) was added, 3, 4'-bipyridyl (0.095 g, 0.6 mmol), and the reaction was stirred at 70 °C for 48 hours. The reaction mixture was cooled to room temperature and acetone (10 mL) was added to induce further precipitation of a pale yellow solid. The precipitate was centrifuged, washed with acetone (2x 10 mL) and dried under a stream of argon (0.17 g, 45% yield). ^{1}H NMR (500 MHz, D_2O) δ 9.47 (s ,1H), 9.03 (m, 3H), 8.38 (d, J=5Hz, 1H), 8.25 (m, 1H), 7.81 (m, 1H), 7.60 (m ,5H), 6.14(s, 2H), 6.09(s, 2H); ^{13}C NMR (126 MHz, D_2O) δ 150.83, 146.77, 136.24, 132.30, 130.90, 127.31, 66.61. ^{11}B NMR (160 MHz, D_2O) δ +29.94.

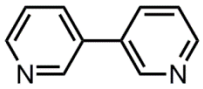

Preparation of 3,3' bipyridyl.[84] To an oven dried double neck round bottom flask (25 mL) fitted with a condenser and purged under argon, $[NiCl_2(PPh_3)_2]$ (0.327 g, 0.5 mmol), acid-washed zinc (0.164 g, 2.5 mmol), Et_4NI (0.435 g, 1.7 mmol), and dry THF (10 mL) was added. The mixture stirred under argon for 30 min at room temperature to give a brown-red solution to which 3-bromopyridine (0.16 mL, 1.7 mmol) was added and the mixture was brought to reflux and stirred for 24 h. The reaction mixture was then cooled to room temperature and poured into 2 M aqueous ammonia (50 mL) and filtered with ethyl acetate (25 mL). The aqueous layer was extracted with ethyl acetate (2x 25 mL) and the combined organic layers were extracted with 2 M hydrochloric acid (2x 25 mL). The acidic aqueous layers were combined and neutralized with Na_2CO_3. The neutralized solution was extracted with ethyl acetate (2x 25 mL) and organic layers were dried over anhydrous $MgSO_4$ and evaporated to give the product as a pale yellow oil (0.09 g, 70%). ^{1}H NMR (500 MHz, $CDCl_3$) δ 8.86 (s, 2H), 8.66 (d, J= 5 Hz, 2H), 7.89 (d, J=10 Hz, 2H), 7.41 (m, 2H); ^{13}C NMR (126 MHz, $CDCl_3$) δ 149.31, 148.18, 134.48, 133.52, 123.80.

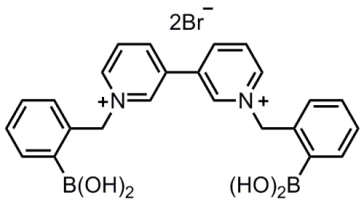

Preparation of 3,3'-o-BBV.[81] To a solution of 2-bromomethylphenyl boronic acid (0.45 g, 2.85 mmol) in dry MeCN (10 mL) was added MeOH (0.65 mL) dropwise, 3,3'-bipyridyl (0.194 g, 1.2 mmol), and the reaction was stirred at 55 °C for 48 h. The reaction mixture was cooled to room temperature and acetone (10 mL) was added to induce further precipitation of a pale yellow solid. The precipitate was centrifuged, washed with acetone (2x 10 mL) and dried under a stream of argon (0.5 g, 70%yield). ^{1}H NMR (500 MHz, D_2O) δ 9.15 (s, 2H), 9.03 (d, J=10 Hz, 2H), 8.85 (d, J=5 Hz, 2H), 8.22 (t, J=5, 10 Hz, 2H), 7.80 (d, J=5 Hz, 2H), 7.56 (m, 6H), 6.10 (s, 4H); ^{13}C NMR (126 MHz, D_2O) δ 146.70, 145.84, 144.38, 136.53, 136.28, 135.41, 132.39, 130.95, 129.80, 66.48; ^{11}B NMR (160 MHz, D_2O) δ +29.94.

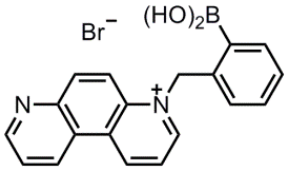

Preparation of *N*-(benzyl–2-boronic acid)-4,7-phenanthrolinium bromide (*o*-PBV).[79] An oven dried 100-mL round bottom flask equipped with a magnetic stir bar was cooled under argon and charged with 4,7-phenanthroline (5.20 mmol, 0.95 g) and 2-bromomethylphenyl boronic acid (5.10 mmol, 1.105 g). The flask was fit with a reflux condenser and purged with argon. CH_3CN (30 mL) was added via cannula and the reaction mixture was heated to reflux for 16 h. The solution was cooled under argon and the solvent removed under reduced pressure. The residue was triturated with acetone (2 x 50 mL), transferred to a fritted funnel, and washed with additional acetone (3 x 50 mL). The yellow-orange powder was dried under reduced pressure and isolated under a blanket of argon (1.70 g, 80%).^{1}H NMR (D_2O, 500 MHz) δ 9.88 (d, J=5 Hz, 1H), 9.23 (dd, J= 5, 20 Hz, 1H), 9.06 (d, J=5 Hz, 1H), 8.94 (d, J=5 Hz, 1H), 8.38 (d, J=10, 1H), 8.25 (d, J= 5 Hz, 1H), 7.88 (dd, J= 5, 20 Hz, 1H), 7.73 (d, J= 5 Hz, 2H), 7.45 (m, 2H), 7.08 (d, J= 5 Hz) , 6.49 (s, 2H). ^{13}C NMR (126 MHz, D_2O) δ 63.324, 121.541, 124.610, 126.038, 129.335, 129.882, 130.490, 131.690, 134.303, 134.440, 135.047, 137.660, 139.514, 140.851, 143.844, 147.915, 149.556, 154.676. ^{11}B NMR (160 MHz, D_2O) δ +29.023

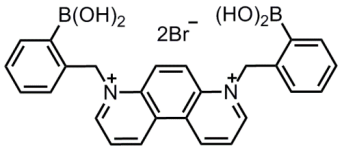

Preparation of 4,7-*o*-PBBV.[79] An oven dried 100 mL side armed round bottom flask equipped with a magnetic stir bar, was cooled under argon and charged with ***o*-PBV** (2.5 mmol, 1.01 g) and 2-bromomethylphenyl boronic acid (25 mmol, 5.5 g). The flask was fit with a reflux condenser and purged with argon. DMF (45 mL) was added to the side arm and the reaction mixture was heated to 55 ° C for 3 h. The reaction mixture was cooled to room temperature and dripped into ice-cold acetone (150 mL) to induce precipitation. The material was allowed to sit at 4 °C overnight and then was washed with additional ice-cold acetone (2 × 225 mL). After removal of the solvent and drying under reduced pressure, a viscous red oil remained. The oil was dissolved in MeOH (4 mL) and added dropwise via cannula to a rapidly stirring ice-cold acetone (500 mL) solution to give a yellow-orange solid. The solid was isolated under argon and dried under reduced pressure. Further purification on a Biotage Flash 40+ C18 cartridge (20% methanol, 0.02% formic acid, in water) gave an orange powder (0.50 g, 35%).^{1}H NMR (D_2O, 500 MHz) δ 6.781 (s, 4H), 7.356 (d, *J* = 10 Hz, 2H), 7.680 (m, 4H), 7.972 (d, *J*= 10 Hz, 2H), 8.675 (dd, *J* = 5,10 Hz, 2H), 9.189 (s, 2H), 9.591 (dd, *J* = 5 Hz, 10 Hz, 2H), 10.370 (d, *J* = 5, 10 Hz, 2H); ^{13}C NMR (D_2O, 125 MHz) δ 63.56, 126.85, 127.35, 129.17, 130.40, 130.55, 132.53, 136.40, 136.83, 140.24, 144.24, 151.63. ^{11}B NMR (106 MHz, D_2O) δ +30.97.

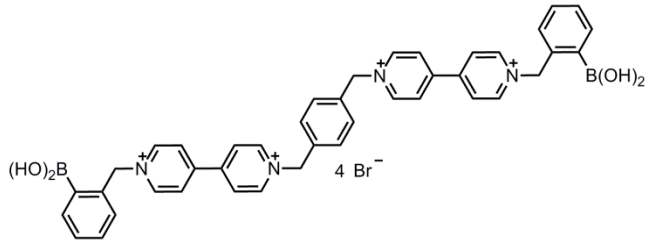

Preparation of pB*o*B.[82] To a solution of 4,4'-monoalkylated bipyridyl boronic acid salt (0.5 g, 1.3 mmol) in DMF (15 mL) was added α, α'-dibromo-*p*-xylene (0.17 g, 0.67 mmol), and the reaction was stirred at 65 ^{o} C for 24 h. The resulting yellow precipitate was collected by centrifugation. The DMF supernatant was decanted, the yellow solid washed several times with acetone, then dried under a stream of argon to yield a yellow powder (0.50 g, 74% yield).^{1}H NMR (500 MHz, D_2O) δ 9.17 (d, J=10 Hz, 4H), 9.08 (d, J=10 Hz, 4H), 8.56 (d, J= 5 Hz, 4H), 8.50 (d, J= 5 Hz, 4H), 7.96 (d, J=5 Hz, 2H), 7.81 (d, J= 10 Hz, 2H), 7.60 (m, 10H), 6.12 (s, 4H), 6.00 (s, 4H); ^{13}C NMR (125 MHz, D_2O) δ 172.21, 146.85, 136.31, 132.37, 131.56, 128.46, 127.88, 66.21; ^{11}B NMR (160 MHz, D_2O) δ +30.07.

4.5.2 Lactulose/Riboflavin Measurements

Baseline absorbance spectra of urine

Because the assay uses spectroscopic methods, urine samples were evaluated for interfering absorbance. Urine was collected from volunteers, including subjects with suspected gut hyperpermeability. They were instructed to drink 0.5 - 1.0 L water the night before and in the morning ~3 hrs prior to sample collection. The first morning urine was voided. No food or additional beverages were consumed until after the baseline sample was collected. This reflects current practice prior to initiating the permeability test. Absorbance was scanned from 380-700 nm at the time of collection. Below 380 nm, samples are essentially opaque. Absorbance is negligible from 700-1000 nm.

Permeability test in humans

Subjects consumed 0.5 - 1.0 L water the night before and in the morning ~3 hr prior to sample collection. The first morning urine was voided. No food or other beverages were consumed prior to the test. Permeability probes were ingested after baseline urine collection. Doses were 50 mg riboflavin and 5 g mannitol or 10 g lactulose (15 mL at 0.67 mg/mL). Test subjects were permitted to drink water or coffee as desired. Light snacks were permitted after the fourth hr. Urine volumes were recorded and 50 mL was retained for analysis. Studies were carried out in Sweden according to ethical approval Dnr 2010/184 held at Uppsala University, Sweden. In this jurisdiction, lactulose, mannitol, and riboflavin are available over the counter.

Urine Assays

Sample collection

Freshly collected urine (50 ml) was first centrifuged 2500 RCF, 4 ºC, 10 min. 100 µl supernatant was set aside for riboflavin analysis, the remaining supernatant was frozen at -20 ºC for later mannitol or lactulose analyses.

Riboflavin assay

The above 100 µl urine set aside and standards prepared in pooled baseline samples were diluted in 900 µl EtOH, vortexed and centrifuged. Supernatants were pipetted 40µL/well in duplicate into plates (#3694, Corning, USA). Fluorescence (Exc/Em 450/580 nm) was read on a plate reader (Infinite M200Pro, Tecan, Switzerland). Signal to noise (S/N) was higher at 580 nm than at the 530 nm emission maximum. Concentration was calculated as mg/mL and multiplied by total urine volume in mL, giving total mg in urine. The mg in urine/mg ingested x 100 yielded % ingested.

C18 solid phase extraction of samples for lactulose and mannitol

To remove riboflavin and other colored components, 2 mL urine was processed twice through solid phase extraction (SPE) using 500 mg C18 columns fitted onto a Waters/Millipore SPE vacuum manifold (max -50 kPa, ~0.5 mL/min). The SPE column was cleaned with MeOH and H_2O between runs. Mannitol and lactulose recovery were both ~91%. Data was corrected for a 9% loss. After SPE, samples were directed to the various assays.

Two-component assay for lactulose and mannitol permeability in humans

Ready-made assay 96 well plates were prepared (#3694, Corning, USA). A 4X premix buffer was prepared (0.1 M sodium phosphate, 0.1 M HEPES, 0.04% Triton X-100, pH 7.4). To this was added HPTS (16 µM) and quencher (1.6 mM 4,4'oBBV or 2.0 mM 4,4'oMBV), each 4 times above final concentration. The different viologen concentrations were chosen to achieve similar extents of quenching in the absence of sugar (~20% of free fluorophore) while preserving S/N. Blank wells were given 10 µl 4X premix buffer with neither HPTS nor viologen. Some wells received 16 µM HPTS without quencher to determine maximum possible fluorescence. All other wells received 10 µl of the complete 4X premix. Those premixes containing 4,4'oBBV were continuously vortexed because the mixture is a suspension. Plates were sealed with plate tape and stored at 4 ºC until use.

Upon running an assay, 30 µl of standards or samples were pipetted into wells. Final concentrations were 4 µM HPTS and 400 µM 4,4'oBBV or 500 µM 4,4'oMBV. Urine samples were placed in both blank wells (for individual sample blanking) and wells containing complete 4X premix. Plates were put on a shaker for 1 hr, RT. During this time, sugars interacted with the HPTS-viologen complex, liberating HPTS into solution. Plates were then centrifuged at 2500 RCF, 10 min, RT to pull down remaining HPTS-quencher particulate matter, plate tape was removed and fluorescence read on a plate reader (Tecan M-200 Infinite, gain 70, 404/535 nm). The height was adjusted to read from the top of the solution (18 mm). This wavelength combination is pH insensitive and poorly affected by any residual riboflavin or

endogenous fluorophores that might still be present after C18 SPE. A Marquardt 4-parameter curve fit was used. Sugar concentrations were calculated as g/mL and multiplied by total urine volume in mL, giving total g in urine. Values were corrected for % recovery from the C18 SPE step. The g in urine / g ingested x 100 yielded % ingested. Lactulose measurements were confirmed by enzyme assay.[65] Mannitol measurements were confirmed by HPLC-ELSD using a C8 pre-column and Prevail Carbohydrate ES 5µ 250x4.6mm column (Grace Davison Discovery Sciences, IL, USA) with 80:20 MeCN/H_2O.

4.5.3 Discrimination of Permeability Markers and L/M Mixtures

Construction of boronic acid receptor array

The boronic acid array was pipetted onto a 96-well (Fisherbrand®, flat bottom, clear polystyrene, non-sterile) by preparing a stock "probe" solution of each boronic acid receptor at its respective quencher:dye ratio prepared as a twofold concentration in 0.1M NaH_2PO_4/Na_2HPO_4 pH 7.4 buffer. For 4, 4'-, 3, 4'-, 3, 3'-*o*-BBV and 4, 4'-*o*, *m*-BBV a ratio of 125:1 was used. For 4, 7-*o*-PBBV a ratio of 30:1 was used. For pBoB a ratio of 3:1 was used. To each receptor solution was added HPTS (8 µM) to complete the probe solution. Blank wells were given 40 µL of the sodium phosphate buffer. Baseline fluorescence ("probe") wells were given 20 µL of the probe and sodium phosphate buffer. The rest of the wells received 20 µL of probe and analyte (Table 4.5).

Table 4.5. Map of multi-well plate for permeability marker study that outlines the location of each sugar and probe used.

	1	2	3	4	5	6	7	8	9	10	11	12
A		Sugar 1 →			Sugar 2 →			Sugar 3 →			Sugar 4 →	
B		Sugar 5 →			Sugar 6 →			Sugar 7 →			Sugar 8 →	
C		Sugar 9 →			Sugar 10 →			Sugar 11 →			Sugar 12 →	
D		Sugar 13 →			Sugar 14 →			Sugar 15 →			Sugar 16 →	
E		Sugar 17 →			Sugar 18 →			Sugar 19 →			Sugar 20 →	
F		Sugar 21 →			Sugar 22 →			Sugar 23 →			Sugar 24 →	
G		Sugar 25 →			Sugar 26 →			Sugar 27 →			Sugar 28 →	
H		Sugar 29 →			Sugar 30 →			"blank" →			"probe" →	

Discriminant Analysis of GI permeability markers.

Boronic acid arrays were prepared by making a stock probe solution of each boronic acid receptor with its respective quencher to dye ratios (Q:D) and HPTS having an initial concentration of 8 μM in 0.1 M sodium phosphate pH 7.4 buffer. Previous studies showed optimal signal recovery when the probe solution is buffered at 7.4.[85] A microtiter plate was prepared from each one probe solution, seven sugar alcohols or six permeability markers in the same sodium phosphate buffer to obtain a twofold above final concentration before adding to the 96-well plate (Fisherbrand®, flat-bottom, clear polystyrene, non-sterile). Each well contained equal amounts of probe solution and sugar solution to reach a total volume of 80 μL. To ensure

reproducibility, each assay was repeated four times. Fluorescence intensity data was analyzed by PCA or LDA using XLSTAT-Pro© (Addinsoft, Paris, France), a statistical add-on package for Excel© (Microsoft Corp, Redmond, WA, USA).

Analysis of permeability markers in urine.

Baseline urine was obtained from healthy volunteers who had consumed 0.5-1.0 L of water 3 h prior to urine collection. From the urine that was collected, 2 mL was subjected to a C18 solid phase extraction twice to remove the majority of the hydrophobic components found in urine. This purified fraction is considered as the baseline urine without endogenous permeability markers which were then spiked with lactulose or mannitol to obtain lower limits of quantification (LOQ) and detection (LOD) for 4,4'-*o*-BBV, 4,7-*o*-PBBV, and pB*o*B. Lactulose or mannitol was prepared in the baseline urine fraction and serially diluted to obtain five data points. Probe solutions were prepared as a fourfold initial concentration (1.6 mM for 4,4'-*o*-BBV, 800 μM for 4,7-*o*-PBBV, 64 μM for pB*o*B, and 16 μM for HPTS) in 0.1 M sodium phosphate, 0.1 M HEPES, 0.04 % Triton X-100, pH 7.4. Upon running assays, wells for permeability marker (i.e. analyte) analysis received 10 μL of the probe (i.e. BBV + HPTS) and 30 μL of analyte solution. Baseline fluorescence ("probe") wells were given 10 μL of the probe and 30 μL of baseline urine. Blank wells received 10 μL of buffer and 30 μL of baseline urine. Completed plates were put on a shaker for 30 minutes and centrifuged at 2500 RCF for 10 min and the fluorescence was read on a

plate reader (Tecan M-200 Infinite, gain 70, Exc 405 nm, Em 535 nm) (See table 6 for similar plate set-up).

Distinguishing between low and increased lactulose/mannitol ratios. Baseline urine was obtained from healthy volunteers who had consumed 0.5-1.0 L of water 3 h prior to urine collection. From the urine that was collected, 2 mL was subjected to a C18 solid phase extraction twice to remove urobilinogen and riboflavin found in urine.[72] Low and increased permeability ratios of lactulose/mannitol (L/M) were prepared in 0.025 M sodium phosphate-HEPES buffer pH 7.4 containing 0.01 % Triton X-100 for the buffer studies and were prepared in human baseline urine for urine studies. The human baseline urine was processed as mentioned above. Each permeability ratio was obtained by preparing a stock solution of each subgroup mixture and serially diluting to the desired concentration in buffer or human baseline urine. Probe solutions were prepared as fourfold concentration (1.6 mM for 4,4'-*o*-BBV, 3,4'-*o*-BBV, 3,3'-*o*-BBV, and 4,4'-*o,m*-BBV. 800 μM for 4,7-*o*-PBBV, 64 μM for pBoB, and 16 μM for HPTS) in 0.1 M sodium phosphate-HEPES buffer pH 7.4 containing 0.04% Triton X-100. Upon running assay, each well received 10 μL of each probe solution and 30 μL of each L/M mixture. Each concentration data point was repeated six times for reproducibility. Completed plates were put on a shaker for 30 minutes and centrifuged at 2500 RCF for 10 minutes and the fluorescence was

read on a plate reader (Tecan M-200 Infinite, gain 70, excitation: 405nm, emission: 535nm) (Table 4.6).

Table 4.6. Plate map for the discrimination of various L/M mixtures by a 3-probe array.

Probe 1 -6	1	2	3	4	5	6	7	8	9	10	11	12
A				L1					L2			
B				L3					L4			
C				L5					L6			
D				I1					I2			
E				I3					L4			
F				I5					I6			
G				I7					I8			
H				I9					“probe”			

4.6. References

1. Yoon, J.; Czarnik, A. W., Fluorescent Chemosensors of carbohydrates –A means of chemically communicating the binding of polyols in water based on chelation-enhanced quenching. *J. Am. Chem. Soc.***1992,** *114*, 5874-5875.

2. Kondo, K.; Shiomi, Y.; Saisho, M.; Harada, T.; Shinkai, S., Specific complexation of disaccarides with diphenyl-3,3'-diboronic acid that can be detected by circular-dichroism. *Tetrahedron* **1992,** *48*, 8239-8252.

3. Ellis, G. A.; Palte, M. J.; Raines, R. T., Boronate-Mediated Biologic Delivery. *J. Am. Chem. Soc.***2012,** *134*, 3631-3634.

4. Jianzhang, Z.; James, T. D., Chemoselective and enantioselective fluorescent recognition of sugar alcohols by a bisboronic acid receptor. *J. Mat. Chem.* **2005,** *15*, 2896-901.

5. Cheng, Y.; Ni, N.; Yang, W.; Wang, B., A New Class of Fluorescent Boronic Acids That Have Extraordinarily High Affinities for Diols in Aqueous Solution at Physiological pH. *Chem.-a Eur. J.***2010,** *16*, 13528-13538.

6. Zhai, W. L.; Sun, X. L.; James, T. D.; Fossey, J. S., Boronic Acid-Based Carbohydrate Sensing. *Chem.-a Eur. J.***2015,** *10*, 1836-1848.

7. Wang, H. C.; Lee, A. R., Recent developments in blood glucose sensors. *J. Food Drug Anal.* **2015,** *23*, 191-200.

8. Lacina, K.; Skladal, P.; James, T. D., Boronic acids for sensing and other applications - a mini-review of papers published in 2013. *Chem. Centl. J.* **2014,** *8*.

9. Mortellaro, M.; DeHennis, A., Performance characterization of an abiotic and fluorescent-based continuous glucose monitoring system in patients with type 1 diabetes. *Biosens. Bioelectron.* **2014,** *61*, 227-231.

10. Jelinek, R.; Kolusheva, S., Carbohydrate biosensors. *Chem. Rev.* **2004,** *104*, 5987-6015.

11. Kim, K. K.; Escobedo, J. O.; St Luce, N. N.; Rusin, O.; Wong, D.; Strongin, R. M., Postcolumn HPLC detection of mono- and oligosaccharides with a chemosensor. *Org. Lett.* **2003,** *5*, 5007-5010.

12. Wiskur, S. L.; Lavigne, J. L.; Metzger, A.; Tobey, S. L.; Lynch, V.; Anslyn, E. V., Thermodynamic analysis of receptors based on guanidinium/boronic acid groups for the complexation of carboxylates, alpha-hydroxycarboxylates, and diols: Driving force for binding and cooperativity. *Chem.-a Eur. J.* **2004,** *10*, 3792-3804.

13. Bull, S. D.; Davidson, M. G.; Van den Elsen, J. M. H.; Fossey, J. S.; Jenkins, A. T. A.; Jiang, Y.-B.; Kubo, Y.; Marken, F.; Sakurai, K.; Zhao, J.; James, T. D., Exploiting the Reversible Covalent Bonding of Boronic Acids: Recognition, Sensing, and Assembly. *Acc. Chem. Res.* **2013,** *46*, 312-326.

14. Musto, C. J.; Suslick, K. S., Differential sensing of sugars by colorimetric arrays. *Curr. Opinion Chem. Biol.* **2010,** *14*, 758-766.

15. Hansen, J. S.; Christensen, J. B., Recent Advances in Fluorescent Arylboronic Acids for Glucose Sensing. *Biosensors* **2012,** *3*, 400-418.

16. Anslyn, E. V., The Lock and Key Principle. The state of the Art - 100 Years on edited by J.-P. Behr. *Angew. Chem., Int. Ed. Engl.* **1995,** *34*, 2293.

17. You, L.; Zha, D. J.; Anslyn, E. V., Recent Advances in Supramolecular Analytical Chemistry Using Optical Sensing. *Chemical Reviews* **2015,** *115*, 7840-7892.

18. Lee, J. W.; Lee, J. S.; Chang, Y. T., Colorimetric identification of carbohydrates by a pH Indicator/pH change inducer ensemble. *Angew. Chem., Int. Ed.* **2006,** *45*, 6485-6487.

19. Rakow, N. A.; Suslick, K. S., A colorimetric sensor array for odour visualization. *Nature* **2000,** *406*, 710-713.

20. Diaz de Grenu, B.; Moreno, D.; Torroba, T.; Berg, A.; Gunnars, J.; Nilsson, T.; Nyman, R.; Persson, M.; Pettersson, J.; Eklind, I.; Wasterby, P., Fluorescent Discrimination between Traces of Chemical Warfare Agents and Their Mimics. *J. Am. Chem. Soc.***2014,** *136*, 4125-4128.

21. Greene, N. T.; Shimizu, K. D., Colorimetric molecularly imprinted polymer sensor array using dye displacement. *J. Am. Chem. Soc.***2005,** *127*, 5695-5700.

22. Folmer-Andersen, J. F.; Kitamura, M.; Anslyn, E. V., Pattern-based discrimination of enantiomeric and structurally similar amino acids: An optical mimic of the mammalian taste response. *J. Am. Chem. Soc.***2006,** *128*, 5652-5653.

23. Diehl, K. L.; Ivy, M. A.; Rabidoux, S.; Petry, S. M.; Mueller, G.; Anslyn, E. V., Differential sensing for the regio- and stereoselective identification and quantitation of glycerides. *Proc.Nalt. Acad. Sci.U.S.A.* **2015,** *112*, E3977-E3986.

24. Buryak, A.; Severin, K., A chemosensor array for the colorimetric identification of 20 natural amino acids. *J. Am. Chem. Soc.***2005,** *127*, 3700-3701.

25. You, C.-C.; Miranda, O. R.; Gider, B.; Ghosh, P. S.; Kim, I.-B.; Erdogan, B.; Krovi, S. A.; Bunz, U. H. F.; Rotello, V. M., Detection and identification of proteins using nanoparticle-fluorescent polymer 'chemical nose' sensors. *Nature Nanotechnol.* **2007,** *2*, 318-323.

26. Chen, W.; Li, Q.; Zheng, W.; Hu, F.; Zhang, G.; Wang, Z.; Zhang, D.; Jiang, X., Identification of Bacteria in Water by a Fluorescent Array *Angew. Chem., Int.* **2014,** *53*, 13734-13739.

27. Bajaj, A.; Miranda, O. R.; Phillips, R.; Kim, I.-B.; Jerry, D. J.; Bunz, U. H. F.; Rotello, V. M., Array-Based Sensing of Normal, Cancerous, and Metastatic Cells Using Conjugated Fluorescent Polymers. *J. Am. Chem. Soc.***2010,** *132*, 1018-1022.

28. Persaud, K.; Dodd, G., Analysis of discrimination mechanisms in the mammalian olfactory system using a model nose. *Nature* **1982,** *299*, 352-355.

29. Kim, I.-B.; Han, M. H.; Phillips, R. L.; Samanta, B.; Rotello, V. M.; Zhang, Z. J.; Bunz, U. H. F., Nano-Conjugate Fluorescence Probe for the Discrimination of Phosphate and Pyrophosphate. *Chem.-a Eur.J.* **2009,** *15*, 449-456.

30. Koehne, J. E.; Chen, H.; Cassell, A.; Liu, G.-y.; Li, J.; Meyyappan, M., Arrays of carbon nanofibers as a platform for biosensing at the molecular level and for tissue engineering and implantation. *Bio-Medical Materials and Engineering* **2009,** *19* (1), 35-43.

31. Wang, J.; Liu, B., Fluorescence resonance energy transfer between an anionic conjugated polymer and a dye-labeled lysozyme aptamer for specific lysozyme detection. *Chem. Commun.* **2009,** 2284-2286.

32. Li, H.; Bazan, G. C., Conjugated Oligoelectrolyte/ssDNA Aggregates: Self-Assembled Multicomponent Chromophores for Protein Discrimination. *Adv. Mat.* **2009,** *21*, 964.

33. Wright, A. T.; Anslyn, E. V., Differential receptor arrays and assays for solution-based molecular recognition. *Chem. Soc. Rev.***2006,** *35*, 14-28.

34. Jurs, P. C.; Bakken, G. A.; McClelland, H. E., Computational methods for the analysis of chemical sensor array data from volatile analytes. *Chem. Rev.* **2000,** *100*, 2649-2678.

35. Kitamura, M.; Shabbir, S. H.; Anslyn, E. V., Guidelines for Pattern Recognition Using Differential Receptors and Indicator Displacement Assays. *J. Org. Chem.***2009,** *74*, 4479-4489.

36. Leung, D.; Folmer-Andersen, J. F.; Lynch, V. M.; Anslyn, E. V., Using enantioselective indicator displacement assays to determine the enantiomeric excess of alpha-amino acids. *J. Am. Chem. Soc.***2008,** *130*, 12318-12327.

37. Rochat, S.; Gao, J.; Qian, X.; Zaubitzer, F.; Severin, K., Cross-Reactive Sensor Arrays for the Detection of Peptides in Aqueous Solution by Fluorescence Spectroscopy. *Chem. Eur. J.* **2010,** *16*, 104-113, S104/1-S104/36.

38. Buryak, A.; Pozdnoukhov, A.; Severin, K., Pattern-based sensing of nucleotides in aqueous solution with a multicomponent indicator displacement assay. *Chem. Commun.* **2007,** 2366-2368.

39. Zaubitzer, F.; Buryak, A.; Severin, K., Cp*Rh-based indicator-displacement assays for the identification of amino sugars and aminoglycosides. *Chem.-a Eur. J.* **2006,** *12*, 3928-3934.

40. Buryak, A.; Severin, K., Dynamic combinatorial libraries of dye complexes as sensors. *Angew. Chem., Int. Ed.* **2005,** *44*, 7935-7938.

41. Buryak, A.; Severin, K., An organometallic chemosensor for the sequence-selective detection of histidine- and methionine-containing peptides in water at neutral pH. *Angew. Chem., Int. Ed.* **2004,** *43*, 4771-4774.

42. Stewart, S.; Ivy, M. A.; Anslyn, E. V., The use of principal component analysis and discriminant analysis in differential sensing routines. *Chem. Soc. Rev.* **2014,** *43*, 70-84.

43. Shabbir, S. H.; Joyce, L. A.; da Cruz, G. M.; Lynch, V. M.; Sorey, S.; Anslyn, E. V., Pattern-Based Recognition for the Rapid Determination of Identity, Concentration, and Enantiomeric Excess of Subtly Different Threo Diols. *J. Am. Chem. Soc.* **2009,** *131*, 13125-13131.

44. Lim, S. H.; Musto, C. J.; Park, E.; Zhong, W.; Suslick, K. S., A Colorimetric Sensor Array for Detection and Identification of Sugars. *Org. Lett.* **2008,** *10*, 4405-4408.

45. Bjarnason, I.; Macpherson, A.; Hollander, D., Intestinal permeability-an overview. *Gastroenterology* **1995,** *108*, 1566-1581.

46. Welcker, K.; Martin, A.; Kolle, P.; Siebeck, M.; Gross, M., Increased intestinal permeability in patients with inflammatory bowel disease. *Eur. J. Med. Res.* **2004,** *9*, 456-60.

47. Gerova, V. A.; Stoynov, S. G.; Katsarov, D. S.; Svinarov, D. A., Increased intestinal permeability in inflammatory bowel diseases assessed by iohexol test. *World J. Gastroenterology* **2011,** *17*, 2211-2215.

48. Smecuol, E.; Bai, J. C.; Vazquez, H.; Kogan, Z.; Cabanne, A.; Niveloni, S.; Pedreira, S.; Boerr, L.; Maurino, E.; Meddings, J. B., Gastrointestinal permeability in celiac disease. *Gastroenterology* **1997,** *112*, 1129-1136.

49. Meddings, J. B.; Jarand, J.; Urbanski, S. J.; Hardin, J.; Gall, D. G., Increased gastrointestinal permeability is an early lesion in the spontaneously diabetic BB rat. *Am. J. Physiol. Gastrointest. Liver Physiol.***1999,** *276*, G951-G957.

50. Miki, K.; Butler, R.; Moore, D.; Davidson, G., Rapid and simultaneous quantification of rhamnose, mannitol, and lactulose in urine by HPLC for estimating intestinal permeability in pediatric practice. *Clin. Chem.* **1996,** *42*, 71-75.

51. Arrieta, M. C.; Bistritz, L.; Meddings, J. B., Alterations in intestinal permeability. *Gut* **2006,** *55*.

52. Denno, D. M.; VanBuskirk, K.; Nelson, Z. C.; Musser, C. A.; Burgess, D. C. H.; Tarr, P. I., Use of the Lactulose to Mannitol Ratio to Evaluate Childhood Environmental Enteric Dysfunction: A Systematic Review. *Clin. Infect. Dis.* **2014,** *59*, S213-S219.

53. Groschwitz, K. R.; Hogan, S. P., Intestinal barrier function: Molecular regulation and disease pathogenesis. *J. Allergy Clin. Immunol.***2009,** *124*, 3-20.

54. Broer, S., Amino acid transport across mammalian intestinal and renal epithelia. *Physiol. Rev.* **2008,** *88*, 249-286.

55. Ferraris, R. P.; Diamond, J., Regulation of intestinal sugar transport. *Physiol. Rev.* **1997,** *77*, 257-302.

56. Van Itallie, C. M.; Anderson, J. M., Claudins and epithelial paracellular transport. *Ann. Rev. Physiol.* **2006,** *68*, 403-429.

57. Farquhar, M. G.; Palade, G. E., Junctional complexes in various epithela. *J. Cell Biol.* **1963,** *17*, 375.

58. Turner, J. R., Intestinal mucosal barrier function in health and disease. *Nat. Rev. Immunol.* **2009,** *9*, 799-809.

59. Teshima, C. W.; Meddings, J. B., The measurement and clinical significance of intestinal permeability. *Curr. Gastroenter. reports* **2008,** *10*, 443-9.

60. Fihn, B. M.; Sjoqvist, A.; Jodal, M., Permeability of the rat small intestinal epithelium along the villus-crypt axis: Effects of glucose transport. *Gastroenterology* **2000,** *119*, 1029-1036.

61. Camilleri, M.; Nadeau, A.; Lamsam, J.; Nord, S. L.; Ryks, M.; Burton, D.; Sweetser, S.; Zinsmeister, A. R.; Singh, R., Understanding measurements of intestinal permeability in healthy humans with urine lactulose and mannitol excretion. *Neurogastroenterol. Motil.***2010,** *22*, E15-E26.

62. Travis, S.; Menzies, I., Intestinal permeability-Functional assesment and significance. *Clin. Sci.* **1992,** *82*, 471-488.

63. Meddings, J. B.; Gibbons, I., Discrimination of site-specific alterations in gastrointestinal permeability in the rat. *Gastroenterology* **1998,** *114*, 83-92.

64. Farhadi, A.; Keshavarzian, A.; Holmes, E. W.; Fields, J.; Zhang, L.; Banan, A., Gas chromatographic method for detection of urinary sucralose: application to the assessment of intestinal permeability. *J. Chromat. B-Anal. Technol. Biomed. Life Sci.* **2003,** *784*, 145-154.

65. Northrop, C. A.; Lunn, P. G.; Behrens, R. H., Automated enzymatic assay for the determination of intestinal permeability probes in urine.1. Lactulose and lactose. *Clin. Chim. Acta* **1990,** *187*, 79-87.

66. Lunn, P. G.; Northrop, C. A.; Northrop, A. J., Automated enzymatic assay for the determination of intestinal permeability probes in urine .2. Mannitol. *Clin. Chim. Acta* **1989,** *183*, 163-170.

67. Norrild, J. C.; Eggert, H., Boronic acids as fructose sensors. Structure determination of the complexes involved using (1)J(CC) coupling constants. *J. Chem. Soc., Perkin Trans. 2* **1996,** 2583-2588.

68. Yan, J.; Springsteen, G.; Deeter, S.; Wang, B. H., The relationship among pK(a),pH, and binding constants in the interactions between boronic acids and diols - it is not as simple as it appears. *Tetrahedron* **2004,** *60*, 11205-11209.

69. Norrild, J. C.; Eggert, H., Evidence for monodentate and bisdentate boronate complexes of glucose in the furanose form –Application of (1) J(C-C)-coupling-constants as a structural probe. *J. Am. Chem. Soc.***1995,** *117*, 1479-1484.

70. Subramanian, V. S.; Subramanya, S. B.; Rapp, L.; Marchant, J. S.; Ma, T. Y.; Said, H. M., Differential expression of human riboflavin transporters -1, -2, and -3 in polarized epithelia: A key role for hRFT-2 in intestinal riboflavin uptake. *Biochim. Biophys. Acta, Biomembr.* **2011,** *1808*, 3016-3021.

71. Eli, M.; Li, D. S.; Zhang, W. W.; Kong, B.; Du, C. S.; Wumar, M.; Mamtimin, B.; Sheyhidin, I.; Hasim, A., Decreased blood riboflavin levels are correlated with defective expression of RFT2 gene in gastric cancer. *World J. Gastroenterol.* **2012,** *18*, 3112-3118.

72. Resendez, A.; Abdul Halim, M.; Landhage, C. M.; Hellstrom, P. M.; Singaram, B.; Webb, D.-L., Rapid small intestinal permeability assay based on riboflavin and lactulose detected by bis-boronic acid appended benzyl viologens. *Clin. Chim. Acta* **2015,** *439*, 115-121.

73. Cordes, D. B.; Singaram, B., A unique, two-component sensing system for fluorescence detection of glucose and other carbohydrates. *Pure Appl. Chem.* **2012,** *84*, 2183-2202.

74. Resendez, A.; Panescu, P.; Zuniga, R.; Banda, I.; Joseph, J.; Webb, D. L.; Singaram, B., Multiwell Assay for the Analysis of Sugar Gut Permeability Markers:

Discrimination of Sugar Alcohols with a Fluorescent Probe Array Based on Boronic Acid Appended Viologens. *Anal. Chem.***2016,** *88,* 5444-5452.

75. Schiller, A.; Vilozny, B.; Wessling, R. A.; Singaram, B., Recognition of phospho sugars and nucleotides with an array of boronic acid appended bipyridinium salts. *Anal. Chim. Acta* **2008,** *627,* 203-211.

76. Peters, J. A., Interactions between boric acid derivatives and saccharides in aqueous media: Structures and stabilities of resulting esters. *Coord. Chem. Rev.* **2014,** *268*, 1-22.

77. van Wijck, K.; van Eijk, H. M. H.; Buurman, W. A.; Dejong, C. H. C.; Lenaerts, K., Novel analytical approach to a multi-sugar whole gut permeability assay. *J. Chromat. B-Anal. Technol. Biomed. Life Sci.* **2011,** *879,* 2794-2801.

78. McOmber, M. E.; Ou, C.-N.; Shulman, R. J., Effects of Timing, Sex, and Age on Site-specific Gastrointestinal Permeability Testing in Children and Adults. *J.Pediat. Gastroenterol. Nutrit.* **2010,** *50*, 269-275.

79. Suri, J. T.; Cordes, D. B.; Cappuccio, F. E.; Wessling, R. A.; Singaram, B., Monosaccharide detection with 4,7-phenanthrolinium salts: Charge-induced fluorescence sensing. *Langmuir* **2003,** *19,* 5145-5152.

80. Gamsey, S.; Suri, J. T.; Wessling, R. A.; Singaram, B., Continuous Glucose Detection Using Boronic Acid-Substituted Viologens in Fluorescent Hydrogels: Linker Effects and Extension to Fiber Optics. *Langmuir* **2006,** *22,* 9067-9074.

81. Gamsey, S.; Miller, A.; Olmstead, M. M.; Beavers, C. M.; Hirayama, L. C.; Pradhan, S.; Wessling, R. A.; Singaram, B., Boronic acid-based bipyridinium salts as tunable receptors for monosaccharides and alpha-hydroxycarboxylates. *J. Am. Chem. Soc.***2007,** *129*, 1278-1286.

82. Sharrett, Z.; Gamsey, S.; Levine, P.; Cunningham-Bryant, D.; Vilozny, B.; Schiller, A.; Wessling, R. A.; Singaram, B., Boronic acid-appended bis-viologens as a new family of viologen quenchers for glucose sensing. *Tetrahedron Lett.* **2008,** *49*, 300-304.

83. Yang, J.; Liu, S.; Zheng, J.-F.; Zhou, J., Room-Temperature Suzuki-Miyaura Coupling of Heteroaryl Chlorides and Tosylates. *Eur. J. Org.Chem.* **2012,** 6248-6259.

84. Constable, E. C.; Morris, D.; Carr, S., Functionalised 3,3 '-bipyridines - a new class of dinucleating ligands. *New J. Chem.* **1998,** *22*, 287-294.

85. Gamsey, S.; Baxter, N. A.; Sharrett, Z.; Cordes, D. B.; Olmstead, M. M.; Wessling, R. A.; Singaram, B., The effect of boronic acid-positioning in an optical glucose-sensing ensemble. *Tetrahedron* **2006,** *62*, 6321-6331.

Appendix A:

NMR of Selected Compounds

Chapter 2 & 4

Spectra

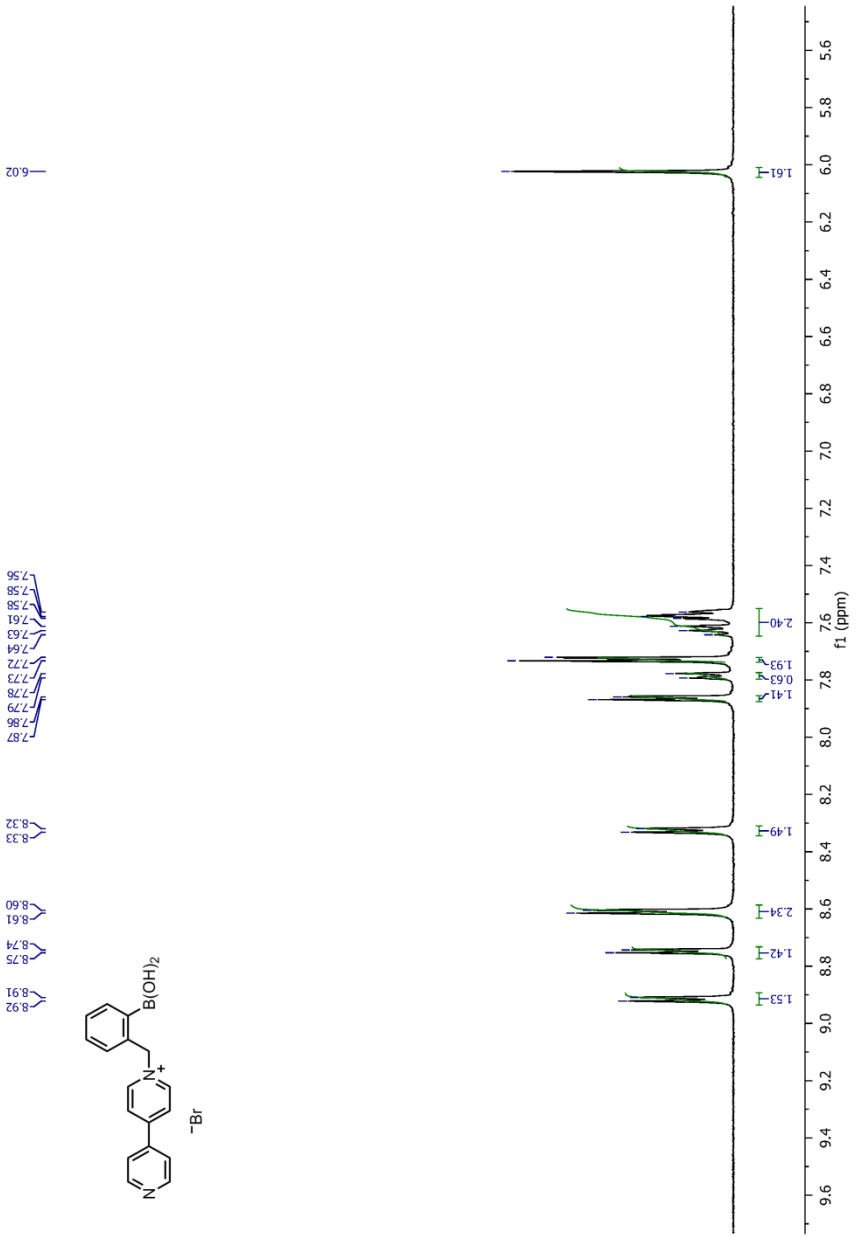

^{1}H NMR of monoalkylated bipyridyl boronic acid salt (**8**)

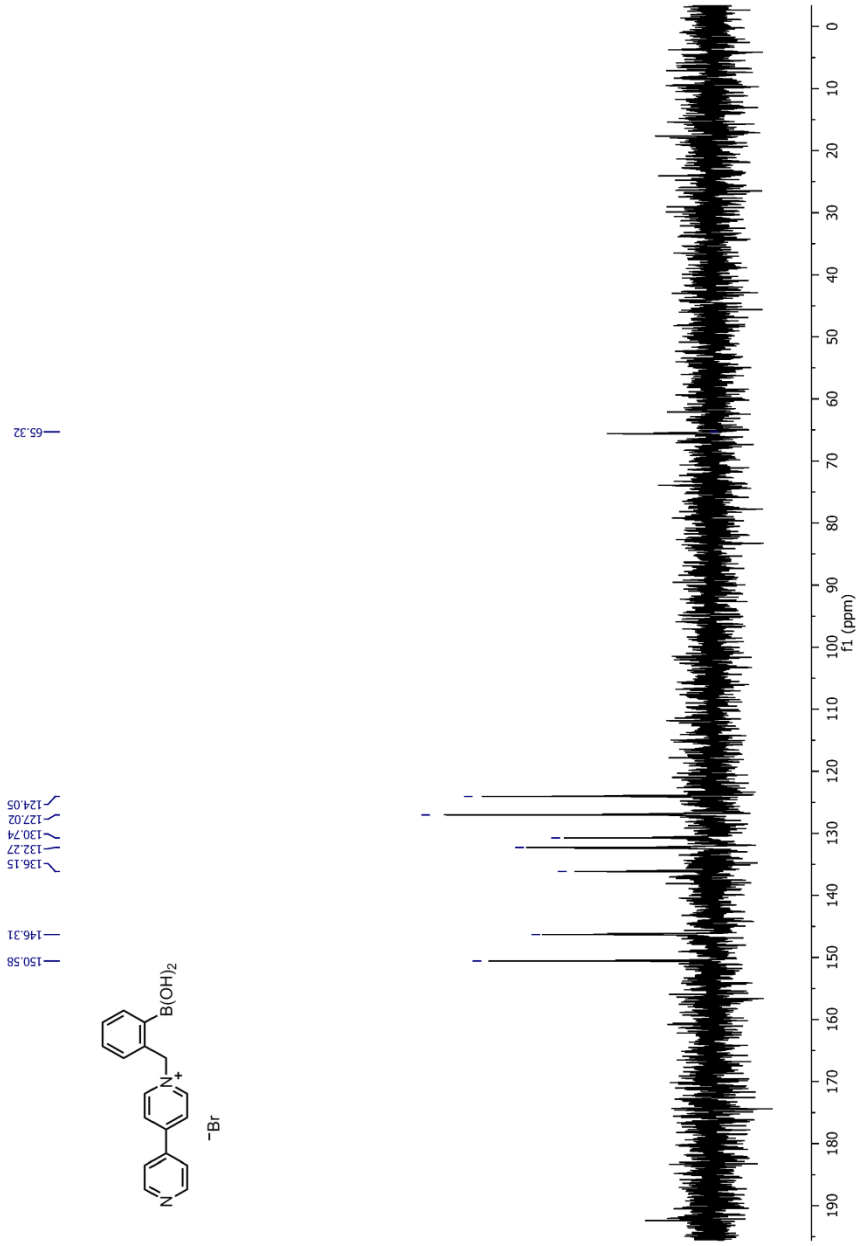

^{13}C NMR of monoalkylated bipyridyl boronic acid salt (**8**)

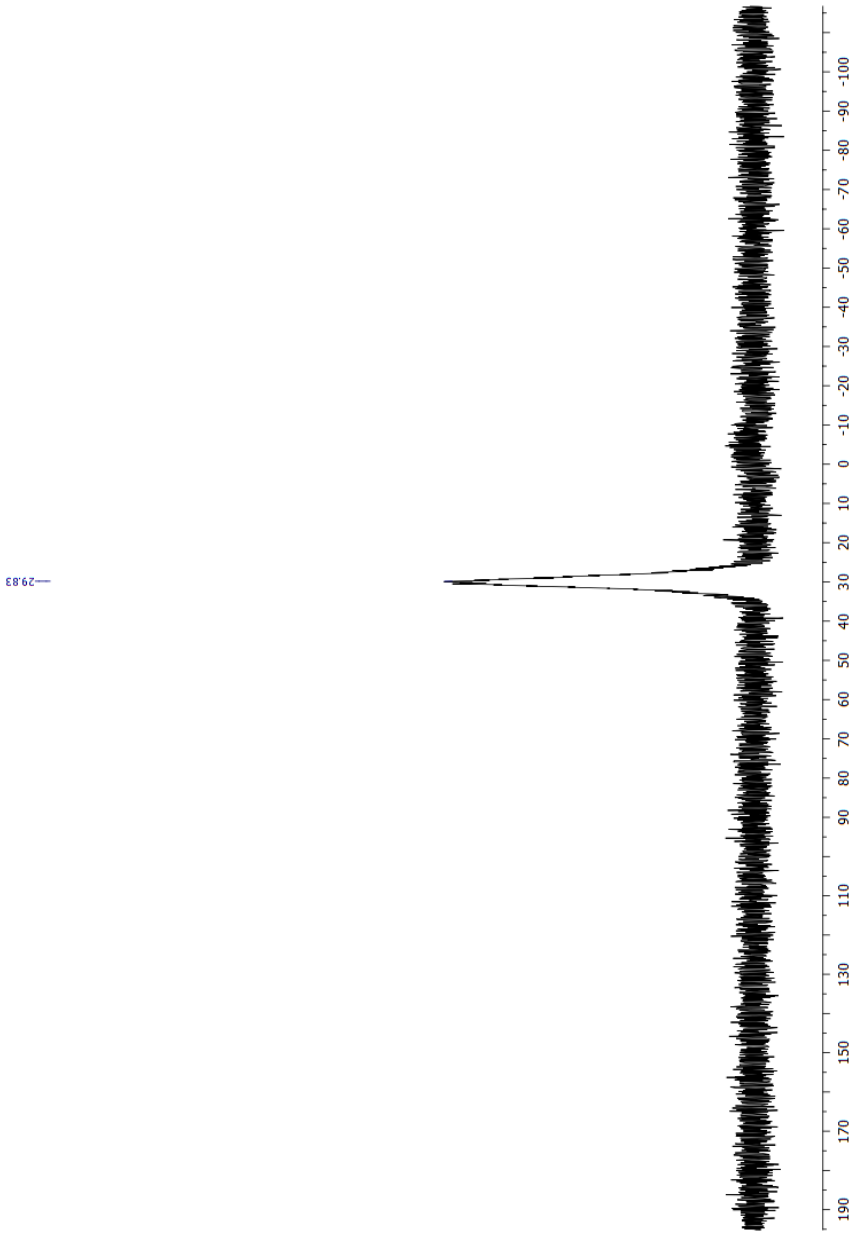

^{11}B NMR of monoalkylated bipyridyl boronic acid salt (**8**)

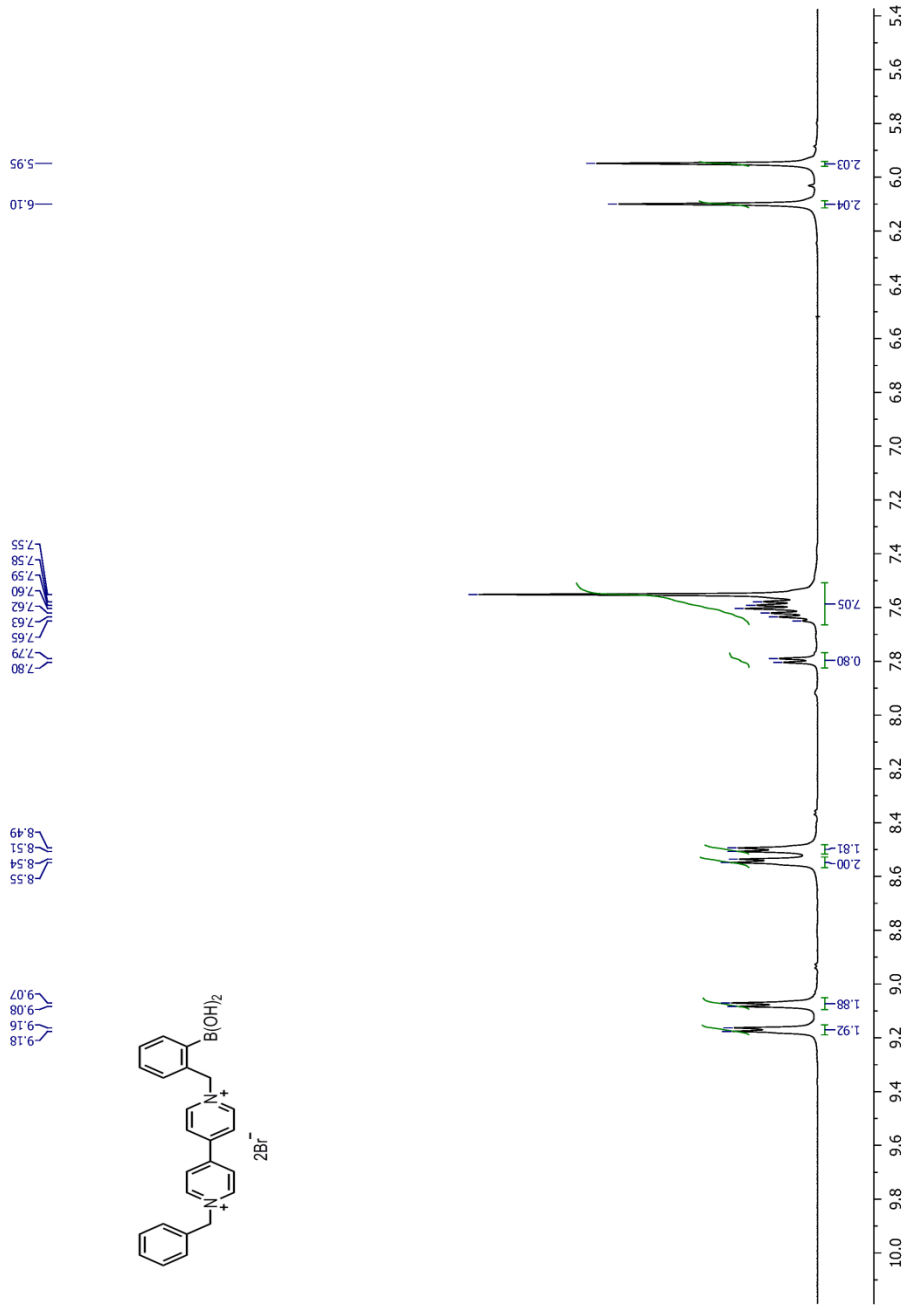

^{1}H NMR of monoalkylated bipyridyl boronic acid salt (oMBV, **9**)

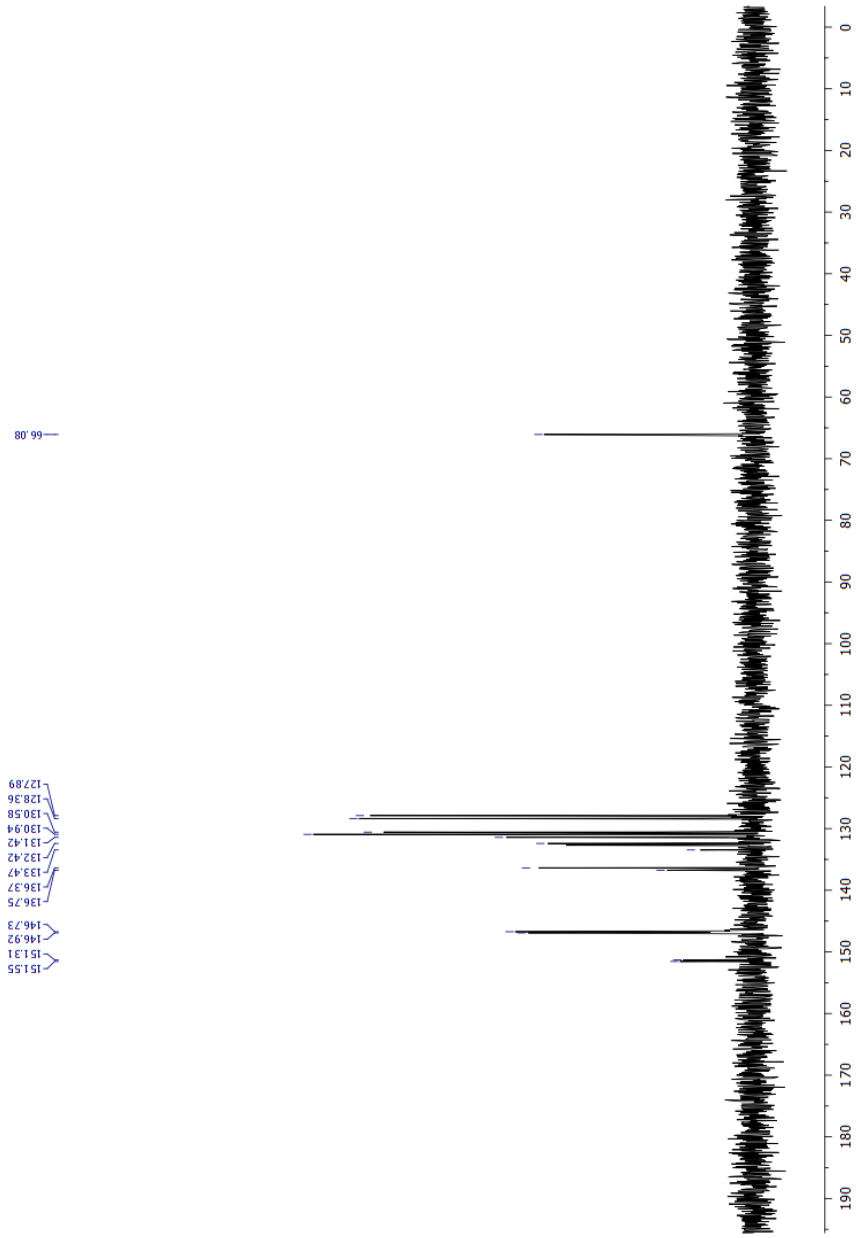

^{13}C NMR of monoalkylated bipyridyl boronic acid salt (oMBV**,9**)

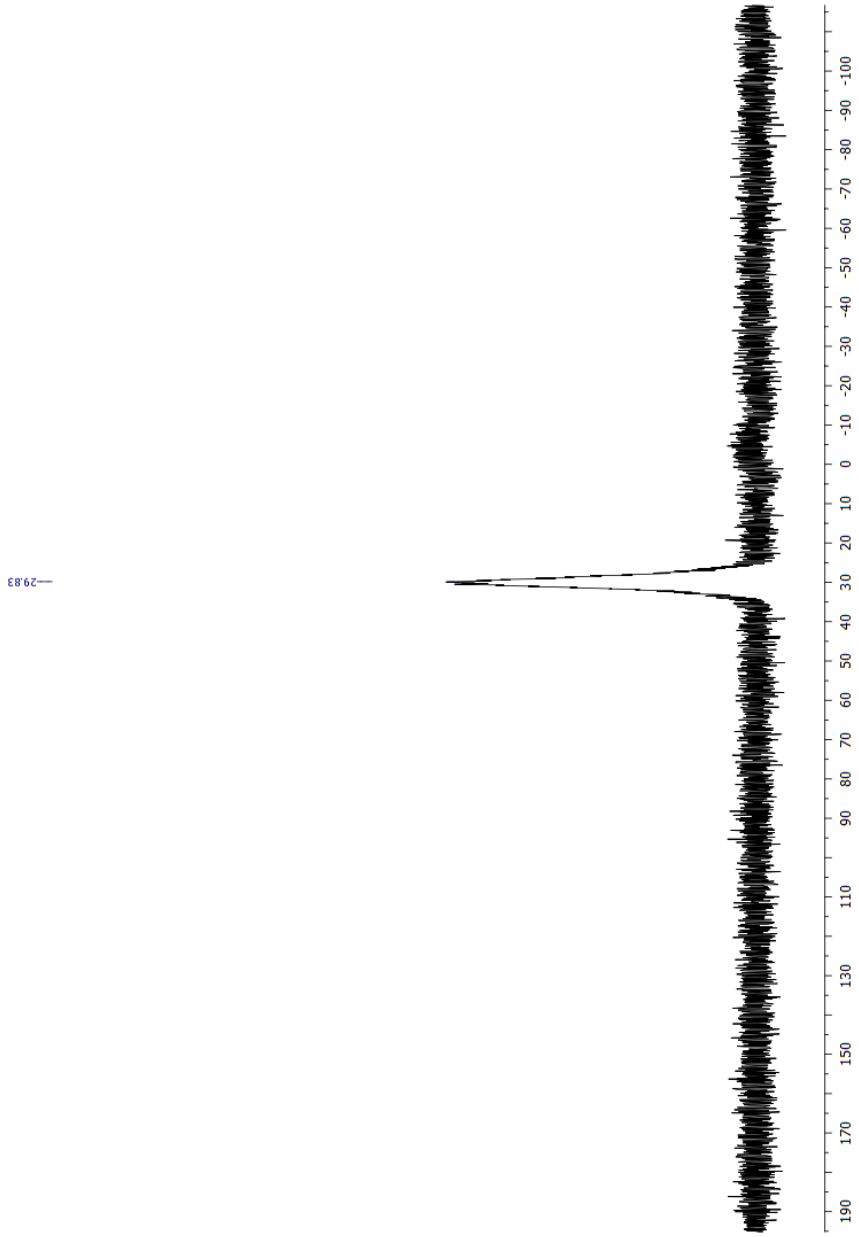

^{11}B NMR of monoalkylated bipyridyl boronic acid salt (oMBV**,9**)

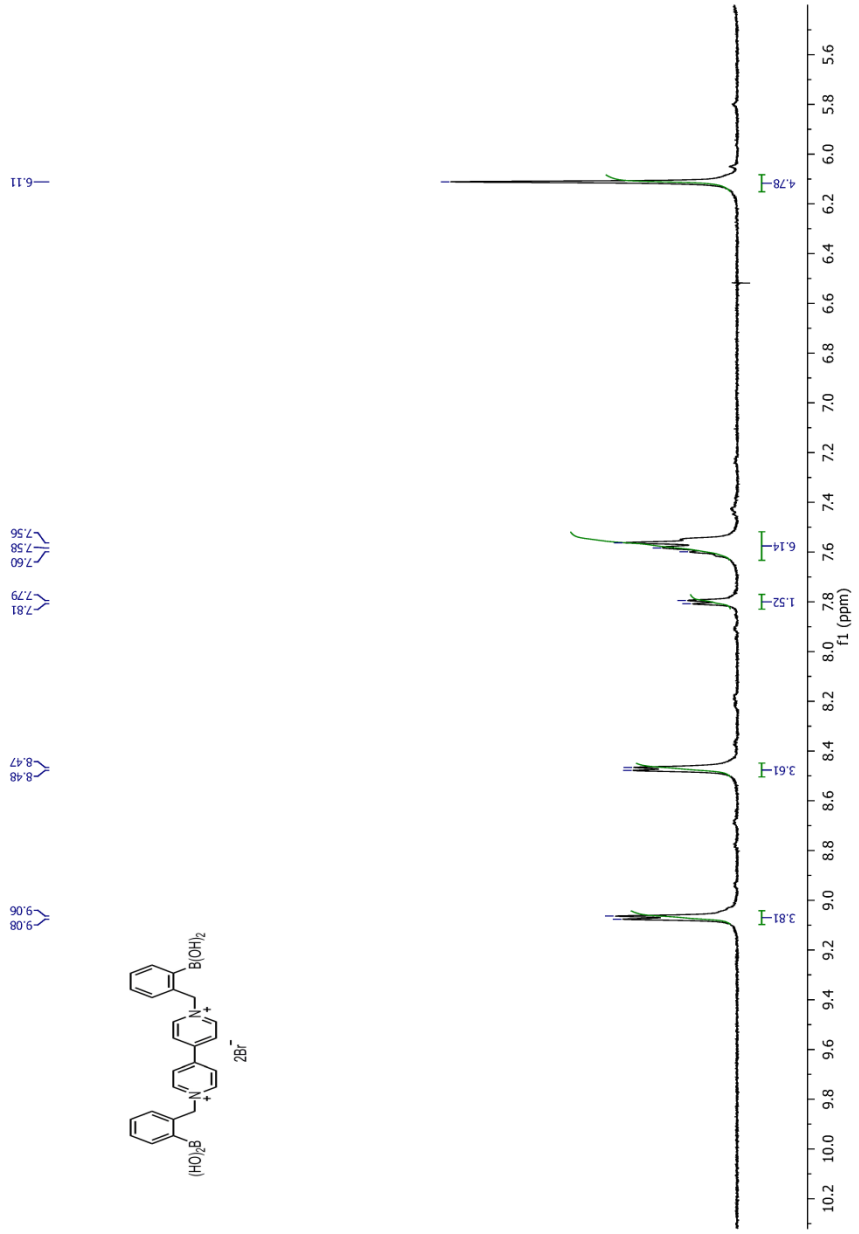

^{1}H NMR of 4,4'-*o*-BBV (**6**)

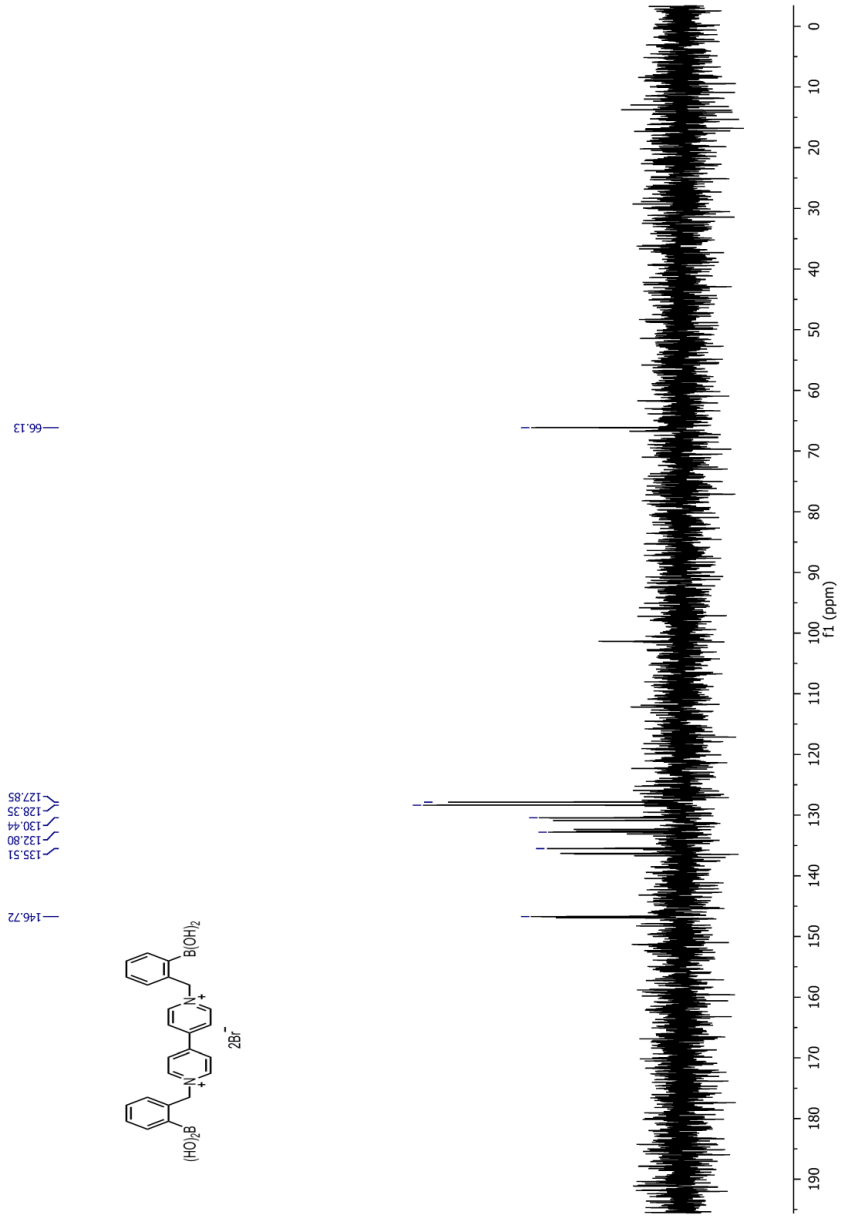

^{13}C NMR of 4,4'-*o*-BBV (**6**)

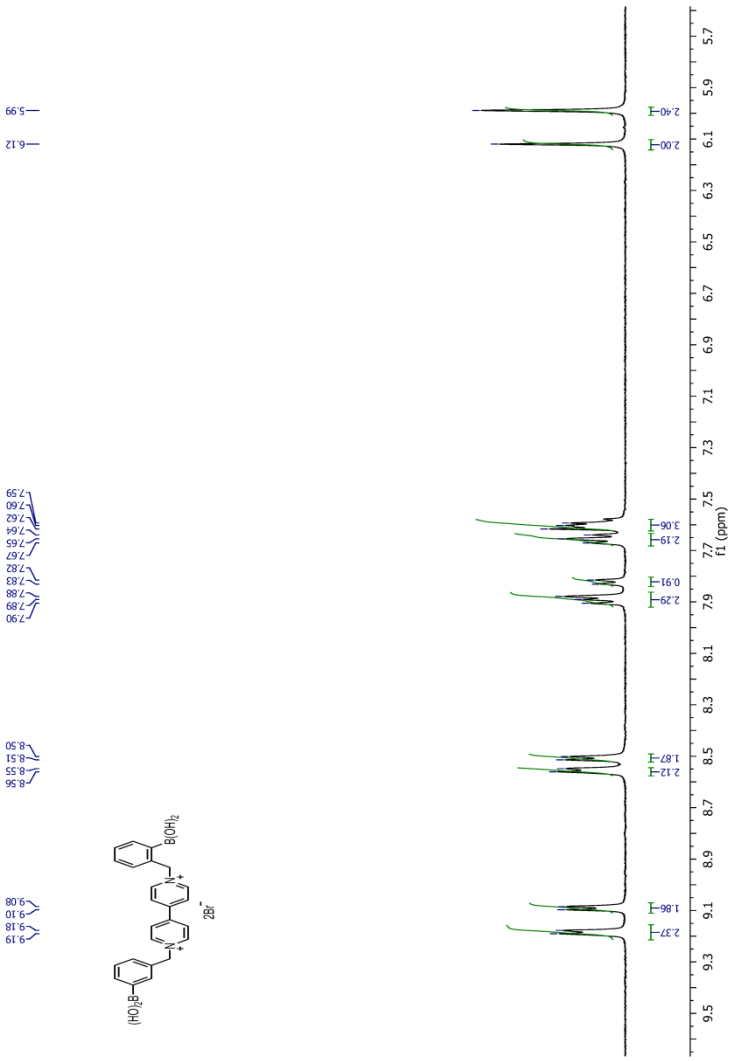

^{1}H NMR of 4,4'-*o,m*-BBV (**11**)

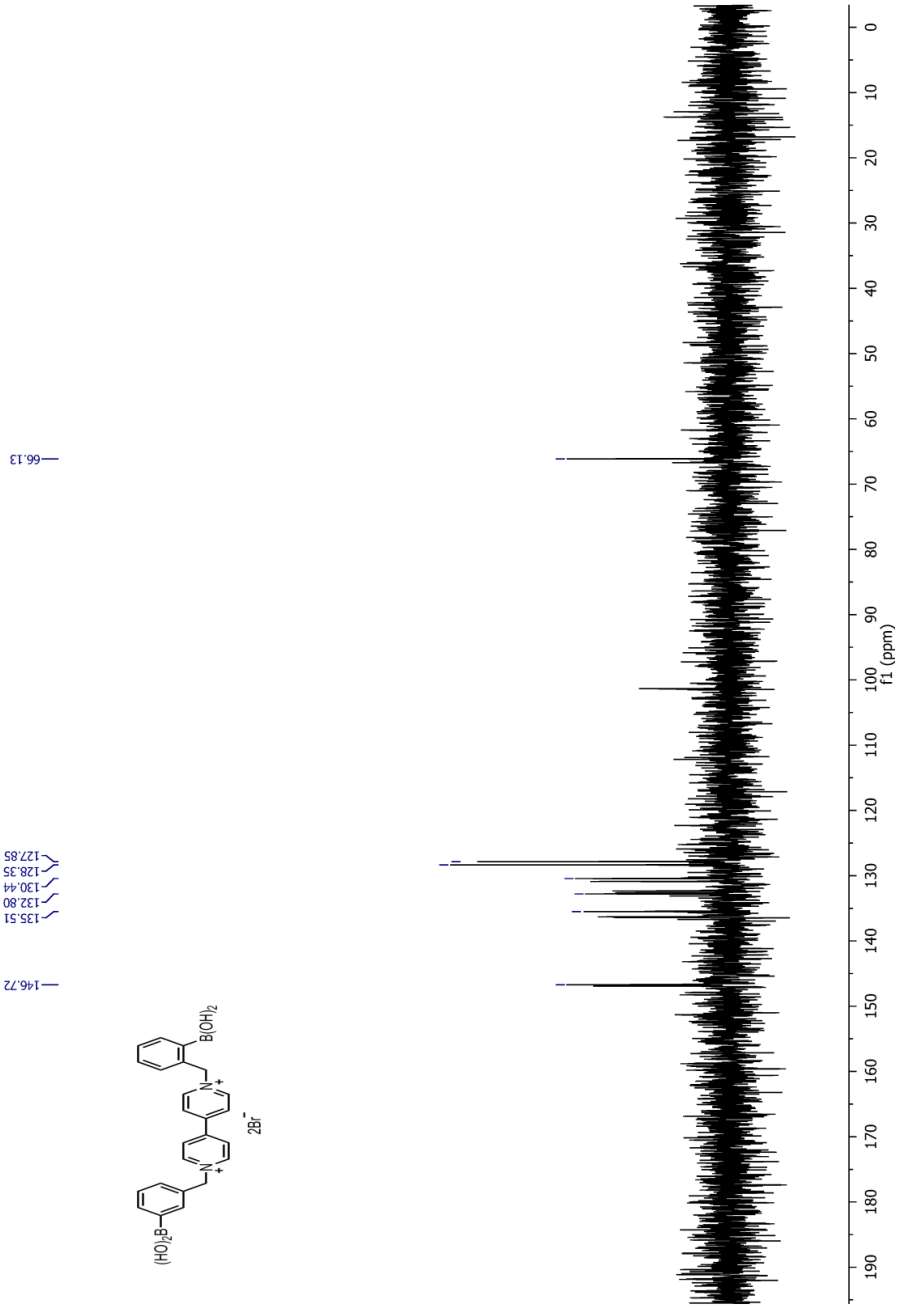

^{13}C NMR of 4,4'-*o,m*-BBV (**11**)

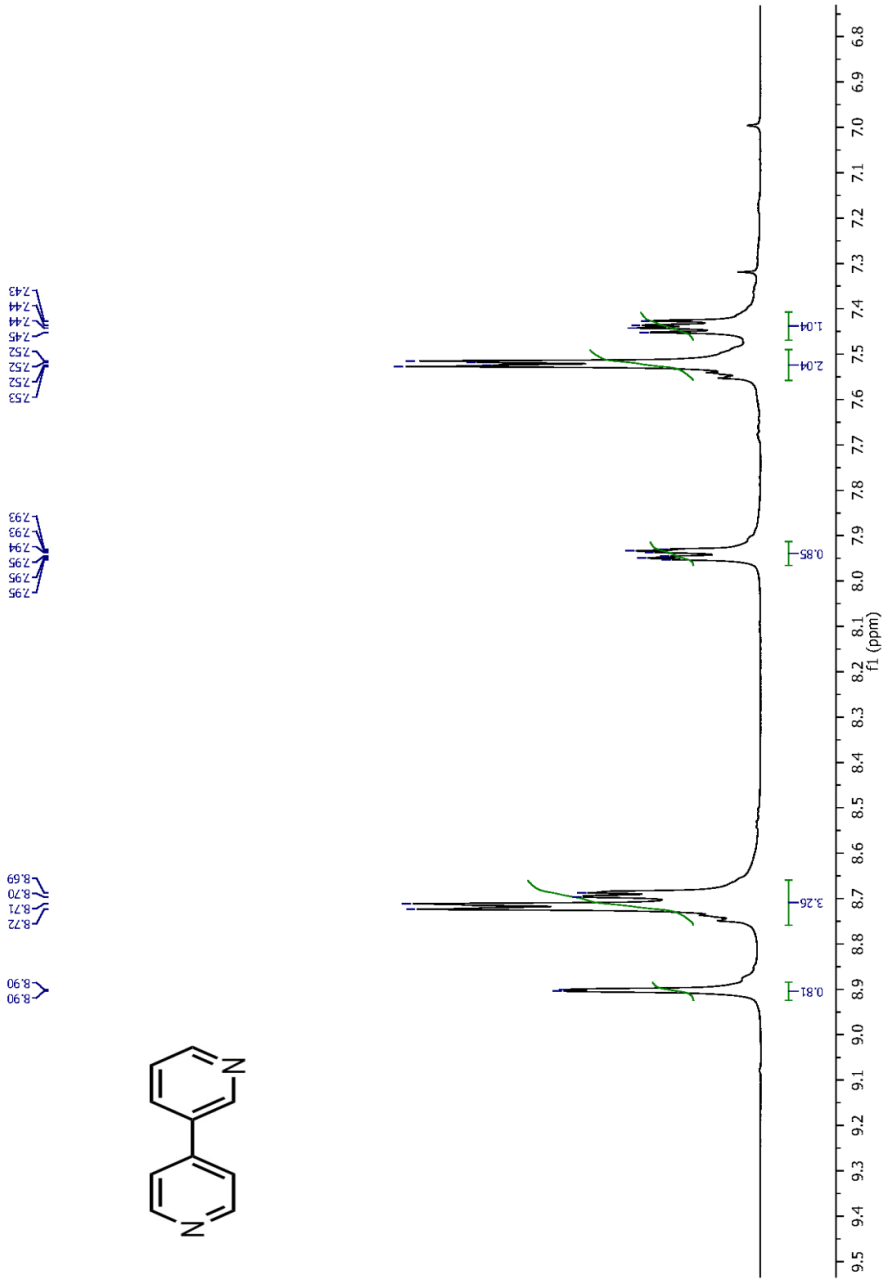

^{1}H NMR of 3,4'- bipyridyl

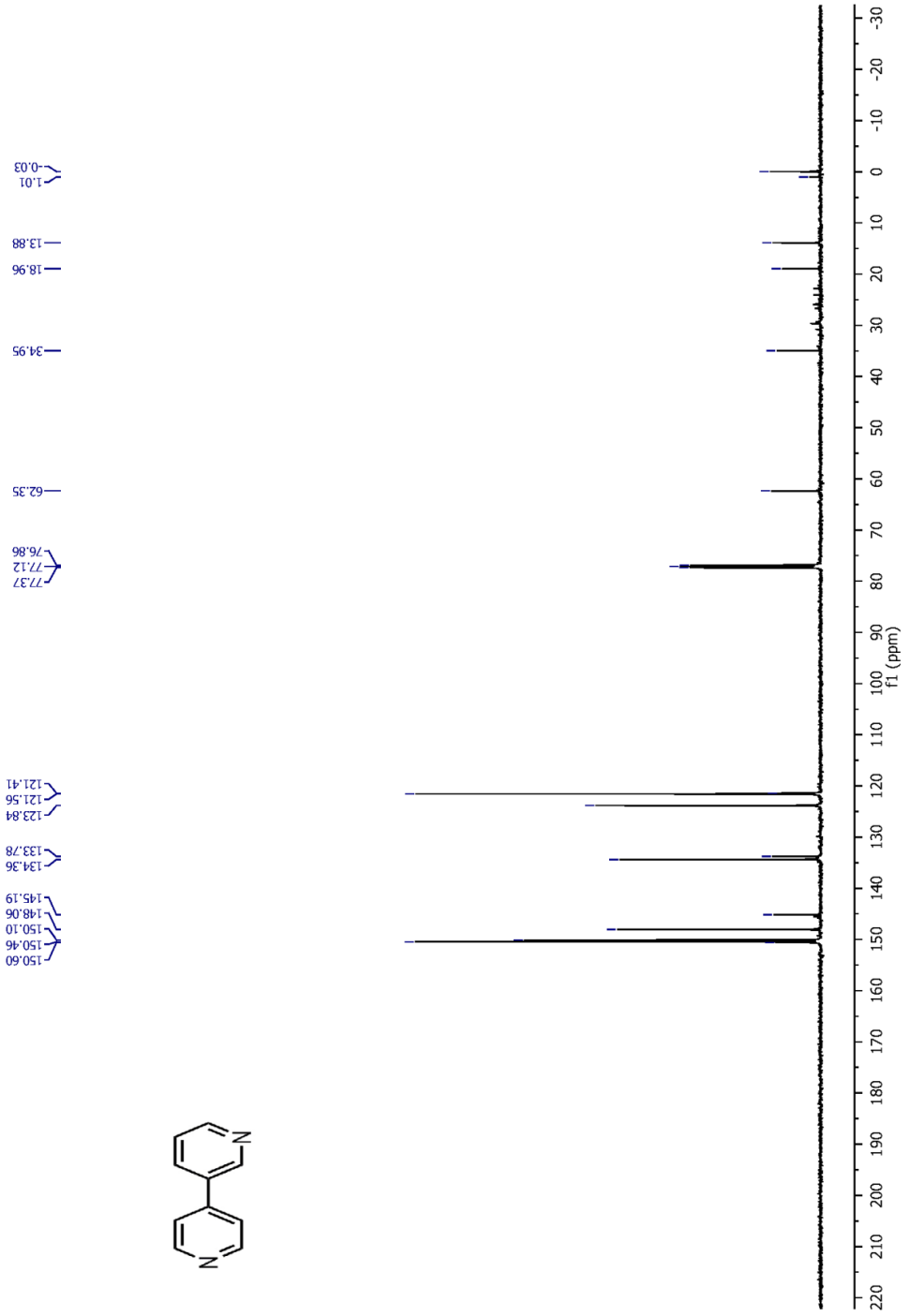

^{13}C NMR of 3,4'-bipyridyl

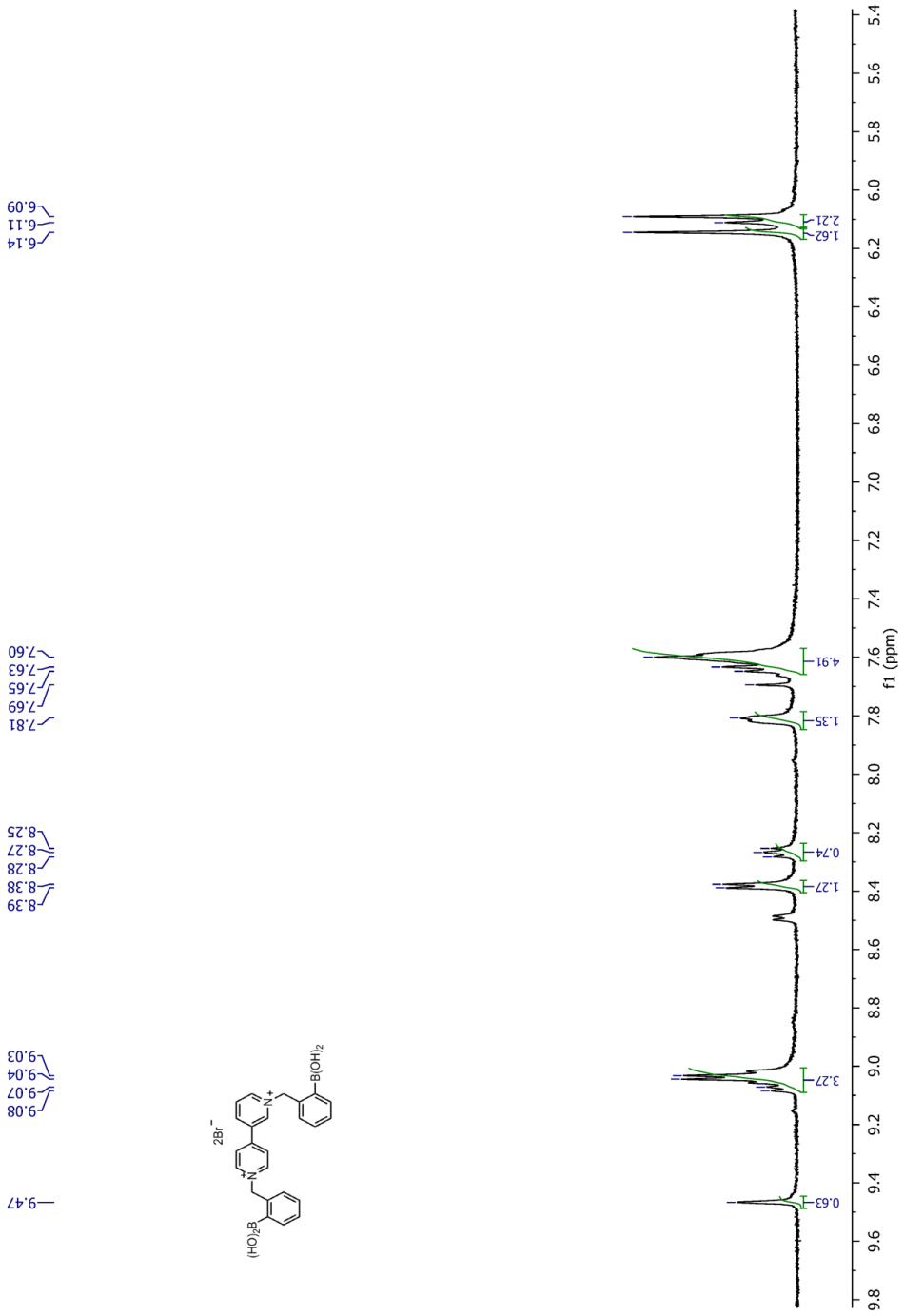

^{1}H NMR of 3,4'-*o*-BBV (**10**)

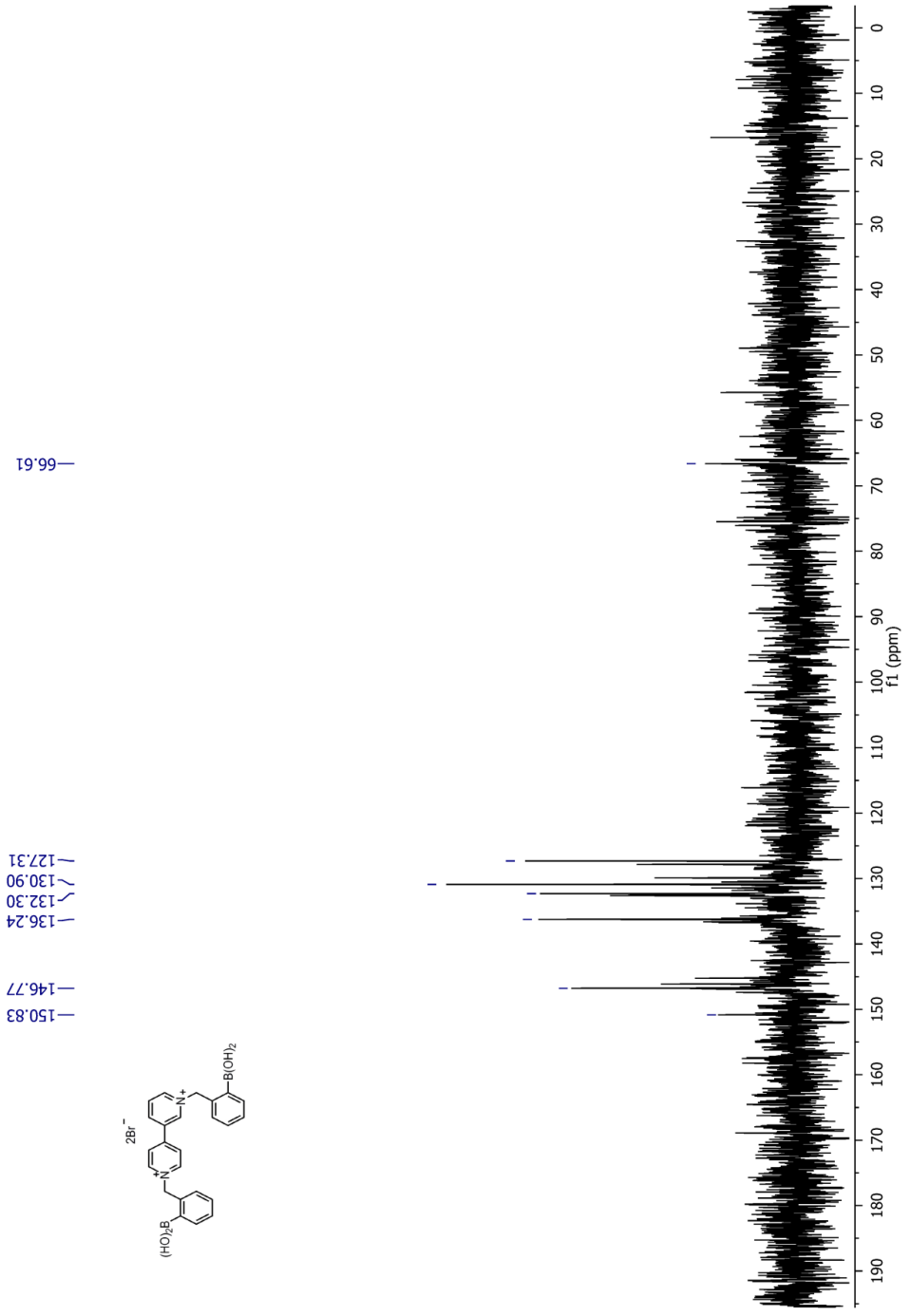

^{13}C NMR of 3,4'-*o*-BBV (**10**)

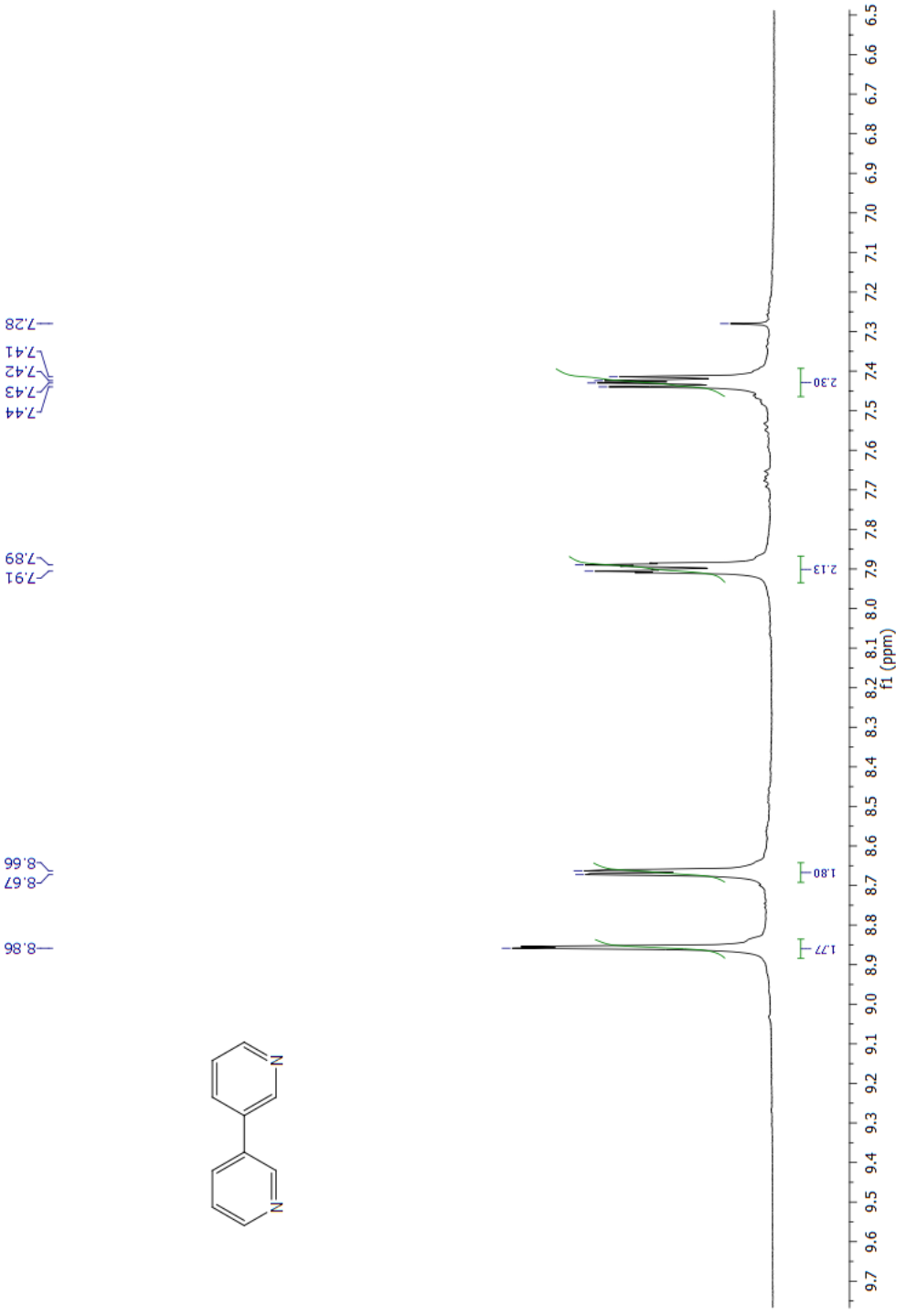

^{1}H NMR of 3,3'-bipyridyl

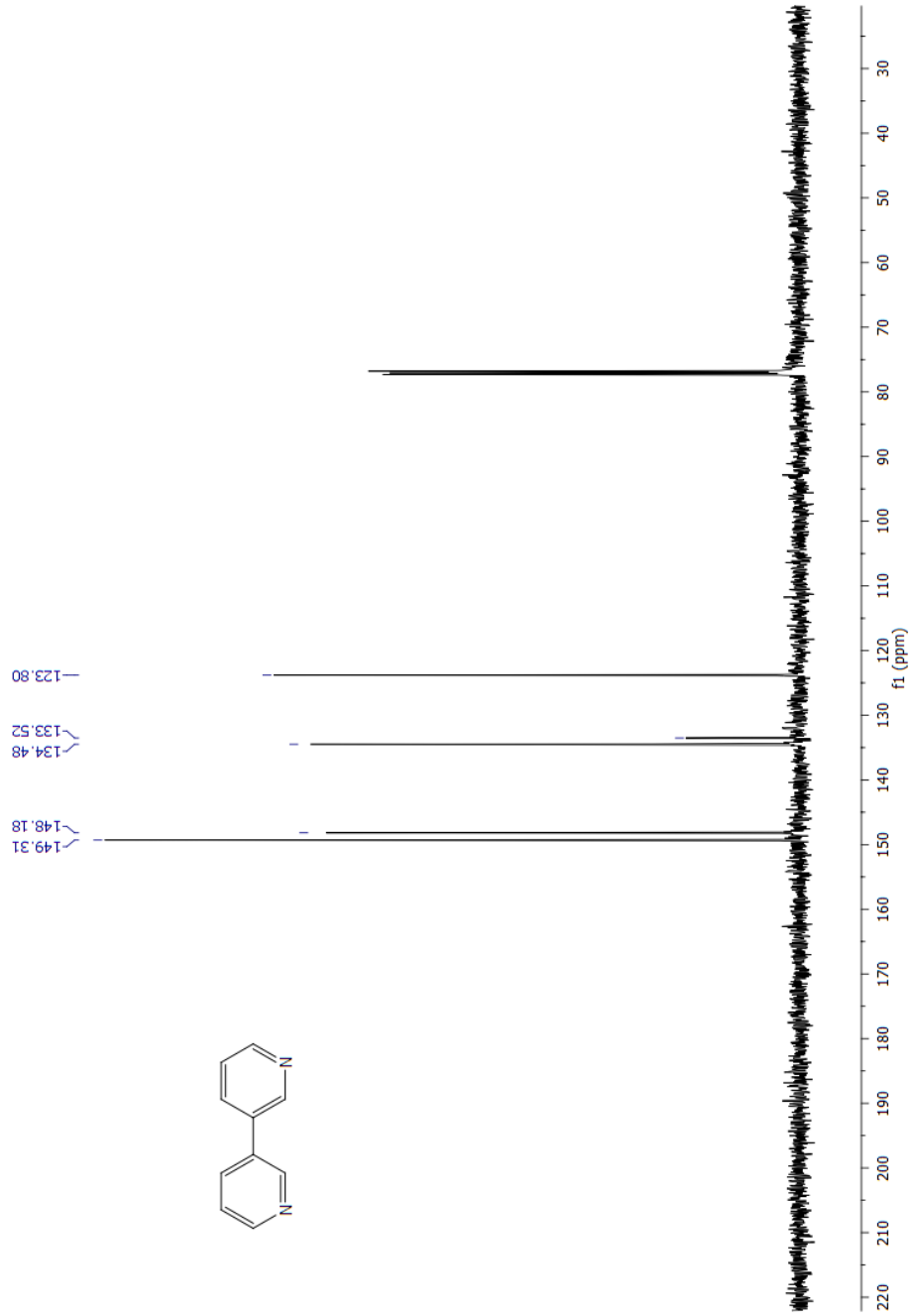

^{13}C NMR of 3,3'-bipyridyl

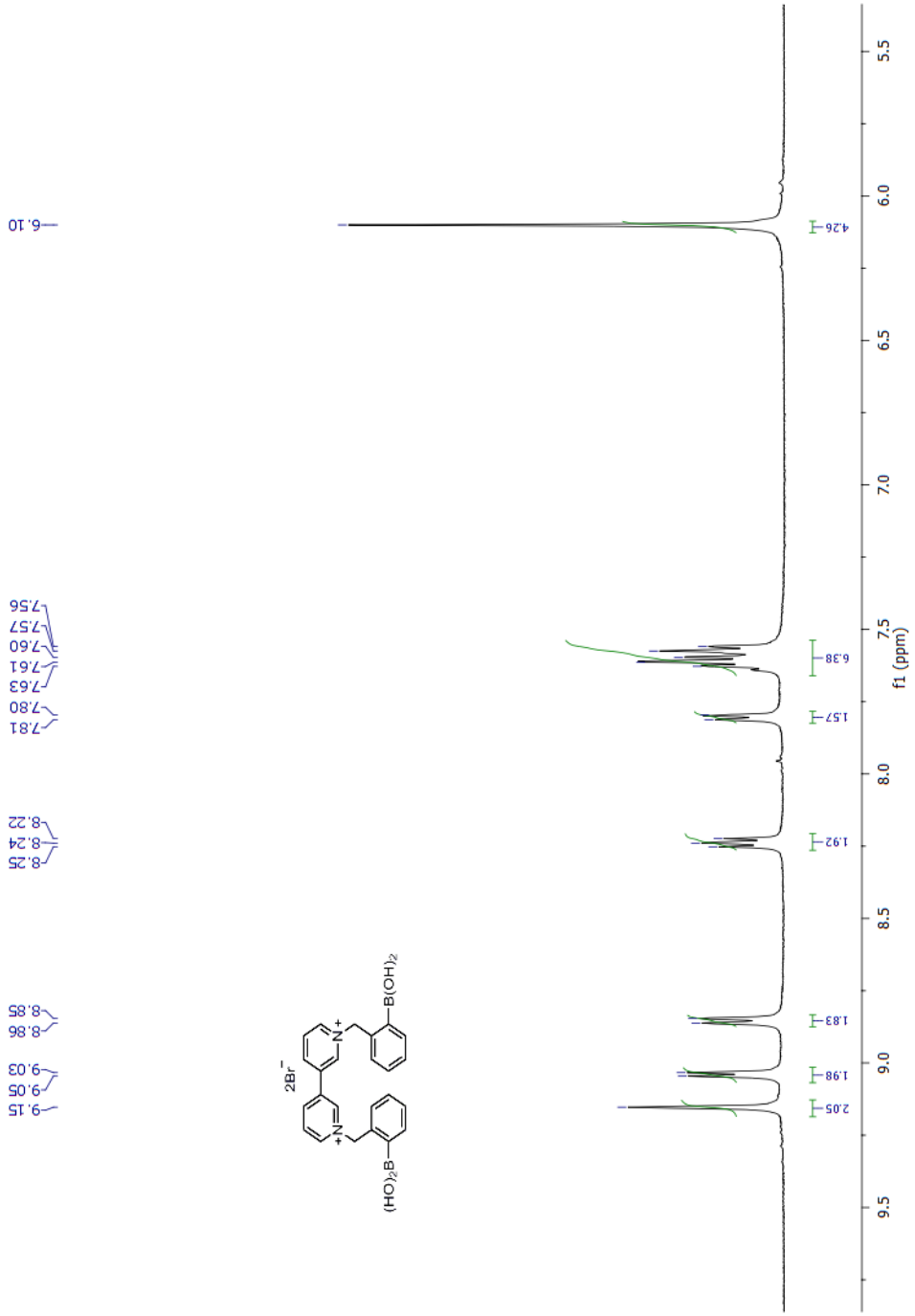

^{1}H NMR of 3,3'-*o*-BBV (**7**)

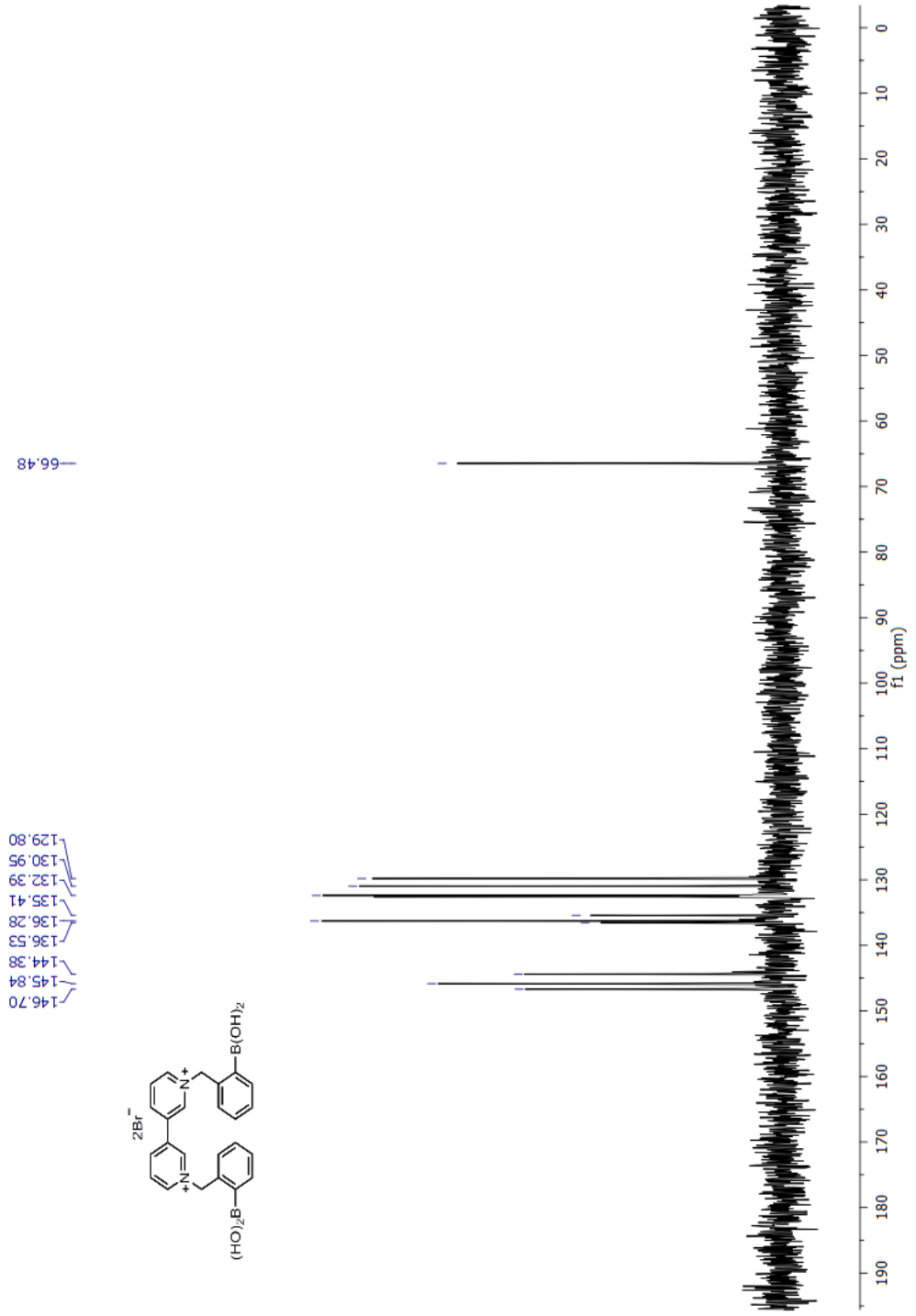

^{13}C NMR of 3,3'-*o*-BBV (**7**)

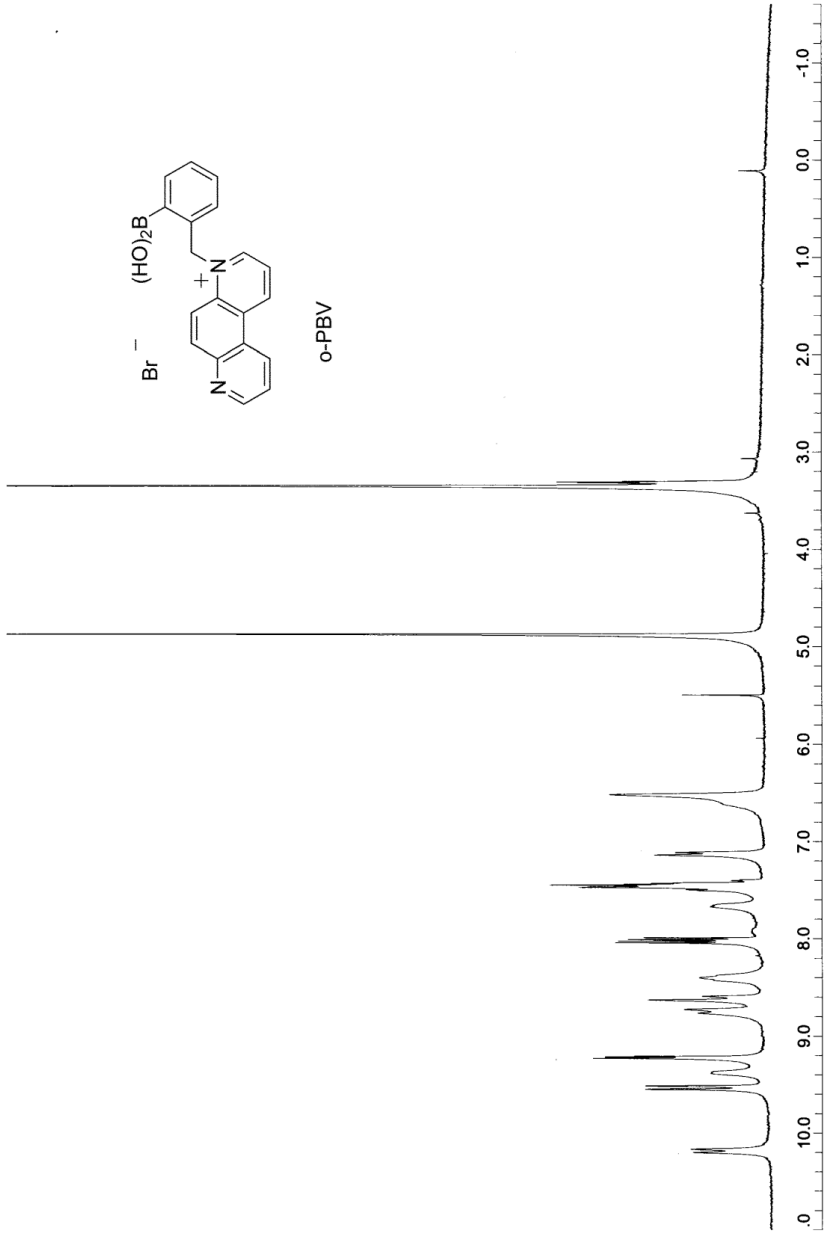

^{1}H NMR of *o*-PBV

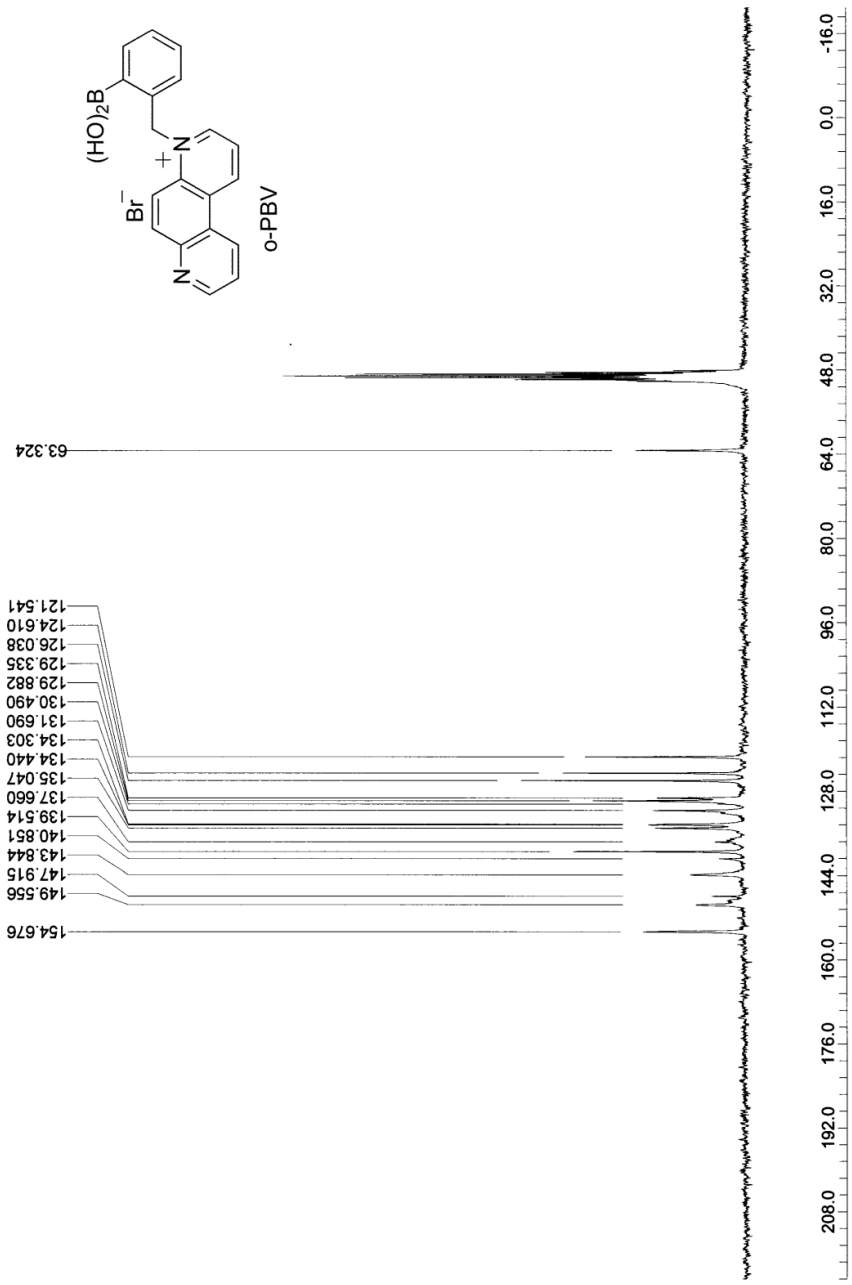

^{13}C NMR of *o*-PBV

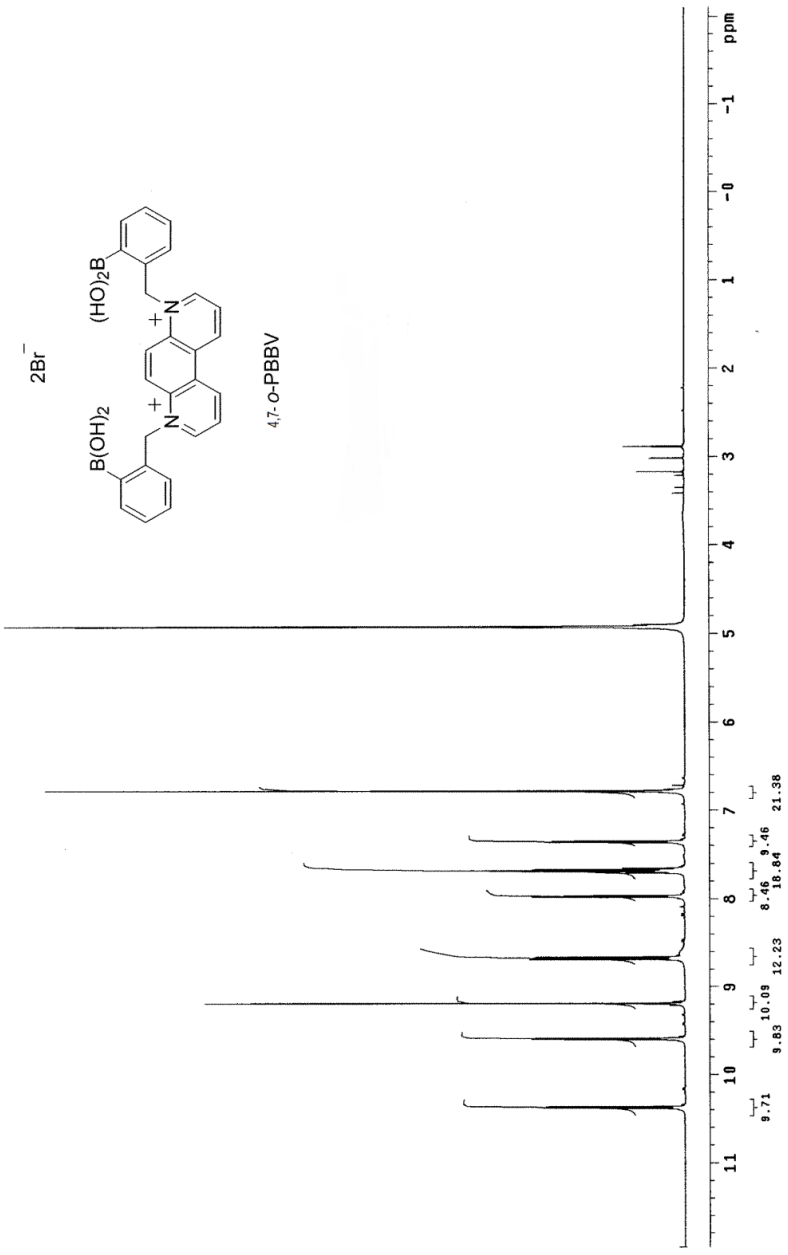

^{1}H NMR of 4,7-*o*-PBBV (**12**)

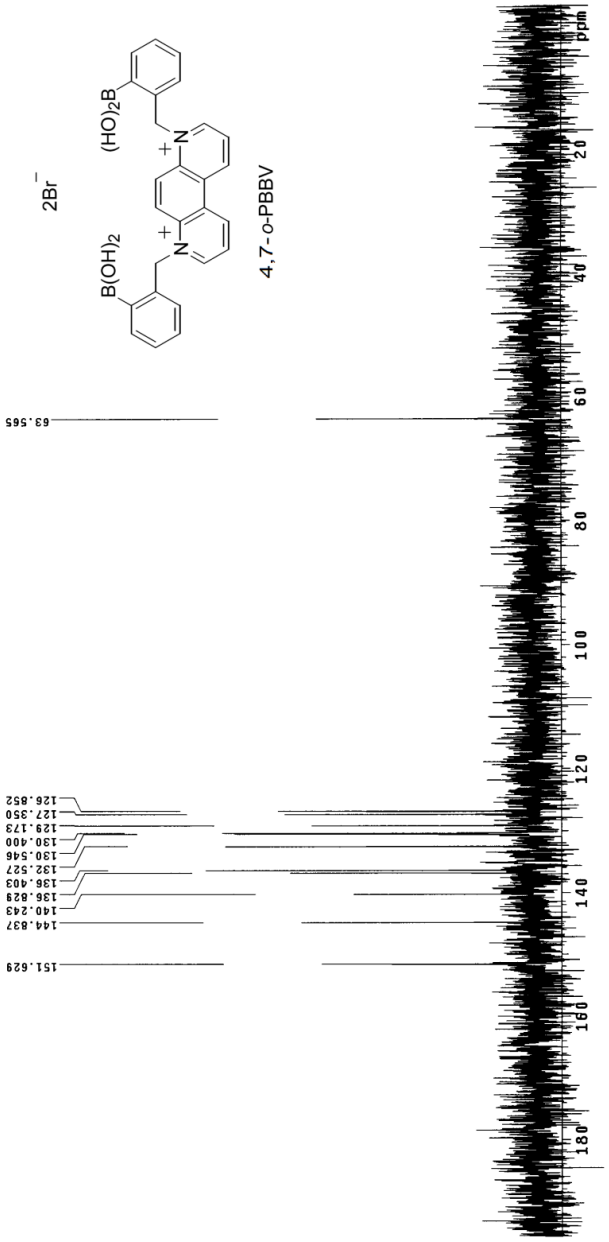

^{13}C NMR of 4,7-*o*-PBBV (**12**)

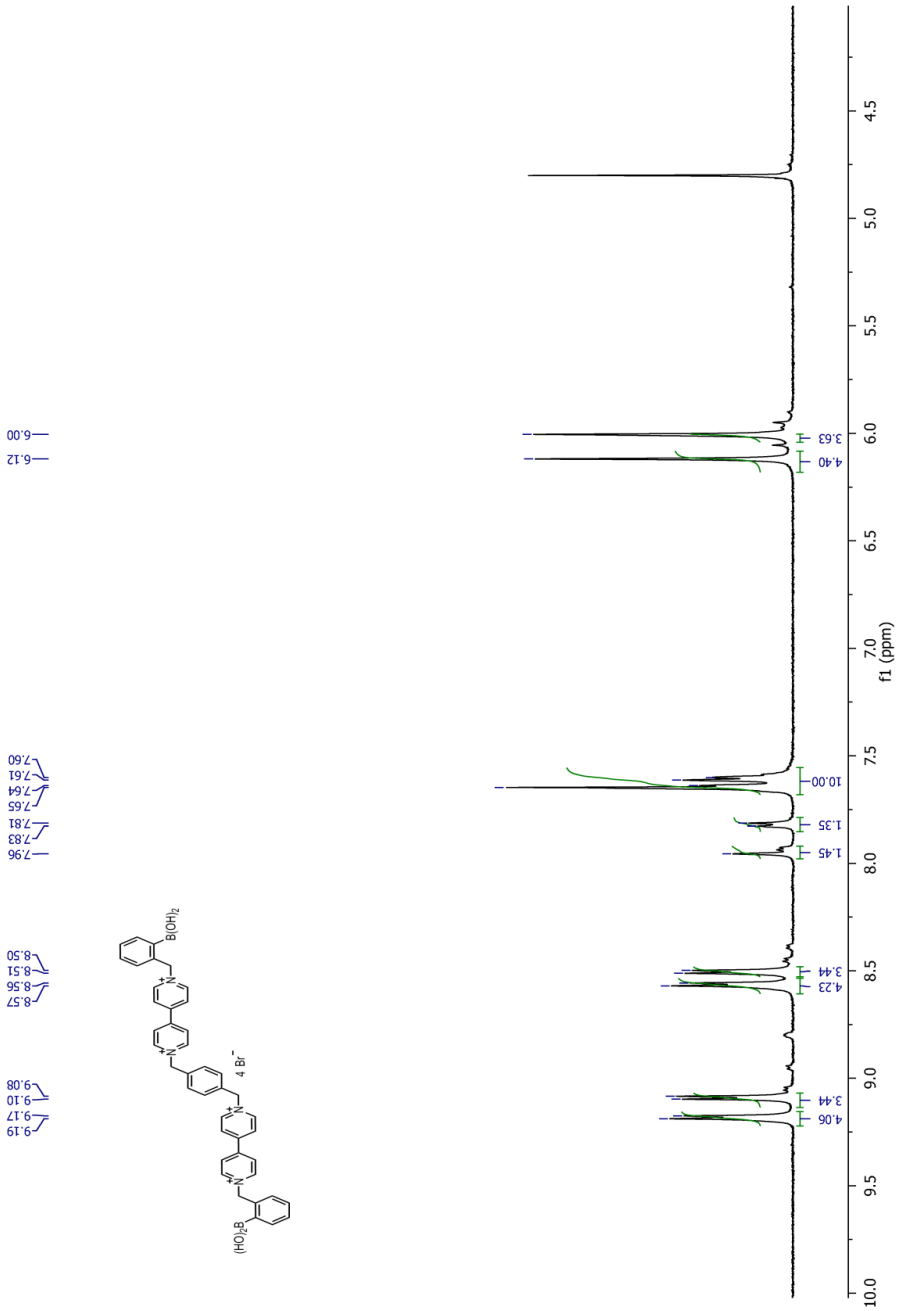

^{1}H NMR of pBo*o*B (**13**)

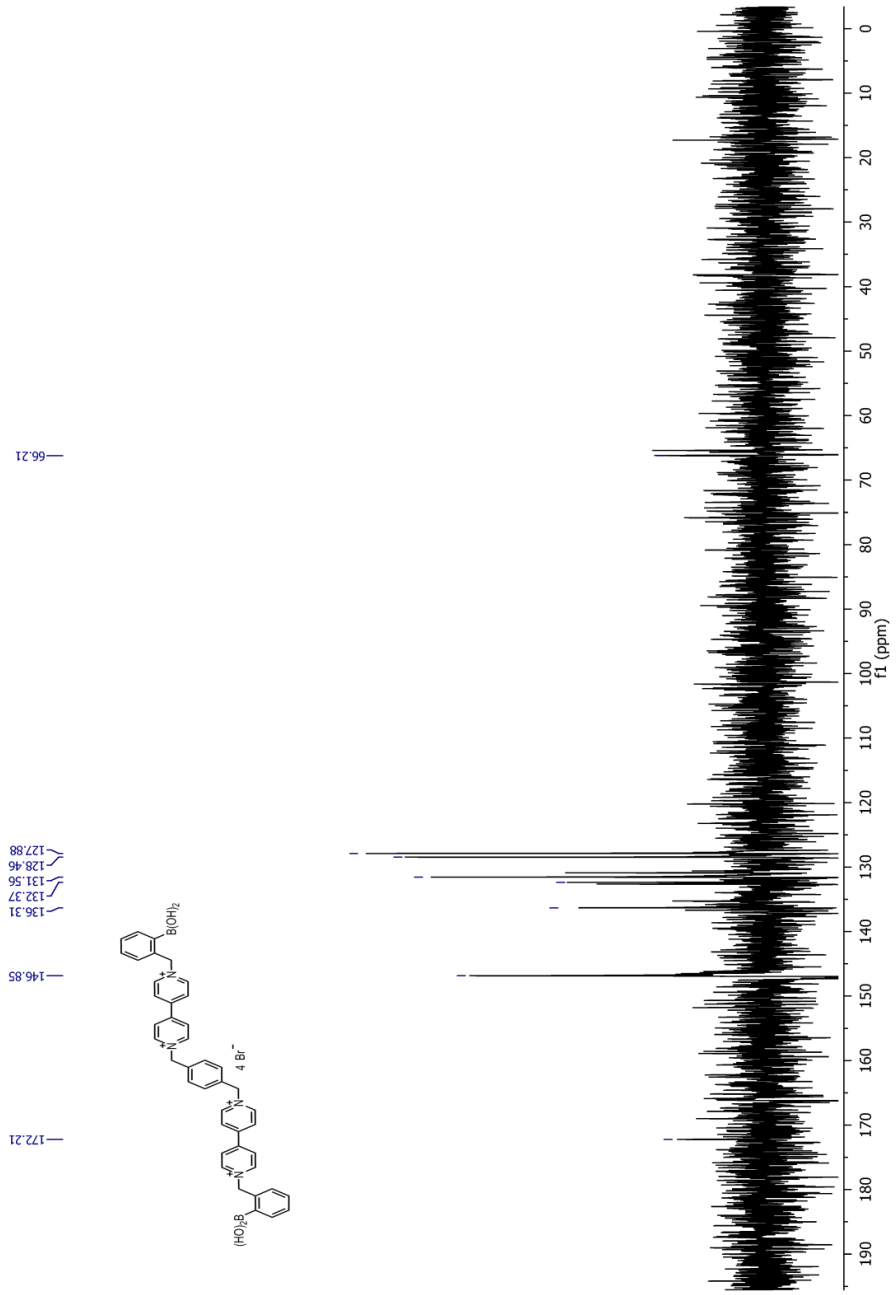

^{13}C NMR of pBoB (**13**)

Appendix B:
LDA Score Plots
Of Triad Arrays

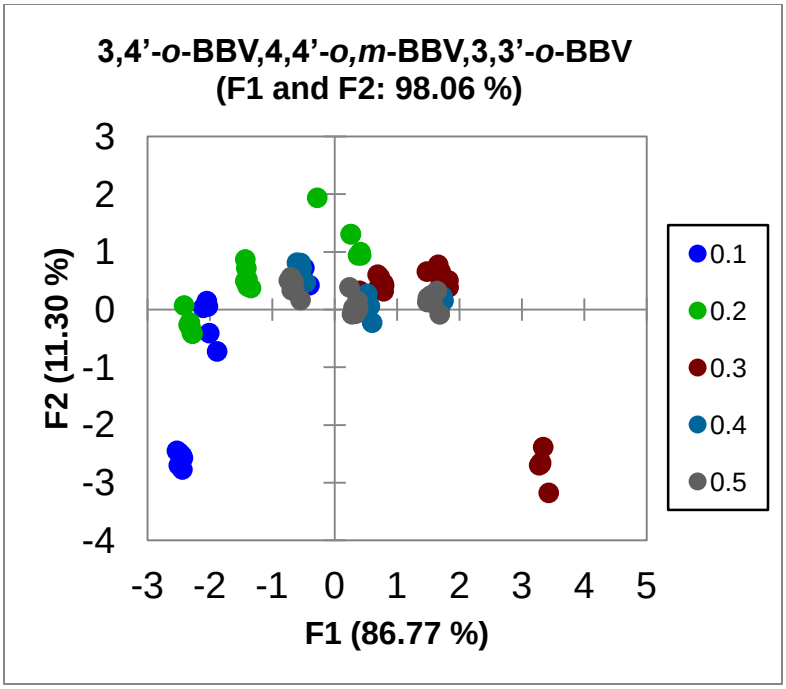

LDA plot (1) of various L/M ratios with the triad array of boronic acid receptors: 3,4'-*o*-BBV, 4,4,'-*o,m*-BBV, and 3,3'-*o*-BBV.

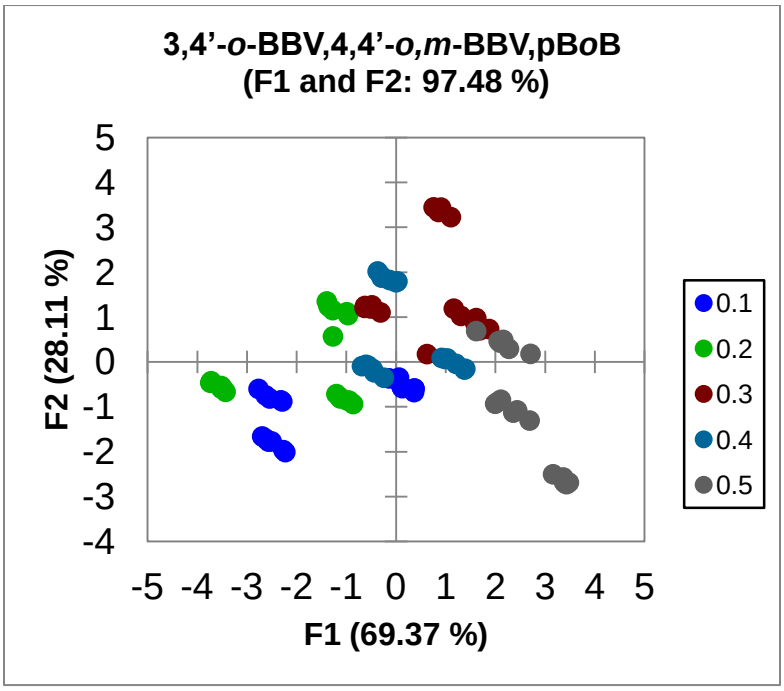

LDA plot (2) of various L/M ratios with the triad array of boronic acid receptors: 3,4'-*o*-BBV, 4,4,'-*o,m*-BBV, and pB*o*B.

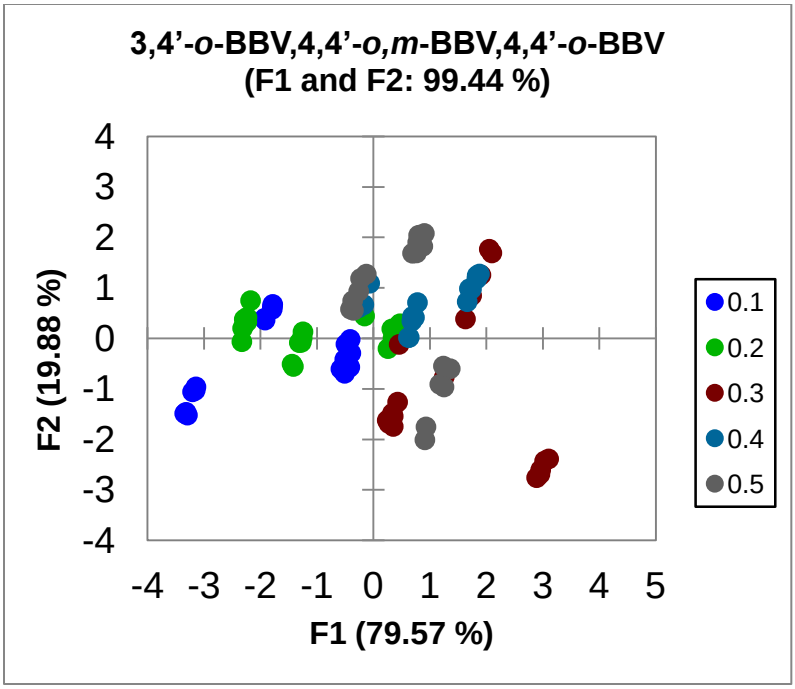

LDA plot (3) of various L/M ratios with the triad array of boronic acid receptors: 3,4'-*o*-BBV, 4,4,'-*o*-*m*-BBV, and 4,4,'-*o*-BBV.

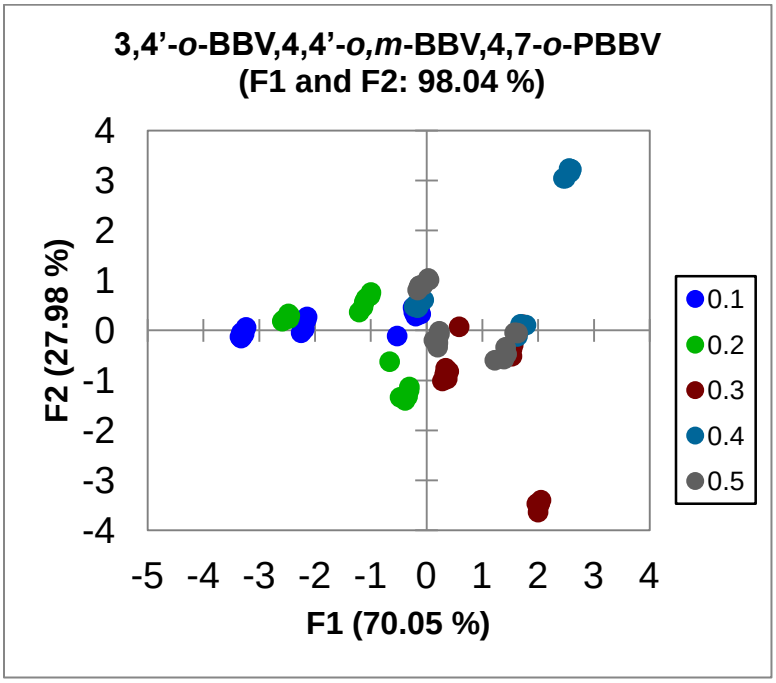

LDA plot (4) of various L/M ratios with the triad array of boronic acid receptors: 3,4'-*o*-BBV, 4,4,'-*o*-*m*-BBV, and 4,7-o-PBBV.

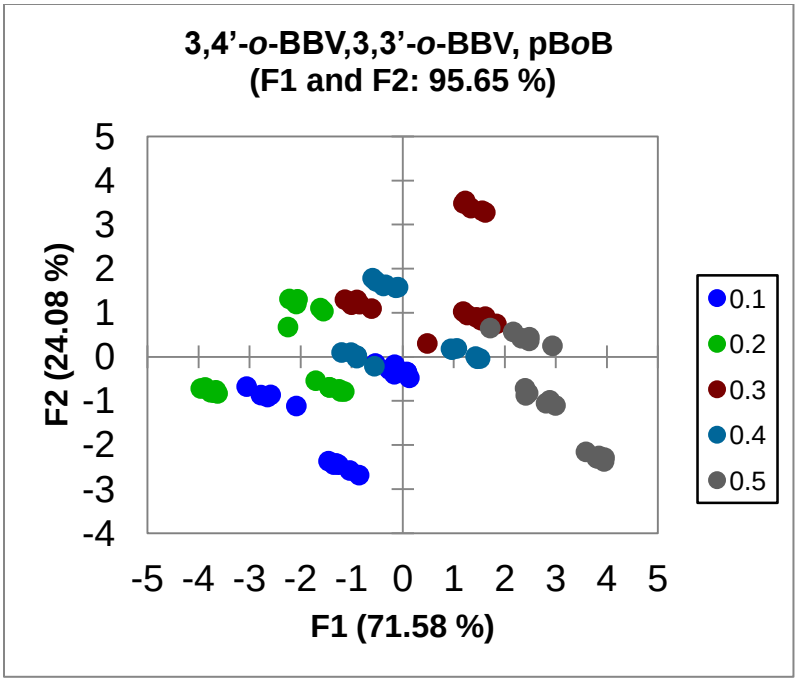

LDA plot (5) of various L/M ratios with the triad array of boronic acid receptors: 3,4'-*o*-BBV, 3,3,'-*o*-BBV, and pB*o*B.

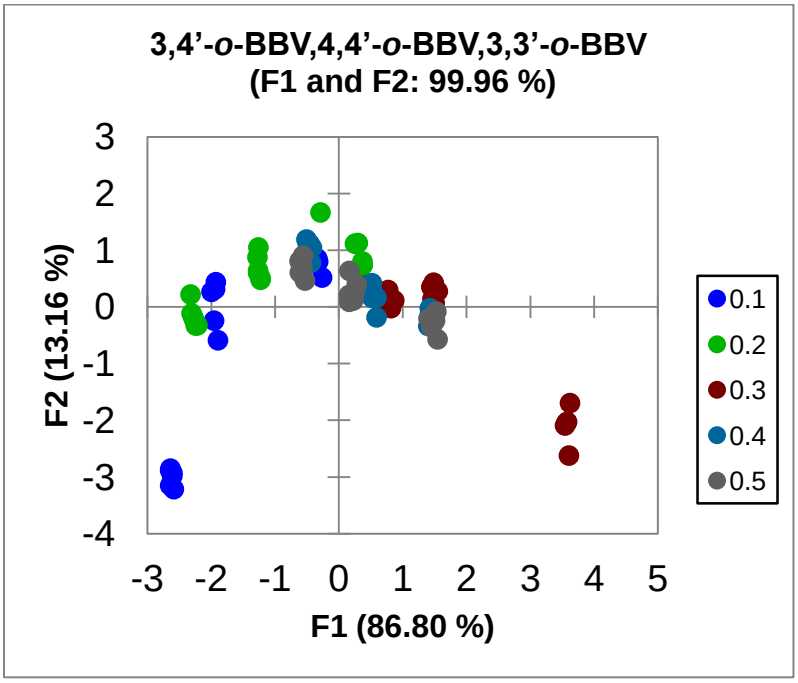

LDA plot (6) of various L/M ratios with the triad array of boronic acid receptors: 3,4'-*o*-BBV, 4,4,'-*o*-BBV and 3,3,'-*o*-BBV.

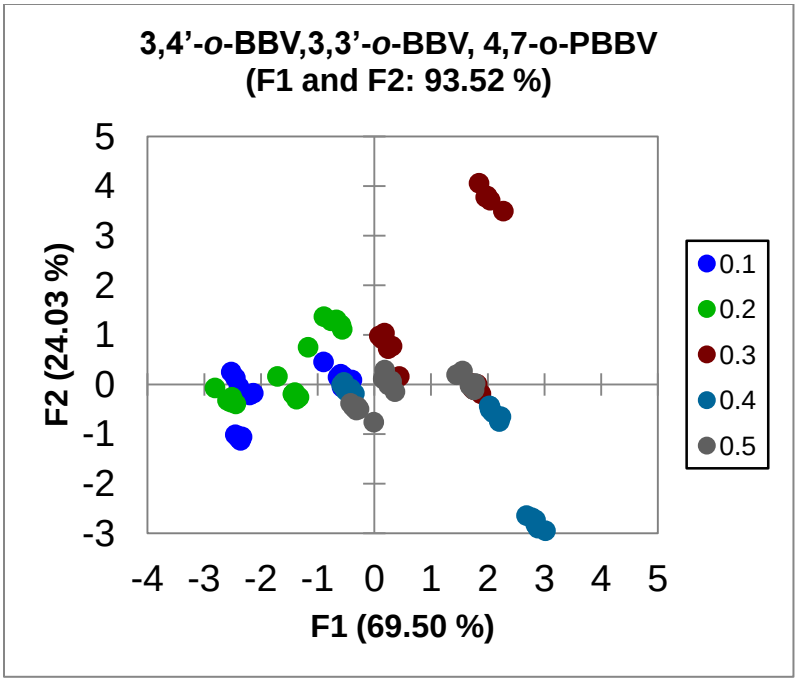

LDA plot (7) of various L/M ratios with the triad array of boronic acid receptors: 3,4'-*o*-BBV, 3,3'-*o*-BBV, 4,7-o-PBBV

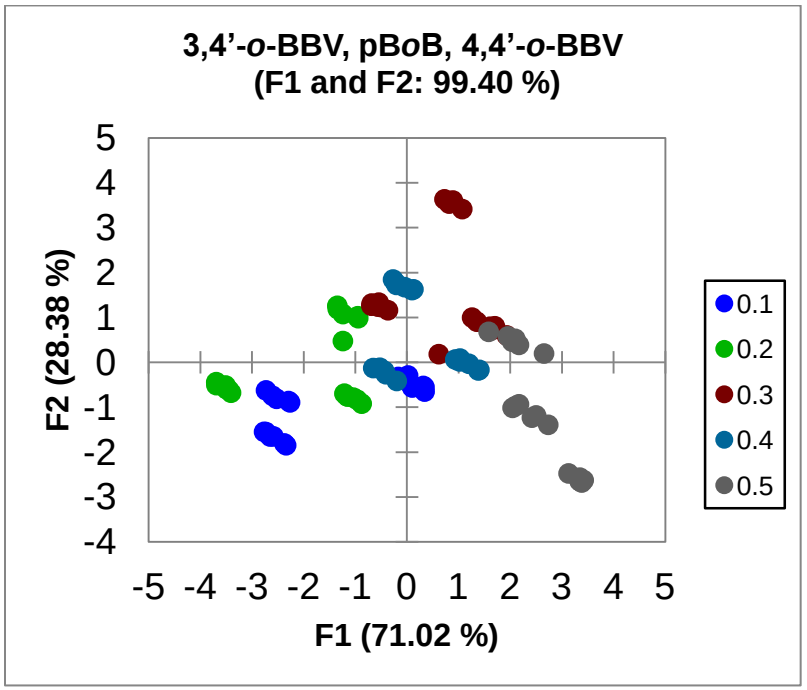

LDA plot (8) of various L/M ratios with the triad array of boronic acid receptors: 3,4'-*o*-BBV, pB*o*B, 4,4'-*o*-BBV.

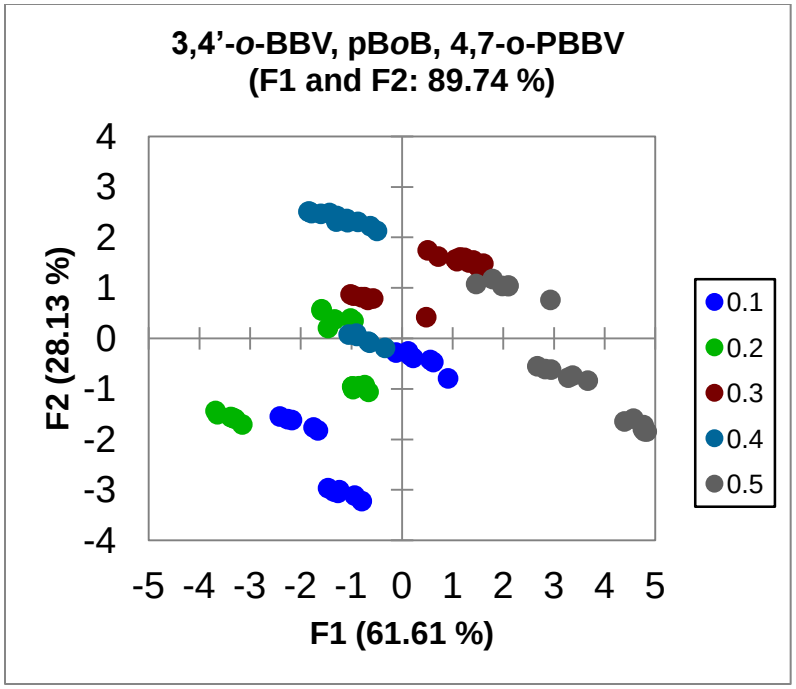

LDA plot (9) of various L/M ratios with the triad array of boronic acid receptors:3,4'-*o*-BBV, pB*o*B, 4,7-*o*-PBBV.

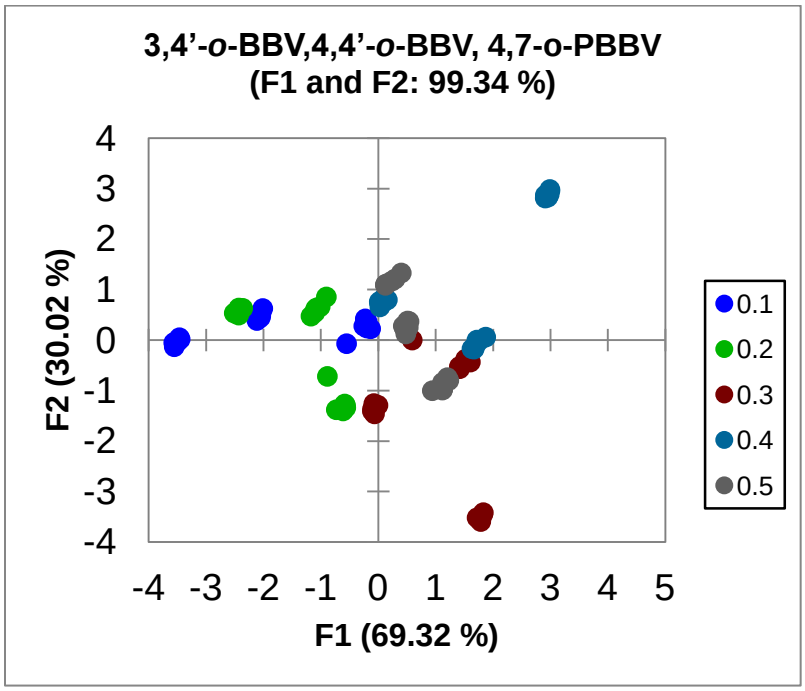

LDA plot (10) of various L/M ratios with the triad array of boronic acid receptors:3,4'-*o*-BBV, 4,4'-*o*-BBV, 4,7-*o*-PBBV.

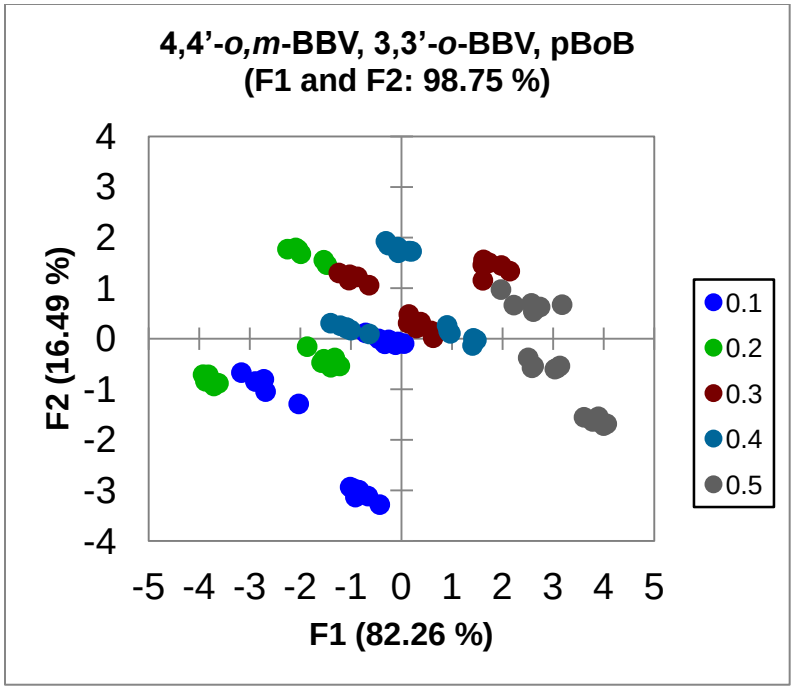

LDA plot (11) of various L/M ratios with the triad array of boronic acid receptors: 4,4'-*o,m*-BBV, 3,3'-*o*-BBV, pB*o*B.

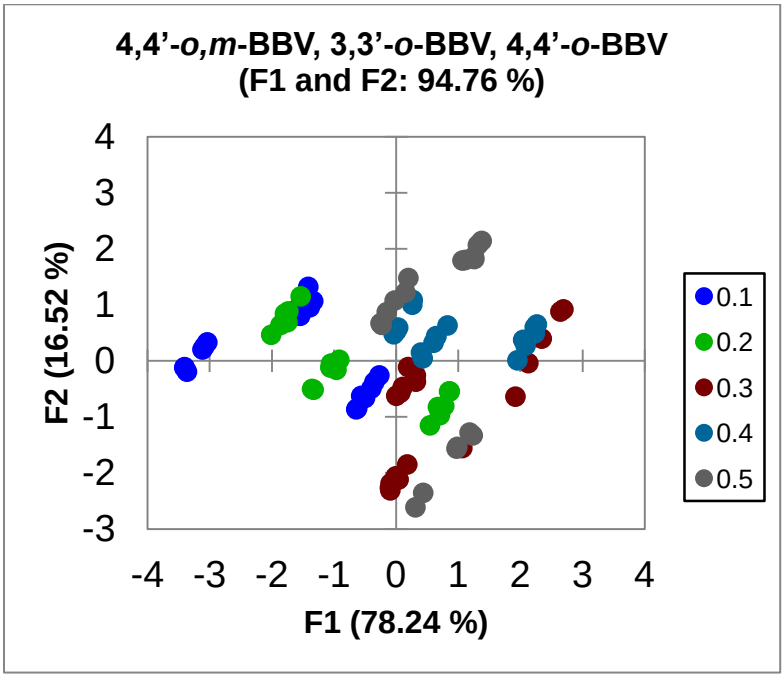

LDA plot (12) of various L/M ratios with the triad array of boronic acid receptors:4,4'-*o,m*-BBV, 3,3'-*o*-BBV, 4,4'-*o*-BBV.

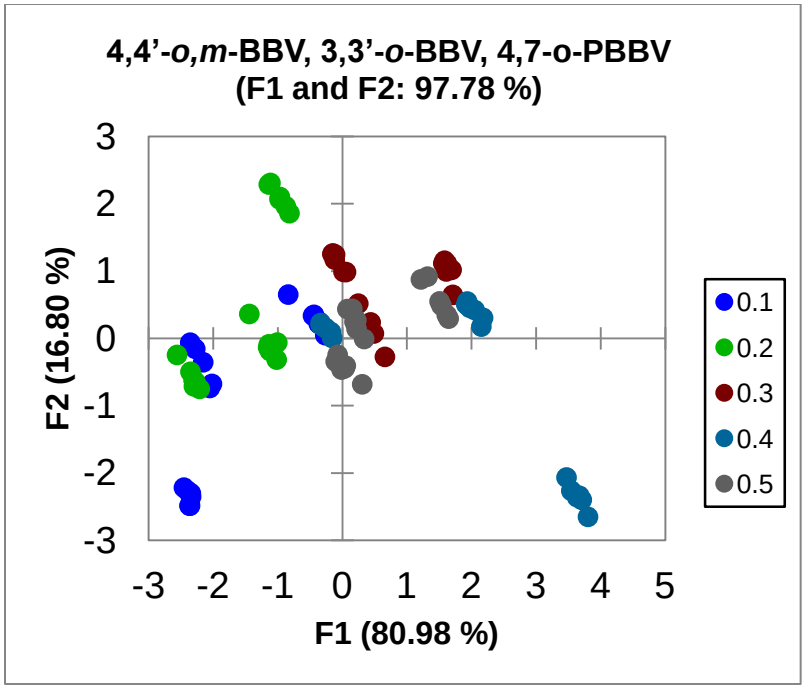

LDA plot (13) of various L/M ratios with the triad array of boronic acid receptors:4,4'-*o,m*-BBV, 3,3'-*o*-BBV, 4,7-*o*-PBBV.

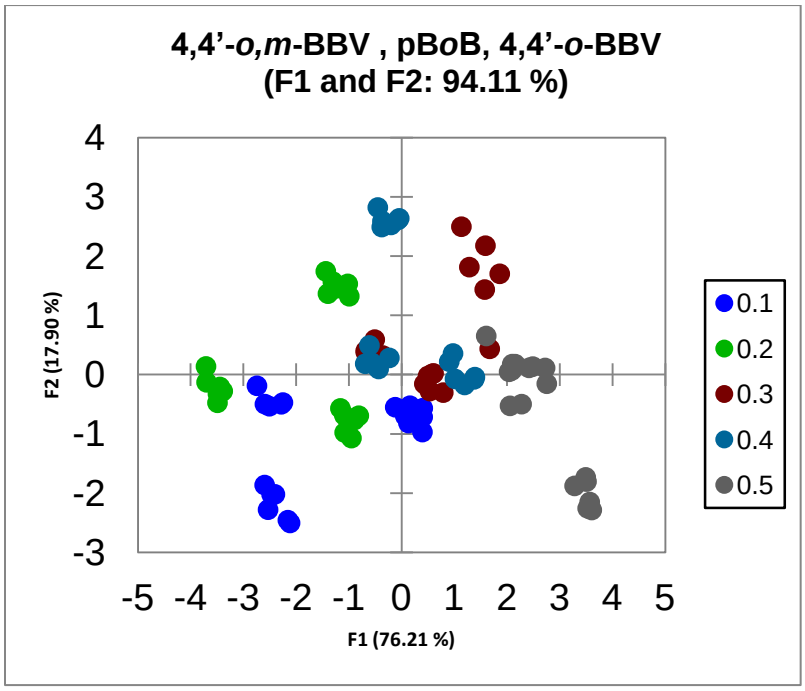

LDA plot (14) of various L/M ratios with the triad array of boronic acid receptors:4,4'-*o,m*-BBV, pB*o*B, 4,4'-*o*-BBV.

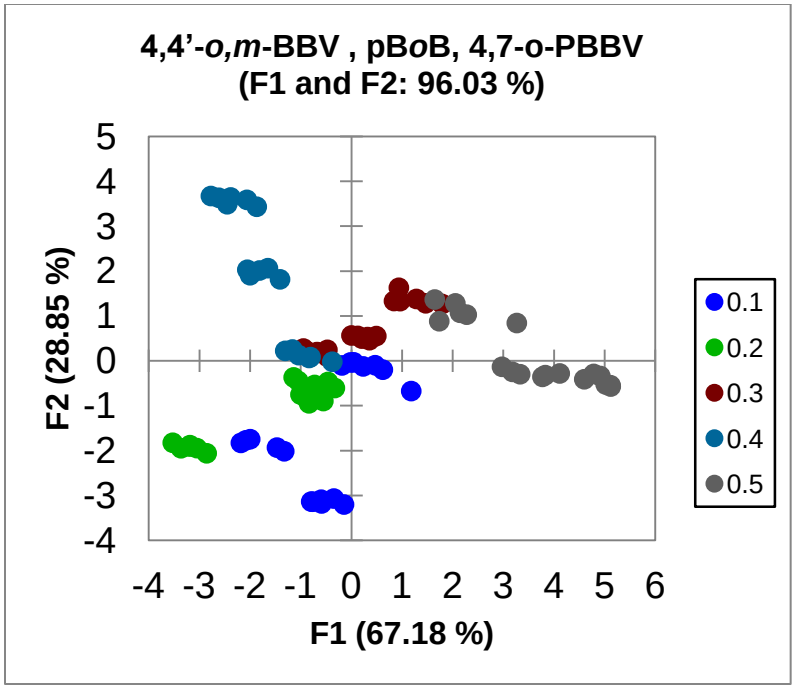

LDA plot (15) of various L/M ratios with the triad array of boronic acid receptors: 3,4'-*o,m*-BBV, pBoB, 4,7-*o*-PBBV.

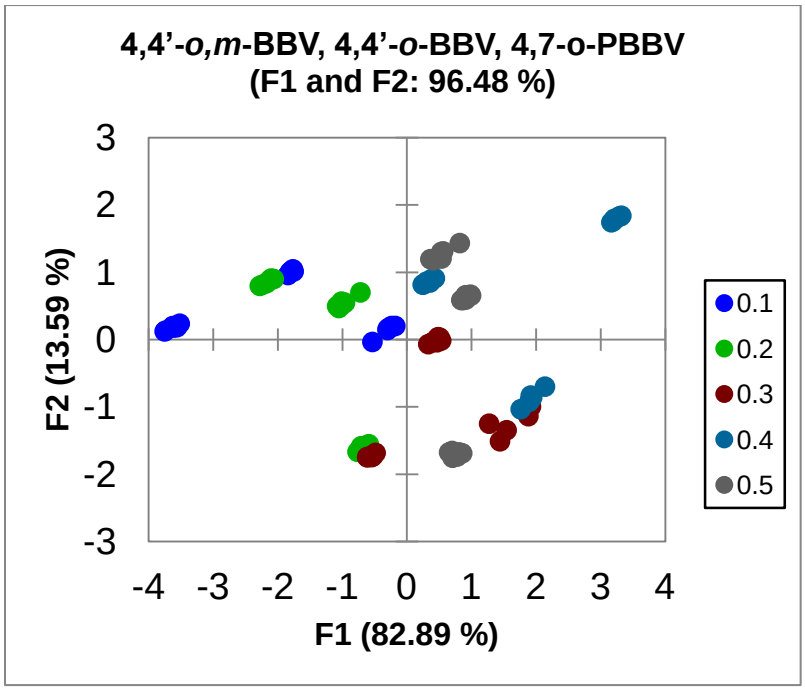

LDA plot (16) of various L/M ratios with the triad array of boronic acid receptors: 4,4'-*o,m*-BBV, 4,4'-*o*-BBV, 4,7-*o*-PBBV.

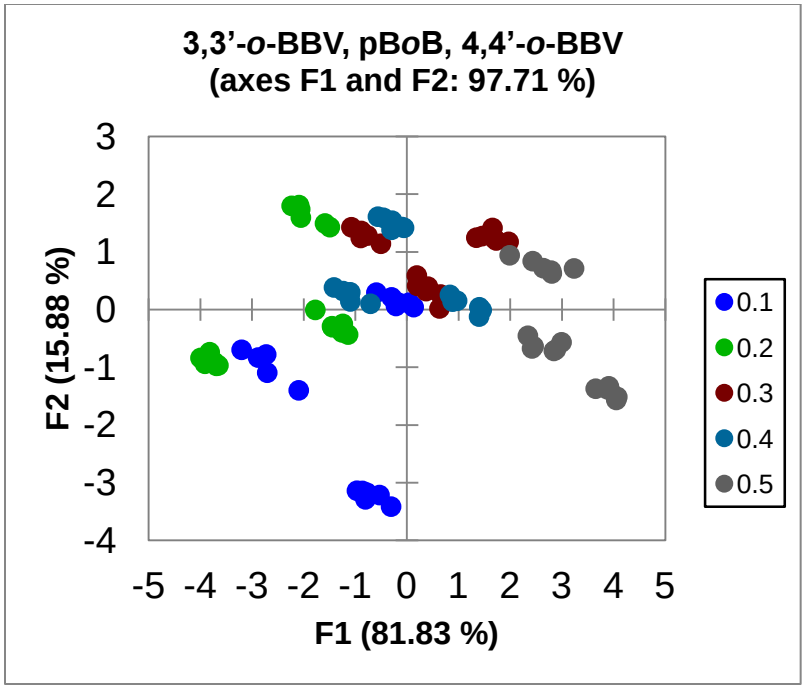

LDA plot (17) of various L/M ratios with the triad array of boronic acid receptors: 3,3'-*o*-BBV, pB*o*B, 4,4'-*o*-BBV.

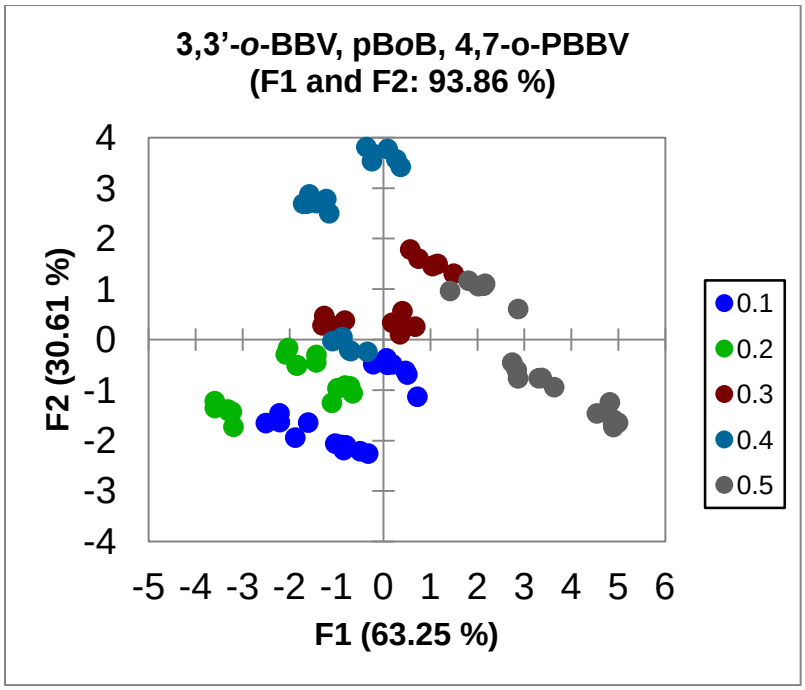

LDA plot (18) of various L/M ratios with the triad array of boronic acid receptors: 3,3'-*o*-BBV, pB*o*B, 4,7-*o*-PBBV.

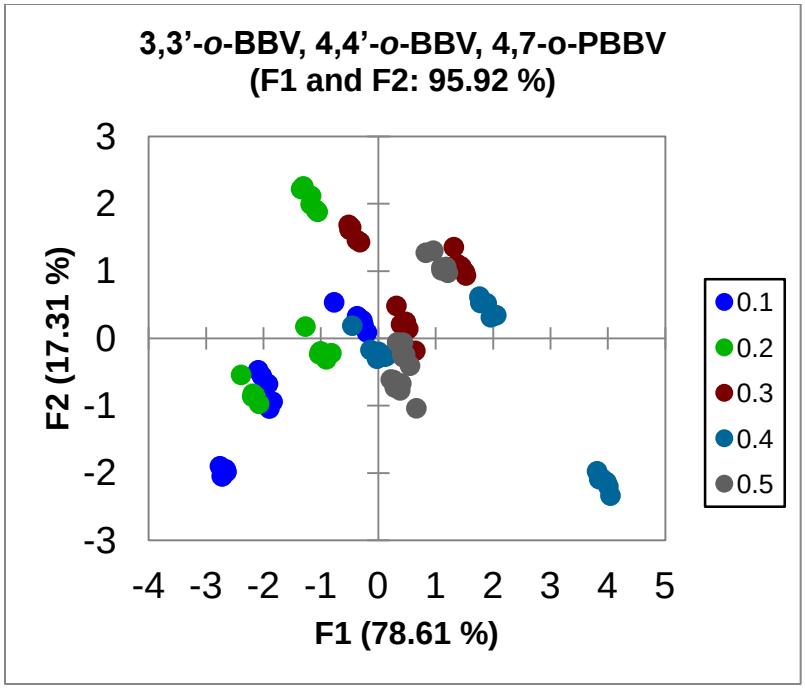

LDA plot (19) of various L/M ratios with the triad array of boronic acid receptors: 3,3'-*o*-BBV, 4,4'-*o*-BBV,4,7-o-PBBV.

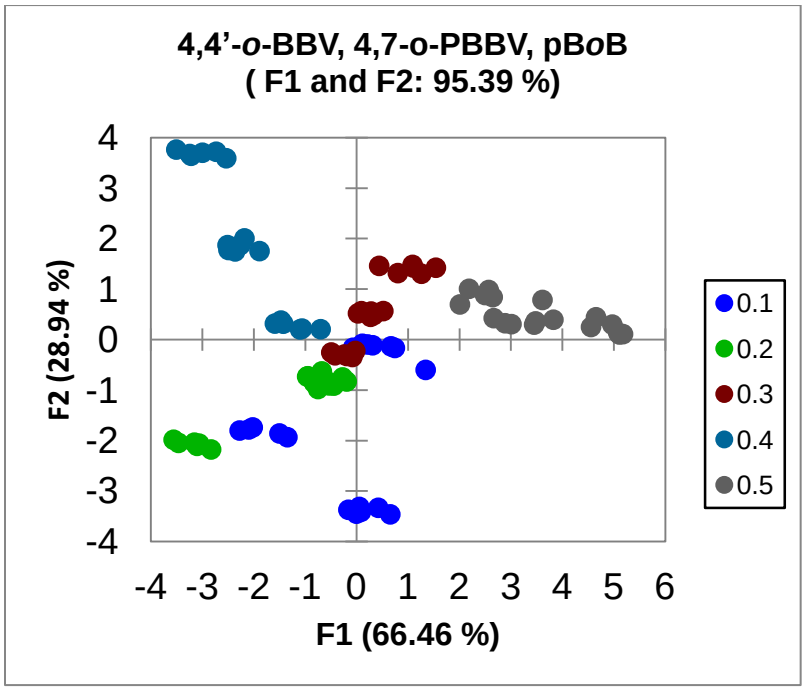

LDA plot (20) of various L/M ratios with the triad array of boronic acid receptors:4,4'-*o*-BBV, 4,7-o-PBBV, pB*o*B.

Bibliography

1) Abdelakher, M.; Hamilton, J. K.; Smith, F., "The reduction of sugars with sodium borohydride." *J. Am. Chem. Soc.***1951**, *73*, 4691-4692.

2) Abouissa, H.; Dwivedi, C.; Curley, R. W.; Kirkpatrick, R.; Koolemansbeynen, A.; Engineer, F. N.; Humphries, K. A.; Elmasry, W.; Webb, T. E., "Basis for the antitumor and chemopreventive activities of glucarate and the glucarate-retinoid combination." *Anticancer Res.* **1993**, *13*, 395-399.

3) Akay, S.; Yang, W. Q.; Wang, J. F.; Lin, L.; Wang, B. H., "Synthesis and evaluation of dual wavelength fluorescent benzo b thiophene boronic acid derivatives for sugar sensing." *Chem. Biol. & Drug Design* **2007**, *70*, 279-289.

4) Alivisatos, P., "The use of nanocrystals in biological detection." *Nat. Biotechnol.* **2004**, *22*, 47-52.

5) Andersen, K. E.; Bjergegaard, C.; Sorensen, H., "Analysis of reducing carbohydrates by reductive tryptamine derivatization prior to micellar electrokinetic capillary chromatography." *J. Agri. Food Chem.* **2003**, *51*, 7234-7239.

6) Anslyn, E. V., Supramolecular Analytical Chemistry. *J. Org. Chem.* **2007**, *72*, 687-699.

7) Anslyn, E. V., "The Lock and Key Principle. The state of the Art - 100 Years on edited by J.-P. Behr." Angew. *Chem., Int. Ed. Engl.* **1995**, *34*, 2293.

8) Anumula, K. R., "Quantitative-determination of monosaccharides in glycoproteins by high-performance liquid-chromatography with highly sensitive fluorescence detection." *Anal. Biochem.* **1994**, *220*, 275-283.

9) Anumula, K. R., "Single tag for total carbohydrate analysis." *Anal. Biochem.* **2014**, *457*, 31-37.

10) Arimori, S.; Murakami, H.; Takeuchi, M.; Shinkai, S., "Sugar-Controlled Association and Photoinduced Electron-Transfer in Boronic-Acid-Appended Porphyrins." *J. Chem. Soc., Chem. Commun.*, **1995**, 961-962.

11) Arrieta, M. C.; Bistritz, L.; Meddings, J. B., "Alterations in intestinal permeability." *Gut* **2006**, 55.

12) Aslan, K.; Zhang, J.; Lakowicz, J. R.; Geddes, C. D., “Saccharide sensing using gold and silver nanoparticles - A review.” *J. Fluores.* **2004**, *14*, 391-400.

13) Badugu, R.; Lakowicz, J. R.; Geddes, C. D., “Fluorescence sensors for monosaccharides based on the 6-methylquinolinium nucleus and boronic acid moiety: potential application to ophthalmic diagnostics.” *Talanta* **2005**, *65*, 762-768.

14) Bajaj, A.; Miranda, O. R.; Phillips, R.; Kim, I.-B.; Jerry, D. J.; Bunz, U. H. F.; Rotello, V. M., “Array-Based Sensing of Normal, Cancerous, and Metastatic Cells Using Conjugated Fluorescent Polymers.” *J. Am. Chem. Soc.* **2010**, *132*, 1018-1022.

15) Bao, L. G.; Ma, S. W.; van Huystee, R. B., “Glycosylation of the cationic peanut peroxidase gene expressed in transgenic tobacco.” *Plant Sci.* **2000**, *156*, 55-63.

16) Bard, A. J.; Ledwith, A.; Shine, H. J., “Formation, properties and reactions of cation radicals in solution.” *Adv. Phys. Org. Chem.* **1976**, *13*, 155-278.

17) Beck, E.; Hopf, H., “7 - Branched-chain Sugars and Sugar Alcohols. In Methods in Plant Biochemistry,” P.M, D. E. Y., Ed. Academic Press: **1990**; Vol. 2, 235-289.

18) Berezenko, S.; Sturgeon, R. J., “The enzymatic determination of D-mannitol with dehydrogenase from agaricus-bisporus.” *Carbohydr. Res.* **1991**, *216*, 505-509.

19) Bhat, V. T.; Caniard, A. M.; Luksch, T.; Brenk, R.; Campopiano, D. J.; Greaney, M. F., “Nucleophilic catalysis of acylhydrazone equilibration for protein-directed dynamic covalent chemistry.” *Nat. Chem.* **2010**, *2*, 490-497.

20) Bidon, N.; Brichory, F.; Bourguet, P.; Le Pennec, J.-P.; Dazord, L., “Galectin-8: a complex sub-family of galectins.” *Int. J. Mol. Med.* **2001**, *8*, 245-250.

21) Bieleski, R. L., Loewus, F. A.; Tanner, W., “Sugar Alcohols. In Plant Carbohydrates I: Intracellular Carbohydrates,” Eds. Springer Berlin Heidelberg: Berlin, Heidelberg, **1982**; 158-192.

22) Bird, C. L.; Kuhn, A. T., “Electrochemistry of the Viologens.” *Chem. Soc. Rev.* **1981**, *10*, 49-82.

23) Bjarnason, I.; Macpherson, A.; Hollander, D., “Intestinal permeability-an overview.” *Gastroenterology* **1995**, *108*, 1566-1581.

24) Blumenthal, H. J.; Lucuta, V. L.; Blumenthal, D. C., "Specific enzymatic assay for D-glucarate in human serum." *Anal. Biochem.* **1990**, *185*, 286-293.

25) Boul, P. J.; Reutenauer, P.; Lehn, J. M., "Reversible Diels-Alder reactions for the generation of dynamic combinatorial libraries." *Org. Lett.* **2005**, *7*, 15-18.

26) Boulton, R., "Relationships Between Total Acidity, Titratable Acidity and pH in Wine." *Am. J. Enol. Viticul.* **1980**, *31*, 76-80.

27) Broer, S., "Amino acid transport across mammalian intestinal and renal epithelia." *Physiol. Rev.* **2008**, *88*, 249-286.

28) Bull, S. D.; Davidson, M. G.; Van den Elsen, J. M. H.; Fossey, J. S.; Jenkins, A. T. A.; Jiang, Y.-B.; Kubo, Y.; Marken, F.; Sakurai, K.; Zhao, J.; James, T. D., "Exploiting the Reversible Covalent Bonding of Boronic Acids: Recognition, Sensing, and Assembly." *Acc. Chem. Res.* **2013**, *46*, 312-326.

29) Bull, S. D.; Davidson, M. G.; Van den Elsen, J. M. H.; Fossey, J. S.; Jenkins, A. T. A.; Jiang, Y.-B.; Kubo, Y.; Marken, F.; Sakurai, K.; Zhao, J.; James, T. D., "Exploiting the Reversible Covalent Bonding of Boronic Acids: Recognition, Sensing, and Assembly." *Acc. Chem. Res.* **2013**, *46*, 312-326.

30) Burgemeister, T.; Grobe-Einsler, R.; Grotstollen, R.; Mannschreck, A.; Wulff, G., "Fast Thermal Breaking and Formation of a B-N Bond in 2-(Aminomethyl) benzeneboronates)." *Chemis. Berich.* **1981**, *114*, 3403-3411.

31) Buryak, A.; Pozdnoukhov, A.; Severin, K., "Pattern-based sensing of nucleotides in aqueous solution with a multicomponent indicator displacement assay." *Chem. Commun.* **2007**, 2366-2368.

32) Buryak, A.; Severin, K., "A chemosensor array for the colorimetric identification of 20 natural amino acids." *J. Am. Chem. Soc.* **2005**, *127*, 3700-3701.

33) Buryak, A.; Severin, K., "An organometallic chemosensor for the sequence-selective detection of histidine- and methionine-containing peptides in water at neutral pH." *Angew. Chem., Int. Ed.* **2004**, *43*, 4771-4774.

34) Buryak, A.; Severin, K., "Dynamic combinatorial libraries of dye complexes as sensors." *Angew. Chem., Int. Ed.* **2005**, *44*, 7935-7938.

35) Cacciapaglia, R.; Di Stefano, S.; Mandolini, L., "Metathesis reaction of formaldehyde acetals: An easy entry into the dynamic covalent chemistry of cyclophane formation." *J. Am. Chem. Soc.* **2005**, *127*, 13666-13671.

36) Camara, J. N.; Suri, J. T.; Cappuccio, F. E.; Wessling, R. A.; Singaram, B., "Boronic acid substituted viologen based optical sugar sensors: modulated quenching with viologen as a method for monosaccharide detection." *Tetrahedron Lett.* **2002**, *43*, 1139-1141.

37) Camilleri, M.; Nadeau, A.; Lamsam, J.; Nord, S. L.; Ryks, M.; Burton, D.; Sweetser, S.; Zinsmeister, A. R.; Singh, R., "Understanding measurements of intestinal permeability in healthy humans with urine lactulose and mannitol excretion." *Neurogastroenterol. Motil.* **2010**, *22*, E15-E26.

38) Cao, H. S.; Heagy, M. D., "Fluorescent chemosensors for carbohydrates: A decade's worth of bright spies for saccharides in review." *J. Fluores.* **2004**, *14*, 569-584.

39) Cappuccio, F. E.; Suri, J. T.; Cordes, D. B.; Wessling, R. A.; Singaram, B., "Evaluation of Pyranine Derivatives in Boronic Acid Based Saccharide Sensing: Significance of Charge Interaction Between Dye and Quencher in Solution and Hydrogel." *J. Fluoresc.* **2004**, *14*, 521-533.

40) Chen, L. H.; McBranch, D. W.; Wang, H. L.; Helgeson, R.; Wudl, F.; Whitten, D. G., "Highly sensitive biological and chemical sensors based on reversible fluorescence quenching in a conjugated polymer." *Proc. Nalt. Acad. Sci.U.S.A.***1999**, *96*, 12287-12292.

41) Chen, W. B.; Elfeky, S. A.; Nonne, Y.; Male, L.; Ahmed, K.; Amiable, C.; Axe, P.; Yamada, S.; James, T. D.; Bull, S. D.; Fossey, J. S., "A pyridinium cation-pi interaction sensor for the fluorescent detection of alkyl halides." *Chem. Commun.* **2011**, *47*, 253-255.

42) Chen, W.; Li, Q.; Zheng, W.; Hu, F.; Zhang, G.; Wang, Z.; Zhang, D.; Jiang, X., "Identification of Bacteria in Water by a Fluorescent Array." *Angew. Chem., Int. Ed.* **2014**, *53*, 13734-13739.

43) Chen, Y.; Xianyu, Y.; Jiang, X., "Surface Modification of Gold Nanoparticles with Small Molecules for Biochemical Analysis." *Acc. Chem. Res.* **2017**, *50*, 310-319.

44) Cheng, Y.; Ni, N.; Yang, W.; Wang, B., "A New Class of Fluorescent Boronic Acids That Have Extraordinarily High Affinities for Diols in Aqueous Solution at Physiological pH." *Chem.-a Eur. J.* **2010**, *16*, 13528-13538.

45) Constable, E. C.; Morris, D.; Carr, S., “Functionalised 3,3 '-bipyridines - a new class of dinucleating ligands.” *New J. Chem.* **1998**, *22*, 287-294.

46) Corbett, P. T.; Leclaire, J.; Vial, L.; West, K. R.; Wietor, J. L.; Sanders, J. K. M.; Otto, S., “Dynamic combinatorial chemistry.” *Chem. Rev.* **2006**, *106*, 3652-3711.

47) Cordes, D. B.; Gamsey, S.; Sharrett, Z.; Miller, A.; Thoniyot, P.; Wessling, R. A.; Singaram, B., “The interaction of boronic acid-substituted viologens with pyranine: The effects of quencher charge on fluorescence quenching and glucose response.” *Langmuir* **2005**, *21*, 6540-6547.

48) Cordes, D. B.; Miller, A.; Gamsey, S.; Sharrett, Z.; Thoniyot, P.; Wessling, R.; Singaram, B., “Optical glucose detection across the visible spectrum using anionic fluorescent dyes and a viologen quencher in a two-component saccharide sensing system.” *Org. Biomol. Chem.* **2005**, *3*, 1708-1713.

49) Cordes, D. B.; Singaram, B., “A unique, two-component sensing system for fluorescence detection of glucose and other carbohydrates.” *Pure Appl. Chem.* **2012**, *84*, 2183-2202.

50) da Cunha, A. L.; de Oliveira, L. G.; Maia, L. F.; de Oliveira, L. F. C.; Michelacci, Y. M.; de Aguiar, J. A. K., “Pharmaceutical grade chondroitin sulfate: Structural analysis and identification of contaminants in different commercial preparations.” *Carbohydr. Poly.* **2015**, *134*, 300-308.

51) De Borba, E. B.; Amaral, C. L. C.; Politi, M. J.; Villalobos, R.; Baptista, M. S., “Photophysical and Photochemical Properties of Pyranine/Methyl Viologen Complexes in Solution and in Supramolecular Aggregates: A Switchable Complex.” *Langmuir* **2000**, *16*, 5900-5907.

52) de Silva, A. P.; Gunaratne, H. Q. N.; Gunnlaugsson, T.; Nieuwenhuizen, M., “Fluorescent switches with high selectivity towards sodium ions: Correlation of ion-induced conformation switching with fluorescence function.” *Chem. Commun.***1996**, 1967-1968.

53) Denno, D. M.; VanBuskirk, K.; Nelson, Z. C.; Musser, C. A.; Burgess, D. C. H.; Tarr, P. I., “Use of the Lactulose to Mannitol Ratio to Evaluate Childhood Environmental Enteric Dysfunction: A Systematic Review.” *Clin. Infect. Dis.* **2014**, *59*, S213-S219.

54) Di Cesare, N.; Lakowicz, J. R., "Wavelength-ratiometric probes for saccharides based on donor-acceptor diphenylpolyenes." *J. Photochem. and Photobiol. a-Chem.* **2001**, *143*, 39-47.

55) Diaz de Grenu, B.; Moreno, D.; Torroba, T.; Berg, A.; Gunnars, J.; Nilsson, T.; Nyman, R.; Persson, M.; Pettersson, J.; Eklind, I.; Wasterby, P., "Fluorescent Discrimination between Traces of Chemical Warfare Agents and Their Mimics." *J. Am. Chem. Soc.* **2014**, *136*, 4125-4128.

56) DiCesare, N.; Lakowicz, J. R., "Spectral properties of fluorophores combining the boronic acid group with electron donor or withdrawing groups. Implication in the development of fluorescence probes for saccharides." *J. Phys. Chem. A* **2001**, *105*, 6834-6840.

57) DiCesare, N.; Pinto, M. R.; Schanze, K. S.; Lakowicz, J. R., "Saccharide detection based on the amplified fluorescence quenching of a water-soluble poly(phenylene ethylene) by a boronic acid functionalized benzyl viologen derivative." *Langmuir* **2002**, *18*, 7785-7787.

58) Dickert, F. L., "The Viologens. Physicochemical properties, synthesis and applications of the salts of 4,4'-bipyridine." *Angew. Chem., Int. Ed.* **1999**, *38*, 2456-2457.

59) Diehl, K. L.; Ivy, M. A.; Rabidoux, S.; Petry, S. M.; Mueller, G.; Anslyn, E. V., "Differential sensing for the regio- and stereoselective identification and quantitation of glycerides." *Proc.Nalt. Acad. Sci.U.S.A.* **2015**, *112*, E3977-E3986.

60) Djanashvili, K.; Frullano, L.; Peters, J. A., "Molecular recognition of sialic acid end groups by phenylboronates." *Chem.-a Eur. J.* **2005**, *11*, 4010-4018.

61) Dwivedi, C.; Heck, W. J.; Downie, A. A.; Larroya, S.; Webb, T. E., "Effect of calcium glucarate on beta-glucuronidase activity and glucarate content of certain vegetables and fruits." *Biochem. Med. Metabol. Biol.* **1990**, *43*, 83-92.

62) Eli, M.; Li, D. S.; Zhang, W. W.; Kong, B.; Du, C. S.; Wumar, M.; Mamtimin, B.; Sheyhidin, I.; Hasim, A., "Decreased blood riboflavin levels are correlated with defective expression of RFT2 gene in gastric cancer." *World J. Gastroenterol.* **2012**, *18*, 3112-3118.

63) Ellis, G. A.; Palte, M. J.; Raines, R. T., "Boronate-Mediated Biologic Delivery." *J. Am. Chem. Soc.* **2012**, *134*, 3631-3634.

64) Evans, W. J.; McCourtney, E. J.; Carney, W. B., “A comparative analysis of the interaction of borate ion with various polyols.” *Anal. Biochem.* **1979**, *95*, 383-386.

65) Farhadi, A.; Keshavarzian, A.; Holmes, E. W.; Fields, J.; Zhang, L.; Banan, A., “Gas chromatographic method for detection of urinary sucralose: application to the assessment of intestinal permeability.” *J. Chromat. B-Anal. Technol. Biomed. Life Sci.* **2003**, 784, 145-154.

66) Farquhar, M. G.; Palade, G. E., “Junctional complexes in various epithelial.” *J. Cell Biol.* **1963**, *17*, 375.

67) Fenton, H. J. H.; Gostling, M., “The action of hydrogen bromide on carbohydrates.” *J. Am. Chem. Soc.***1901**, *79*, 361-365.

68) Ferraris, R. P.; Diamond, J., “Regulation of intestinal sugar transport.” *Physiol. Rev.* **1997**, *77*, 257-302.

69) Fihn, B. M.; Sjoqvist, A.; Jodal, M., “Permeability of the rat small intestinal epithelium along the villus-crypt axis: Effects of glucose transport.” *Gastroenterology* **2000**, *119*, 1029-1036.

70) Folmer-Andersen, J. F.; Kitamura, M.; Anslyn, E. V., “Pattern-based discrimination of enantiomeric and structurally similar amino acids: An optical mimic of the mammalian taste response.” *J. Am. Chem. Soc.* **2006**, *128*, 5652-5653.

71) Frank, J. M.; Vavilov, S. I., “Effective spheres in the extinction process in fluorescent liquids.” *Z. Phys.* **1931**, *69*, 100-10.

72) Fuchs, M.; Hoekstra, J. B. L.; Mudde, A. H., “Glucose and cardiovascular risk.” *Nether. J. Med.* **2002**, *60*, 192-199.

73) Fujieda, T.; Kitamura, Y.; Yamasaki, H.; Furuishi, A.; Motobayashi, K., “An experimental study on whole paddy saccharification and fermentation for rice ethanol production.” *Biomass Bioener.* **2012**, *44*, 135-141.

74) Fukasawa, Y.; Tateno, O.; Hagiwara, Y.; Hirose, D.; Osono, T., “Fungal succession and decomposition of beech cupule litter.” *Ecol. Res.* **2012**, *27*, 735-743.

75) Fukuda, M., “Carbohydrate-dependent cell adhesion.” *Biorg. Med. Chem.* **1995**, *3*, 207-215.

76) Gamsey, S.; Baxter, N. A.; Sharrett, Z.; Cordes, D. B.; Olmstead, M. M.; Wessling, R. A.; Singaram, B., "The effect of boronic acid-positioning in an optical glucose-sensing ensemble." *Tetrahedron* **2006**, *62*, 6321-6331.

77) Gamsey, S.; Miller, A.; Olmstead, M. M.; Beavers, C. M.; Hirayama, L. C.; Pradhan, S.; Wessling, R. A.; Singaram, B., "Boronic acid-based bipyridinium salts as tunable receptors for monosaccharides and alpha-hydroxycarboxylates." *J. Am. Chem. Soc.* **2007**, *129*, 1278-1286.

78) Gamsey, S.; Suri, J. T.; Wessling, R. A.; Singaram, B., "Continuous Glucose Detection Using Boronic Acid-Substituted Viologens in Fluorescent Hydrogels: Linker Effects and Extension to Fiber Optics." *Langmuir* **2006**, *22*, 9067-9074.

79) Gao, X. M.; Zhang, Y. L.; Wang, B. H., "New boronic acid fluorescent reporter compounds. 2. A naphthalene-based on-off sensor functional at physiological pH." *Org. Lett.* **2003**, *5*, 4615-4618.

80) Gaylord, B. S.; Wang, S. J.; Heeger, A. J.; Bazan, G. C., "Water-soluble conjugated oligomers: Effect of chain length and aggregation on photoluminescence-quenching efficiencies." *J. Am. Chem. Soc.* **2001**, *123*, 6417-6418.

81) Gerova, V. A.; Stoynov, S. G.; Katsarov, D. S.; Svinarov, D. A., "Increased intestinal permeability in inflammatory bowel diseases assessed by iohexol test." *World J. Gastroenterology* **2011**, *17*, 2211-2215.

82) Globisch, D.; Moreno, A. Y.; Hixon, M. S.; Nunes, A. A. K.; Denery, J. R.; Specht, S.; Hoerauf, A.; Janda, K. D., "Onchocerca volvulus-neurotransmitter tyramine is a biomarker for river blindness." *Proc. Nalt. Acad. Sci. U.S.A.* **2013**, *110*, 4218-4223.

83) Golovchenko, V. V.; Khramova, D. S.; Ovodova, R. G.; Shashkov, A. S.; Ovodov, Y. S., "Structure of pectic polysaccharides isolated from onion Allium cepa L. using a simulated gastric medium and their effect on intestinal absorption." *Food Chem.* **2012**, *134*, 1813-1822.

84) Gray, C. W.; Houston, T. A., "Boronic acid receptors for alpha-hydroxycarboxylates: High affinity of Shinkai's glucose receptor for tartrate." *J. Org. Chem.* **2002**, *67*, 5426-5428.

85) Greene, N. T.; Shimizu, K. D., “Colorimetric molecularly imprinted polymer sensor array using dye displacement.” *J. Am. Chem. Soc.* **2005**, *127*, 5695-5700.

86) Grill, E.; Huber, C.; Oefner, P.; Vorndran, A.; Bonn, G., “Capillary zone of electrophoresis of p-aminobenzoic acid-derivatives of aldoses, ketoses, and uronic-acids.” *Electrophoresis* **1993**, *14*, 1004-1010.

87) Groschwitz, K. R.; Hogan, S. P., “Intestinal barrier function: Molecular regulation and disease pathogenesis.*” J. Allergy Clin. Immunol.* **2009**, *124*, 3-20.

88) Hansen, J. S.; Christensen, J. B., “Recent Advances in Fluorescent Arylboronic Acids for Glucose Sensing.” *Biosensors* **2012**, *3*, 400-418.

89) Heerdt, A. S.; Young, C. W.; Borgen, P. I., “Calcium glucarate as a chemopreventive agent in breast-cancer.” *Israel J. Med. Sci.* **1995**, *31*, 101-105.

90) Honda, S.; Akao, E.; Suzuki, S.; Okuda, M.; Kakehi, K.; Nakamura, J., “High-performance liquid chromatography of reducing carbohydrates as strongly ultraviolet-absorbing and electrochemically sensitive 1-phenyl-3-methyl-5-pyrazolone derivatives.” *Anal. Biochem.***1989**, *180*, 351-357.

91) Hosseinzadeh, R.; Mohadjerani, M.; Pooryousef, M., “A new selective fluorene-based fluorescent internal charge transfer (ICT) sensor for sugar alcohols in aqueous solution.” *Anal. Bioanal. Chem.* **2016**, *408*, 1901-1908.

92) Huang, Y. J.; Ouyang, W. J.; Wu, X.; Li, Z.; Fossey, J. S.; James, T. D.; Jiang, Y. B., “Glucose Sensing via Aggregation and the Use of "Knock-Out" Binding To Improve Selectivity.” *J. Am. Chem. Soc.***2013**, *135*, 1700-1703.

93) Hui, H. K.; Soonkap, H.; Bankert, C. S. “Optical-fiber pH microsensor and method of manufacture.” EP481740A2, **1992**.

94) James, T. D.; Sandanayake, K. R. A. S.; Shinkai, S., “A glucose-specific molecular fluorescence sensor.” *Angew. Chem.* **1994**, *106*, 2287-9.

95) James, T. D.; Sandanayake, K.; Iguchi, R.; Shinkai, S., “Novel Saccharide-Photoinduced Electron-Transfer Sensors Based on the Interaction of Boronic Acid and Amine.” *J. Am. Chem. Soc.* **1995**, *117*, 8982-8987.

96) James, T. D.; Sandanayake, K.; Shinkai, S., “Saccharide sensing with molecular receptors based on boronic acid.” *Angew. Chem.-Intl. Ed. Engl.* **1996**, *35*, 1911-1922.

97) James, T. D.; Shinkai, S., "Artificial receptors as chemosensors for carbohydrates. Host-Guest Chemistry: Mimetic Approaches to Study Carbohydrate Recognition" **2002**, *218*, 159-200.

98) Jelinek, R.; Kolusheva, S., "Carbohydrate biosensors." *Chem. Rev.* **2004**, *104*, 5987-6015.

99) Jianzhang, Z.; James, T. D., "Chemoselective and enantioselective fluorescent recognition of sugar alcohols by a bisboronic acid receptor." *J. Mat. Chem.* **2005**, *15*, 2896-901.

100) Jin, S.; Zhu, C. Y.; Cheng, Y. F.; Li, M. Y.; Wang, B. H., "Synthesis and carbohydrate binding studies of fluorescent alpha-amidoboronic acids and the corresponding bisboronic acids." *Bioorg.Med. Chem.* **2010**, *18*, 1449-1455.

101) Jurs, P. C.; Bakken, G. A.; McClelland, H. E., "Computational methods for the analysis of chemical sensor array data from volatile analytes." *Chem. Rev.* **2000**, *100*, 2649-2678.

102) Kim, I.-B.; Han, M. H.; Phillips, R. L.; Samanta, B.; Rotello, V. M.; Zhang, Z. J.; Bunz, U. H. F., "Nano-Conjugate Fluorescence Probe for the Discrimination of Phosphate and Pyrophosphate." *Chem.-a Eur. J.* **2009**, *15*, 449-456.

103) Kim, K. K.; Escobedo, J. O.; St Luce, N. N.; Rusin, O.; Wong, D.; Strongin, R. M., "Postcolumn HPLC detection of mono- and oligosaccharides with a chemosensor." *Org. Lett.* **2003**, *5*, 5007-5010.

104) Kitamura, M.; Shabbir, S. H.; Anslyn, E. V., "Guidelines for Pattern Recognition Using Differential Receptors and Indicator Displacement Assays." *J. Org. Chem.* **2009**, *74*, 4479-4489.

105) Kobata, A., "Glycobiology - An expanding research area in carbohydrate-chemistry." *Acc. Chem. Res.* **1993**, *26*, 319-324.

106) Koehne, J. E.; Chen, H.; Cassell, A.; Liu, G.-y.; Li, J.; Meyyappan, M., "Arrays of carbon nanofibers as a platform for biosensing at the molecular level and for tissue engineering and implantation." *Bio-Med. Mat. Eng.* **2009**, *19*, 35-43.

107) Kondo, K.; Shiomi, Y.; Saisho, M.; Harada, T.; Shinkai, S., "Specific complexation of disaccarides with diphenyl-3,3'-diboronic acid that can be detected by circular-dichroism." *Tetrahedron* **1992**, *48*, 8239-8252.

108) Kuivila, H. G.; Keough, A. H.; Soboczenski, E. J., "Areneboronates from diols and polyols." *J. Org. Chem.* **1954**, *19*, 780-783.

109) Lacina, K.; Skladal, P.; James, T. D., "Boronic acids for sensing and other applications - a mini-review of papers published in 2013." *Chem. Centl. J.* **2014**, *8*.

110) Lakowicz, J. R., "Principles of Fluorescence Spectroscopy." 3rd ed.; Springer: New York, **2006**; 954.

111) Lamari, F.; Theocharis, A.; Hjerpe, A.; Karamanos, N. K., "Ultrasensitive capillary electrophoresis of sulfated disaccharides in chondroitin dermatan sulfates by laser-induced fluorescence after derivatization with 2-aminoacridone." *J. Chromat. B* **1999**, *730*, 129-133.

112) Lattova, E.; Perreault, H., "Labeling saccharides with phenylhydrazine for electrospray and matrix-assisted laser desorption-ionization mass spectrometry." *J.Chromat. B-Anal. Technol. in the Biomed. Life Sci.* **2003**, *79*, 167-179.

113) Lavigne, J. J.; Anslyn, E. V., "Teaching Old Indicators New Tricks: A Colorimetric Chemosensing Ensemble for Tartrate/Malate in Beverages." *Angew. Chem.-Intl. Ed.* **1999**, *38*, 3666-3669.

114) Lee, J. W.; Lee, J. S.; Chang, Y. T., "Colorimetric identification of carbohydrates by a pH Indicator/pH change inducer ensemble." *Angew. Chem., Int. Ed.* **2006**, *45*, 6485-6487.

115) Leung, D.; Folmer-Andersen, J. F.; Lynch, V. M.; Anslyn, E. V., "Using enantioselective indicator displacement assays to determine the enantiomeric excess of alpha-amino acids." *J. Am. Chem. Soc.* **2008**, *130*, 12318-12327.

116) Lewis, D. H.; Smith, D. C., "Sugar alcohols (polyols) in fungi and green plants in distribution physiology and metabolism." *New Phyto.* **1967**, *66*, 143.

117) Li, H.; Bazan, G. C., "Conjugated Oligoelectrolyte/ssDNA Aggregates: Self-Assembled Multicomponent Chromophores for Protein Discrimination." *Adv. Mat.* **2009**, *21*, 964.

118) Liang, X.; James, T. D.; Zhao, J., "6,6 '-Bis-substituted BINOL boronic acids as enantio selective and chemoselective fluorescent chemosensors for D-sorbitol." *Tetrahedron* **2008**, *64*, 1309-1315.

119) Lim, S. H.; Musto, C. J.; Park, E.; Zhong, W.; Suslick, K. S., "A Colorimetric Sensor Array for Detection and Identification of Sugars." *Org. Lett.* **2008**, *10*, 4405-4408.

120) Liu, J. W.; Lu, Y., "Colorimetric biosensors based on DNAzyme-assembled gold nanoparticles." *J. Fluores.* **2004**, *14*, 343-354.

121) Liu, S.; Bai, H.; Sun, Q.; Zhang, W.; Qian, J., "Naphthalimide-based fluorescent photoinduced electron transfer sensors for saccharides." *RSC Adv.* **2015**, *5*, 2837-2843.

122) Lorand, E. J.; Edwards, E. I., "Para-methylbenzyl hydroperoxide." *J. Am. Chem. Soc.* **1955**, *77*, 4035-4037.

123) Lorand, J. P.; Edwards, J. O., "Polyol complexes and structure of the bezeneboronate ion." *J. Org. Chem.* **1959**, *24*, 769-774.

124) Lunn, P. G.; Northrop, C. A.; Northrop, A. J., "Automated enzymatic assay for the determination of intestinal permeability probes in urine. 2. Mannitol." *Clin. Chim. Acta* **1989**, *183*, 163-170.

125) Luo, X. L.; Morrin, A.; Killard, A. J.; Smyth, M. R., "Application of nanoparticles in electrochemical sensors and biosensors." *Electroanal.* **2006**, *18*, 319-326.

126) McOmber, M. E.; Ou, C.-N.; Shulman, R. J., "Effects of Timing, Sex, and Age on Site-specific Gastrointestinal Permeability Testing in Children and Adults." *J. Pediat. Gastroenterol. Nutrit.* **2010**, *50*, 269-275.

127) McPhie, P., "Principles of Fluorescence Spectroscopy," Second ed. Joseph R. Lakowicz. *Anal. Biochem.* **2000**, *287*, 353-354.

128) McShane, M. J., "Potential for glucose monitoring with nanoengineered fluorescent biosensors." *Diabetes Technol. Ther.* **2002**, *4*, 533-538.

129) Meddings, J. B.; Gibbons, I., "Discrimination of site-specific alterations in gastrointestinal permeability in the rat." *Gastroenterology* **1998**, *114*, 83-92.

130) Meddings, J. B.; Jarand, J.; Urbanski, S. J.; Hardin, J.; Gall, D. G., "Increased gastrointestinal permeability is an early lesion in the spontaneously diabetic BB rat." *Am. J. Physiol. Gastrointest. Liver Physiol.***1999**, *276*, G951-G957.

131) Miki, K.; Butler, R.; Moore, D.; Davidson, G., "Rapid and simultaneous quantification of rhamnose, mannitol, and lactulose in urine by HPLC for estimating intestinal permeability in pediatric practice." *Clin. Chem.* **1996**, *42*, 71-75.

132) Miron, C. E.; Petitjean, A., "Sugar Recognition: Designing Artificial Receptors for Applications in Biological Diagnostics and Imaging." *Chembiochem* **2015**, *16*, 365-379.

133) Mohr, G. J.; Werner, T.; Wolfbeis, O. S., "Application of a novel lipophilized fluorescent dye in an optical nitrate sensor." *J. Fluoresc.* **1995**, *5*, 135-8.

134) Mortellaro, M.; DeHennis, A., "Performance characterization of an abiotic and fluorescent-based continuous glucose monitoring system in patients with type 1 diabetes." "Biosens. Bioelectron." **2014**, *61*, 227-231.

135) Musto, C. J.; Suslick, K. S., "Differential sensing of sugars by colorimetric arrays." *Curr. Opinion Chem. Biol.* **2010**, *14*, 758-766.

136) Nagai, Y.; Kobayashi, K.; Toi, H.; Aoyama, Y., "Stabilization of sugar-boronic esters of indolylboronic acid in water via sugar indole interaction-a notable selectivity in oligosaccharides." *Bull. Chem. Soc. Japan* **1993**, 66, 2965-2971.

137) Nakashima, K.; Kido, N., "Fluorescence quenching of 1-pyrenemethanol by methylviologen in polystyrene latex dispersions." *J. Photochem. Photobiol.* **1996**, *64*, 296-302.

138) Nguyen, B. T.; Anslyn, E. V., "Indicator-displacement assays." *Coord. Chem. Rev.* **2006**, *250*, 3118-3127.

139) Noe, C. R.; Freissmuth, J., "Capillary zone electrophoresis of aldose enantiomers-separation after derivatization with S-(-)-1-phenylethylamine." *J.Chromat. A.* **1995**, *704*, 503-512.

140) Norrild, J. C., "An illusive chiral aminoalkylferroceneboronic acid. Structural assignment of a strong 1 [ratio] 1 sorbitol complex and new insight into boronate-polyol interactions." J. Chem. Soc., Perkin Trans. 2 **2001**, 719-726.

141) Norrild, J. C.; Eggert, H., "Boronic acids as fructose sensors. Structure determination of the complexes involved using (1)J(CC) coupling constants." J. *Chem. Soc., Perkin Trans. 2* **1996**, 2583-2588.

142) Norrild, J. C.; Eggert, H., "Evidence for Mono- and Bisdentate Boronate Complexes of Glucose in the Furanose Form. Application of JC-C Coupling Constants as a Structural Probe." *J. Am. Chem. Soc.* **1995**, *117*, 1479-84.

143) Northrop, C. A.; Lunn, P. G.; Behrens, R. H., "Automated enzymatic assay for the determination of intestinal permeability probes in urine.1. Lactulose and lactose." *Clin. Chim. Acta* **1990**, *187*, 79-87.

144) Otto, S.; Furlan, R. L. E.; Sanders, J. K. M., "Dynamic combinatorial libraries of macrocyclic disulfides in water." *J. Am. Chem. Soc.* **2000**, *122*, 12063-12064.

145) Palmer, D. R. J.; Gerit, J. A., "Evolution of enzymatic activities: Multiple pathways for generating and partitioning a common enolic intermediate by glucarate dehydrogenase from Pseudomonas putida." *J. Am. Chem. Soc.* **1996**, *118*, 10323-10324.

146) Persaud, K.; Dodd, G., "Analysis of discrimination mechanisms in the mammalian olfactory system using a model nose." *Nature* **1982**, *299*, 352-355.

147) Peters, J. A., "Interactions between boric acid derivatives and saccharides in aqueous media: Structures and stabilities of resulting esters." *Coord. Chem. Rev.* **2014**, *268*, 1-22.

148) Poirier, F.; Kimber, S., "Cell surface carbohydrates and lectins in early development." *Mol. Hum. Reprod.* **1997**, *3*, 907-918.

149) Rakow, N. A.; Suslick, K. S., "A colorimetric sensor array for odour visualization." *Nature* **2000**, *406*, 710-713.

150) Renard, E., "Monitoring glycemic control: the importance of self-monitoring of blood glucose." *Am. J. of Med.* **2005**, *118*, 12S-19S.

151) Resendez, A.; Abdul Halim, M.; Landhage, C. M.; Hellstrom, P. M.; Singaram, B.; Webb, D.-L., "Rapid small intestinal permeability assay based on riboflavin and lactulose detected by bis-boronic acid appended benzyl viologens." *Clin. Chim. Acta* **2015**, *439*, 115-121.

152) Resendez, A.; Panescu, P.; Zuniga, R.; Banda, I.; Joseph, J.; Webb, D. L.; Singaram, B., "Multiwell Assay for the Analysis of Sugar Gut Permeability Markers: Discrimination of Sugar Alcohols with a Fluorescent Probe Array Based on Boronic Acid Appended Viologens." *Anal. Chem.* **2016**, *88*, 5444-5452.

153) Robbins, G. B.; Upson, F. W., "Some Fully Acetylated Sugar Acids and their Derivatives." *J. Am. Chem. Soc.* **1940**, *62*, 1074-1076.

154) Rochat, S.; Gao, J.; Qian, X.; Zaubitzer, F.; Severin, K., "Cross-Reactive Sensor Arrays for the Detection of Peptides in Aqueous Solution by Fluorescence Spectroscopy." *Chem. Eur. J.* **2010**, *16*, 104-113.

155) Russell, A. P. "Photometric method and means involving dyes for detecting vicinal polyhydroxyl compounds." WO9104488A1, **1991**.

156) Schiller, A.; Vilozny, B.; Wessling, R. A.; Singaram, B., "Recognition of phospho sugars and nucleotides with an array of boronic acid appended bipyridinium salts." *Anal. Chim. Acta* **2008**, *627*, 203-211.

157) Schwaiger, H.; Oefner, P. J.; Huber, C.; Grill, E.; Bonn, G. K., "Capillary zone of electrophoresis and micellar electrokinetic chromatography of 4-aminobenzonitrile carbohydrate derivatives." *Electrophoresis* **1994**, *15*, 941-952.

158) Shabbir, S. H.; Joyce, L. A.; da Cruz, G. M.; Lynch, V. M.; Sorey, S.; Anslyn, E. V., "Pattern-Based Recognition for the Rapid Determination of Identity, Concentration, and Enantiomeric Excess of Subtly Different Threo Diols." *J. Am. Chem. Soc.* **2009**, *131*, 13125-13131.

159) Shabbir, S. H.; Regan, C. J.; Anslyn, E. V., "A general protocol for creating high-throughput screening assays for reaction yield and enantiomeric excess applied to hydrobenzoin." *Proc. Nalt. Acad. Sci.U.S.A.* **2009**, *106*, 10487-10492.

160) Sharrett, Z.; Gamsey, S.; Fat, J.; "Cunningham-Bryant, D.; Wessling, R. A.; Singaram, B., The effect of boronic acid acidity on performance of viologen-based boronic acids in a two-component optical glucose-sensing system." *Tetrahedron Lett.* **2007**, *48*, 5125-5129.

161) Sharrett, Z.; Gamsey, S.; Levine, P.; Cunningham-Bryant, D.; Vilozny, B.; Schiller, A.; Wessling, R. A.; Singaram, B., "Boronic acid-appended bis-viologens as a new family of viologen quenchers for glucose sensing." *Tetrahedron Lett.* **2008**, *49*, 300-304.

162) Shiomi, Y.; Saisho, M.; Tsukagoshi, K.; Shinkai, S., "Specific complexation of glucose with a diphenylmethane-3,3'-diboronic acid derivative: correlation between the absolute configuration of mono- and disaccharides and the circular dichroic-activity of the complex." *J. Chem. Soc., Perkin Trans. 1* **1993**, 2111-17.

163) Smecuol, E.; Bai, J. C.; Vazquez, H.; Kogan, Z.; Cabanne, A.; Niveloni, S.; Pedreira, S.; Boerr, L.; Maurino, E.; Meddings, J. B., "Gastrointestinal permeability in celiac disease." *Gastroenterology* **1997**, *112*, 1129-1136.

164) Springsteen, G.; Wang, B., "A detailed examination of boronic acid-diol complexation." *Tetrahedron* **2002**, *58*, 5291-5300.

165) Stewart, S.; Ivy, M. A.; Anslyn, E. V., "The use of principal component analysis and discriminant analysis in differential sensing routines." *Chem. Soc. Rev.* **2014**, *43*, 70-84.

166) Sturgeon, R. J., "Monosaccharides. In Methods in Plant Biochemistry," P.M, D. E. Y., Ed. Academic Press: **1990**; vol. *2*, 1-37.

167) Sturgeon, R. J., "A reinvestigation of the borohydride reduction of carbohydrates." *Carbohydr. Res.* **1992**, *227*, 375-377.

168) Subramanian, V. S.; Subramanya, S. B.; Rapp, L.; Marchant, J. S.; Ma, T. Y.; Said, H. M., "Differential expression of human riboflavin transporters -1, -2, and -3 in polarized epithelia: A key role for hRFT-2 in intestinal riboflavin uptake." *Biochim. Biophys. Acta, Biomembr.* **2011**, *1808*, 3016-3021.

169) Suenaga, H.; Mikami, M.; Sandanayake, K.; Shinkai, S., "Screening of fluorescent boronic acids for sugar sensing which show a large fluorescence change." *Tetrahedron Lett.* **1995**, *36*, 4825-4828.

170) Summers, L. A. "In Chemical constitution and activity of bipyridinium herbicides, Pergamon:" **1979**; 244-7.

171) Summers, L. A., "The Bipyridines. In Advances in Heterocyclic Chemistry," Alan, R. K., Ed. Academic Press: **1984**; Vol. *35*, 281-374.

172) Suri, J. T.; Cordes, D. B.; Cappuccio, F. E.; Wessling, R. A.; Singaram, B., "Continuous glucose sensing with a fluorescent thin-film hydrogel." *Angew. Chem., Int. Ed.* **2003**, *42*, 5857-5859.

173) Suri, J. T.; Cordes, D. B.; Cappuccio, F. E.; Wessling, R. A.; Singaram, B., "Monosaccharide detection with 4,7-phenanthrolinium salts: Charge-induced fluorescence sensing." *Langmuir* **2003**, *19*, 5145-5152.

174) Suzuki, H.; Kato, E.; Matsuzaki, A.; Ishikawa, M.; Harada, Y.; Tanikawa, K.; Nakagawa, H., "Analysis of Saccharides Possessing Post-translational Protein Modifications by Phenylhydrazine Labeling Using High-Performance Liquid Chromatography." *Anal. Sci.* **2009**, *25*, 1039-1042.

175) Swamy, K. M. K.; Jang, Y. J.; Park, M. S.; Koh, H. S.; Lee, S. K.; Yoon, Y. J.; Yoon, J., "A sorbitol-selective fluorescence sensor." *Tetrahedron Lett.* **2005**, *46*, 3453-3456.

176) Takeuchi, M.; Yamamoto, M.; Shinkai, S., "Fluorescent sensing of uronic acids based on a cooperative action of boronic acid and metal chelate." *Chem. Commun.* **1997**, 1731-1732.

177) Taylor, M. S., "Catalysis Based on Reversible Covalent Interactions of Organoboron Compounds." *Acc. Chem. Res.* **2015**, *48*, 295-305.

178) Teshima, C. W.; Meddings, J. B., "The measurement and clinical significance of intestinal permeability." *Curr. Gastroenter. reports* **2008**, *10*, 443-9.

179) Thoniyot, P.; Cappuccio, F. E.; Gamsey, S.; Cordes, D. B.; Wessling, R. A.; Singaram, B., "Continuous glucose sensing with fluorescent thin-film hydrogels. 2. Fiber optic sensor fabrication and in vitro testing." *Diabetes Technol. Ther.* **2006**, *8*, 279-287.

180) Torres, C. I.; Ramakrishna, S.; Chiu, C.-A.; Nelson, K. G.; Westerhoff, P.; Krajmalnik-Brown, R., "Fate of Sucralose During Wastewater Treatment." *Environ. Eng. Sci.* **2011**, *28*, 325-331.

181) Travis, S.; Menzies, I., "Intestinal permeability-Functional assessment and significance." *Clin. Sci.* **1992**, *82*, 471-488.

182) Trudgill, P. W.; Widdus, R., "D-glucarate catabolism by pseudomonadaceae and enterobacteriaceae." *Nature* **1966**, *211*, 1097.

183) Turner, J. R., "Intestinal mucosal barrier function in health and disease." *Nat. Rev. Immunol.* **2009**, *9*, 799-809.

184) Van den Berg, R.; Peters, J. A.; van, B. H., "The structure and (local) stability constants of borate esters of mono- and disaccharides as studied by 11B and 13C NMR spectroscopy." *Carbohydr. Res.* **1994**, *253*, 1-12.

185) Van den Berghe, G.; Wilmer, A.; Hermans, G.; Meersseman, W.; Wouters, P. J.; Milants, I.; Van Wijngaerden, E.; Bobbaers, H.; Bouillon, R., "Intensive insulin therapy in the medical ICU." *New Eng. J. Med.* **2006**, *354*, 449-461.

186) Van den Berghe, G.; Wouters, P.; Weekers, F.; Verwaest, C.; Bruyninckx, F.; Schetz, M.; Vlasselaers, D.; Ferdinande, P.; Lauwers, P.; Bouillon, R., "Intensive insulin therapy in critically ill patients." *New Eng. J. Med.* **2001**, *345*, 1359-1367.

187) Van den Berghe, G., "Disorders of gluconeogenesis." *J. Inher. Metabol. Dis.* **1996**, *19*, 470-477.

188) Van Duin, M.; Peters, J. A.; Kieboom, A. P. G.; Van Bekkum, H., "Studies on borate esters." *Tetrahedron* **1985**, *41*, 3411-3421.

189) Van Itallie, C. M.; Anderson, J. M., "Claudins and epithelial paracellular transport." *Ann. Rev. Physiol.* **2006**, *68*, 403-429.

190) van Wijck, K.; van Eijk, H. M. H.; Buurman, W. A.; Dejong, C. H. C.; Lenaerts, K., "Novel analytical approach to a multi-sugar whole gut permeability assay." *J. Chromat. B-Anal. Technol. Biomed. Life Sci.* **2011**, *879*, 2794-2801.

191) Vanduin, M.; Peters, J. A.; Kieboom, A. P. G.; Vanbekkum, H., "Studies on borate esters. Synergic coordination of calcium in borate polyhydroxycarboxylate systems." *Carb. Res.* **1987**, *162*, 65-78.

192) Vanduin, M.; Peters, J. A.; Kieboom, A. P. G.; Vanbekkum, H., "The pH-dependence of the stability esters of boronic-acid and borate in aqueous-medium studied by B-11 NMR." *Tetrahedron* **1984**, *40*, 2901-2911.

193) Varki, A., "Essentials of glycobiology." Essentials of glycobiology **1999**, 653.

194) Vilozny, B.; Schiller, A.; Wessling, R. A.; Singaram, B., "Enzyme assays with boronic acid appended bipyridinium salts." *Anal. Chim. Acta* **2009**, *649*, 246-251.

195) Vorndran, A. E.; Grill, E.; Huber, C.; Oefner, P. J.; Bonn, G. K., "Capillary zone of electrophoresis of aldoses, ketoses and uronic-acids derivatized with ethyl para-aminobenzoate." *Chromatographia* **1992**, *34*, 109-114.

196) Vougioukalakis, G. C.; Grubbs, R. H., "Ruthenium-Based Heterocyclic Carbene-Coordinated Olefin Metathesis Catalysts." *Chem. Rev.* **2010**, *110*, 1746-1787.

197) Walaszek, Z.; Szemraj, J.; Narog, M.; Adams, A. K.; Kilgore, J.; Sherman, U.; Hanausek, M., "Metabolism, uptake, and excretion of a D-glucaric acid salt and its potential use in cancer prevention." *Cancer Det. Prev.* **1997**, *21*, 178-190.

198) Wang, D. L.; Gong, X.; Heeger, P. S.; Rininsland, F.; Bazan, G. C.; Heeger, A. J., "Biosensors from conjugated polyelectrolyte complexes." *Proc. Nalt. Acad. Sci.U.S.A.* **2002**, *99*, 49-53.

199) Wang, D.; Wang, J.; Moses, D.; Bazan, G. C.; Heeger, A. J., "Photoluminescence Quenching of Conjugated Macromolecules by Bipyridinium Derivatives in Aqueous Media: Charge Dependence." *Langmuir* **2001**, *17*, 1262-1266.

200) Wang, H. C.; Lee, A. R., "Recent developments in blood glucose sensors." *J. Food Drug Anal.* **2015**, *23*, 191-200.

201) Wang, J. F.; Jin, S.; Akay, S.; Wang, B. H., "Design and synthesis of long-wavelength fluorescent boronic acid reporter compounds." *Eur. J. Org. Chem.* **2007**, 2091-2099.

202) Wang, J. F.; Jin, S.; Lin, N.; Wang, B. H., "Fluorescent indolylboronic acids that are useful reporters for the synthesis of boronolectins." *Chem. Biol. & Drug Design* **2006**, *67*, 137-144.

203) Wang, J.; Liu, B., "Fluorescence resonance energy transfer between an anionic conjugated polymer and a dye-labeled lysozyme aptamer for specific lysozyme detection." *Chem. Commun.* **2009**, 2284-2286.

204) Wang, J.; Liu, G. D.; Jan, M. R., "Ultrasensitive electrical biosensing of proteins and DNA: Carbon-nanotube derived amplification of the recognition and transduction events." *J. Am. Chem. Soc.* **2004**, *126*, 3010-3011.

205) Wang, P.; Lin, Z.; Su, X.; Tang, Z., "Application of Au based nanomaterials in analytical science." *Nano Today* **2017**, *12*, 64-97.

206) Wang, Y.; Chalagalla, S.; Li, T.; Sun, X.-l.; Zhao, W.; Wang, P. G.; Zeng, X., "Multivalent interaction-based carbohydrate biosensors for signal amplification." *Biosens. Bioelectron.* **2010**, *26*, 996-1001.

207) Welcker, K.; Martin, A.; Kolle, P.; Siebeck, M.; Gross, M., "Increased intestinal permeability in patients with inflammatory bowel disease." *Eur. J. Med. Res.* **2004**, *9*, 456-460.

208) Wiklund, A.-K. E.; Breitholtz, M.; Bengtsson, B.-E.; Adolfsson-Erici, M., "Sucralose - An ecotoxicological challenger?" *Chemosphere* **2012**, *86*, 50-55.

209) Wiskur, S. L.; Ait-Haddou, H.; Lavigne, J. J.; Anslyn, E. V., "Teaching old indicators new tricks." *Acc. Chem. Res.* **2001**, *34*, 963-972.

210) Wiskur, S. L.; Lavigne, J. L.; Metzger, A.; Tobey, S. L.; Lynch, V.; Anslyn, E. V., "Thermodynamic analysis of receptors based on guanidinium/boronic acid groups for the complexation of carboxylates, alpha-hydroxycarboxylates, and diols: Driving force for binding and cooperativity." *Chem.-a Eur. J.* **2004**, *10*, 3792-3804.

211) Wright, A. T.; Anslyn, E. V., "Differential receptor arrays and assays for solution-based molecular recognition." *Chem. Soc. Rev.* **2006**, *35*, 14-28.

212) Wulff, G., "Selective Binding to Polymers Via Covalent Bonds- The Construction of Chiral Cavities as Specific Receptor-Sites." *Pure Appl. Chem.* **1982**, *54*, 2093-2102.

213) Yamamoto, M.; Takeuchi, M.; Shinkai, S., "Molecular design of a PET-based chemosensor for uronic acids and sialic acids utilizing a cooperative action of boronic acid and metal chelate." *Tetrahedron* **1998**, *54*, 3125-3140.

214) Yan, J.; Fang, H.; Wang, B. H., "Boronolectins and fluorescent boronolectins: An examination of the detailed chemistry issues important for the design." *Med. Res. Rev.* **2005**, *25*, 490-520.

215) Yan, J.; Springsteen, G.; Deeter, S.; Wang, B. H., "The relationship among pK(a),pH, and binding constants in the interactions between boronic acids and diols - it is not as simple as it appears." *Tetrahedron* **2004**, *60*, 11205-11209.

216) Yang, J.; Liu, S.; Zheng, J.-F.; Zhou, J., "Room-Temperature Suzuki-Miyaura Coupling of Heteroaryl Chlorides and Tosylates." *Eur. J. Org. Chem.* **2012**, 6248-6259.

217) Yang, W. Q.; Yan, J.; Fang, H.; Wang, B. H., "The first fluorescent sensor for D-glucarate based on the cooperative action of boronic acid and guanidinium groups." *Chem. Commun.* **2003**, 792-793.

218) Yang, W.; He, H.; Drueckhammer, D. G., "Computer-guided design in molecular recognition: design and synthesis of a glucopyranose receptor." *Angew. Chem., Int. Ed.* **2001**, *40*, 1714-1718.

219) Yang, W.; Lin, L.; Wang, B., "A new type of boronic acid fluorescent reporter compound for sugar recognition." *Tetrahedron Lett.* **2005**, *46*, 7981-7984.

220) Yang, W.; Yan, J.; Springsteen, G.; Deeter, S.; Wang, B., "A novel type of fluorescent boronic acid that shows large fluorescence intensity changes upon binding with a carbohydrate in aqueous solution at physiological pH." *Bioorg. Med. Chem. Lett.* **2003**, *13*, 1019-1022.

221) Yoo, E. H.; Lee, S. Y., "Glucose Biosensors: An Overview of Use in Clinical Practice." *Sensors* **2010**, *10*, 4558-4576.

222) Yoon, J.; Czarnik, A. W., "Fluorescent Chemosensors of Carbohydrates - a Means of Chemically Communicating the Binding of Polyols in Water Based on Chelation-Enhanced Quenching." *J. Am. Chem. Soc.* **1992**, *114*, 5874-5875.

223) You, C.-C.; Miranda, O. R.; Gider, B.; Ghosh, P. S.; Kim, I.-B.; Erdogan, B.; Krovi, S. A.; Bunz, U. H. F.; Rotello, V. M., "Detection and identification of proteins using nanoparticle-fluorescent polymer 'chemical nose' sensors." *Nat. Nanotechnol.* **2007**, *2*, 318-323.

224) You, L.; Zha, D. J.; Anslyn, E. V., "Recent Advances in Supramolecular Analytical Chemistry Using Optical Sensing." *Chem. Rev.* **2015**, *115*, 7840-7892.

225) Yu, X.; Munge, B.; Patel, V.; Jensen, G.; Bhirde, A.; Gong, J. D.; Kim, S. N.; Gillespie, J.; Gutkind, J. S.; Papadimitrakopoulos, F.; Rusling, J. F., "Carbon nanotube amplification strategies for highly sensitive immunodetection of cancer biomarkers." *J. Am. Chem. Soc.* **2006**, *128*, 11199-11205.

226) Zaubitzer, F.; Buryak, A.; Severin, K., "Cp*Rh-based indicator-displacement assays for the identification of amino sugars and aminoglycosides." *Chem.-a Eur. J.* **2006**, *12*, 3928-3934.

227) Zhai, W. L.; Sun, X. L.; James, T. D.; Fossey, J. S., "Boronic Acid-Based Carbohydrate Sensing." *Chem.-a Eur. J.* **2015**, *10*, 1836-1848.

228) Zhao, J. Z.; Davidson, M. G.; Mahon, M. F.; Kociok-Kohn, G.; James, T. D., "An enantioselective fluorescent sensor for sugar acids." *J. Am. Chem. Soc.* **2004**, *126*, 16179-16186.

229) Zhao, Z.; Shen, T.; Xu, H., "Photoinduced interaction between eosine and viologen." *J. Photochem. Photobiol., A* **1990**, *52*, 47-53.

230) Zhu, L.; Anslyn, E. V., "Facile quantification of enantiomeric excess and concentration with indicator-displacement assays: An example in the analyses of alpha-hydroxyacids." *J. Am. Chem. Soc.* **2004**, *126*, 3676-3677.